Nowcasting and very short range forecasting SAF

Prototype Scientific Description for Météo-France/CMS

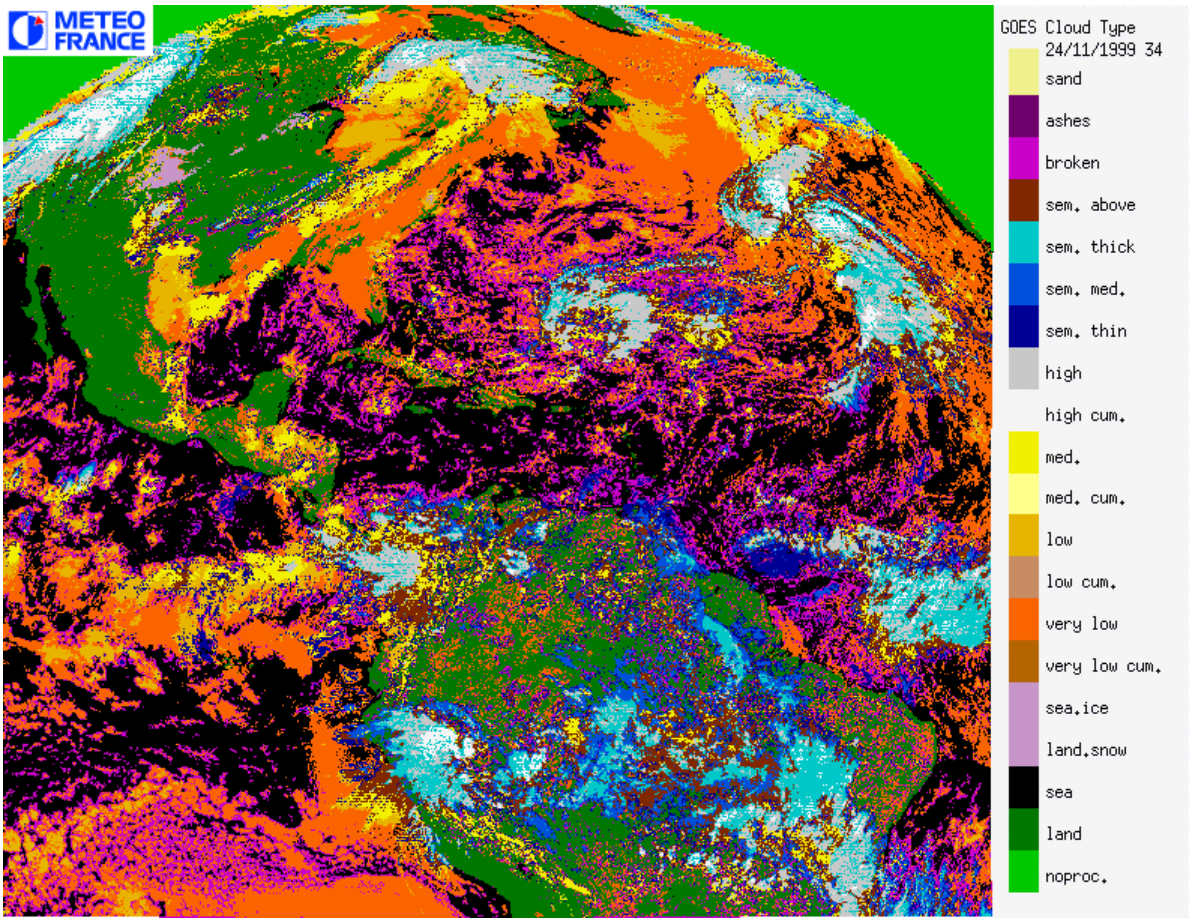

May 2000

SAF/NWC/MFCMS/MTR/PSD, Issue 1, Rev. 1

Prepared by METEO-FRANCE/CMS

REPORT SIGNATURE TABLE

Function	Name	Signature	Date
Prepared by	H. LeGleau & M. Derrien		May 2000
Reviewed by			May 2000
Authorised by			May 2000

DOCUMENT CHANGE RECORD

Version	Date	Pages	CHANGE(S)	Approval
0.1	Dec, 1999		SAF/NWC/MFCMS/MTR/PSD	
1.0	Feb. 2000	210	MF internal comments	
1.1	May 2000	210	MTR RIDs	

Table of Contents

List of Tables

List of Figures

Introduction

Within the EUMETSAT SAF for support to Nowcasting and Very Short Range Forecasting (hereafter referred as SAF NWC), Météo-France is responsible for the development of a software to extract cloud parameters from MSG SEVIRI imagery over MSG N area (see Serdan et al., 1998). These parameters must be extracted successively and are the cloud mask (CMa), the cloud type (CT) and the cloud top temperature and height (CTTH)). The Swedish Meteorological Institute (SMHI) is responsible for the adaptation (if needed) of the algorithm and software to high latitude conditions, and the development of a specific module (using window channels only) to retrieve cloud top temperature.

During the first development phase (1997-1999), prototypes to extract these cloud parameters have been developed at Météo-France and validated in a pre-operational environment during one year:

- NOAA/AVHRR images (locally received at CMS Lannion) have allowed to test algorithms in European conditions. We improved and adapted an existing AVHRR processing scheme (Derrien et al , 1993).
- NOAA/HIRS data (locally received at CMS Lannion) has allowed to compare various cloud top pressure retrieval techniques using window and sounding channels.
- GOES-East images, which are received at CMS Lannion every 30 minutes have allowed to test geostationary conditions. A completely new scheme has been developed, meeting most of the specifications defined within the SAF NWC.

No adaptation to high latitude conditions, nor specific cloud top temperature retrieval modules has yet been provided by SMHI.

The final software tuned to MSG SEVIRI spectral characteristics will be elaborated during a second development phase planned in 2000, taking advantage of experience gained at Météo-France during the prototyping phase.

This report contains a detailed scientific description of the cloud parameters prototyping performed during the first development phase by Météo-France / CMS. It is separated in three main chapters (one for each studied cloud parameters), and a set of annexes referenced in the main text. Although the interdependency of the three products is highlighted in the report, each main chapter is stand alone.

For each cloud parameter, we have detailed the algorithm, present its practical implementation, given validation results and drawn conclusions for its adaptation to SEVIRI.

1. Cloud mask prototyping

1.1. Introduction

This chapter is a scientific description of the cloud mask (CMa) prototyping performed by Météo-France during the SAF NWC first development phase (compliant with science and project plan).

The adaptation of the cloud mask algorithm to high latitude conditions is studied by SMHI and described in a separate document. To allow this study, we have delivered to SMHI the GOES prototyped software that we have developed, and a training dataset (see annex A 3.1). No feedback has been provided yet by SMHI.

1.2. Overview

1.2.1. Objective

The cloud mask (CMa), developed within the SAF NWC context, aims to support nowcasting applications, and additionally the remote-sensing of continental and oceanic surfaces. The CMa allows identifying cloud free areas where other products (total or layer precipitable water, land or sea surface temperatures, snow/ice cover delineation) may be computed. It also allows identifying cloudy areas where other products (cloud types and cloud top temperature/height) may be derived.

The central aim of the CMa is therefore to delineate all cloud-free pixels in a satellite scene with a high confidence. In addition, the product provides information on the presence of aerosols (i.e., smoke, dust clouds or volcanic plumes) and snow/sea ice.

The main application is nowcasting over the MSG N area. The consequences are twofold :

- the CMa prototypes have been developed, keeping in mind that the final software must be efficient in term of computing time and that all the ancillary data needed by the software must be available in real time.
- the prototypes have been validated in mid-latitude regions, but when available results for polar or tropical regions are indicated.

1.2.2. *Background*

Cloud detection algorithms are based on the fact that the spectral behaviour of clouds and earth surfaces are different in window channels. The main difficulties are that the earth surfaces' characteristics very much depend on the surface type, on the atmospheric conditions, on the sun and satellite respective positions, and that the contrast between the cloud and earth surface's characteristics may be very low under certain circumstances.

Three techniques may be applied to detect clouds :

- Clustering techniques are scene dependent methods : they use pixel values of the entire scene through histogram analysis or other calculations to segment the image according to pre-defined rules.

- Artificial neural networks are advanced multidimensional regression techniques which are capable of treating predictands and predictors in a very flexible way (allowing non linear relations).
- Multi-spectral threshold techniques are based on a pixel by pixel analysis of radiances where cloudy pixels are identified if pixel radiance pass a sequence of threshold tests.

The chosen method should be efficient in term of computing time, make the maximum use of SEVIRI channels, be easily adapted (e.g., if one channel is missing), and be mature. Moreover, it should be possible to easily tune the algorithm (prototyped with AVHRR and GOES imagery) to SEVIRI spectral conditions, even before SEVIRI data are available. The multispectral thresholding technique has been chosen for the generation of the CMa :

- The clustering techniques have been considered to be too scene-dependant.
- Although artificial neural network techniques are promising methods, they have not be retained for day-1 SW (i. e. SW to be ready when MSG is launched) : the main reason is that the training of such methods, very sensitive to the learning data set, cannot rely only on simulated data.
- One of the main advantage of the multispectral thresholding technique is that it is relatively easy to adapt thresholds to varying meteorological conditions, earth surface types, viewing geometry using external data (NWP model forecast fields, RTM calculations, climatological atlas). This physical approach will also allow an easy tuning of the CMa prototypes to MSG SEVIRI spectral characteristics. Moreover, Météo-France has a 10-years experience in applying such technique to process AVHRR imagery (see Derrien et al, 1993).

1.2.3. Cloud mask inputs

The CMa has been prototyped with AVHRR images and GOES-East imagery locally received at CMS. The input and output data for these two prototypes are slightly different, as the AVHRR prototype is based on an existing software and the GOES-East prototype is a completely new scheme.

<u>The input for the GOES-East prototype are :</u>

- satellite imagery (see annex A.1.3) :

4 window channels (0.6 µm, 3.9 µm, 11 and 12 µm) over the Extended Northern Hemisphere at full IR spatial resolution (the visible has been averaged at the IR resolution) every slot in the satellite projection. Sun and satellite angles associated to GOES imagery, are computed at the segment resolution (i.e., 4*4 IR pixels).

- NWP outputs (see annex A.2.2) :

The French NWP model ARPEGE has been used during prototyping. Six-hourly short term forecast fields of the following parameters, remapped onto satellite images (at the segment resolution, i.e. 4*4 IR pixels), are used as input (the elevation of the NWP model grid is also needed):

  - 2 m temperatures and surface temperatures,
  - total water vapour content of the atmosphere,

- Ancillary data sets (see annex A.2.1) :

The following ancillary data, remapped onto satellite images (at the segment resolution, i.e. 4*4 IR pixels), are used as input :

  - Land/sea/coast atlas,
  - Elevation atlas,
  - Monthly minimum SST climatology,
  - Monthly mean 0.6 µm atmospheric-corrected reflectance climatology (land),

The input for the AVHRR prototype are:

- satellite imagery (see annex A.1.1) :

5 or 6 window channels (0.6 µm, 0.9 µm, 1.6 µm, 3.9 µm, 11 and 12 µm) at full spatial resolution in the satellite projection. Only 4 passes are processed every day. Sun and satellite angles associated to AVHRR imagery, are computed every HIRS FOV (i.e., 34*39 AVHRR pixels).

- NWP outputs (see annex A.2.2) :

The French NWP model ARPEGE has been used during prototyping. Six-hourly short term forecast fields of the following parameters, remapped onto satellite images (at the HIRS spatial resolution, i.e. 34*39 AVHRR pixels), are used as input (the elevation of the NWP model grid is also needed) :

  - 2 m air temperatures,

- Ancillary data sets (see annex A.2.1) :

The following ancillary data, remapped onto satellite images (at the segment resolution, i.e. 34*39 pixels), are used as input :

  - Land/sea/coast atlas,
  - Elevation atlas,
  - Monthly minimum SST climatology,
  - Monthly mean 0.6 µm atmospheric-corrected reflectance climatology (land),

1.2.4. Cloud mask outputs

The CMa output for the GOES-East prototype are available over the Northern Hemisphere at full spatial resolution for every slots (i.e., every 30 minutes). They follow most of the specification retained for SEVIRI. These outputs are :

- The CMa itself is coded on a short unsigned integer and contains seven categories:
  - Not processed : containing no data or corrupted data,
  - Cloud free : completely cloud free, and no contamination by snow/ice covered surface,
  - Contaminated by cloud : clouds present in the FOV,
  - Cloud filled : opaque cloud completely filling the FOV,
  - Contaminated by aerosols (i.e., smoke, dust clouds or volcanic plumes),
  - Contaminated by snow or by ice,
  - Unclassified (if the distinction between cloudy or cloud-free cannot be done),

- Quality flag:

The quality flag is coded on a short unsigned integer and encloses :

  - one bit to flag not-processed pixels,
  - six bits to identify the conditions in which the product has been processed: use of NWP outputs in the processing, illumination conditions (day, night, dawn, sunglint), high viewing angles, missing channels,
  - three bits to describe the quality of the CMa itself : cloud-free, cloudy and ice/snow areas that may be mis-classified are flagged,
  - one bit to indicate that the pixel, classified as cloudy by the threshold tests, has been re-set as cloud free by the filtering process,
  - one bit to indicate whether aerosol detection has been attempted,

- Threshold test flag :

This flag is used for validation purposes and allows the identification of the first test that has detected clouds. Each bits of this flag (coded on a short unsigned integer) are devoted to one specific threshold test.

The CMa output for the AVHRR prototype are available at full spatial resolution for every processed pass. These outputs are coded on a short unsigned integer as described below. They do not follow the specifications retained for SEVIRI, because the AVHRR prototype is an adaption of an existing software :

- one bit to flag not processed area (i.e., containing no data or corrupted data),
- two bits to aerosols (i.e., smoke, dust clouds, and volcanic plume),

- one bit to flag ice or snow,
- one bits to flag cloud free areas,
- one bit to flag oceanic cloud free areas (specifically developed not to mask thermal front),
- three bits to describes which test has detected the clouds,

1.3. Algorithm detailed description

1.3.1. Algorithm outline

The algorithm is based on multispectral threshold technique. Each pixel of the image is classified by a succession of tests applied to various combinations of channels.

A first set of tests allows the identification of pixels contaminated by clouds or snow/ice : this first process stops if one test is really successful (i.e., if the threshold is not too close to the measured value). A test is applied to cloud contaminated pixels to check whether the cloud cover is opaque and completely fills the FOV. A second process (much more experimental) allows the identification of aerosol events (dust clouds or volcanic plume) ; during the prototyping, this aerosol detection is applied to all pixels (even if already classified as cloud-free or contaminated by clouds) : it means that the classes are not completely exclusive. The combinations of channels used depend on the geographical location of the pixel (land, sea or coast), on the solar illumination and on the viewing angles (daytime, nigh-time, twilight, sunglint).

The computation of the thresholds is the most critical task of the cloud masking. They are determined off-line, either as empirical values, or as functions/pre-computed tables tuned using RTM calculations. The on-line preparation of thresholds is then performed by these functions/pre-computed tables, using as input the viewing geometry (sun and satellite viewing angles), NWP forecast fields (surface temperature and total atmospheric water vapour content) and ancillary data (elevation and climatological data). The thresholds are computed on segment, which size is 4*4 IR pixels for the GOES prototyping (see also a discussion of the segment's size in 1.4.3), and 34 * 39 pixels in the AVHRR prototyping.

In the GOES prototyping, an assessment of the cloud and snow detection's quality is performed by analysing how much close the thresholds and the measures are.

A filtering is applied, allowing to reclassify pixels having a class type different from their neighbours.

1.3.2. Tests sequence

A first set of tests allows the identification of pixels contaminated by clouds or snow/ice : this first process stops if one test is really successful (i.e., if the threshold is not too close to the measured value). The combinations of channels used depend on the geographical location of the pixel (land, sea or coast), on the solar illumination and on the viewing angles (daytime, night-time, twilight, sunglint, defined in Table 1.3.2.1).

	Nighttime	**Twilight**	**Daytime**	**Sunglint**
GOES prototype	Solar elevation < 0	0<Solar elevation<10	10 < Solar elevation	Cox & Munck > 10% Solar elevation > 15
AVHRR prototype	Solar elevation < 0	0<Solar elevation <7	7 < Solar elevation	Cox & Munck > 10% Solar elevation > 15

(Cox & Munck stands for the reflectance computed using Cox & Munck theory (see Cox and Munck, 1954) ; the solar elevation is expressed in degrees)..

Table 1.3.2.1 Definition of the illumination conditions.

The geographical location is defined, using the land/sea atlas value. A processing specific to coastal areas is performed in the AVHRR prototyping : the inaccuracy of the image navigation may lead to a confusion between sea and land pixels in coastal areas and has to be accounted for. This processing, not needed for geostationary satellites (neither GOES, nor SEVIRI), is not detailed in this document.

The test applied to land or sea pixels are listed in Tables 1.3.2.2, 1.3.2.3 and 1.3.2.4 (the test sequences are not the same in the AVHRR and GOES prototype, because the AVHRR prototype is based on an already existing scheme).

A second process (much more experimental) allows the identification of aerosol (dust clouds and volcanic plume) and is applied to all pixels (even already classified as cloud-free or contaminated by clouds).

[T3.9µm, T11µm and T12µm stand for brightness temperatures at 3.9, 11 and 12 micrometer ; R0.6µm and R0.9µm stand for VIS/NIR bi-directional top of atmosphere reflectances at 0.6 and 0.9 micrometer normalised for solar illumination ; SST is the split-window (used for SST calculation) computed from T11µm and T12µm measurements. Low Clouds in Sunglint is a specific module (detailed in 1.3.3) for low clouds identification in sunglint areas.]

GOES			AVHRR		
Daytime	**Twilight**	**Nighttime**	**Daytime**	**Twilight**	**Nighttime**
Snow detection	T11µm	T11µm	Snow detection	T11µm	T11µm
T11µm	R0.6µm	T11µm-T12µm	T11µm	T11µm-T12µm	T3.9µm-T12µm
R0.6µm	T11µm-T12µm	T11µm-T3.9µm	R0.6µm	T11µm-T3.9µm	T11µm-T3.9µm
T11µm-T12µm	T11µm-T3.9µm	T3.9µm-T11µm	T11µm-T12µm	R0.6µm	T11µm-T12µm
T11µm-T3.9µm	Spatial coherence	Spatial coherence	T11µm-T3.9µm	(T11µm-T3.9µm) / (T11µm-T12µm)	(T11µm-T3.9µm) / (T11µm-T12µm)
Spatial coherence	(T11µm-T3.9µm) / (T11µm-T12µm)	(T11µm-T3.9µm) / (T11µm-T12µm)			

Table 1.3.2.2 Test sequence over land

GOES prototype			
Daytime	**Sunglint**	**Twilight**	**Nighttime**
Ice detection	Ice detection	SST	SST
SST	SST	R0.6µm	T11µm-T12µm
R0.6µm	T11µm-T12µm	T11µm-T12µm	T11µm-T3.9µm
T11µm-T12µm	Spatial coherence	T11µm-T3.9µm	T3.9µm-T11µm
T11µm-T3.9µm	R0.6µm	Spatial coherence	Spatial coherence
Spatial coherence	T11µm-T3.9µm		
	Low Clouds in Sunglint		

Table 1.3.2.3 Test sequence over sea in the GOES prototype

AVHRR prototype			
Daytime	**Sunglint**	**Twilight**	**Nighttime**
Ice detection	Ice detection	Spatial coherence	SST
SST	SST	SST	T3.9µm-T12µm
R0.9µm	Spatial coherence	T11µm-T12µm	T11µm-T3.9µm
Spatial coherence	T11µm-T12µm	T11µm-T3.9µm	Spatial coherence
T11µm-T12µm	R0.9µm	R0.9µm	T11µm-T12µm
T11µm-T3.9µm	Low Clouds in Sunglint		
	T11µm-T3.9µm		

Table 1.3.2.4 Test sequence over sea in the AVHRR prototype

1.3.3. Tests description

In this paragraph, we describe each cloud detection test, focusing on the computation of the thresholds. The cloud free targets gathered in the interactive test file (see annex A.3.1) are used to illustrate the thresholds' quality.

1.3.3.1. Test on SST

1.3.3.1.1. Aim of the test

The test is the following :

A pixel is classified as cloud contaminated if :

- SST(T11µm, T12µm) < SSTthreshold.

A split window algorithm, using T11µm and T12µm brightness temperatures to compute Sea Surface Temperature, is applied to all pixels over the ocean. A pixel is then classified as cloudy if its split window value is lower that the estimated Sea Surface Temperature. This test allows to detect most of the clouds over the ocean for any solar illumination. Problems may be encountered where the oceanic SST is varies rapidly in space and time. This test is more efficient than directly thresholding the T11µm using an offset that accounts for the atmospheric absorption and the surface emissivity variation with satellite angle.

1.3.3.1.2.Threshold computation

The threshold is computed from a monthly climatological minimum SST (see Annexe A.2.1.3) by substracting a offset (4°C). This offset is needed to account for the imperfection of the climatology, especially in areas with persistent cloudiness, and in areas where the oceanic SST varies rapidly in space and time.

The split window algorithm that has been used in the GOES and AVHRR prototype is the one developed by SAF O&SI. For example, the following algorithm is used in the GOES-08 prototype :

SST(T11µm, T12µm) = 0.981*T11µm+(0.063*sstclim+1.143*(sec-1))*(T11µm-T12µm)+1.085 [sec is the secante of the satellite zenith angle, sstclim is the climatological SST in °C].

On figure 1.3.3.1, satellite-retrieved SST are compared to climatological minimum SST for cloud free oceanic targets of the GOES interactive test file. This figure illustrates why an offset of at least 4°C is needed to compute the threshold.

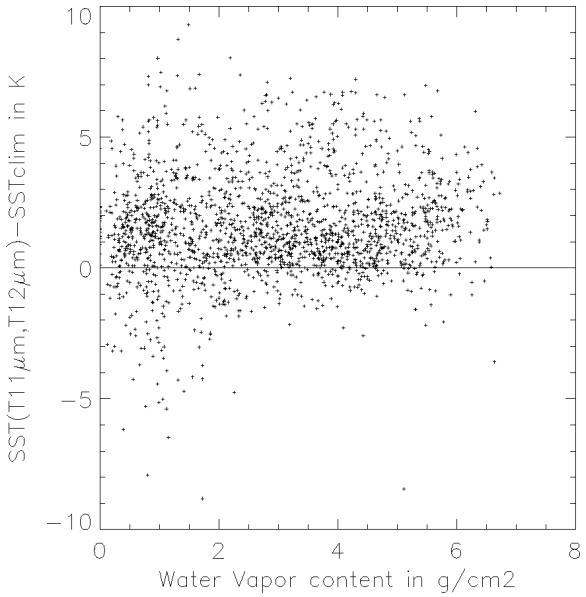

Figure 1.3.3.1 Comparison between the SST derived from satellite data and the climatological SST, for GOES oceanic cloud free targets :

1.3.3.2. Test on T11μm (only over land)

1.3.3.2.1. Aim of the test

The test is the following :

A pixel is classified as cloud contaminated if :

- T11μm < T11threshold.

This test, applied only over land, allows the detection of the clouds having a 11 μm brightness temperature lower than the surface brightness temperature. The surface brightness temperatures are estimated from air or surface temperatures forecast by a NWP model. Thereby the test accuracy depends both on the forecast's quality and on the methodology applied to transform this forecast temperature into a best estimate of the clear-sky surface brightness temperature.

1.3.3.2.2.Threshold computation

The differences between the surface temperature (forecast by ARPEGE for the time of observation) and the T11μm brightness temperatures are illustrated on figure 1.3.3.2, using the GOES interactive test file. These differences are rather low at night-time; whereas at daytime, they strongly increase with the solar elevation [especially for highly reflective surfaces] and seem to decrease with water vapour content. The reasons for these behaviours are shortly analysed below:

- The high differences between brightness temperature and NWP surface temperature for high solar elevation and bright surfaces are due to the different physical meaning of both temperatures. The brightness temperature is very close to the skin temperature which is the warmest part of the vertical temperature profile at daytime (especially in case high solar elevation and arid surfaces). The computation of the NWP surface temperature depends on the land surface parametrisation scheme used in the NWP model ; surface temperatures computed in ARPEGE correspond to the first 4-5 cm in the ground, which present a weaker diurnal cycle than the skin temperatures.

- The slight decrease of the difference between brightness and surface temperatures with water vapour content can be explained by atmospheric absorption, which is in fact higher for high water vapour content over warm surfaces.

The T11μm threshold over land is computed from temperatures forecast by ARPEGE model, by accounting for atmospheric absorption and small scale height effects as described below [the different physical meaning of brightness temperature and NWP surface temperature (dependent on the NWP model) is not accounted for] :

- 6-hourly fields (0h, 6h, 12h and 18h TU) forecast by ARPEGE are used. The surface temperature for a given GOES slot is then estimated from the two nearest NWP fields (spatially interpolated at the segment's spatial resolution) by retaining the minimum value, whereas the nearest in time 2m air temperature is used in the AVHRR processing. The rough spatial resolution of ARPEGE over America (nearly 200km) does not allow fine scale structures' description.

- In the GOES prototype, the atmospheric absorption is accounted for through an offset computed as a function of satellite zenith angle, integrated atmospheric water vapour content and solar zenith angle. Two tables have been pre-computed by applying RTTOV to radio-soundings from TIGR data set (Annex A.2.3). One table is used for night-time conditions [the surface temperature used in the RTTOV simulations has been assumed to

be colder than the air of the lowest layer by 5°C]; the second table is used for daytime condition at 30 degrees solar elevation [the surface temperature used in the RTTOV simulation has been assumed to be warmer than the air of the lowest layer by 5°C]. The satellite zenith angle and the water vapour content are used to interpolate in these tables, whereas the solar zenith angle is used to interpolate or extrapolate between the night-time and the daytime values. In the AVHRR prototype, a constant offset is applied (10 °C).

- A dry adiabatic law is used to account for the height difference between the elevation of the NWP grid and of the pixel (available at a much finer spatial resolution that ARPEGE resolution over America (see Annexe A.2.1.2)) : this simple process (applied both in the AVHRR and GOES prototypes) allows to roughly simulate small scale height effects in mountainous regions.

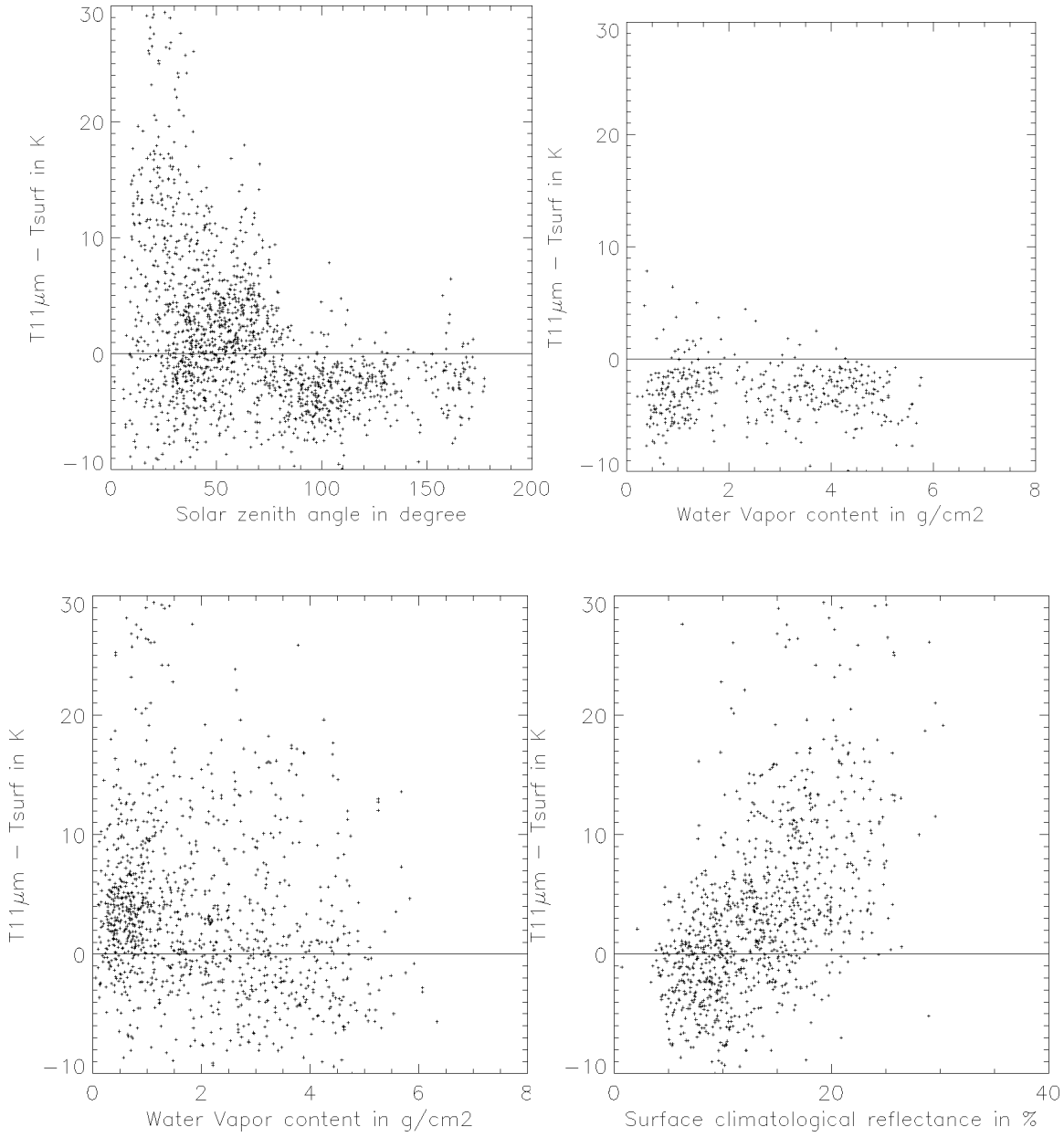

Figure 1.3.3.2 Comparison between T11µm and ARPEGE surface temperature for GOES continental clear-sky targets. Top right : night-time cases. Bottom (right and left) : daytime cases.

1.3.3.3. Test on T11µm-T12µm

1.3.3.3.1. Aim of the test

The test is the following :

A pixel is classified as cloud contaminated if :

- T11µm -T12µm > T11T12threshold.

This test, which can be applied over all surfaces in any solar illumination, allows the detection of thin cirrus clouds and cloud edges characterised by a higher T11µm-T12µm than cloud-free surfaces. The difficulty is to estimate the cloud free surfaces T11µm-T12µm difference which depends on the difference of atmospheric absorption (mainly due to water vapour) and surface emissivity in the two infrared wavelengths. This test will be useless if the estimated clear-sky T11µm-T12µm difference is too high, which may be the case at daytime.

1.3.3.3.2.Threshold computation over sea

The thresholds are functions of satellite zenith angle and T11µm brightness temperatures of the pixel in the AVHRR prototype, of satellite zenith angle, water vapour content and climatological SST in the GOES prototype. They are calculated from pre-computed tables, which have been elaborated by applying RTTOV to radio-soundings from the TIGR dataset, using Masuda emissivities (Masuda et al., 1988).

In the AVHRR prototype, only one pre-computed table is used. The satellite zenith angle and the T11µm brightness temperatures of the pixel are used to interpolate in this table.

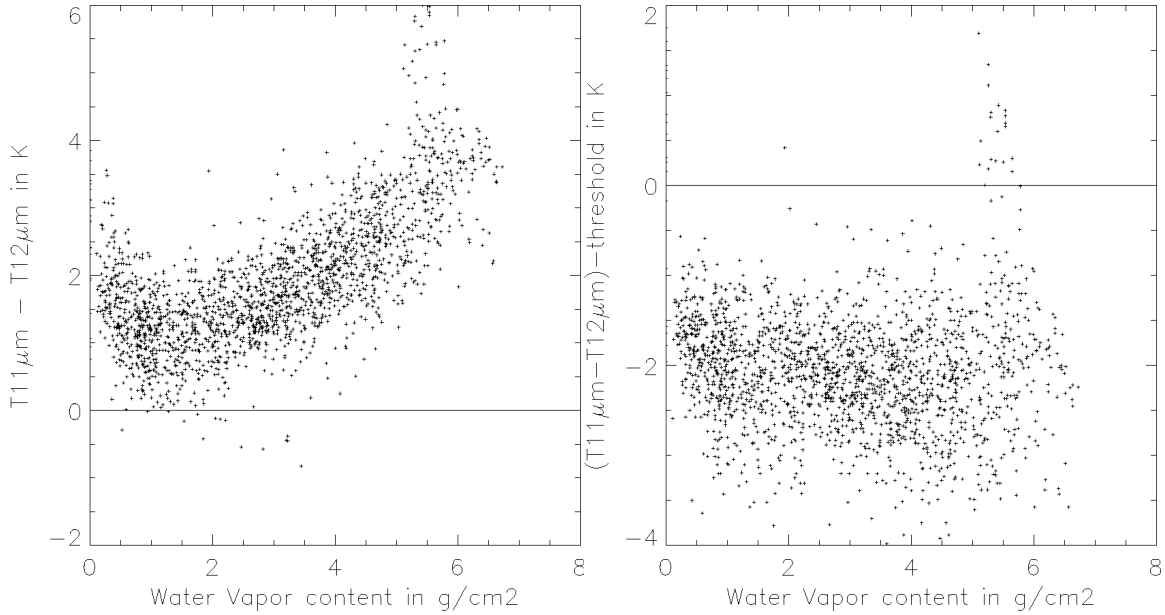

Figure 1.3.3.3.1 For GOES oceanic clear sky targets :Left : variation of T11µm-T12µm with water vapour content. Right : comparison of T11µm-T12µm and the associated threshold.

.

In the GOES prototype, two pre-computed tables are used. One table is used for cold seas conditions [the surface temperature used in the RTTOV simulations has been assumed to be colder than the air of the lowest layer by 3°C] ; the second table is used for warm seas condition [the surface

temperature used in the RTTOV simulation has been assumed to be equal to the air of the lowest layer]. The satellite zenith angle and the water vapour content are used to interpolate in these tables, whereas the climatological SST allows to interpolate between the two tables.

The quality of the threshold is illustrated on figure 1.3.3.3.1, using the GOES interactive test file. The variation of T11µm-T12µm difference with water vapour content is well accounted for, even if the scatter remains. Some very high T11µm-T12µm values (larger than 4°C) are observed for high water vapour content and correspond to high solar elevation : they are not well simulated in the threshold. The plot on figure 1.3.3.3.1 shows brightness temperatures averaged on targets of 5 by 5 IR GOES pixels ; in fact T11µm-T12µm difference presents a large scatter in each target (as high as 1°C), which must be accounted for by the threshold : it is therefore advisable that the quantity (T11µm-T12µm - threshold) is not too closed to zero for cloud free values.

1.3.3.3.3.Threshold computation over land

The thresholds are functions of satellite zenith angle and T11µm brightness temperatures of the pixel in the AVHRR prototype, of satellite zenith angle, water vapour content and solar zenith angles in the GOES prototype. They are calculated from pre-computed tables, which have been set up by applying RTTOV to radio-soundings from the TIGR dataset, using a constant emissivity of 0.98 in both channels (Salisbury et al., 1992).

In the AVHRR prototype, a single pre-computed table is used. The satellite zenith angle and the T11µm brightness temperatures of the pixel are used to interpolate in this table.

In the GOES prototype, two pre-computed tables are used. One table is used for night-time conditions [the surface temperature used in the RTTOV simulations has been assumed to be colder than the air of the lowest layer by 3°C (see figure 1.3.3.3.2)] ; the second table is used for daytime condition at 30 degrees solar elevation [the surface temperature used in the RTTOV simulation has been assumed to be warmer than the air of the lowest layer by 10°C (see figure 1.3.3.3.2)]. The satellite zenith angle and the water vapour content are used to interpolate in these tables, whereas the solar zenith angle is used to interpolate or extrapolate between the night-time and the daytime values.

The quality of the threshold is illustrated on figure 1.3.3.3.3 (night-time conditions) and figure 1.3.3.3.4 (daytime conditions), using the GOES interactive test file. At night-time, the increase of T11µm-T12µm difference with water vapour content is not very well simulated. At daytime, it is even worse. As shown by the RTTOV simulations on figure 1.3.3.3.2, for relatively high water vapour content the T11µm-T12µm difference is very dependent on the temperature difference between the surface and the air just above. As this quantity is not directly available : its impact on T11µm-T12µm difference has been estimated using the solar illumination to interpolate or extrapolate between a night-time and a daytime values. This uncertainty, linked with the possible inaccuracy of the water vapour content forecast may explain why the very large scatter observed in T11µm-T12µm difference is not retrieved in the threshold. This very large uncertainty on the simulation of T11µm-T12µm difference and the large cloud free values observed may make this test nearly useless at daytime.

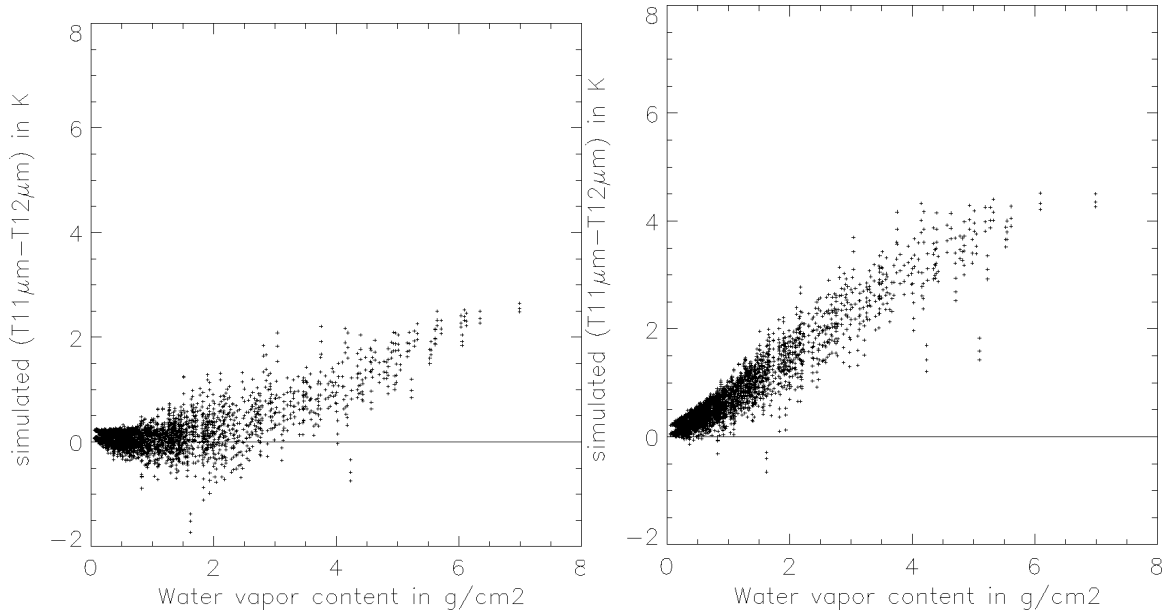

Figure 1.3.3.3.2 GOES T11µm-T12µm simulated with RTTOV applied to TIGR radio-soundings. Left : nighttime conditions. Right : daytime conditions.

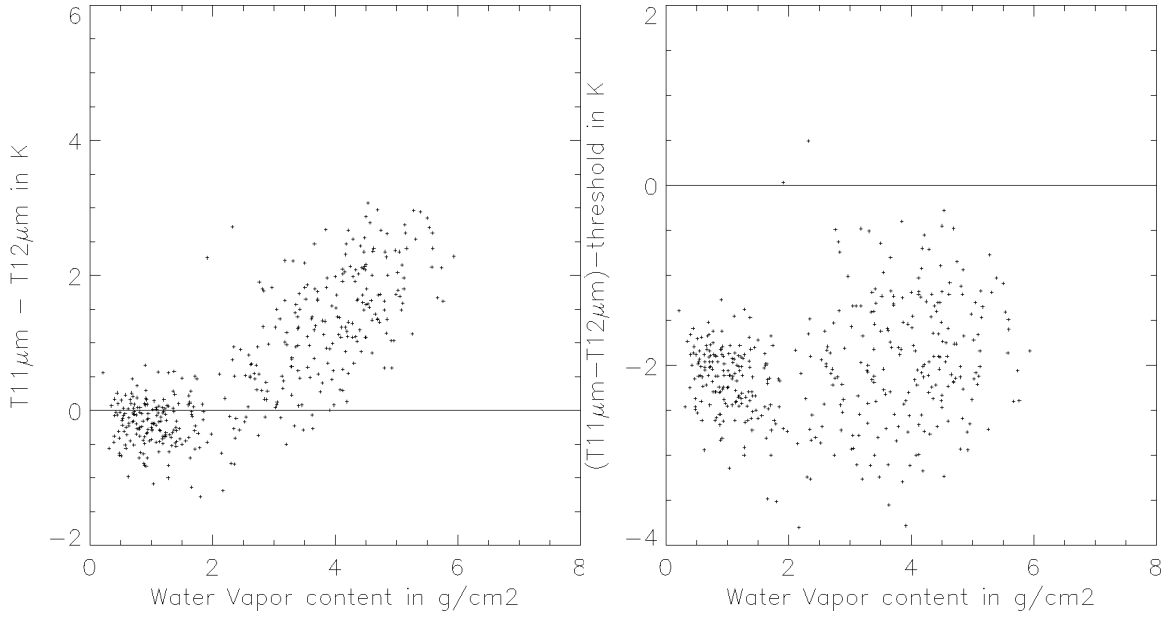

Figure 1.3.3.3.3 For GOES continental clear sky targets at night-time .Left : variation of T11µm-T12µm with water vapour content. Right : comparison of T11µm-T12µm and the associated threshold.

.

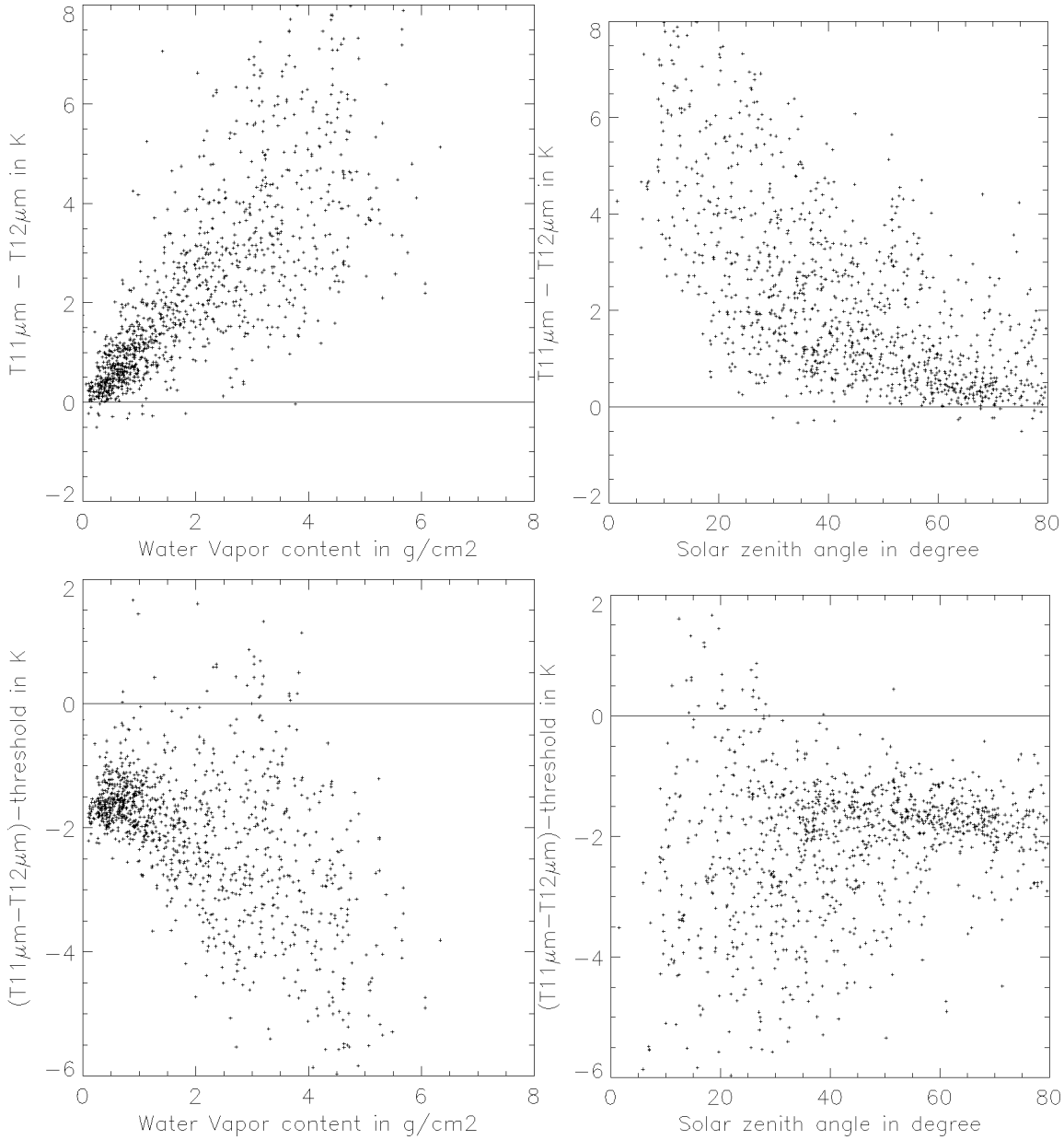

Figure 1.3.3.3.4 For GOES continental clear sky targets at daytime Top : variation of T11µm-T12µm with water vapour content and solar zenith angle. Bottom : comparison of T11µm-T12µm and the associated threshold.

1.3.3.4. Test on T11µm-T3.9µm

1.3.3.4.1. Aim of the test

The test is the following :

A pixel is classified as cloud contaminated if :

- T11µm - T3.9µm > T11T39threshold.

This test allows the detection of low water clouds at night-time, but also low clouds shadowed by higher clouds. It is based on the fact that the water cloud emissivity is lower at 3.9µm than at 11µm (Hunt, 1973), which is not the case for cloud free surfaces (except sandy desertic areas). A basic assumption is that the 3.9µm channel is not affected by the solar irradiance, which is the case at night-time and in shadows. The cloud free surfaces T11µm-T3.9µm difference (depending on the difference of atmospheric absorption (mainly due to water vapour) and surface emissivity in the two infrared wavelengths) has to be accurately estimated to allow this test to detect most low water clouds. An additional difficulty is the high radiometric noise (enhanced for cold temperatures) that affects the 3.9µm channel.

1.3.3.4.2.Threshold computation over sea

The threshold is a constant value (1.5°C) in the AVHRR prototype, and is a function of satellite zenith angle, water vapour content in the GOES prototype.

In the GOES prototype, one pre-computed table is used. It has been elaborated by applying RTTOV to radio-soundings from the TIGR dataset, using Masuda emissivities (Masuda et al., 1988). The surface temperature used in the RTTOV simulations has been assumed to be colder than the air of the lowest layer by 3°C. The satellite zenith angle and the water vapour content are used to interpolate in this table.

The quality of the threshold is illustrated on figure 1.3.3.4.1, using the GOES interactive test file. The variation of T11µm-T3.9µm difference with water vapour content is well accounted for, even if the scatter (especially large for high water vapour content) remains. The plot on figure 1.3.3.4.1 shows brightness temperatures averaged on targets of 5 by 5 IR GOES pixels ; in fact T11µm-T3.9µm difference presents a large scatter in each target (especially for cold targets), which must be accounted for by the threshold : it is therefore advisable that the quantity (T11µm-T3.9µm - threshold) is not too close to zero for cloud free values.

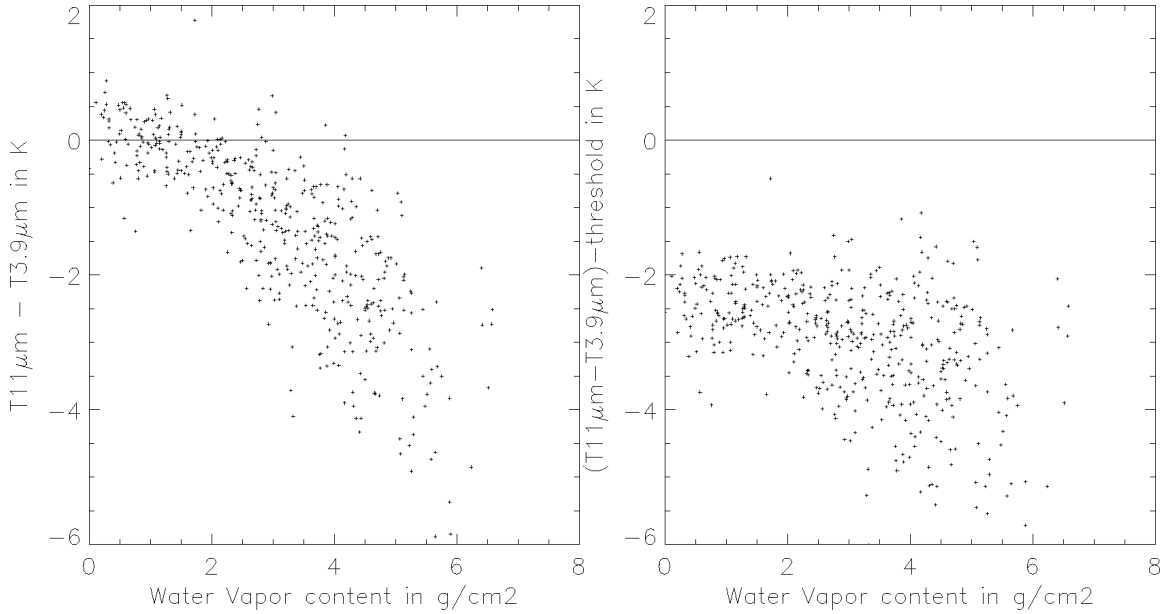

Figure 1.3.3.4.1 For GOES oceanic cloud free targets :Left : variation of T11µm-T3.9µm with water vapour content. Right : comparison of T11µm-T3.9µm and the associated threshold.

1.3.3.4.3.Threshold computation over land

In the AVHRR prototype, the threshold is a constant value depending on the surface type (from 1.5°C up to 3.5°C for the brighter areas (deserts)), whereas it is a function of satellite zenith angle, water vapour content and climatological visible reflectance in the GOES prototype.

In the GOES prototype, two pre-computed tables are used. They have been established by applying RTTOV to radio-soundings from the TIGR dataset, assuming that the surface temperature used in the RTTOV simulations is colder than the air of the lowest layer by 5°C. Two sets of emissivities (Salisbury et al., 1992) have been used to create two tables : one corresponding to vegetated areas (0.98 in both channel), one to arid areas (sandstone (0.88 and 0.96 at 3.9µm and 11µm respectively) and silicate (0.80 and 0.96 at 3.9µm and 11µm respectively)). The satellite zenith angle and the water vapour content are used to interpolate in this table, whereas the climatological visible reflectance allows to interpolate between the two tables corresponding to vegetated and arid surfaces.

The quality of the threshold is illustrated on figure 1.3.3.4.2, using the GOES interactive test file. The variation of T11µm-T3.9µm difference with water vapour content is not well accounted for.

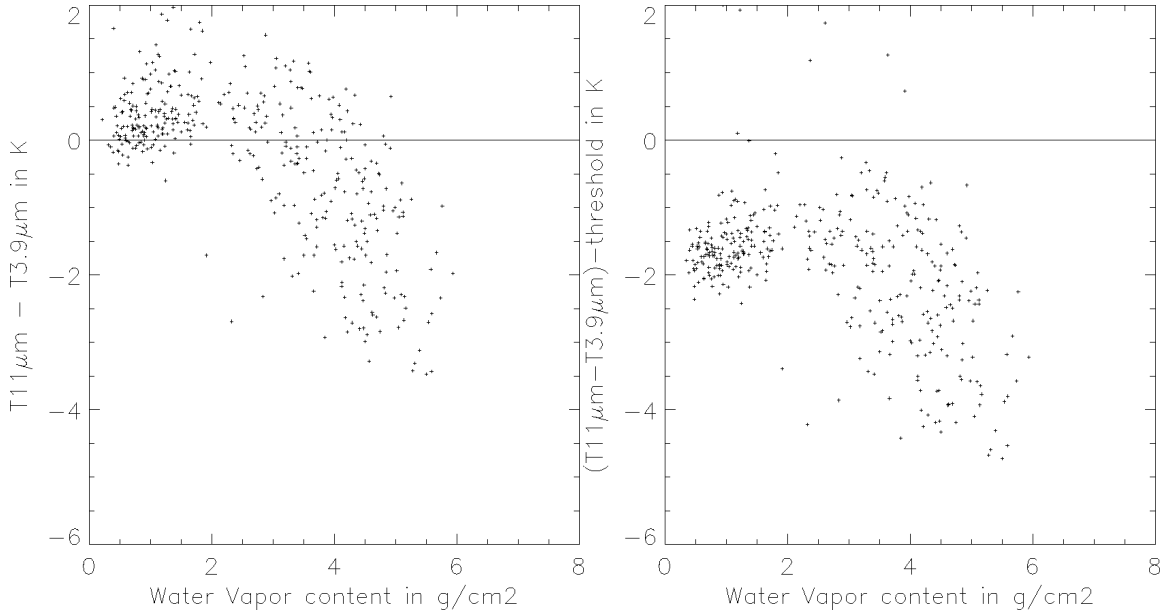

Figure 1.3.3.4.2 For GOES continental cloud free targets .Left : variation of T11µm-T3.9µm with water vapour content. Right : comparison of T11µm-T3.9µm and the associated threshold.

1.3.3.5. Test on T3.9µm-T11µm (GOES prototype) or T3.9µm-T12µm (AVHRR prototype)

1.3.3.5.1. Aim of the test

The test is the following :

A pixel is classified as cloud contaminated if :

- T3.9µm - T11µm > T39T11threshold (T3.9µm - T12µm > T39T12threshold in the AVHRR prototype)

This test allows the detection of high semi-transparent clouds at night-time. It is based on the fact that the contribution of the relatively warm grounds to the brightness temperature is higher at 3.9µm than at 11µm, due to a lower ice cloud transmittance (Hunt, 1973), and to the high non-linearity of the Planck function at 3.9µm. This test is usable only at night-time, when solar irradiance does not act upon the 3.9µm channel radiance. The cloud free surfaces T11µm-T3.9µm difference (depending on the difference of atmospheric absorption (mainly due to water vapour) and surface emissivity in the two infrared wavelengths) has to be accurately estimated to allow this test to detect most semi-transparent clouds. An additional difficulty is the high radiometric noise (enhanced for cold temperatures) that affects the 3.7µm channel. But the non linearity effect makes this test much more efficient than the T11µm-T12µm test to detect high semi-transparent clouds over rather warm grounds at night-time. T3.9µm-T11µm is preferred because it is less sensitive to atmospheric water vapour.

1.3.3.5.2.Threshold computation over sea

In the AVHRR prototype, the threshold is a constant value depending on the season (from 3.5°C in winter up to 6°C in summer) whereas it is a function of satellite zenith angle, water vapour content and climatological SST in the GOES prototype.

In the GOES prototype, two pre-computed tables are used, that have been elaborated by applying RTTOV to radio-soundings from the TIGR dataset, using Masuda emissivities (Masuda et al., 1988. One table is used for cold seas conditions [the surface temperature used in the RTTOV simulations has been assumed to be equal to the air of the lowest layer] ; the second table is used for warm seas condition [the surface temperature used in the RTTOV simulation has been assumed be warmer than the air of the lowest layer by 3°C]. The satellite zenith angle and the water vapour content are used to interpolate in these tables, whereas the climatological SST allows to interpolate between the two tables.

The quality of the threshold is illustrated on figure 1.3.3.5.1, using the GOES interactive test file. The large scatter of T39µm-T11µm difference (especially at high water vapour content) is not accounted for by the threshold.

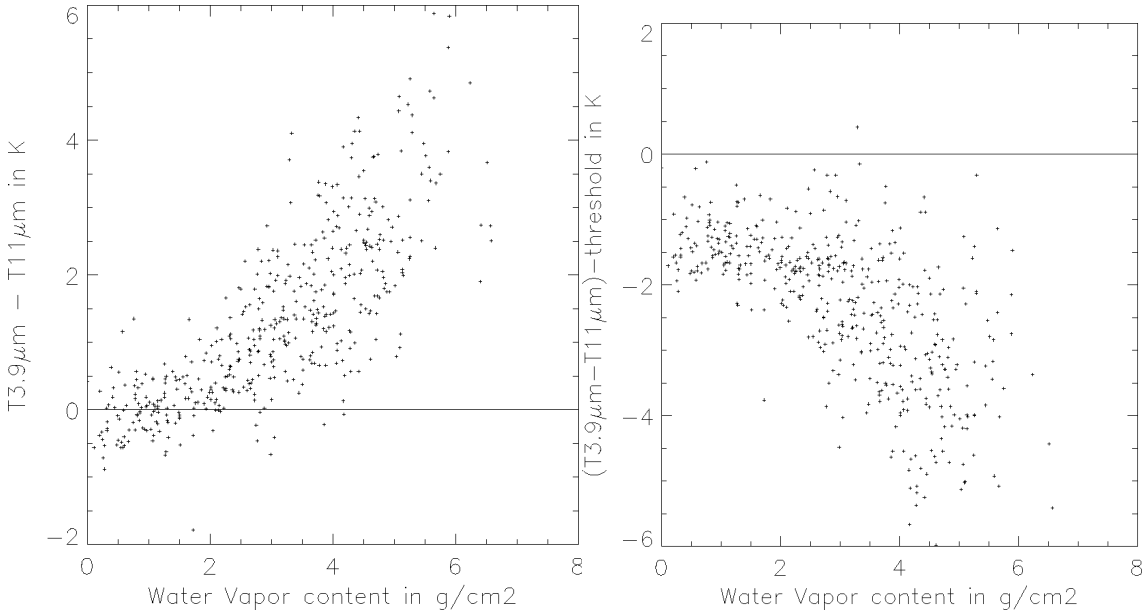

Figure 1.3.3.5.1 For GOES oceanic cloud free targets :Left : variation of T3.9µm-T11µm with water vapour content. Right : comparison of T3.9µm-T11µm and the associated threshold.

1.3.3.5.3.Threshold computation over land

In the AVHRR prototype, the threshold is a constant value depending on the season (from 3.5°C in winter up to 5°C in summer) whereas it is a function of satellite zenith angle, water vapour content and forecast surface temperature in the GOES prototype.

In the GOES prototype, two pre-computed tables are used, that have been elaborated by applying RTTOV to radio-soundings from the TIGR dataset, using a constant emissivity of 0.98 in both channel (i.e., valid for vegetated areas). One table is used for cold grounds conditions [the surface temperature used in the RTTOV simulations has been assumed layer be colder than the air of the lowest layer by 3°C] ; the second table is used for warm grounds condition [the surface temperature used in the RTTOV simulation has been assumed be equal to the air of the lowest layer]. The satellite zenith angle and the water vapour content are used to interpolate in these tables, whereas the forecast surface temperature allows to interpolate between the two tables.

The quality of the threshold is illustrated on figure 1.3.3.5.2, using the GOES interactive test file. The large scatter of T39µm-T11µm difference (especially at high water vapour content) is not accounted for by the threshold.

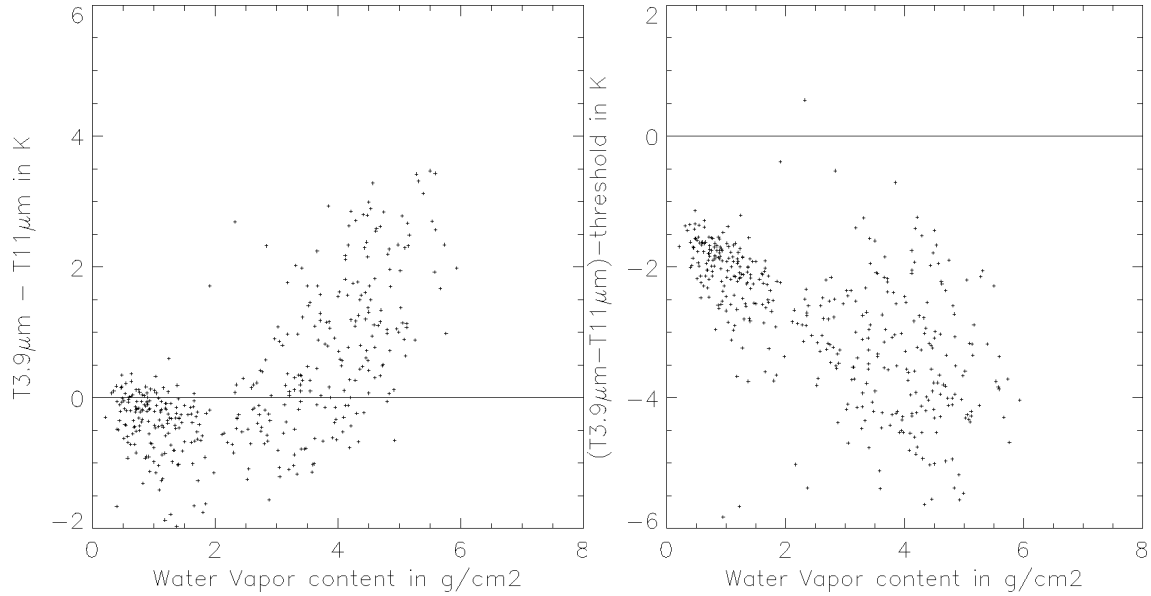

Figure 1.3.3.5.2 For GOES continental cloud free targets :Left : variation of T3.9µm-T11µm with water vapour content. Right : comparison of T3.9µm-T11µm and the associated threshold.

1.3.3.6. Test on R0.6µm or R0.9µm

1.3.3.6.1. Aim of the test

The test is the following :

A pixel is classified as cloud contaminated if :

- R0.6µm > R0.6threshold. (0.9µm channel is used over sea in AVHRR prototype).

This test applied to the visible (0.6µm) or near-infrared (0.9µm) TOA reflectances aims to detect clouds having a reflectance higher than the underlying surfaces.

The visible or near-infrared reflectance measured over the cloud-free oceans mainly corresponds to Rayleigh and aerosol scattering (weaker in the near-infrared band) and to the solar reflection over the ocean, which is very low apart from sunglint conditions, and in turbid areas (for the visible channel only). Therefore 0.9µm reflectance should be preferably used over the ocean (but not available in GOES imagery).

As the cloud-free land reflectance is usually much higher in the near-infrared wavelength than in the visible (due to the vegetation spectral radiative behaviour at these two wavelengths), the test is therefore applied to the visible channel. To make it efficient, it is necessary to near the TOA reflectances of the underlying land or sea surface, by accounting for surface bi-directional effects, atmospheric effects and land spectral characteristics.

1.3.3.6.2.Threshold computation over sea

The threshold is computed from the simulation of the ocean TOA reflectance by adding an offset.

The TOA reflectance is simulated as :

TOA Reflectance = a0 + a1*surface/(1-a2*surface) where :

- a0, a1 and a2 are coefficients computed from satellite and solar angles, water vapour and ozone content using a very fast model based on 6S (see A.4.2)
- surface is the oceanic surface reflectance computed using Cox & Munck theory (see Cox & Munck, 1954).

A maritime aerosol of 70km horizontal visibility is assumed (thicker aerosol leads to an overestimation of the reflectance especially for large zenith angles). For the oceanic surface reflectance, we compute the maximum reflectance given by the Cox & Munck model, for the satellite and solar angles and for wind speed between 0 and 20 m/s : this approach overestimates the reflectance in sunglint conditions.

The dependence of simulated TOA oceanic reflectance on the viewing geometry is shown in figure 1.3.3.6.1. The simulation accuracy is illustrated with the GOES interactive file on figure 1.3.3.6.3. Reflectances are obviously overestimated in sunglint conditions, due to the lack of information on wind speed and direction ; the simulation is rather accurate in the backward scatter direction (less than 2-3 % overestimation, up to 5% for large zenith angles).

An offset of 5% is applied in the AVHRR prototype to account for the calibration inaccuracy (pre-launch calibration coefficients are used), whereas the offset used for GOES images (7% in coastal regions, 4% elsewhere) accounts for relatively high turbid waters reflectances at 0.6µm. The GOES pixels containing less than 50% land are considered as oceanic pixels and could be flagged as cloudy by the visible test : these misclassifications are in fact not so numerous, thanks to the use of a 7% offset in coastal regions.

1.3.3.6.3.Threshold computation over land

The threshold is computed from the simulation of the land TOA reflectance by adding an offset.

The TOA reflectance is simulated as :

TOA Reflectance = a0 + a1*surface/(1-a2*surface) where :

- a0, a1 and a2 are coefficients computed from satellite and solar angles, water vapour and ozone content using a very fast model based on 6S (see A.4.2)
- surface is the land surface reflectance computed from a monthly climatological visible reflectance value (see A2.1.4) using a model developed by Roujean (see Roujean et al., 1992) to simulate the bi-directional effects.

A continental aerosol of 70km horizontal visibility is assumed (thicker aerosol leads to an overestimation of the reflectance especially for large zenith angles). For the land surface bi-directional effects, we use the model of Roujean with 2 sets of coefficients that have been derived empirically [(k1=0.15, k2=1.0) for low reflectance and (k1=0.05, k2=0.5) for highly reflective areas].

The dependence of simulated TOA continental reflectances with the viewing geometry is shown in figure 1.3.3.6.2. The simulation accuracy is illustrated with the GOES interactive file on figure 1.3.3.6.4. The difference between the simulated and the measured reflectances presents a higher scatter than over the ocean. The simulation overestimates the reflectances generally by less than 5% (up to 10% for high zenith angles). Moreover, a slight trend is observed with the climatological visible reflectance, and may be related to the choice of coefficients used in the model of Roujean.

An offset of 8% is applied in the AVHRR prototype to account for the calibration inaccuracy (pre-launch calibration coefficients are used) and inaccuracy of the visible reflectance climatology. In the GOES prototype, an offset of 8% accounts for the inaccuracy of the visible reflectance climatology, but also for the larger filter of the visible channel (up to 0.8µm for GOES-11) which makes this channel slightly more sensitive to vegetation than the AVHRR visible channel (from which the climatological visible map has been derived).

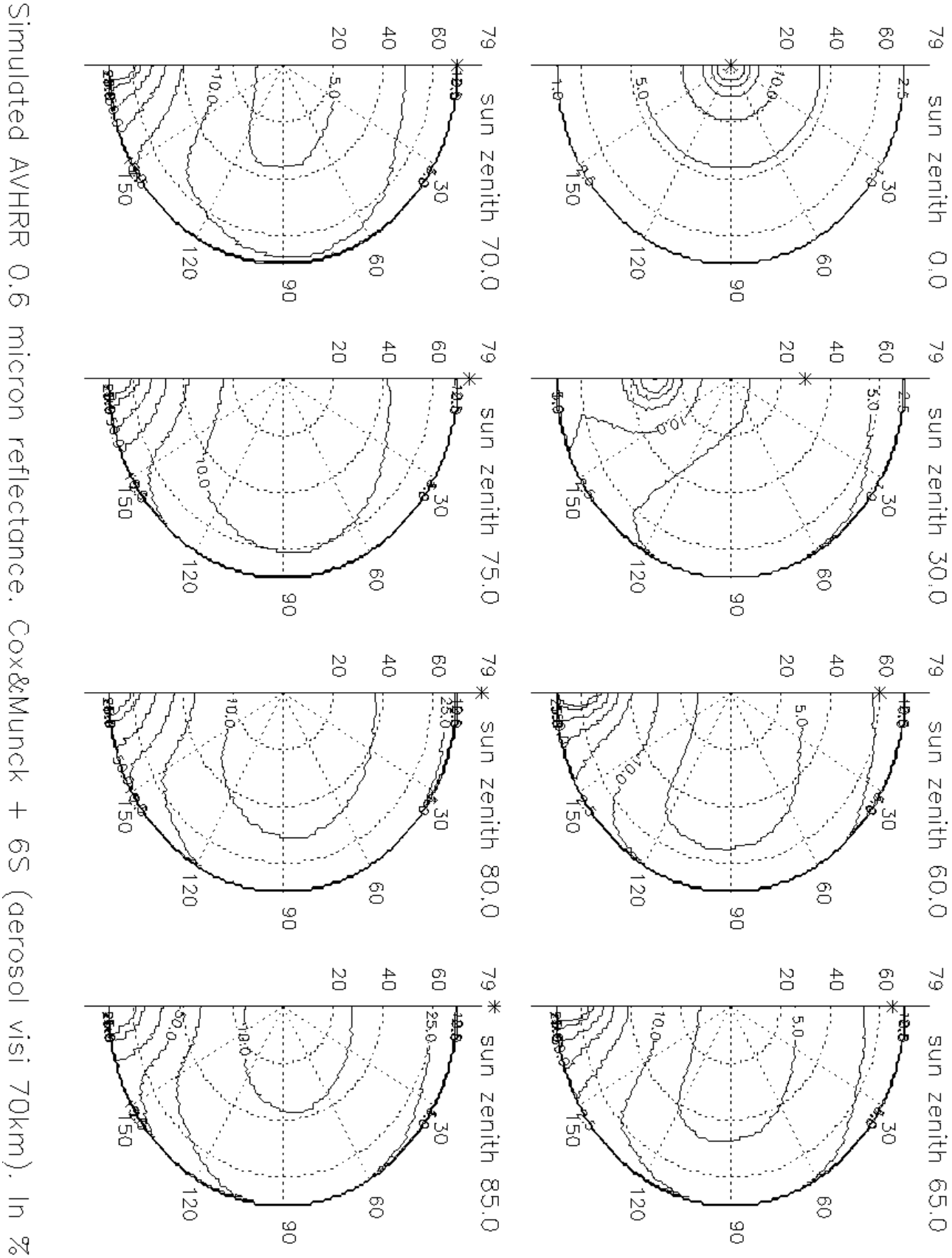

Figure 1.3.3.6.1 Sea Top Of Atmosphere AVHRR 0.6µm reflectance simulated using Cox & Munck model and 6S model (maritime aerosol 70km visibility).

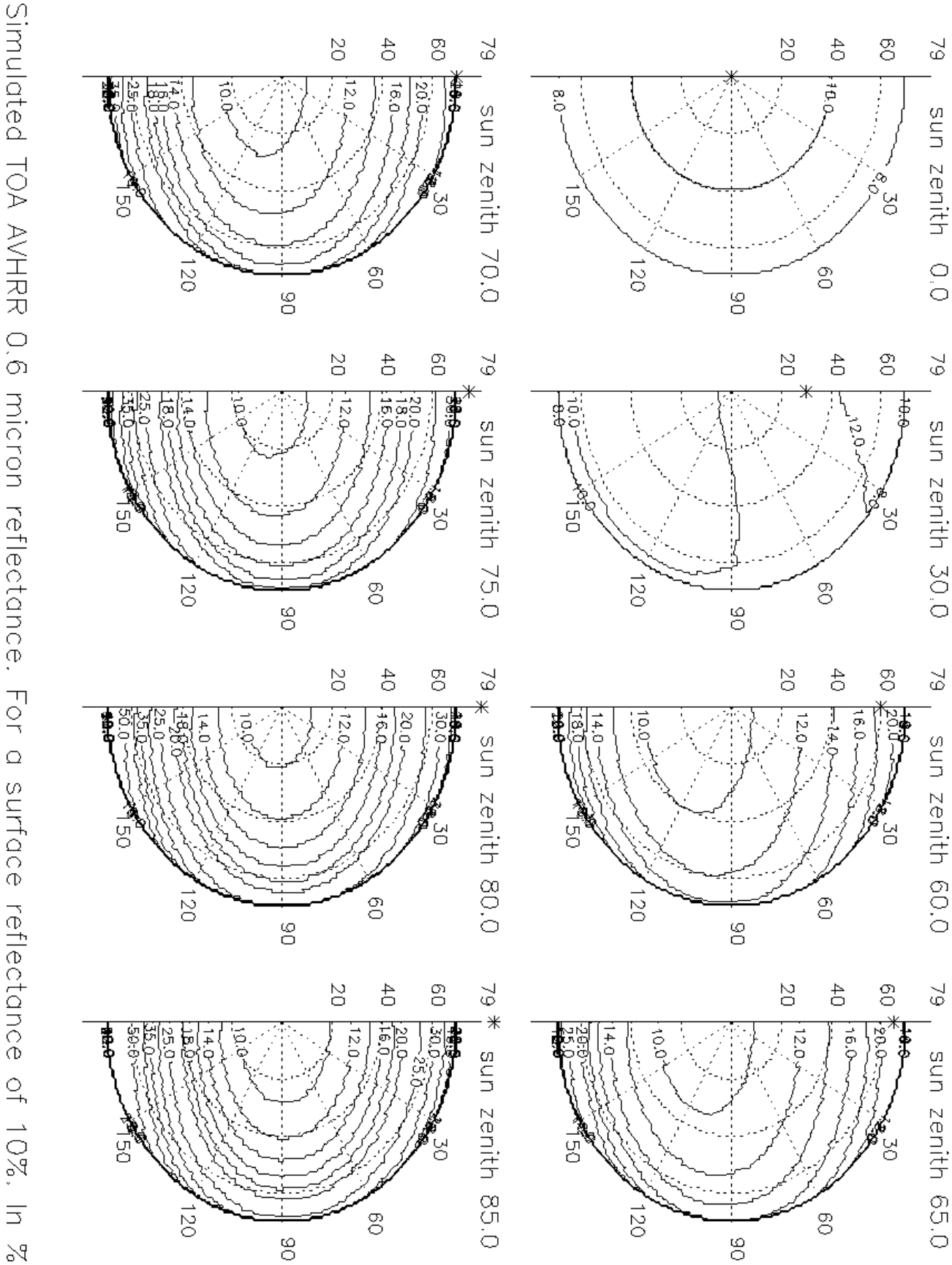

Figure 1.3.3.6.2 Land Top Of Atmosphere AVHRR 0.6µm reflectance simulated using Roujean model and 6S model (continental aerosol 70km visibility). For a continental surface of 10% climatological surface reflectance

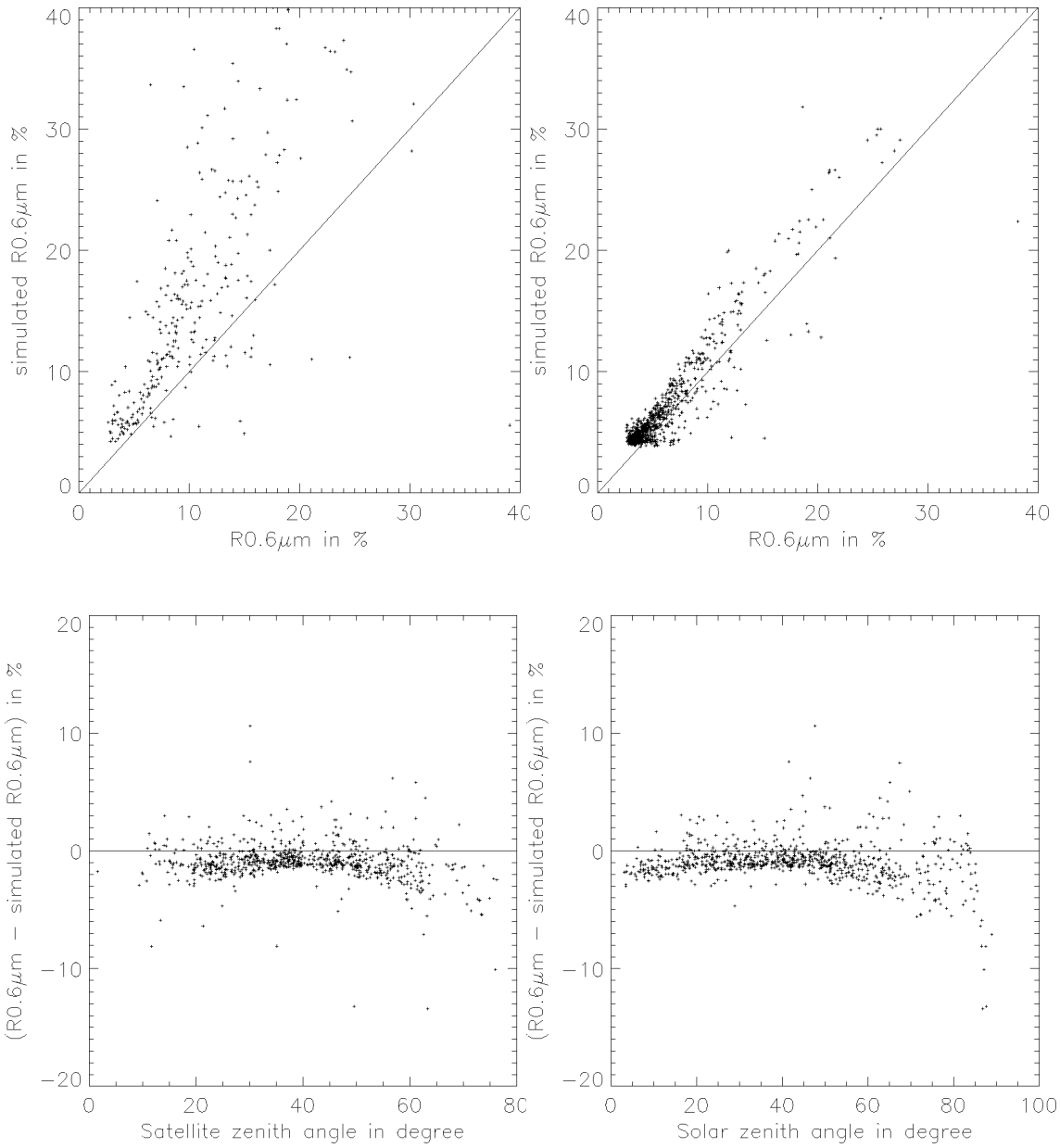

Figure 1.3.3.6.3 Illustration of the accuracy of simulated TOA 0.6µm reflectance over sea using GOES interactive test file. Top left : in forward scattering direction. Top right and bottom : backward scattering direction. GOES visible reflectances are computed using updated calibration coefficients.

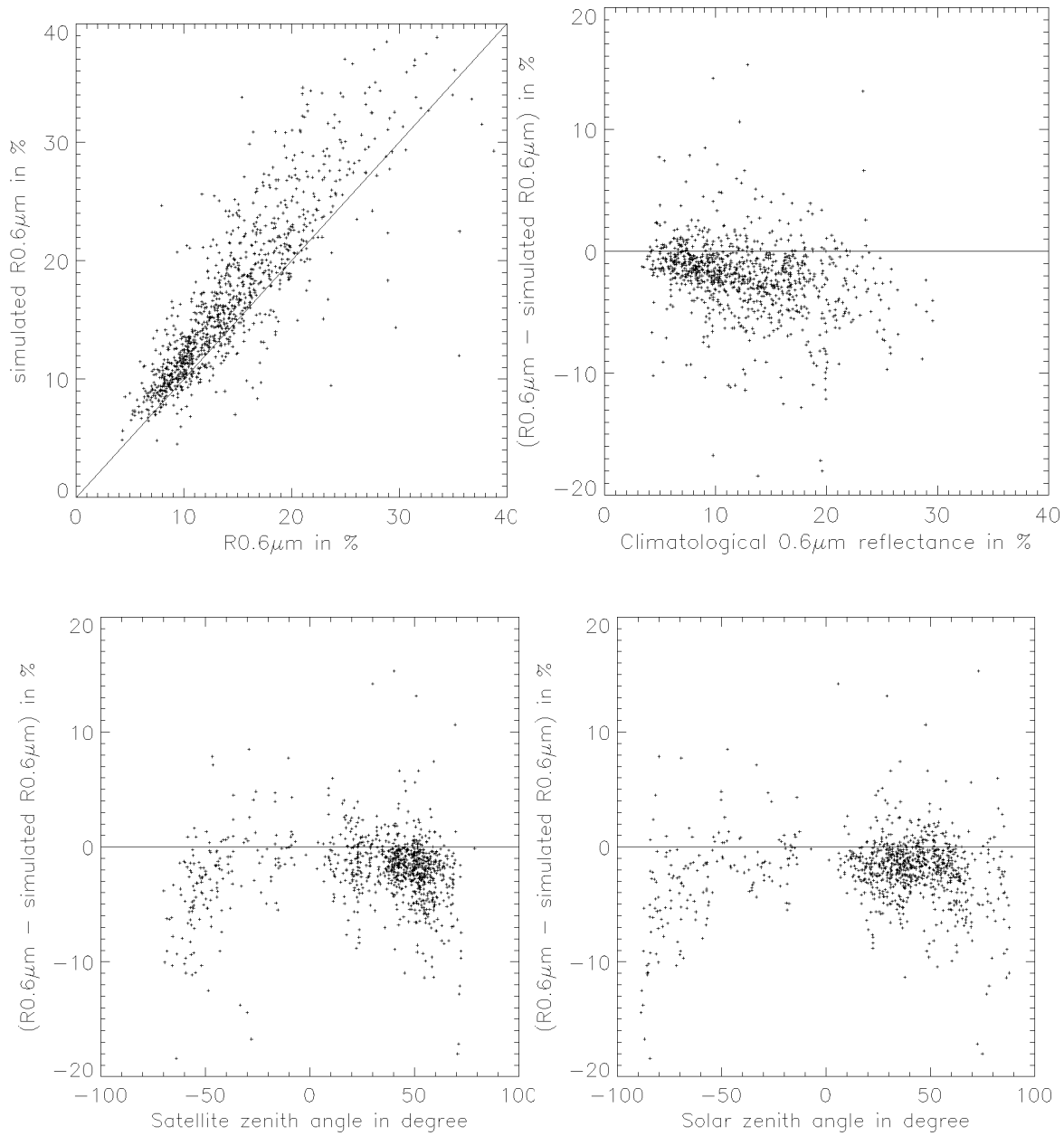

Figure 1.3.3.6.4 Illustration of the accuracy of simulated TOA 0.6µm reflectance over land using GOES interactive test file. Negative solar or satellite zenith angles corresponds to forward scatter direction (positive for backward scatter direction). GOES visible reflectances are computed using updated calibration coefficients

1.3.3.7. Low Cloud Test in Sunglint

1.3.3.7.1. Aim of the test

As shown in 1.3.3.6, low clouds can easily be detected at daytime over the ocean by their high visible (R0.6μm) or preferably near-infrared (R0.9μm) reflectances. This is not possible in case of sunglint, because the sea reflectance at these wavelengths may then be higher than that of clouds. The use of both 0.6μm (alternatively 0.9μm) and 3.9μm channels allows to detect low clouds even in areas affected by sunglint. Indeed, oceanic areas with high 0.6μm reflectances have also very high 3.9μm reflectances, which is usually not the case for low clouds. One difficulty of this test is that the thermal part of the 3.9μm radiance must be removed to get access to the reflectance. The rapid saturation of the 3.9μm radiance also limits the use of this test in case of strong sunglint (frequent in AVHRR imagery).

1.3.3.7.2.Delineation of areas affected by sunglint

The theory developed by Cox and Munck (see Cox & Munck, 1954) allows to estimate the sea bi-directional reflectance (at any wavelength) as a function of wind speed, of satellite and viewing geometry. The area that may be affected by sunglint is determined as a function of satellite and solar angles. We assume that sunglint is possible if the simulated R0.6μm reflectance, for wind speed between 0m/s and 20m/s) is less than 10% and if the solar elevation is higher than 15 degrees.

1.3.3.7.3.Description of the test

A convenient way to estimate the solar contribution in the 3.9μm channel in case of sunglint is to use (T3.9μm-T11μm)/cos(θ_{sol}). Figures 1.3.3.7.1 and 1.3.3.7.2 illustrates the efficiency of using R0.6μm and (T3.9μm-T11μm) /cos(θ_{sol}) to detect low clouds in sunglint areas, both with AVHRR and GOES imagery. A sharper increase of (T3.9μm-T11μm) /cos(θ_{sol}) with R0.6μm for oceanic areas affected by sunglint is observed in the AVHRR interactive test file. This different behaviour, which can be simulated using Cox and Munck theory, the Planck function at 3.9μm and an atmospheric simulation at 0.6μm (see figure 1.3.3.7.3), seems to be related to the different sun-satellite geometry available in the AVHRR and GOES interactive test file [note that GOES targets are chosen in slots 12, 24, 36 and 48 only, and sunglint conditions may therefore not be adequately sampled in the GOES interactive test file].

Finally, the following test (applied only if the sun elevation is higher than 15 degrees) has been implemented both in the AVHRR and GOES prototype :

A pixel is classified as cloud contaminated if :

- T3.9μm < 320K (to make sure 3.9μm is not saturated)
- R0.6μm > 20%
- (T3.9μm-T11μm)/cos(θ_{sol}) > 16 °C
- R0.6μm > slope*(T3.9μm-T11μm)/cos(θ_{sol}) for GOES and
  R0.9μm > slope*(T3.9μm-T11μm)/cos(θ_{sol}) for AVHRR

where θ_{sol} is the solar zenith angle, and
slope is a parameter value linked with the sun-satellite geometry (0.8 for GOES and 2 for AVHRR).

Note that a more accurate test should include a computation of the slope using the sun and satellite geometry, not performed in the prototypes. We could also consider to compute the 3.9μm reflectivity (Ruff and Gruber, 1983).

In the GOES prototype where the sunglint is not very strong, this test did not prove very efficient to detect low clouds, because they were usually identified by the other tests.

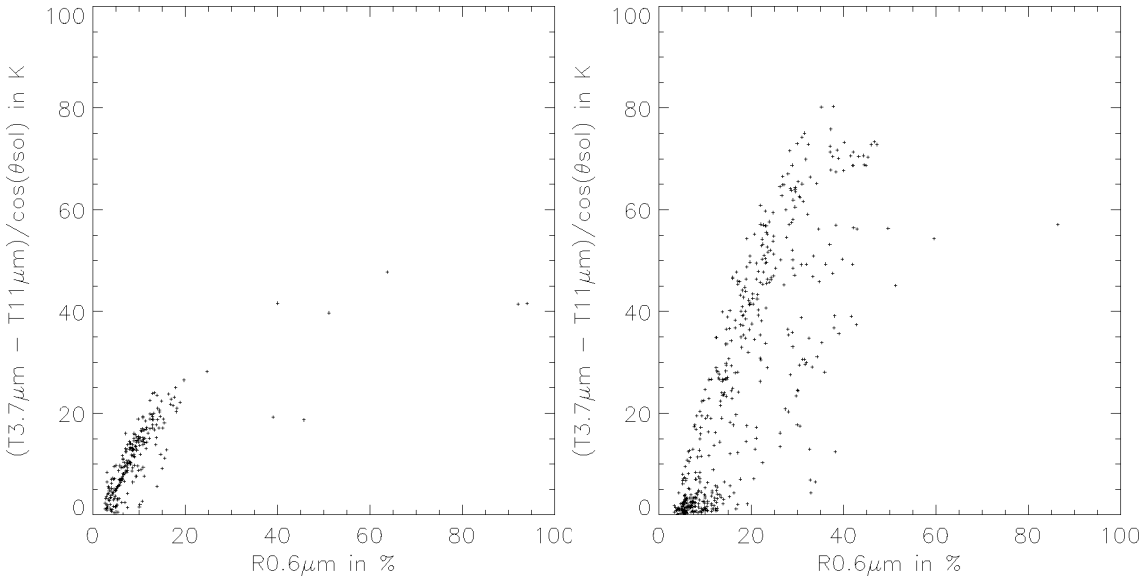

Figure 1.3.3.7.1 Dependency of (T3.9µm-T11µm) /cos(θ_{sol}) on R0.6µm for sunglint areas.GOES (left) and AVHRR (right).

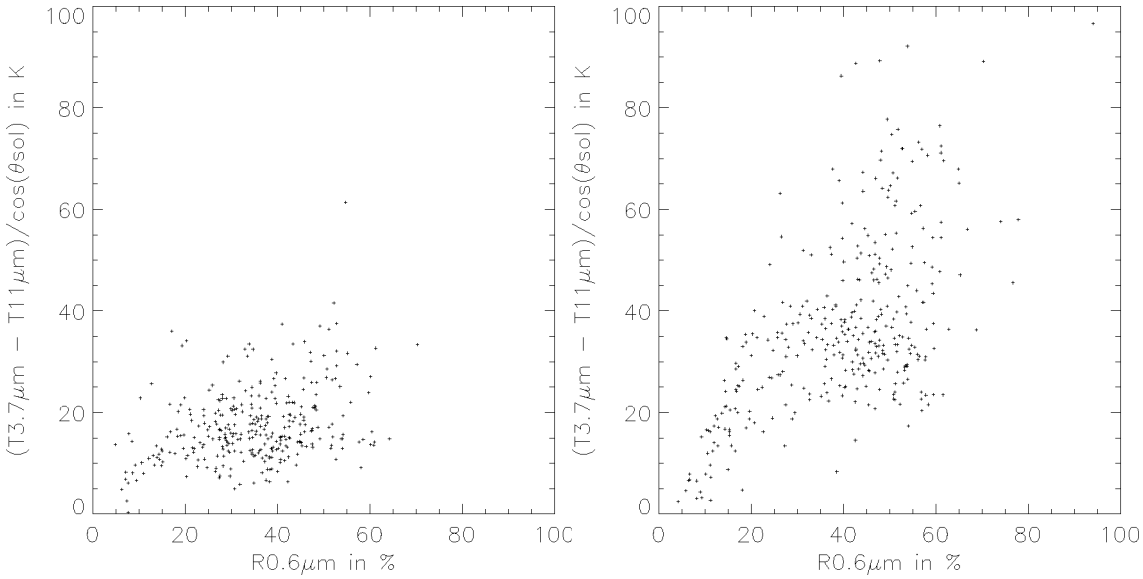

Figure 1.3.3.7.2 Dependency of (T3.9µm-T11µm) /cos(θ_{sol}) with R0.6µm for low clouds.GOES (left) and AVHRR (right).

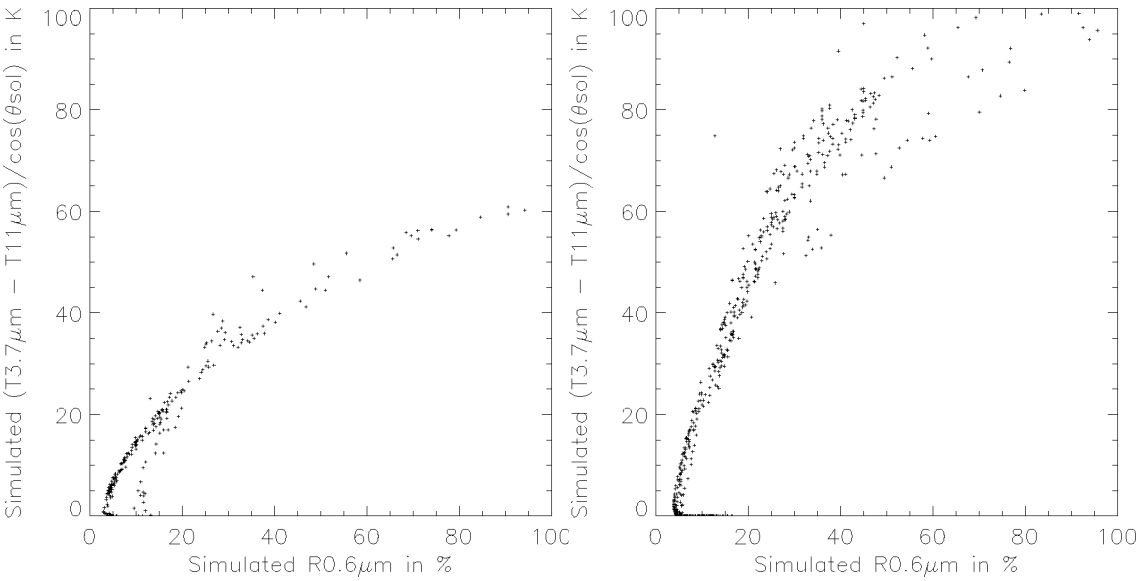

Figure 1.3.3.7.3 Simulation of (T3.9µm-T11µm) /cos(θ_{sol}) vs R0.6µm for sunglint areas.GOES (left) and AVHRR (right).

1.3.3.8. Snow or Ice detection Test

1.3.3.8.1. Aim of the test

Ice or snow appear rather cold and bright, and may therefore be confused with cloud (especially with low clouds) during the cloud detection process. A test, which detects pixels contaminated by snow or ice, has been developed and is the first applied in the daytime cloud detection process : if this test is satisfied, the pixels are classified as snow or ice and no further cloud detection is attempted.

The basis of this test, restricted to daytime conditions, is the following :

- Snow & ice are distinguished from water clouds by their low reflectance at 1.6 µm (not available on GOES) or at 3.9 µm.
- Snow & ice are separated from cloud free oceanic or continental surfaces by their higher R0.6µm visible reflectance and slightly colder T11µm brightness temperature.
- T11µm - T12µm brightness temperature difference helps to discern cirrus from snow or ice.
- R0.9µm (not available on GOES) is useful to separate shadows from snow or ice.

The use of 3.9µm reflectance is complicated, because :

- the computation of the 3.9µm reflectance is not accurate, as the thermal part of the 3.9µm radiance must first be removed.
- low 3.9 µm reflectance may be observed also in low clouds.

1.3.3.8.2.Snow or ice detection test using 3.9µm

The most important feature of the test is the low reflectivity of snow and ice covers at 3.9µm. This reflectivity ρ3.9µm can be computed as (see Ruff and Gruber, 1983):

$$\rho 3.9\mu m = (Planck(T3.9\mu m) - Planck(T11\mu m)) / ((Fsol/\pi)*\cos(\theta sol) - Planck(T11\mu m)),$$

where : Planck is the Planck function for the 3.9µm channel,
θsol is the solar zenith angle and
Fsol is the solar flux in the 3.9µm channel.

This approximation assumes a lambertian pixel without transmittance, no atmospherical effects, and an emissivity at 11µm equal to unity. For example, this is not true for cirrus clouds.

A convenient (and popular) way to estimate the solar contribution in the 3.9µm channel is to use the brightness temperatures differences corrected from solar elevation : (T3.9µm-T11µm)/cos(θsol), which may be approximated (with the same assumption and notation as previously) as :

$$(T3.9\mu m - T11\mu m) = Planck^{-1} [\rho 3.9\mu m * (Fsol/\pi)*\cos(\theta sol) + (1-\rho 3.9\mu m)*Planck(T11\mu m)] - T11\mu m$$

This equation allows to understand why the strong non-linearity of the Planck function at 3.9µm will affect the use of this difference to estimate the solar contribution in the 3.9µm channel. The impact of T11µm is illustrated on figure 1.3.3.8.1

The effectiveness of both features is illustrated with the interactive test file on figures 1.3.3.8.2 and 1.3.3.8.3 : (T11µm-T39µm)/cos(θsol) is efficient to detect snow & ice, and misclassify rather few clouds as snow/ice (provided that the sun elevation is not too low). The use of ρ3.9µm allows a better identification of snow & ice, but more clouds are then misclassified, especially cirrus clouds for which the assumptions used when computing ρ3.9µm are not satisfied.

An additional thresholding of T11µm, T11µm - T12µm, R0.6µm and R0.9µm (for AVHRR only) is applied to separate snow or ice from cloud free surfaces, cirrus clouds, shadows. The thresholds have been empirically set up using the interactive test file.

Finally, the following snow and ice detection test (applied only if the sun elevation is larger than 20 degrees) has been implemented both in the AVHRR and GOES prototype :

A pixel is classified as contaminated by snow if :

- (T3.9µm-T11µm)/cos(θsol) < 15°C
- (T11threshold - 5°C) < T11µm < 4°C
- T11µm-T12µm < 2°C
- R0.6threshold < R0.6µm
- 20% < R0.9µm (only in AVHRR prototype)

where T11threshold and R0.6threshold are thresholds previously described in 1.3.3.2 and 1.3.3.6, and θsol is the solar zenith angle.

A pixel is classified as contaminated by ice if :

- Climatological SST < 4°C
- (T3.9µm-T11µm)/cos(θsol) < 15°C
- (T11threshold - 5°C) < T11µm < 4°C
- T11µm-T12µm < 2°C
- R0.6threshold < R0.6µm
- 20% < R0.9µm (only in AVHRR prototype)

where T11threshold and R0.6threshold are thresholds previously described in 1.3.3.2 and 1.3.3.6, and θsol is the solar zenith angle.

The efficiency of snow and ice detection attempted only when sun elevation is larger than 20 degrees and estimated using the GOES interactive test file can be assessed though the following figures:

- 1.7% of cloudy pixels are confused with snow, whereas 5% of snowy pixels are not detected.
- less than 1% of cloudy pixels are confused with ice, whereas 15% of icy pixels are not detected.

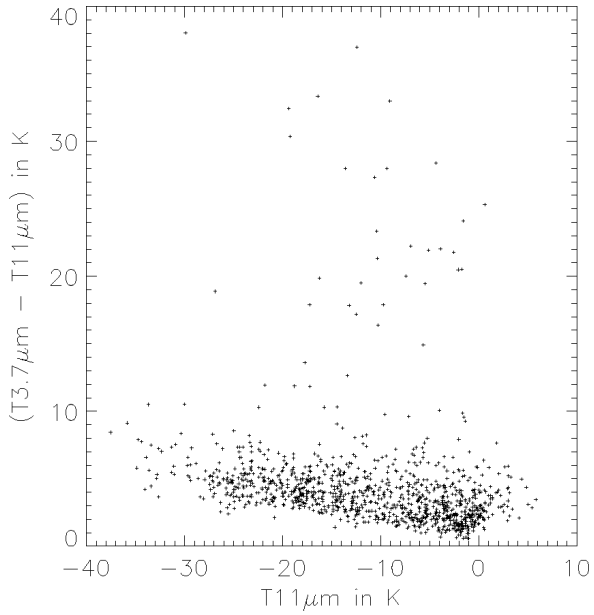

Figure 1.3.3.8.1 (T3.9µm-T11µm) as a function of T11µm. For GOES ice & snow targets.

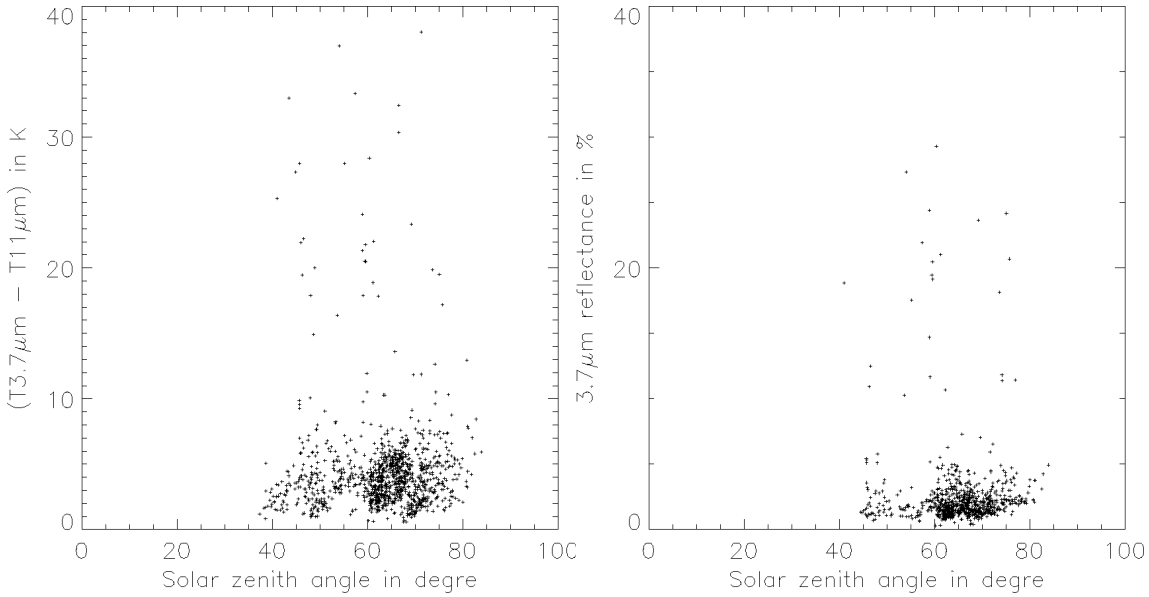

Figure 1.3.3.8.2 (T3.9µm-T11µm) and ρ3.9µm as a function of solar zenith angle.
For GOES ice & snow targets.

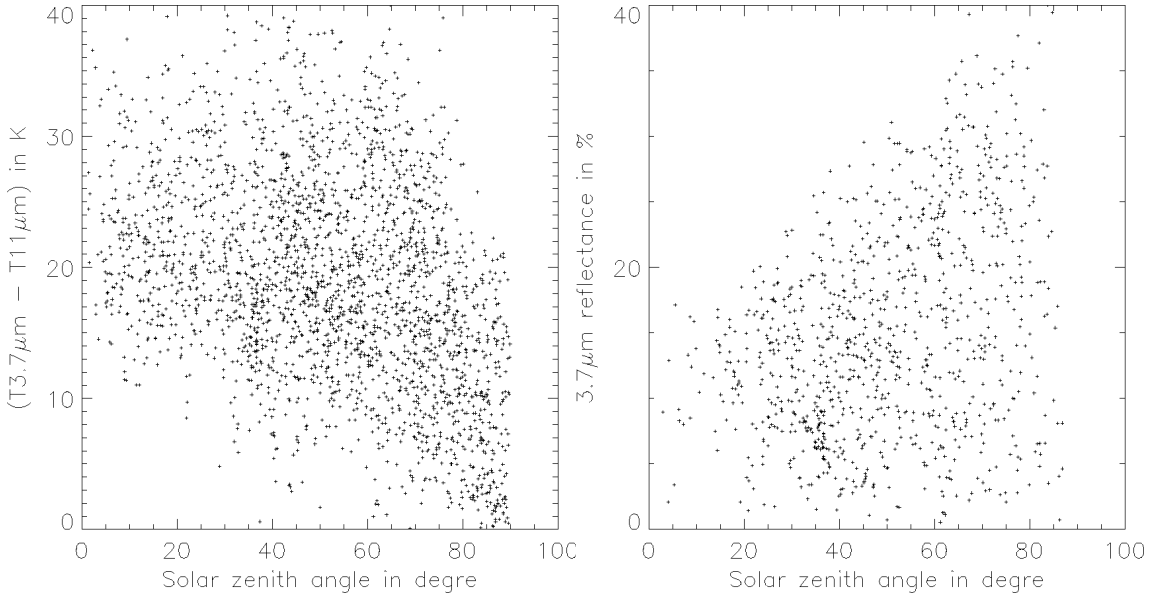

Figure 1.3.3.8.3 (T3.9µm-T11µm) and ρ3.9µm as a function of solar zenith angle.
For GOES cloudy targets.

1.3.3.8.3.Snow or Ice detection test using1.6µm

Ice and snow have low reflectance at 1.6µm (except in sunglint conditions), which is usually not the case for water clouds, but for broken small cumulus cloud covers. This is illustrated with the AVHRR interactive file on figures 1.3.3.8.4 and 1.3.3.8.5. Surface snow reflectances have been tabulated for various viewing geometries and for hexagonal particle shape (3 different sizes) with the radiative transfer model developed by C.Le Roux (see Le Roux et al, 1996). Top of Atmosphere snow reflectance at 1.6µm are then computed using these tables (250µm hexagonal particles have been retained) together with a module (based on 6S) to simulate the atmospheric effects, and plotted

on figure 1.3.3.8.6. The relatively high 1.6µm reflectances of snow in sunglint conditions are rather well simulated, as shown on figure 1.3.3.8.7. The threshold applied to the 1.6µm channel is derived from this simulation by adding an offset (5%).

An additional thresholding of T11µm, T11µm - T12µm, R0.6µm and R0.9µm is applied to separate snow or ice from cloud free surfaces, cirrus clouds, shadows. The thresholds used have been empirically set up using the interactive test file.

Finally, the following snow and ice detection test (applied only if the sun elevation is larger than 20 degrees) has been implemented in the AVHRR prototype :

A pixel is classified as contaminated by snow if :

- (R1.6µm) < R1.6threshold
- (T11threshold - 5°C) < T11µm < 4°C
- T11µm-T12µm < 2°C
- R0.6threshold < R0.6µm
- 20% < R0.9µm

where R1.6thrshold is the threshold described above, T11threshold and R0.6threshold are thresholds previously described in 1.3.3.2 and 1.3.3.6, and θsol is the solar zenith angle.

A pixel is classified as contaminated by ice if :

- Climatological SST < 4°C
- (R1.6µm) < R1.6thrshold
- (T11threshold - 5°C) < T11µm < 4°C
- T11µm-T12µm < 2°C
- R0.6threshold < R0.6µm
- 20% < R0.9µm

where R1.6thrshold is the threshold described above, T11threshold and R0.6threshold are thresholds previously described in 1.3.3.2 and 1.3.3.6, and θsol is the solar zenith angle.

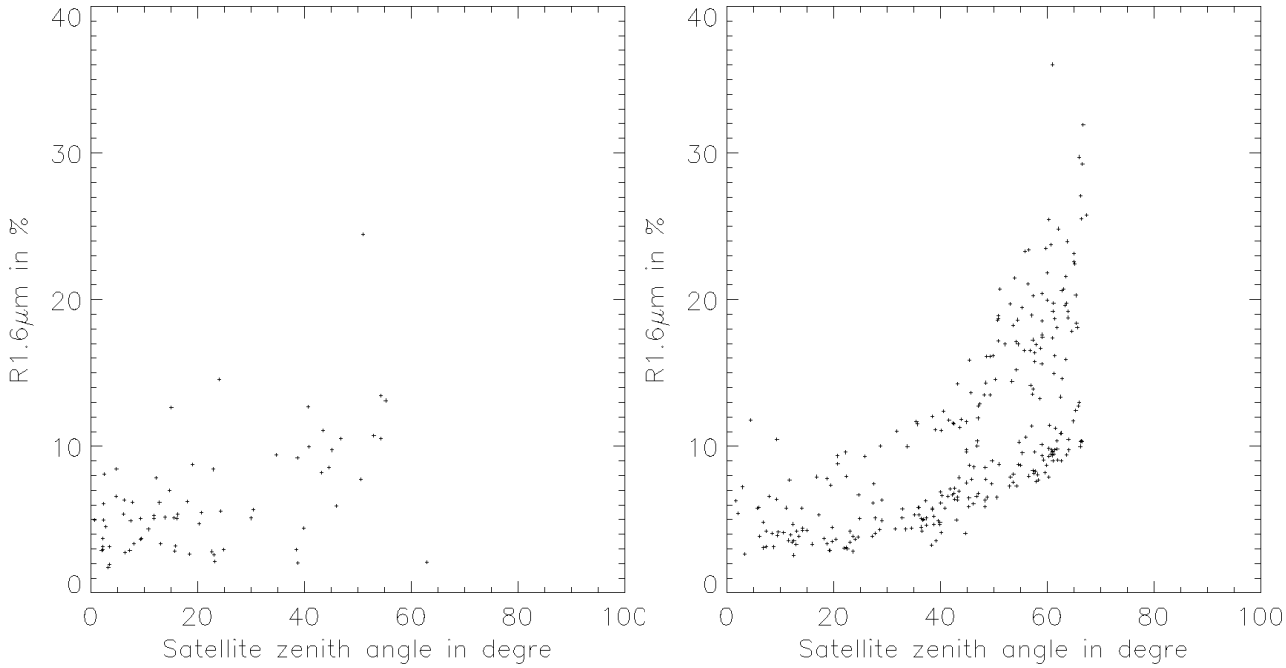

Figure 1.3.3.8.4 R1.6µm as a function of satellite zenith angle.
Left : backward scattering direction ; Right : forward scattering direction.
For AVHRR ice and snow targets.

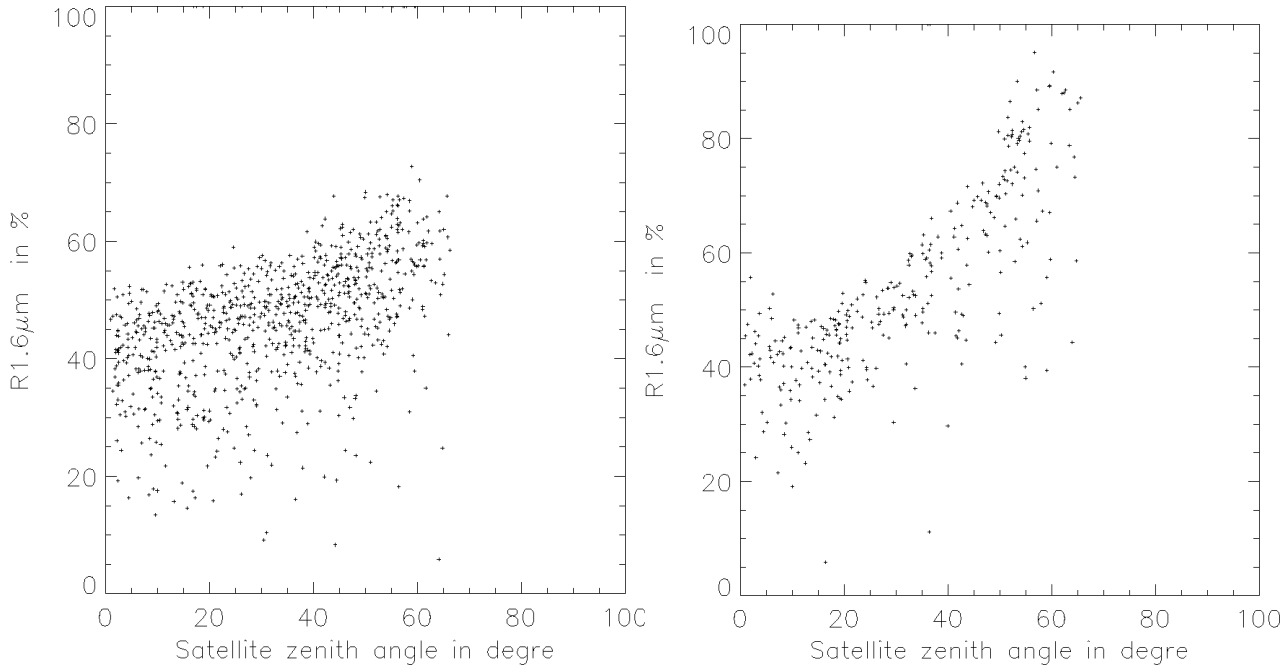

Figure 1.3.3.8.5 R1.6µm as a function of satellite zenith angle.
Left : backward scattering direction ; Right : forward scattering direction.
For AVHRR stratus and stratocumulus clouds.

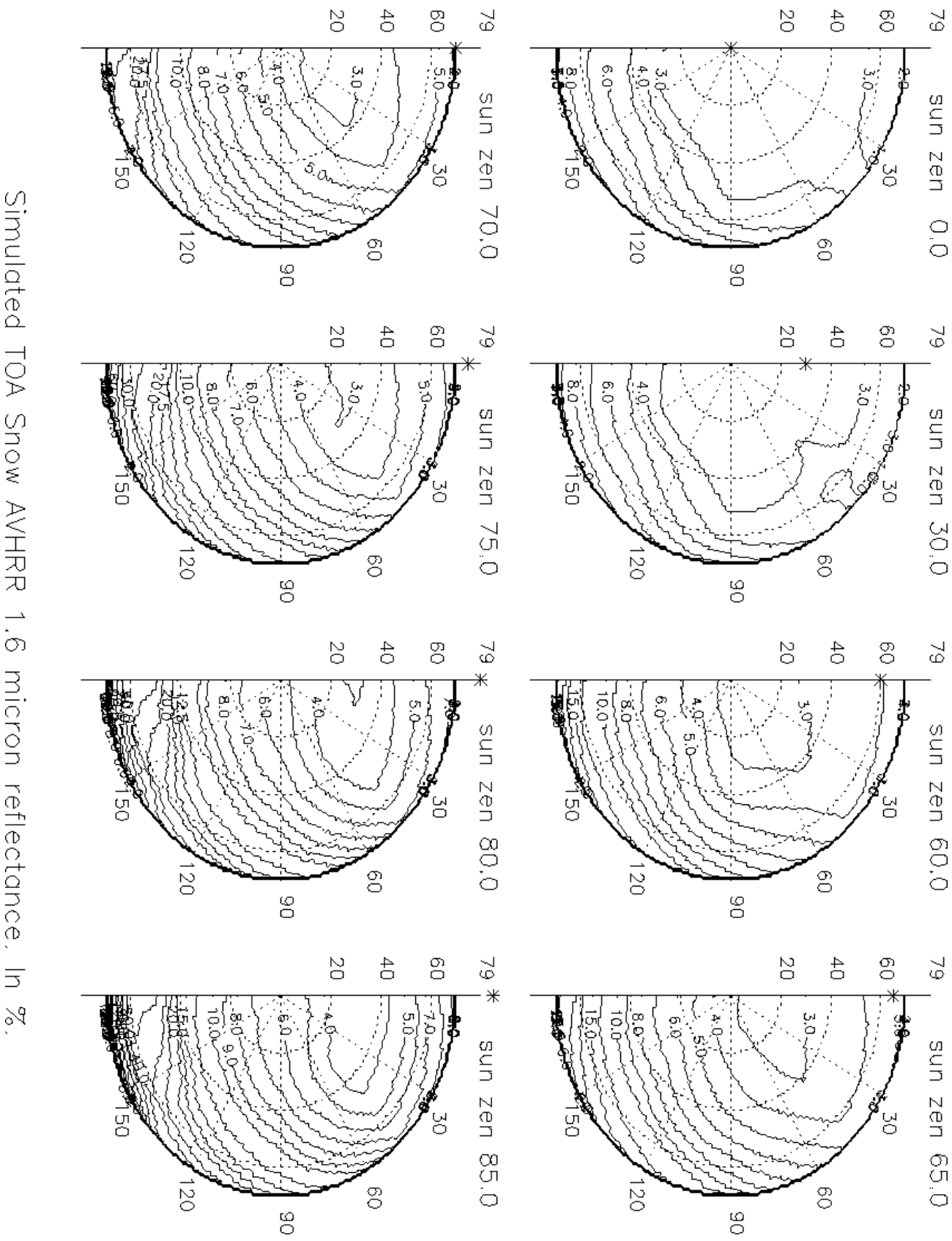

Figure 1.3.3.8.6 Snow Top Of Atmosphere AVHRR 1.6µm reflectance simulated using Le Roux model (250µm hexagonal particles) and 6S model (continental aerosol 70km visibility).

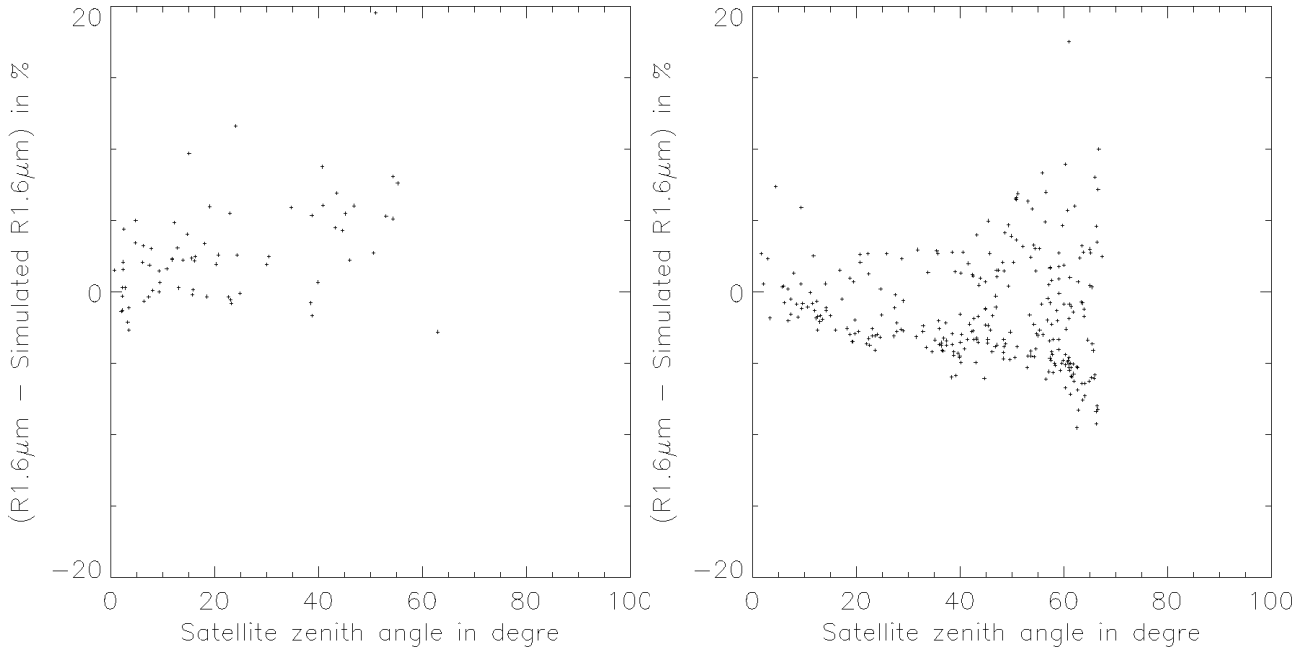

Figure 1.3.3.8.7 Illustration of the accuracy of simulated TOA 1.6µm reflectance over snow & ice using AVHRR interactive test file. In backward (left) and forward (right) scatter direction.

1.3.3.9. Spatial Coherence Tests

1.3.3.9.1. Aim of these tests

These tests detect small broken clouds, thin cirrus or cloud edges, by using their high spatial variations in the visible, near infrared or infrared channels. The difficulty comes from the natural heterogeneity of the surface background : Oceanic areas are rather homogeneous, with the exception of strong thermal fronts (large T11µm variation), turbid coastal areas (large R0.6µm variation), sunglint areas (large R0.6µm and R0.9µm variation) ; Land surfaces are generally much more inhomogeneous, especially in mountainous or desertic regions. The simultaneous analysis of spatial coherency in two spectral bands allows to overcome the difficulty .

- Over Ocean, the combined use of T11µm & T11µm-T39µm for all illumination conditions, and of T11µm & R0.6µm at daytime, is efficient for detecting clouds, and avoids misclassification of turbid areas or thermal front.
- Over land, the combined use of T11µm & T11µm-T39µm for all illumination conditions allows to minimise misclassification, except in very mountainous or in arid areas.
- Continental areas at daytime may present as large R0.6µm, R0.9µm and T11µm horizontal differences as clouds do. But, a cloud-free surface having higher R0.6µm than the neighbourhood is less vegetated and therefore warmer, whereas a pixel contaminated by clouds and having higher R0.6µm than its neighbours should be more cloud contaminated, and therefore colder. This property, not observed in arid areas, is used at daytime over land in the Spatial Coherence Test.

In practice, the Spatial Coherence technique is applied in a 3*3 box surrounding the current pixel.

1.3.3.9.2.Implementation in the AVHRR prototype

In the AVHRR prototype, this technique has only been applied over the ocean, using the T11µm channel with a constant threshold (0.2 °C) :

A pixel is classified as cloud contaminated if :
- SD(T11µm) > SD11threshold. (SD stands for standard deviation)

It obviously leads to misclassification of most of the marine thermal fronts as clouds.

1.3.3.9.3.Implementation in the GOES prototype

The Spatial Coherence technique taking into account the above mentioned remarks has been implemented in the GOES prototypes. As highly heterogeneous cloud free areas such as oceanic thermal fronts have not been specifically included in the interactive test file, the thresholds have been empirically determined using not only the interactive test file, but also full images.

The local standard deviations (denoted SD) of T11µm ,T11µm-T39µm and R06µm are computed for every pixel, using the 8 surrounding pixels image (provided they correspond to the same surface type, i.e. sea or land) :

A pixel is classified as cloudy if :
- SD(T11µm) > SD11threshold and SD(T11µm-T39µm) > SDT11T39threshold over sea and land
- SD(T11µm) > SD11threshold and SD(R0.6µm) > SDT11R0.6threshold over sea at daytime only

This process is not applied in very mountainous or arid regions ; moreover T11µm-T39µm is not used in too cold areas (due to noise effects).

	Thresholds applied to SD(T11µm)	**Thresholds applied to SD(T11µm-T39µm)**	**Thresholds applied to SD(R06µm)**
Land	from 1°C (nighttime) up to 2°C (daytime)	from 1°C (nighttime) up to 2°C (daytime)	Specific test described below.
Sea	0.4°C	0.5°C	0.5%

Table 1.3.3.9.1 Local standard deviation's thresholds

Over land at daytime, the maximum difference between the visible reflectance of a pixel and its eight neighbours (DR0.6µm), and the corresponding T11µm brightness temperature difference (DT11µm) are retained for every pixel, and the ratio R=(DT11µm) / (DR0.6µm) is then computed.

A pixel is classified as cloudy if :

- DR0.6µm > f(DT11µm) / (DR0.6µm) over land (except arid areas) at daytime only

The f(R) function, which is tabulated on the next table, has been derived empirically using the interactive test file.

R=(DT11µm) / (DR0.6µm)	-5	-3	0	0.25	0.5	1
Threshold applied to (DR0.6µm)	2%	2%	5%	10%	15%	15%

Table 1.3.3.9.2 Threshold applied to (DR0.6µm) as a function of R=(DT11µm) / (DR0.6µm)

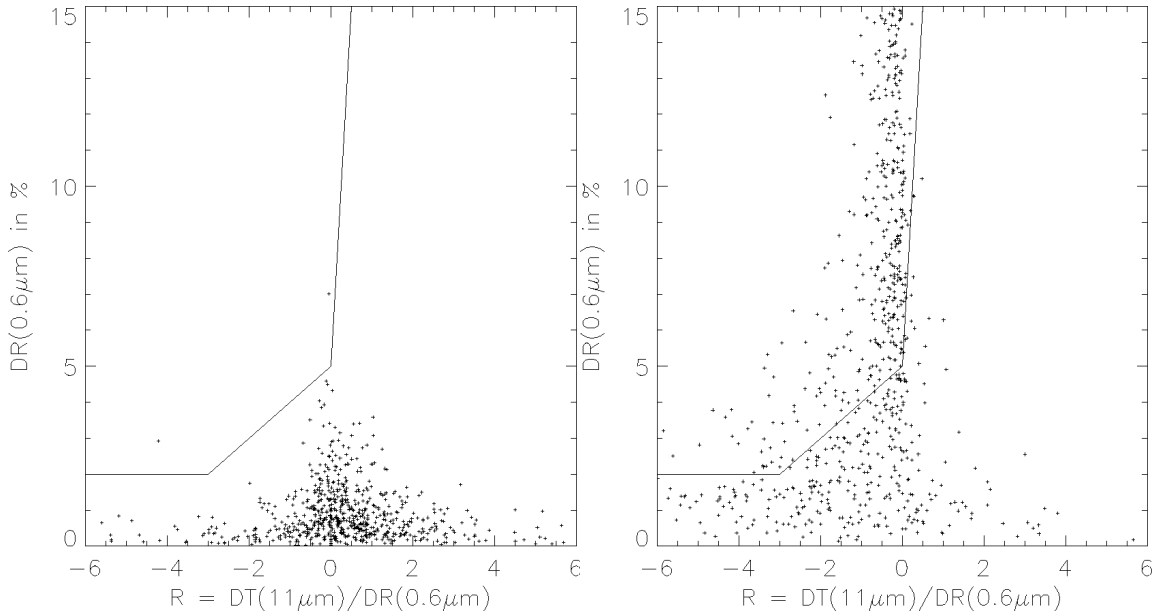

Figure 1.3.3.9.1 Illustration of the test applied to (DR0.6µm) over land at daytime. Cloud free measurement (left) and cloudy (cumulus and thin cirrus) measurements (right) are compared to the threshold (straight-line).

1.3.3.10.Test on (T11µm-T3.9µm)/(T11µm-T12µm) (only over land at nighttime)

At nighttime, some low clouds are very difficult to detect with the test applied to (T11µm-T3.9µm) and are too warm to be detected with T11µm. These situations have been observed with AVHRR imagery over France : they correspond generally to stratocumulus layers invading western Europe, inside warm sectors, with rain or drizzle. Those marine clouds, compared to continental ones, are supposed to have properties influenced by variations in the source and abundance of cloud condensation nuclei affecting their spectral characteristics. Generally low continental stratiform layers contain greater concentration of small droplets due to more numerous condensation nuclei (Sassen, 1999). These clouds were characterised by rather low (T11µm-T3.9µm) value and rather high (T11µm-T12µm). This empirical test tries to improve as much as possible the use of (T11µm-T3.9µm) by using (T11µm-T12µm). But figure 1.3.3.3.10 shows that some low clouds still remains undetected.

The test that has been empirically developed is based on the analysis of figure 1.3.3.10 :

A pixel is classified as cloud contaminated if :

- T11µm -T12µm > F(T11µm -T3.9µm)

where F(T11µm -T3.9µm) = 0.5°C if (T11µm -T3.9µm)>1.8°C

F(T11µm -T3.9µm) = - (T11µm -T3.9µm -1.8) +0.5°C if (T11µm -T3.9µm)<1.8°C

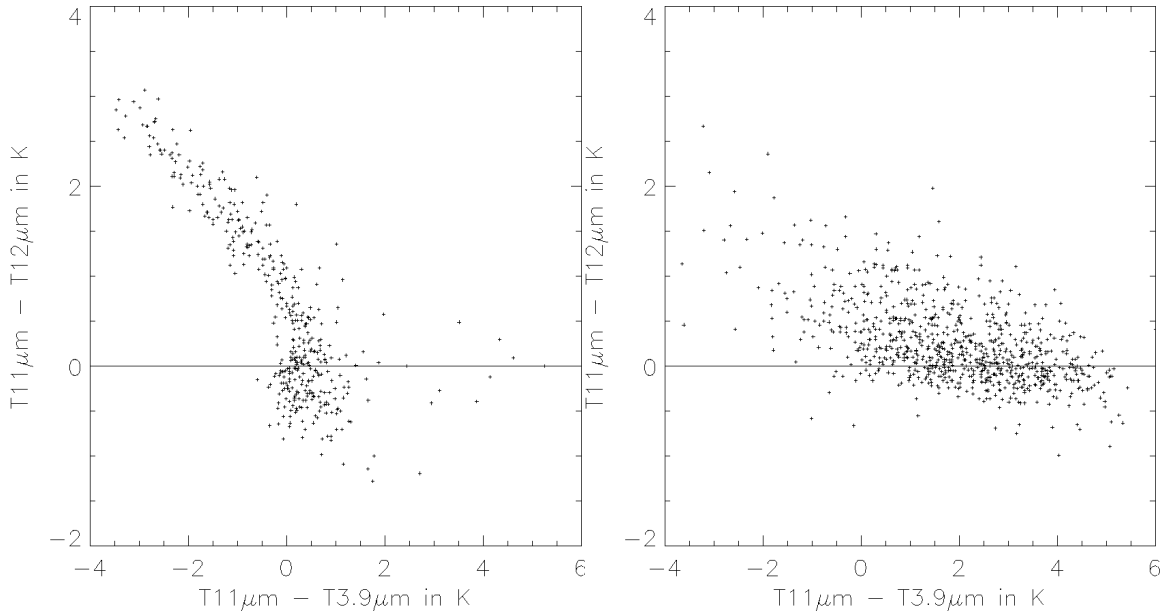

Figure 1.3.3.10 Variation of GOES T11µm-T12µm with T11µm-T3.9µm at nighttime. Left : continental cloud free targets. Right : low clouds.

1.3.3.11.Aerosol detection Tests

The aim is not to map aerosol in general, but to identify some events that could be useful for nowcasting purposes. A need was expressed to detect dust clouds and volcanic plumes. We have also investigated the possibility to detect smoke.

1.3.3.11.1.Smoke identification

The aim was to identify smoke due to fires over both continental and oceanic surfaces. Smoke targets have been specially gathered from GOES imagery (134 targets over ocean & 86 over land, all at daytime) with the interactive procedure (see annex A.3.1) to check the possibility to identify smoke. It has not been possible to select visually smoke targets at nightime, which shows that their automatic identification is practically impossible. At daytime, smoke can be identified in the visible channel over dark surface (ocean or even vegetated area) by their higher reflectance. No strong enough impact is observed in thermal channels to allow their use for automatic smoke detection. Smoke will therefore generally be confused with cloud-free area, except thick enough smoke that can be mis-classified as clouds at daytime over the ocean or vegetated areas. The use of visible and near-infrared channels to distinguish thick smoke from clouds has not been analysed as no AVHRR targets were available. No specific processing to detect smoke has been implemented in the prototypes.

1.3.3.11.2.Dust cloud identification

The aim is to identify dust that is transported out of deserts over both continental and oceanic surfaces. These events are rather frequent over North Africa and adjacent seas (Atlantic Ocean and Mediterranean sea). The difficulty is to separate dust clouds from cloud free areas (the detection step) without confusing them with water clouds (the classification step). Techniques proposed in literature are based on brightness temperature differences [11 and 3.7µm (Ackerman, 1989), or 11 and 12µm (used by NOAA to map dust clouds)], or on visible reflectances spatial homogeneity (Jankowiak and Tanre, 1992).

Dust cloud targets have been specially gathered from AVHRR (305 targets over ocean & 170 over land (60 of them have the 1.6µm channel instead the 3.7µm), all at daytime) and GOES imagery (only 19 targets over ocean at daytime) with the interactive procedure (see annex A.3.1) to check the efficiency of published techniques.

The decrease of T11µm brightness temperature due to dust is rather small : over the ocean, from 1-2°C at satellite nadir up to 10°C for high satellite zenith angles ; around 10°C over continental surfaces (but difficult to estimate accurately). It is not possible to automatically use this too low thermal contrast to detect dust clouds, except over the ocean at large viewing angles. Dust clouds have generally larger visible reflectances than the ocean (except in the sunglint area), which enable their automatic detection. This is not the case over bright continental surfaces such as deserts. The T11µm-T12µm and T3.9µm-T11µm infrared brightness temperatures differences are respectively decreasing and increasing with dust cloud thickness, as shown on figures 1.3.3.11. At daytime, dust cloud can be detected using the visible channel over the ocean (except in sunglint conditions), and the T3.9µm-T11µm infrared brightness temperatures differences over land (care should then be taken to account for thermal saturation). The figures 1.3.3.11 indicate that, at nighttime, only the thickest dust clouds could be detected using the T11µm-T12µm infrared brightness temperatures differences.

Once dust clouds have been detected (i.e., separated from cloud free surfaces), they must be distinguished from thin ice clouds or low water clouds. Dust clouds are easily distinguished from

ice clouds (cirrus) or sub pixels clouds (small cumulus) by their high visible and infrared spatial homogeneity, and their lower T11µm-T12µm infrared brightness temperatures differences. They are more difficult to distinguished from low water clouds (stratus and stratocumulus) : they usually have higher visible and infrared spatial homogeneity, and lower visible reflectance.

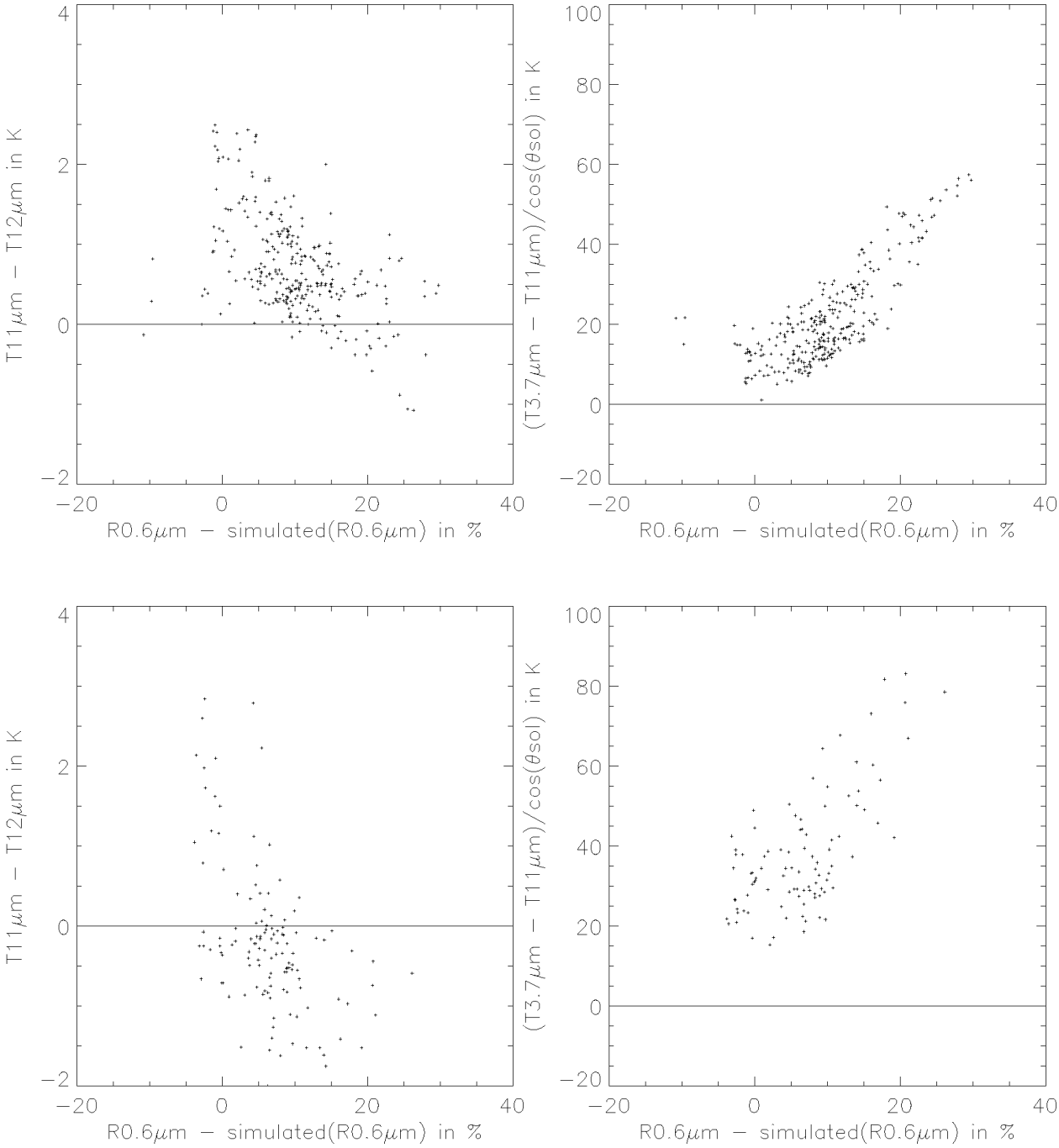

Figure 1.3.3.11 For AVHRR dust cloud targets at daytime. Variation of T11µm-T12µm & T3.9µm-T11µm (corrected from solar elevation) with the difference between observed visible reflectance and corresponding cloud-free simulated visible reflectance (assuming a 35km horizontal visibility).Top : over the ocean ; bottom : over continental surfaces.

Considering these remarks, we have empirically derived the following algorithm to detect and classify dust clouds at daytime:

Over the ocean, a pixel is classified as contaminated by dust cloud if :

- R0.6threshold < R0.6μm < R0.6threshold +30% [R0.6threshold defined in 1.3.3.6]
- -5°C - 5*(1/cos(θsat) -1) < T11μm - SSTclim [where θsat is the satellite zenith angle]
- SD(T11μm) < 0.4°C and SD(R0.6μm) < 0.6 % [SD is the standard deviation]

Over continental surfaces, a pixel is classified as contaminated by dust cloud if :

- 0°C < T11μm < 37°C & (T3.9μm - T11μm) /cos(θsol) > 30 °C [θsol is the solar zenith angle]
- R0.6threshold -15% < R0.6μm < R0.6threshold +30% [R0.6threshold defined in 1.3.3.6]
- SD(T11μm) < 1.0 °C and SD(R0.6μm) < 1.0 % [SD is the standard deviation]

Just to get an insight into its efficiency, we have tested it on the AVHRR interactive file and derived the following contingency tables [A target is classified as « dust » if all its pixels are classified dust, and classified as « not dust » is all its pixels are not dust]. These tables indicate that the dust classification, performed at daytime (over both ocean and continental surfaces), has a rather low accuracy. We have preferred to choose an algorithm that seldom confuses cloud free areas or cloud with dust ; the drawback is that around 40% of dust events (thin dust clouds, but also too inhomogeneous thick dust clouds) are not detected. Moreover, as we have only used afternoon AVHRR passes, the proposed algorithm should also be tested in various illumination conditions. Nevertheless, the algorithm described above has been implemented in the AVHRR and GOES prototypes.

	Observed as dust	Observed as clouds	Observed as Cloud-free
Classified as « dust »	182	3	13
Classified as « not dust »	96	1987	1004

Table 1.3.3.11.1 Contingency tables based on AVHRR interactive file. Over the Ocean at daytime.

	Observed as dust	Observed as clouds	Observed as Cloud-free
Classified as « dust »	58	4	3
Classified as « not dust »	37	272	231

Table 1.3.3.11.2 Contingency tables based on AVHRR interactive file. Over continental surfaces at daytime (targets having the 1.6μm instead the 3.7μm have not been analysed).

1.3.3.11.3.Volcanic plumes identification

The aim is to identify the volcanic plumes that can be observed just after a volcanic eruption, before the eruption cloud has spread and thinned making it more difficult to distinguish. These rare events when accompanied of important ashes emission in the atmosphere are dangerous for aviation, and their identification is therefore required. The difficulty lies in the separation of volcanic plumes from ice or water clouds. Techniques proposed in literature are based on brightness temperature differences : T11μm-T12μm should help in identifying semi-transparent volcanic clouds constituted of very small particles (Prata,1989, Wen et al., 1994).

Volcanic cloud targets have been specially gathered from AVHRR (14 targets over ocean & 66 over land, all at daytime) and GOES imagery (368 targets over ocean (198 at daytime) & 18 over land) with the interactive procedure (see annex A.3.1) to check the efficiency of published techniques. Table 1.3.3.3 details the location and date of the analysed eruptions.

In the case of the Popocatepetl eruption (only 15 targets), the major part of the plume corresponds to strongly negative T11μm-T12μm brightness temperature differences (up to -6°C) which allow their easy separation from water or ice clouds. According to simulations performed by Wen (Wen et al.,

1994), these strong negative differences could be explained by a semi-transparent volcanic plume constituted with small particles. These negative T11μm-T12μm brightness temperature differences can also be found for the other eruptions, but only in very narrow parts of the volcanic plumes ; moreover, the values are not so strongly negative (-1°C over Vatnajökull, Iceland, -0.5°C for Etna, Sicily, -3°C for Soufriere Hills, Montserrat island) and usually do not allow an efficient distinction with clouds. Otherwise, the major part of the volcanic plumes present positive T11μm-T12μm brightness temperature differences similar to those of ice or water clouds.

Considering these insufficient results, we have not yet implemented any algorithm to detect volcanic plumes.

Location	Date	Satellite	Number of targets
Popocatepetl, Mexico 19.023N, 98.622W, 5426m	12/03/1996 (15h-21h UTC)	GOES-08	15
Soufriere Hills, Montserrat, West Indies, 16.72N, 62.18 W, 915m	18/09/1996 (7h-15hUTC)	GOES-08	158
Soufriere Hills, Montserrat, West Indies	08/08/1997 (15h-18h UTC)	GOES-08	17
Soufriere Hills, Montserrat,West Indies	14/12/1998 (12h-15h UTC)	GOES-08	39
Soufriere Hills, Montserrat,West Indies	13/01/1999 (12h-17h UTC)	GOES-08	105
Soufriere Hills, Montserrat,West Indies	10/05/1999 (7h-9h UTC)	GOES-08	4
Etna, Sicily Island, Italy 37.73N, 15.00^{E}, 3315m	23/01/1999	NOAA-15/AVHRR	14
Etna (Italy)	02/02/1999	NOAA-15/AVHRR	3
Vatnajökull glacier, Iceland SE of island	03/10/1996	NOAA-14/AVHRR	26
Vatnajökull (Iceland)	18/12/1998	NOAA-14 & 15/AVHRR	37

Table 1.3.3.3 Details on the eruptions cases available the interactive test file.

1.3.3.12. Opaque clouds detection Test

The initial aim is to identify pixels fully covered by a single cloud layer whose infrared emissivity is close to unity, and are therefore not contaminated in the infrared wavelength by the surface. The calculation of the cloud top temperature and height of these pixels would then have only required a correction for atmospheric attenuation above the cloud. In practice, the opaque cloud flag is effectively used in the AVHRR prototype to retrieve the cloud top temperature, but not in the GOES prototype where the cloud type has been used instead.

The opaque cloud identification is applied to pixels previously detected as cloud contaminated. It relies on the analysis of the T11µm -T12µm brightness temperature difference : this difference is higher for semi-transparent ice clouds (due to their higher transmittivity at 11µm) and broken clouds, than for opaque clouds. The T11µm -T12µm brightness temperature differences of opaque clouds are illustrated on figure 1.3.3.12 : they depend on the atmospheric attenuation above the clouds (increase with integrated atmospheric water vapour for low clouds (stratus and stratocumulus)); but they remain surprisingly high for high clouds (cumulonimbus and perturbation clouds).

Following these remarks, we have implemented this very simple (not very satisfactory) test to identify opaque cloud :

A cloud contaminated pixel is classified as opaque cloud if :

- T11µm -T12µm < 2°C

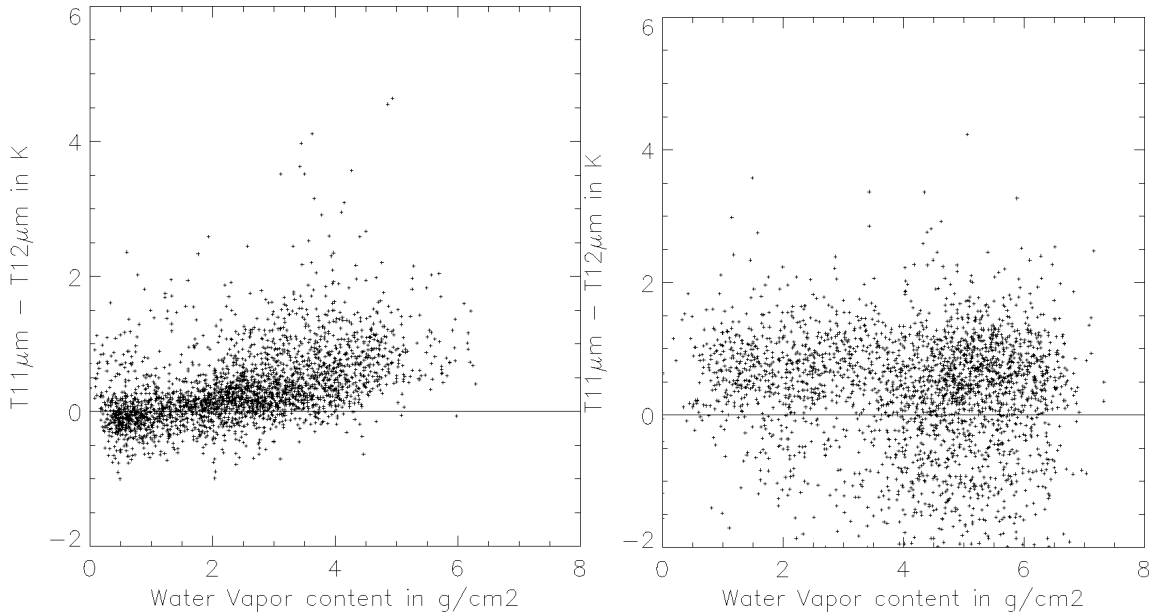

Figure 1.3.3.12 Variation of GOES T11µm-T12µm with atmospheric water vapour content integrated from surface to tropopause .
Left : stratus and stratocumulus. Right : cumulonimbus and perturbation clouds.

1.3.4. Spatial filtering

The following spatial filtering process is applied after the sequence of thresholding tests:

- all the isolated cloudy pixels that have been detected by a test using the 3.9µm are reclassified as cloud-free.

- all the isolated cloud free pixels are reclassified as cloudy.

1.3.5. Quality flag computation (GOES prototype only)

A quality flag (whose content is detailed in 1.2.4) is appended to the CMa. Three bits are dedicated to the identification of cloud-free, cloudy and snowy pixels that may have been misclassified.

- a pixel classified as cloudy is flagged as of bad quality if no cloud detection test has been really successful. A threshold test is said really successful if the difference between the threshold and the measurement is larger than a offset depending on the test itself (see table 1.3.5).

Cloud Test	SST	T11µm	T11µm-T12µm	T11µm-T3.9µm	T3.9µm-T11µm	R0.6µm	Spatial Coherence
Offset	2 °C	3 °C	0.5 °C	0.5 °C	0.5 °C	0.2*threshold	0.2*threshold

Table 1.3.5 Offsets used in the thresholding tests during the cloud detection's quality assessment.

- a pixel classified as cloud free is flagged as of bad quality if the difference between the threshold and the measurement is lower than a quantity (see table 1.3.5) for at least one cloud detection test.
- a pixel classified as snow/ice is flagged as of bad quality if the difference between its observed (T3.9µm-T11µm) and the corresponding threshold of this feature used in the snow/ice detection test is lower than 0.2*threshold.

Such a quality flag should allow to identify good quality cloud free areas for surface parameters computation. On the other hand, the identification of extended cloudy or cloud free area flagged as bad quality should help in identifying areas where the algorithm may be not accurate enough [note that it is understandable that cloud edges or cloud free areas bordering clouds are flagged as of bad quality].

1.4. Practical application

1.4.1. Implementation of the cloud mask scheme

1.4.1.1. AVHRR prototype

We have just modified an existing operational software described in details in Derrien et al., 1993, and summed up below :

- the AVHRR imagery is processed in satellite projection,
- in a first step, most of the thresholds are computed in segments (boxes of 34*39 AVHRR pixels centred on HIRS FOV), using monthly climatological maps, atlas and NWP model forecast fields available at $1/6^{th}$ degree horizontal resolution on the Lannion HRPT acquisition area.
- in a second step, the CMa is computed at the AVHRR pixel resolution using thresholds available at the segment resolution.
- the modified scheme is daily applied on a development workstation : the four AVHRR passes the most centred over France are processed every day.

- the result is available over the whole processed pass in satellite projection.

1.4.1.2. GOES prototype

As already mentioned, the GOES prototype is a completely new scheme that complies with most of the specifications addressed to the SEVIRI software. It is detailed in this paragraph.

- The software is implemented on a pre-operational workstation financed by Eumetsat. This workstation receives half-hourly GOES images, and all the needed NWP fields to allow the CMa computation every half an hour.
- The software may process several regions (rectangular in the satellite projection) located in the GOES Extended Northern Hemisphere (illustrated in the annex A.5), and defined by their name, the location of their north-west corner and their number of rows/lines. The user may choose the whole Extended Northern Hemisphere itself.
- The user must define the size of segments for each processed regions. Segments are square boxes (in the satellite projection). All the solar and satellite angles, the NWP model forecast values, the atlas values and the thresholds will be derived over all the processed regions at the horizontal resolution of the segment. During the prototyping, we have usually used segments of 4*4 GOES IR pixels, but have also tested segment of one individual GOES IR pixel (see 1.4.3). Note that the size of the processed regions must be a multiple of the segment size. Note also that the land/sea atlas will be available at the full GOES IR resolution, allowing the identification of the surface type (land or sea) of all IR pixels, whatever the segment size.
- When the regions are defined, a script prepares automatically for the user (only once) the regional monthly climatological and atlas maps, as well as latitude/longitude and satellite angles information for his regions at the full IR horizontal resolution. These regional atlas and maps are extracted from maps available on the whole northern hemisphere, and stored on a dedicated directory, to be used during the routine processing.
- The routine processing is performed in three steps. All the regions are processed sequentially.
    - the preliminary step is the reprojection of NWP model forecast fields on the regional regions at the segment horizontal resolution. This is regularly scheduled by instructions given through crontab UNIX command.
    - the preparation step, also scheduled by crontab, includes the computation on the regional areas at the segment horizontal resolution of solar & satellite angles, monthly climatological & atlas maps, and thresholds.
    - the execution step is the real-time processing of the GOES images itself over the regions. This process is activated by a home-made scheduler (called ARCHIPEL2) when all the input images (on the whole GOES extended northern hemisphere) are available. The CMa is computed at the IR GOES pixel resolution [the visible reflectances available at 1km resolution are averaged on the corresponding pixel (4km)].

1.4.2. Impact of missing NWP information

The prototypes that have been developed are not robust : they require the availability of all satellite channels and auxiliary data (climatological and atlas maps, and NWP output). Climatological and atlas maps are stored on the disk of the satellite image processing system, and therefore always available. We have never faced a situation where a single satellite channel was missing : this would happen in case a failure of the radiometer itself.. On the contrary, NWP fields are produced by a NWP model (external to the satellite processing system), transferred to the satellite processing system : there are therefore reasons why some fields may be missing. We have analysed the impact of missing NWP fields on the results' accuracy, using the GOES interactive file.

Table 1.4.2.1 compares the clear and cloud failure score (defined in 1.5.1) for various illumination over land and sea using integrated water vapour content (W) output by NWP or extracted from climatology (see annex A.2.1). The main impact of using climatological values is the increase of the clear failure score, especially over sea and also at daytime over land : when the climatological integrated water vapour content is lower than the true atmospheric water vapour content, the T11μm-T12μm of T3.9μm-T11μm thresholds computed from the climatology are then underestimated, leading to an increase of clear failures.

	Cloud failure W from NWP	**Cloud failure Climatological W**	**Clear failure W from NWP**	**Clear failure Climatological W**
Night over Sea	0.7%	0.5%	1.6%	5%
Day over Sea	0.9%	0.9%	6.6%	9.1%
Twilight over Sea	1.3%	0.8%	1.1%	3.2%
Sunglint over Sea	2.5%	2.5%	6.0%	12.0%
Night over land	1.8%	1.8%	5.9%	6.6%
Day over Land	5.5%	4.5%	7.9%	16.2%
Twilight over land	9.6%	8.3%	1.1%	1.1%

Table 1.4.2.1 Statistical characteristics of CMa result based on targets types from GOES interactive file. Using integrated water vapour content (W) extracted from NWP or from climatology.

Table 1.4.2.2 compares the clear and cloud failure scores (defined in 1.5.1) for various illumination over land using surface temperature, either output by NWP, or computed from climatological air temperature at 1000hPa (see annex A.2.1) using dry adiabatic cooling to account for height. The impact of using climatology instead NWP output depends on illumination : the clear failure score is strongly increased at nighttime due to too warm climatological values, whereas the cloud failure score is increased at daytime.

	Cloud failure Tsurf from NWP	**Cloud failure Tsurf from climatology**	**Clear failure Tsurf from NWP**	**Clear failure Tsurf from climatology**
Night over land	1.8%	3.3%	5.9%	12.7%
Day over Land	5.5%	12.2%	7.9%	8.0%
Twilight over land	9.6%	25.1%	1.1%	6.5%

Table 1.4.2.2 Statistical characteristics of CMa result based on targets types from GOES interactive file. Using surface temperature (Tsurf) extracted from NWP or computed from climatology.

1.4.3. Segment size analysis

In the GOES prototype, most of the thresholds are computed at the spatial resolution of segment. The CMa is then computed at the IR pixel resolution. During the prototyping, a segment's size of 4*4 IR pixel has been generally used.

Segments are used to decrease the processing time and the needed memory without debasing too much the CMa quality. In fact, most thresholds are computed from NWP output, atlas and climatological maps which are usually not available at GOES IR pixels spatial resolution.

The impact of the segment size on the CMa quality and the processing time has been studied using two images (17 may 1999 at 12hTU and 18hTU) on a region of 768 by 768 pixels covering North and Central America. Segment size of 1*1, 2*2, 4*4 and 8*8 GOES IR pixels have been tested.

- The CMa quality is very slightly dependent on the segment size (for segment between 1*1 (i.e., 4*4km) and 8*8 (i.e., 32*32km)), as shown on table 1.4.2. As expected, the impact of the segment's size is more sensitive over land.
- The processing time of the off-line step (the threshold's preparation), which consists of lots of computation every segments of the image, is closely linked to the number of segments contained in the image : the processing time is increased by a factor between 3 and 4 when the number of pixels of the segment is divided by 4 (i.e., from 4*4 to 2*2...). Of course, we can argue that the processing time of this step is not so important, as this process is performed before the satellite imagery availability. But we must note that this time has to be added to the other ones, and this processing applied to the full GOES northern hemisphere with a segment reduced to one pixel would have been too much time consuming !
- The processing of the real time CMa computation is nearly independent of the segment size ; this is due to the fact that the thresholds arrays are read from files, which is a very fast process.

	segment : 1*1	**segment : 2*2**	**segment : 4*4**	**segment : 8*8**
12h TU : Over land	46.627 %	46.167 %	45.511 %	44.638 %
12h TU : Over sea	60.471 %	60.277 %	60.098 %	59.892 %
18h TU : Over land	48.024 %	47.900 %	47.406 %	46.747 %
18h TU : Over sea	55.731 %	55.429 %	55.160 %	55.002 %

Table 1.4.2 Percentage of cloudy pixels in the image for various segment's sizes.

The consequences of using a segment's size of 4*4 during our prototyping are a misclassification of less than 1% continental and 0.5% oceanic pixels, but a processing time of the off-line step divided by 16.

1.4.4. Estimation of needed informatic resources

CPU and virtual memory size required by both the preparation step (offline computation of thresholds) and the execution step (real time computation of the Cloud Mask) have been estimated in the GOES prototype for a 512 by 512 IR pixels region using a segment size of 4 by 4 :

- CMa preparation : CPU time : 14 seconds Virtual memory Size : 5848 Kbytes

- CMa execution : CPU time : 21 seconds Virtual Memory Size : 14592 Kbytes

CPU time and Virtual Memory Size have been measured on a development workstation Sun ULTRA Creator 140E running under SunOS 5.7 for tasks compiled without any optimisation. The exact meanings of « CPU time » and « Virtual Memory Size » are those of the **ps** UNIX command.

1.5. Validation

1.5.1. Comparison with interactive file (GOES only)

As a first step towards verification of the CMa, statistical scores have been computed using results of the CMa applied to the GOES data from the interactive file (see annex A.3.1). This can't be strictly a verification for two reasons. First a part of the tuning of CMa has been based on the use of the interactive file which makes them dependent. Secondly, the interactive file has been built to study clouds and many clear targets have been selected to be worst cases for CMa. The statistical indexes are indicators of how much the automated CMa agrees with the interactively manned targets types.

The CMa is available for the 3x3 central pixels of the 5x5 target. A target is :
- « observed cloudy » when its type corresponds to a cloud (including sand or volcanic ashes),
- « observed clear » when the surface observation is not obstructed by a cloud, sand or volcanic ashes
- « detected cloudy » when more than 60% of its 9 central pixels are masked cloudy,
- « detected clear » when less than 40% of its 9 central pixels are masked cloudy.

According to these definitions contingency tables have been built and the several stastistical scores have been computed :

	Detected Cloudy	Detected Clear
Observed Cloudy	n_a	n_b
Observed Clear	n_c	n_d

Table 1.5.1.1 Contingency tables conventions

- Global score is computed as $100x(n_a+n_d)/(n_a+n_b+n_c+n_d)$, it reflects the general performance of Cma.
- Cloud failure score is computed as $100x(n_b)/(n_a+n_b)$, it reflects the failures among cloudy targets, (CMa underestimation of clouds).
- Clear failure score is computed as $100x(n_c)/(n_c+n_d)$, it reflects the failures among clear targets, (CMa overestimation of clouds).

These statistical characteristics have been associated with changes in latitudes, (for nordic, midlatitude and tropical conditions), scene background (land or sea) and illumination conditions (day, night, twilight, sunglint).

The algorithm performs better over the ocean than over land : lower cloud failure score (0.9% against 4.7%) and lower clear failure score (5.2% against 7.0%). Changes in latitude demonstrates the difficulty to detect clouds in nordic conditions : the clear failure score is especially high (14.3% over ocean and 17.2% over land), but the number of targets is limited.

Surprisingly, results are better in night than in day conditions. Over the ocean, the clear failure score is much higher at daytime (6.6% against 1.6%) ; one explanation is that, at daytime over the ocean, the cloud detection algorithm is more sensitive to fractional or semi-transparent cloudiness than the human eye, thanks to local variance tests. Over land, the cloud failure score is higher at daytime (5.5% against 1.8%), the non-detected clouds are low clouds (small cumulus, much less frequent at nighttime) and semi-transparent clouds (easier to detect at nighttime using the 3.9µm channel).

Areas covered by snow are considered in these statistics as cloud free areas. The snow (or ice) is a class of the CT product, and its quality is analysed in more detail in 2.5.

	Contingency table		Contingency table (normalized)		Global Score	Cloud Failure Score	Clear Failure Score
Global	10972	249	74.0%	1.7%			
(All Targets)	218	3396	1.5%	22.9%	**96.9%**	**2.2 %**	**6.0%**
	7215	63	78.1%	0.7%			
over Sea	102	1856	1.1%	20.1%	**98.2%**	**0.9%**	**5.2%**
Nordic	252	5	56.5%	1.1%			
over Sea	27	162	6.1%	36.3%	92.8%	1.9%	14.3%
Midlatitude	3760	26	79.5%	0.5%			
over Sea	56	889	1.2%	18.8%	98.3%	0.7%	5.9%
Tropical	3203	32	78.9%	0.8%			
over Sea1	19	805	0.5%	19.8%	98.7%	1.0%	2.3%
Night	2411	17	84.0%	0.6%			
over Sea	7	434	0.2%	15.1%	99.2%	0.7%	1.6%
Day	4195	38	74.2 %	0.7%			
over Sea	94	1329	1.7%	23.5%	97.7%	0.9%	6.6%
Twilight	609	8	85.7%	1.1%			
over Sea	1	93	0.1%	13.1%	98.7%	1.3%	1.1%
Sunglint	312	8	66.5%	1.7%			
over Sea	9	140	1.9%	29.9%	96.4%	2.5%	6.0%
	3757	186	67.1%	3.3%			
Land	116	1540	2.1%	27.5%	**94.6 %**	**4.7%**	**7.0%**
Nordic	128	11	63.1%	5.4%			
over Land	11	53	5.4%	26.1%	89.2%	7.9%	17.2%
Midlatitude	2167	125	62.7%	3.6%			
over Land	86	1079	2.5%	31.2%	93.9%	5.5%	7.4%
Tropical	1462	50	75.4%	2.6%			
over Land	19	408	1.0%	21.0%	96.4%	3.3%	4.4 %
Night	1051	19	69.6%	1.3%			
over Land	26	415	1.7%	27.5%	97.0%	1.8%	5.9%
Day	2500	145	66.3%	3.8%			
over Land	89	1034	2.4%	27.4%	93.8%	5.5 %	7.9%
Twilight	206	22	64.4%	6.9%			
over Land	1	91	0.3%	28.4%	92.8%	9.6%	1.1%

Table 1.5.1.2 Contingency tables and statistical characteristics of CMa results based on targets types from the GOES interactive file.

1.5.2. Comparison with surface observation

The quantitative comparison of the GOES CMa prototype with surface synoptic observations has been made possible thanks to the use of the coincident satellite targets and SYNOP data gathered from the two years from July 1st 1997 to July 1st 1999. From the SYNOP data set (see annex A.3.2), ground-based total cloud cover and partial cloud cover from low, medium and high clouds are available. We have applied the GOES CMa prototype to the coincident GOES-08 data set, satellite cloud coverage is then the result of the CMa for the central pixel of the satellite targets and its surroundings. To simulate the surface observations from the satellite pixels, no attempt has been made to take into account the complexity of the observation, and all the nine pixels inside the central part of the satellite data target are used for the evaluation. The slots retained for the satellite targets selections start about 15 minutes before the UTC reference time of the SYNOP observation and end about 3 minutes after the reference time, so that they can be considered as really coincident. During the two years of data gathering, a pre-processing random error of scan line numbering occurred, adding some noise to the geographical collocation of the ground and satellite observations.

The comparison between SYNOP and CMa is not straightforward. The satellite-based observation is a top-down view while the ground-based one is down-top. Then the satellite cloud recognition is more difficult because its background is not uniform and not always dark. Another difficulty, linked to the observing point of view is that the satellite observations miss the cloud layers beneath the top cloud layers while the ground-based observation miss the layers above the low-level clouds.

When analysing the results of the comparison, we discovered that the total cloudiness reported in many SYNOP gathered from the GTS over GOES08 area may result from an automated sky observation system, even when the SYNOP is supposed to be done with presence of personnel (code 1 in table 02001 of BUFR code). Including such observations in our statistics would add wrong cases of clear-sky observations, because the ASOS (Automated Sky Observing System) derived cloudiness is 0 in presence of cloud layers above 3600 m. We have chosen to remove the stations having more than 25% of their cloudy reports generally without cloud type description. Thus we have minimised the number of automated clear cloudiness reports, keeping in mind that some of them may remain doubtful. The distribution of the overall cloudiness from the retained data set is shown in Figure 1.5.2.1

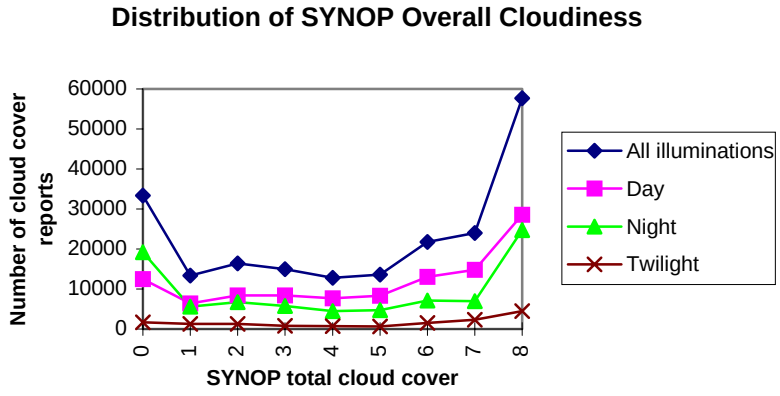

Figure 1.5.2.1 Distribution of total cloud cover from SYNOP reports of retained weather stations as a function of illumination conditions

The first part of the comparison between the GOES CMa and the cloud cover observed from the surface consists in building up contingency tables as for the validation using the interactive file (see 1.5.1) , using the following definition of « observed clear » and « observed cloudy » :

- « observed cloudy » corresponds to a total cloud cover, available in the SYNOP observation, larger or equal to 6 octas (eighths), and such an observed situation is counted as erroneous if its corresponding CMa total cloud cover is below or equal to 2 octas
- « observed clear » corresponds to a total cloud cover, available in the SYNOP observation, less or equal 2 octas, and such a situation is counted as erroneous if its corresponding CMa total cloud cover is greater or equal to 6 octas

The contingency tables are used to quantify clear failure score (targets classified as mainly cloudy, but corresponding to cloud-free observations) and cloud failure score (targets classified as mainly cloud-free, but corresponding to cloud-covered observations). As in the comparison using he interactive file, areas covered by snow are considered in these statistics as cloud free areas.

Contingency tables and statistical scores (cloud failure and clear failure) have been computed for various illumination conditions, and different geographic areas, and are presented in table 1.5.2.1. Note that the definition of clear and cloudy observations eliminates the observations having total cloud cover between 3 and 5 octas from these first statistics. These intermediate observations, and the behaviour of a simple CMa derived total cloud cover are considered in the rest of the study.

	Contingency table		Contingency table (normalized)		Global Score	Cloud Failure Score	Clear Failure Score
Land	80539	10423	55.9%	7.2%			
All Illuminations	10658	42502	7.4%	29.5%	**85.4%**	**11.5%**	**20%**
Land	43327	6083	59.7%	8.4%			
Day	3375	19797	4.6%	27.3%	87.0%	12.3%	14.6%
Land	31576	2883	52.1%	4.7%			
Night	6930	19300	11.4%	31.8%	83.9%	8.2%	26.4%
Land	5636	1507	51.7%	13.8%			
Twilight	353	3405	3.2%	31.2%	82.9%	21.1%	9.4%
Nordic land	7343	451	68.4%	4.2%			
All Illuminations	1378	1564	12.8%	14.6%	**83.0%**	**5.8%**	**46.8%**
Nordic land	3262	130	75.7%	3.0%			
Day	321	594	7.5%	13.8%	89.5%	3.8%	35.1%
Nordic land	3071	97	64.2%	2.0%			
Night	983	630	20.6%	13.2%	77.4%	3.1%	60.9%
Nordic land	1010	224	61.3%	13.6%			
Twilight	74	340	4.5	20.6%	82.0%	18.2%	17.9%
Midlatitude land	35657	3139	55.8%	4.9%			
All Illuminations	4481	20639	7.0%	32.3%	**88.1%**	**8.1%**	**17.8%**
Midlatitude land	18218	1387	61.3%	4.7%			
Day	1472	8666	4.9%	29.1%	90.4%	7.1%	14.5%
Midlatitude land	13832	1002	51.0%	3.7%			
Night	2757	9533	10.2%	35.1%	86.1%	6.8%	22.4%
Midlatitude land	3607	750	51.2%	10.6%			
Twilight	252	2440	3.6%	34.6%	85.8%	17.2%	9.4%
Tropical land	37539	6833	54.0%	9.8%			
All Illuminations	4799	20299	6.9%	29.2%	**83.3%**	**15.4%**	**19.1%**
Tropical land	21847	4566	56.7%	11.8%			
Day	1582	10537	4.1%	27.3%	84.0%	17.3%	13.1%
Tropical land	14673	1734	51.1%	6.0%			
Night	3190	9137	11.1%	31.8%	82.9%	10.6%	25.9%
Tropical land	1019	533	46.2%	24.2%			
Twilight	27	625	1.2%	28.4%	74.6%	34.3%	4.1%

Table 1.5.2.1 Contingency tables and statistical characteristics of CMa results, elaborated from the comparison of CMa and collocated SYNOP cloud covers.

When compared with the CMa results from the interactive file, the SYNOP CMa results present a significant decrease of the overall accuracy of 10%, from 95 to 85% on the land data set. The clear and cloud failure scores are multiplied by 2.8 and 2.4 when computed with SYNOP data set instead of using interactive file, thus confirming the lower accuracy obtained with SYNOP data set. The degradation of cloud and clear failure is strongly increased in night-time condition by a factor of 4.5 instead of 2.2 for daytime condition. Two explanations can be proposed ; the difficulty of visually observing clouds from surface in dark condition that artificially increase the clear failure score ; the interactive selection of cloudy targets in night-time condition has avoided doubtful cloud layers, thus decreasing the cloud failure score artificially.

The results obtained over nordic area confirm the worst results at night-time with a very high clear failure, i.e. when snow detection is impossible making very cold grounds more often confused with clouds. But the cloud failure is better in nordic conditions indicating that the algorithm could be better tuned here. The results for the tropical area outline also a worse cloud detection than for mid-latitude area. That may be explained by the nature of the clouds but also by the higher water vapour loadings increasing the atmospheric contribution into the measurements.

Another technique that can be used to assess the CMa results is to compare its overall cloudiness with that given by the SYNOP. We have studied the distribution of satellite mean CMa cloud cover errror expressed in octas (defined as the difference between CMa and SYNOP cloudiness) as a function of SYNOP observed cloudiness. The CMa cloud cover is computed using the nine central pixels of the satellite target, counting every pixel detected as cloud contaminated as totally covered by clouds. The results are given in Figure 1.5.2.2. For midlatitude area it illustrates a general trend of CMa cloud cover to increase cloud fractions below 4 octas, more widely for night-time cases, one part of this overestimation coming from the simple calculation of CMa cloud fraction assuming pixels as totally cloudy, that is not true in presence of scattered cloud covers. On the contrary , overcast skies are always slightly underestimated. One can also note the obvious trend of CMa to underestimate cloud cover at twilight at any cloud amount. RMS errors present their maximum values (about 3 octas) for scattered cloud covers [3,6], decreasing around 2 or less for overcast skies.

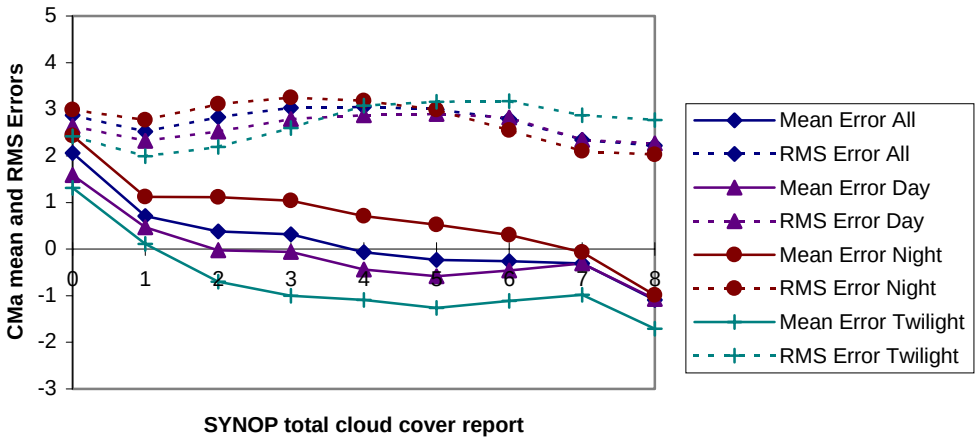

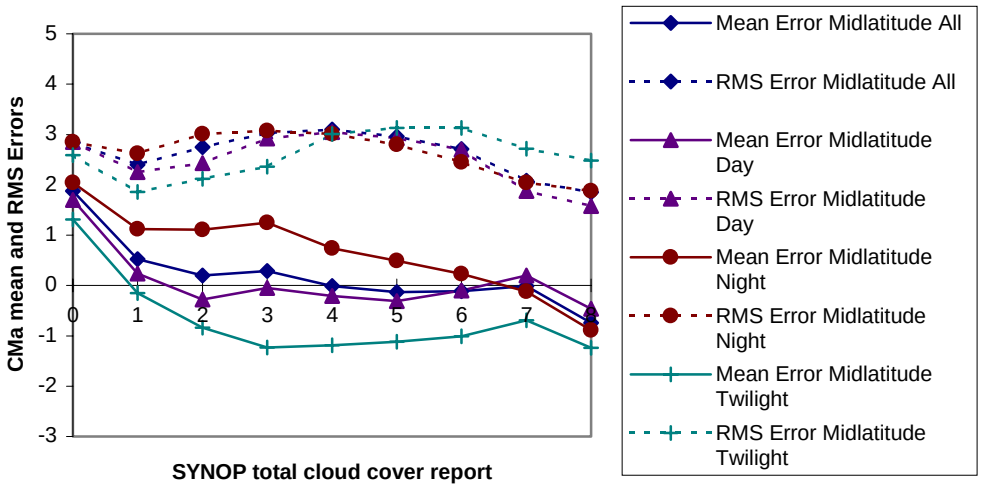

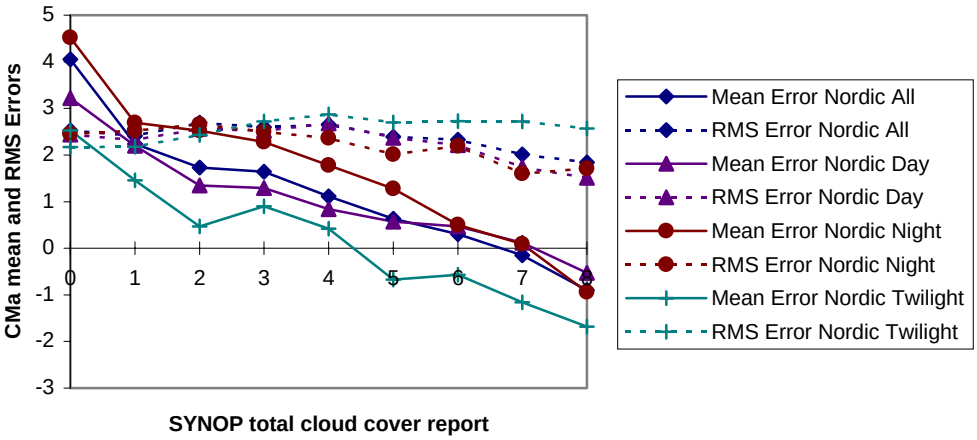

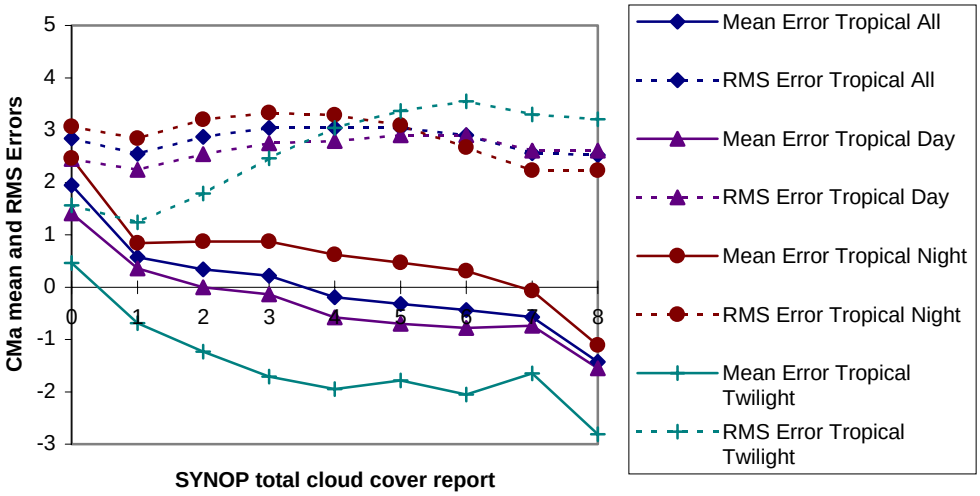

Figure 1.5.2.2 CMa Overall cloudiness mean and RMS errors as function of SYNOP cloud cover and ilumination conditions for the several geographic areas.

The analysis of the percentage of CMa overall cloudiness having a tolerance Δ of 0,1, and 2 octas with the SYNOP (table 1.5.2.2) shows that generally 77% of CMa overall cloudiness is within 2 octas from SYNOP, reaching 80% at daytime and 74% at nighttime for the midlatitude subset. These results can be compared to those obtained with AVHRR by Karrlsson 1993, Kriebel 1997. with Apollo, and by Visa and Iivarinen 1997 with the Self-Organising Map, a neural network based classification, keeping in mind that the GOES-based cloudiness is slightly disadvantaged by the worse horizontal resolution of its radiometer.

	Number of cases	Δ =0	Δ =1	Δ=2
Midlatitude All	82063	39.1%	62.1%	77.0%
Midlatitude Day	38092	38.0%	63.7%	80.1%
Midlatitude Night	34879	42.0%	61.2%	74.1%
Midlatitude Twilight	9092	32.9%	58.5	74.9%

Table 1.5.2.2 Percentage of CMa overall cloudiness having a tolerance Δ of 0,1, and 2 octas with the SYNOP observation.

A last parameter that can also describe the CMa results is the distribution of the differences between CMa and SYNOP overall cloudiness. Its behaviour has been plotted for the various subsets in figure 1.5.2.3. A symetric curve centred on 0 would depict a CMa without any bias to overdetect or underdetect clouds. Their shape confirm again what was observed previously :

- General CMa underdetection of clouds at twilight
- General CMa overdetection of clouds at night.
- On Nordic area, overdetection of clouds at night and day, slight underestimation at twilight.
- On tropical area, general slight underdetection of clouds at daytime, but strong at twilight.

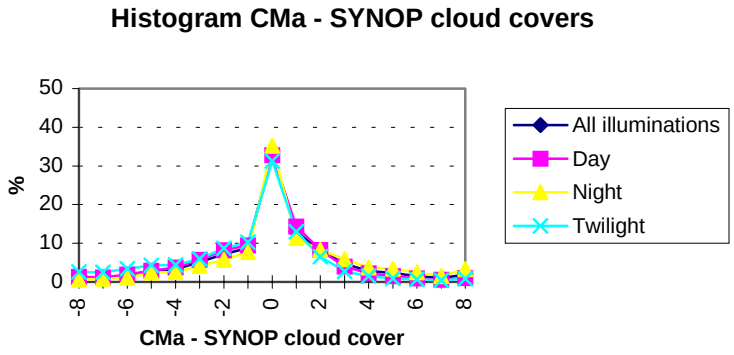

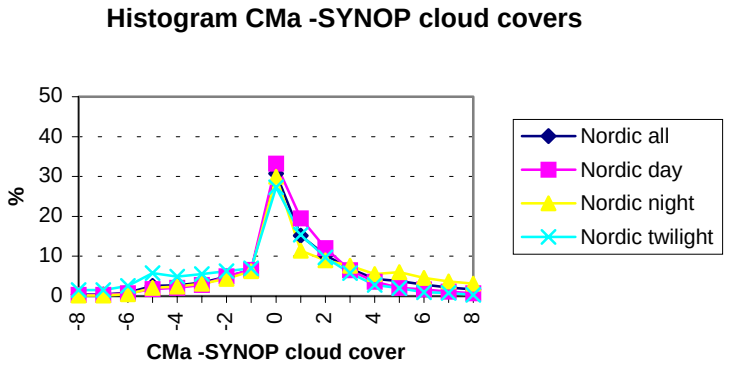

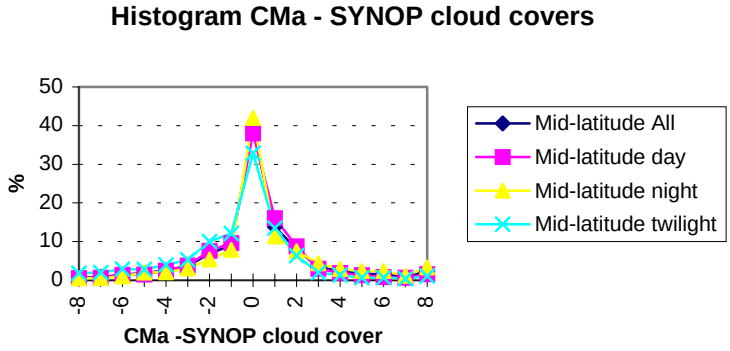

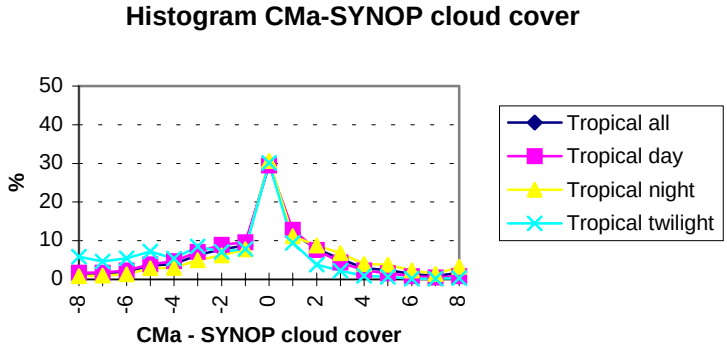

Figure 1.5.2.3 Distribution of the differences between CMa and SYNOP cloud covers

1.5.3. Problems detected by visual inspection

A long-term visual analysis of GOES and AVHRR CMa has allowed to identify the main problems encountered in the cloud masking that are summarised below :

- Non detected clouds :

The main cases of non detection of clouds are listed :

- The most critical problem that we have observed is the non detection of large areas of low warm clouds at night-time over land in the AVHRR imagery. These clouds were accompanied by drizzle or even rain, and were observed in « warm sector ». Their detection has been improved by a combined use of T11µm-T3.9µm and T11µm-T12µm, but still remains problematic (see 1.3.3.10).
- Some low clouds are not detected over land for very low solar elevation. In the GOES prototype, this phenomena usually lasts one slot, during which the sun is too low for the visible channel to be useful, but sufficiently high to contaminate the 3.9µm brightness temperature. This can be seen only when animating sequences of CT images.
- Low clouds shadowed by higher clouds may not be very well detected.
- Low clouds overlaid by very thin cirrus may not be very well detected at night-time.
- Too thin cirrus or broken clouds may not be detected, over both sea and land.
- The snowy areas are not detected at nighttime and for too low solar elevation, and may then be confused with clouds.

Usually, these misclassified clouds are flagged as « bad quality » as their spectral characteristics are very close to the thresholds used during the cloud masking.

- Cloud free areas misclassified as clouds :

It happens that cloud free surfaces, having radiometric characteristics close to the thresholds, are misclassified as cloudy. But they are usually flagged as « bad quality » by the associated quality flag.

1.6. The demonstration experiment

A description of the demonstration experiment is given in annex A.5. During this experiment, the GOES CT has been visually checked, which of course includes the analysis of the quality of the cloud detection. A special validation of the cloud mask with SYNOP measurements during the demonstrator experiment has not been performed, as the results of an extensive validation covering two years are already available (see 1.5.2).

1.7. Future application to SEVIRI

1.7.1. Conclusion from prototyping :

The prototyping with AVHRR and GOES has allowed to gain experience for the development of the algorithm and software to process SEVIRI :

- we have checked the technical feasibility of real time cloud masking using GOES imagery

- we have quantified the accuracy that can be expected if a limited set of SEVIRI channels is used (i.e., those available on GOES).
- we have estimated the interest of additional channels (at 0.9µm or 1.6µm) using AVHRR
- we have visually estimated CMa quality in Europe using AVHRR

Taking into account the result of prototyping, we propose to implement the algorithm described below :

Input data (M indicates mandatory input) :

- Satellite imagery (see annex A.1.3 ; availability of data checked for every pixel :
  - 0.6µm (M), 0.9µm, 1.6µm, 3.9µm (M), 8.7µm, 11µm (M), 12 µm (M) at full IR spatial resolution
  - Sun and satellite angles associated to SEVIRI imagery (M).

- NWP parameters (see annex A.2.2) :

Forecast fields of the following parameters (minimum frequency : 4 per days), remapped onto satellite images (at the segment resolution), are used as input :

  - surface temperatures (required to get good quality results over land ; but not mandatory)
  - air temperature at 950hPa (to check low level inversion)
  - total water vapour content of the atmosphere,
  - elevation of the NWP model grid (required if NWP fields are used as input)

- Ancillary data sets (see annex A.2.1) :

The following ancillary data, remapped onto satellite images, are used as input :

  - Land/sea atlas (M)
  - Land/sea/coast atlas (M)
  - Elevation atlas (M)
  - Monthly minimum SST climatology (M)
  - Monthly mean 0.6µm atmospheric-corrected reflectance climatology (land) (M)
  - Monthly integrated atmospheric water vapor content climatology (M)
  - Monthly climatology of mean air temperature at 1000 hPa (M)

Output data :

The content of the CMa is the following :

- 3 bits to describe cloud mask

0	Non-processed	containing no data or corrupted data
1	cloud-free	no contamination by snow/ice covered surface, no contamination by clouds ; but contamination by thin aerosol (dust clouds or volcanic plume) remains possible
2	Cloud contaminated	partly cloudy or semitransparent. May include also dust clouds or volcanic plumes.
3	Cloud filled	opaque clouds completely filling the FOV. May includes also thick dust clouds or volcanic plumes.
4	Snow/Ice contaminated	
5	Undefined	has been processed but not classified due to known separability problems

- 16 bits to describe which test was successful

1 bit per test used in the CM algorithm is activated if the test is successful.

0	T11µm or SST
1	R0.6µm (land) or R0.9µm (sea)
2	sunglint test using 3.9µm
3	Spatial coherence test
4	T11µm - T12µm
5	T11µm - T39µm

6 T39µm - T11µm
7 spatial smoothing (reclassify isolated cloud-free pixels)
8 T11µm - T12µm /T11µm - T39µm (nighttime)
9 R1.6µm (sea)
10 T11µm -T8.7µm
11 snow using R1.6µm
12 snow using T3.7µm
13-15 spare

- 9 bits for quality

3 bits to define illumination and viewing conditions:
0 Undefined (space)
1 Night
2 Twilight
3 Day
4 Sunglint

2 bits to describe NWP input data
0 Undefined (space)
1 All NWP parameters available (no low level inversion)
2 All NWP parameters available (low level inversion)
3 At least one NWP parameter missing

2 bits to describe SEVIRI input data
0 Undefined (space)
1 All useful SEVIRI channels available ;
2 At least one useful SEVIRI channel missing

2 bits to describe the quality of the processing itself:
0 Non processed (containing no data or corrupted data)
1 Good quality (high confidence)
2 Poor quality (low confidence)
3 Reclassified after spatial smoothing (very low confidence)

- 2 bits for dust detection

0 Non processed (containing no data or corrupted data)
1 dust
2 non dust
3 undefined (due to known separability problems)

- 2 bits for volcanic plume detection

0 Non processed (containing no data or corrupted data)
1 volcanic plume
2 non volcanic plume
3 undefined (due to known separability problems)

Algorithm outline :

The algorithm is based on multispectral threshold technique. Each pixel of the image is classified by a succession of tests applied to various combinations of channels.

A first set of tests allows the identification of pixels contaminated by clouds or snow/ice : this first process stops if one test is really successful (i.e., if the threshold is not too close to the measured value).

- The combinations of channels used depend on the geographical location of the pixel (defined, using the land/sea atlas value), on the solar illumination and on the viewing angles (daytime, night-time, twilight, sunglint, defined in Table 1.7.1.1).

- The tests applied to land or sea pixels are listed in tables 1.7.1.2 and 1.7.1.3. The snow or ice detection test make use of the 1.6µm as the AVHRR prototype (3.7µm is used as a spare channel) ; the spatial coherence tests and the sunglint test are the same as those prototyped with GOES. Over sea, R0.6µm is thresholded if R0.9µm is unavailable.
- The thresholds are computed as in the GOES prototype (in the AVHRR prototype for the snow detection test). They are determined off-line, either as empirical values, or as functions/pre-computed tables tuned using RTM calculations (6S or RTTOV). The on-line preparation of thresholds is then performed by these functions/pre-computed tables, using as input the viewing geometry (sun and satellite viewing angles), NWP forecast fields (surface temperature and total atmospheric water vapour content) and ancillary data (elevation and climatological data). The thresholds are computed on segment, which size is defined by the user.
- A test is applied to cloud contaminated pixels to check whether the cloud cover is opaque and completely fills the FOV.
- A spatial filtering is finally applied, allowing to reclassify pixels having a class type different from their neighbours.

A second process allows the identification of dust clouds and is applied to all pixels (even already classified as cloud-free or contaminated by clouds). The algorithm will be similar to the GOES prototype. The use of additional channel will be considered only when SEVIRI images are available

	Nighttime	Twilight	Daytime	Sunglint
SEVIRI algorithm	Solar elevation < 0	0<Solar elevation<10	10 < Solar elevation	Cox & Munck > 10% Solar elevation > 15

(Cox & Munck stands for the reflectance computed using Cox & Munck theory (see Cox and Munck, 1954) ; the solar elevation is expressed in degrees).

Table 1.7.1.1 Definition of the illumination conditions for SEVIRI algorithm

[T3.9µm, T8.7µm , T11µm and T12µm stand for brightness temperatures at 3.9, 8.7, 11 and 12 micrometer ; R0.6µm,R0.9µm and R1.6µm stand for VIS/NIR bi-directional top of atmosphere reflectances at 0.6, 0.9 and 1.6 micrometer normalised for solar illumination ; SST is the split-window (used for SST calculation) computed from T11µm and T12µm measurements. Low Clouds in Sunglint is a specific module (detailed in 1.3.3) for low clouds identification in sunglint areas.]

Daytime	Twilight	Nighttime
Snow detection	T11µm	T11µm
T11µm	R0.6µm	T11µm-T12µm
R0.6µm	T11µm-T12µm	T11µm-T8.7µm
T11µm-T12µm	T11µm-T8.7µm	T11µm-T3.9µm
T11µm-T8.7µm	T11µm-T3.9µm	T3.9µm-T11µm
T11µm-T3.9µm	Spatial coherence	Spatial coherence
Spatial coherence	(T11µm-T3.9µm) / (T11µm-T12µm)	(T11µm-T3.9µm) / (T11µm-T12µm)

Table 1.7.1.2 Test sequence over land for SEVIRI algorithm

Daytime	Sunglint	Twilight	Nighttime
Ice detection	Ice detection	SST	SST
SST	SST	R0.9µm (R0.6µm)	T11µm-T12µm
R0.9µm (R0.6µm)	T11µm-T12µm	R1.6µm	T11µm-T8.7µm
R1.6µm	T11µm-T8.7µm	T11µm-T12µm	T11µm-T3.9µm
T11µm-T12µm	Spatial coherence	T11µm-T8.7µm	T3.9µm-T11µm
T11µm-T8.7µm	R0.9µm (R0.6µm)	T11µm-T3.9µm	Spatial coherence
T11µm-T3.9µm	T11µm-T3.9µm	Spatial coherence	
Spatial coherence	Low Clouds in Sunglint		

Table 1.7.1.3 Test sequence over sea for SEVIRI algorithm

1.7.2. Pre-launch activity :

The CMa phase 1 prototype will be used to develop PGE01 (Product Generation Element 01 : the software to extract the Cloud Mask (CMa) from SEVIRI images).

- PGE01 will :
  follow previous description
  use as much as possible SAFNWC common functions
  be spectrally tuned to process both GOES and SEVIRI channels
- PGE01 will be tested with GOES images by comparison with CMa phase-1 prototype : this validates PGE01 if the mandatory set of SEVIRI channels is used.
- PGE-01 will be implemented in a CMS pre-operational SEVIRI environment to prepare their full validation as soon as SEVIRI images are available at CMS.

1.7.3. Post-launch activity :

- The PGE01 will be run in a CMS pre-operational SEVIRI environment. It will include a visual inspection.
- As during the prototyping phase-1, test and validation files will be gathered interactively (with a procedure based on the WAVE commercial software see annex A.3.1, with an updated list of clouds, including for instance fractional clouds and marine originated stratiform and more numerous classes of aerosols) and automatically (collocated satellite imagery and surface observations extracted from SYNOP, see annex A.3.2).
- The products will be validated, and the algorithm tuned if needed (especially, the use of the new channel 8.7µm and the aerosol detection).
- A scientific report, including validation results, will be written.

1.7.4. Integration activity :

- The PGE01 will be prepared for their delivery to INM (systematic use of common functions),
- The informatic documentation will be written,
- A test case will be defined : the PGE01 to be delivered to INM will be validated at CMS (must give same result as PGE01 implemented at CMS),

The PGE01, the test case and the informatic documentation will be made available to INM.

2. Cloud type prototyping

2.1. Introduction

This chapter is a scientific description of the cloud type (CT) prototyping performed by Météo-France during the SAF NWC first development phase.

The adaptation of the cloud type to high latitude conditions is studied by SMHI and described in a separate document. To allow this study, we have delivered to SMHI a GOES training dataset (see annex A 3.1).

2.2. Overview

2.2.1. Objective

The cloud type (CT), developed within the SAF NWC context, mainly aims to support nowcasting applications. The main objective of this product is to provide a detailed cloud analysis. It may be used as input to an objective meso-scale analysis (which in turn may feed a simple nowcasting scheme), as an intermediate product input to other SAFNWC PGE, or as a final image product for display at a forecaster's desk. The CT product is essential for the generation of the cloud top temperature and height product and for the identification of precipitation clouds. Finally, it is also essential for the computation of radiative fluxes over sea or land, which are SAF Ocean & Sea Ice products.

The CT product therefore contains information on the major cloud classes : fractional clouds, semitransparent clouds, high, medium and low clouds (including fog) for all the pixels identified as cloudy in a scene. A second priority is the distinction between convective and stratiform clouds, and the identification of clouds for which the top mainly consists of water droplets.

The main application is nowcasting over the MSG N area. The consequences are twofold :

- the CT prototypes have been developed, keeping in mind that the final software must be efficient in term of computing time and that all the ancillary data needed by the software must be available in real time.
- the prototypes have been validated only in mid-latitude regions, but when available, results for polar and tropical regions are indicated

2.2.2. Background

Cloud classification algorithms are based on the fact that in window channels the spectral characteristics of clouds depend on their type, mainly through the cloud top temperature/height, (low, medium or high clouds), particle phase (ice or water clouds), and optical depth and cloud amount in the field of view (opaque or semitransparent, and completely or partially filled pixels). From the CMa product, it is assumed that cloudy (overcast opaque or partially filled) pixels are determined. The problem is then to find the set of adequate combinations of spectral channels and textural information that will separate clouds presenting different characteristics in the most satisfactory manner for the nowcasting and very short range forecast purposes, and to determine how these features are concerned by atmospheric conditions and viewing geometry.

Three techniques may be applied to classify clouds :

- Clustering techniques are scene dependent methods : they use pixel values of the entire scene or wide areas through histogram analysis or other calculations to segment the image according to predefined rules.
- Artificial neural networks are advanced multidimensional regression techniques which are capable of treating predictands and predictors in a very flexible way (allowing non linear relations).
- Multi-spectral threshold techniques are based on a pixel by pixel analysis of radiances where the cloud type of the pixel is determined when the pixel radiance goes through a sequence of threshold tests.

The chosen method should be efficient in term of computing time, make the maximum use of SEVIRI channels, be easily adapted (e.g., if one channel is missing), and be mature. Moreover, it should be possible to easily tune the algorithm (prototyped with AVHRR and GOES imagery) to SEVIRI spectral conditions before SEVIRI data are available. The multispectral thresholding technique has been chosen for the generation of the CT :

- The clustering techniques have been considered to be too scene-dependent. Making them more independent would require a pre-processing using a huge amount of previous scenes that does not seem adapted to nowcasting requirements
- Although artificial neural network techniques are promising methods, they have not been retained for day-1 software (i. e. software to be ready when MSG is launched) : the main reason is that the training of such methods, very sensitive to the learning data set, cannot rely only on simulated data. The too short period of SEVIRI availability before SAFNWC software delivery and our lack of knowledge about such methods made their use too risky for Day 1.
- One of the main advantages of the multispectral thresholding method is that it is relatively easy to adapt thresholds to varying meteorological conditions, viewing geometry using external data (NWP data, RTM calculation, climatological atlas). This physical approach will also allow an easy tuning to of the CT prototypes to MSG SEVIRI spectral characteristics. Moreover, Météo-France has a 10-years experience in applying such a technique to process AVHRR imagery (see Derrien et al, 1993).

But, even with Météo-France experience on AVHRR cloud classification based on such a thresholding technique, some differences between AVHRR and GOES imagery make necessary the study of GOES CT prototype results :

- GOES spatial resolution 4km is large enough, when compared to AVHRR 1.1 km, that there may be differences in the characterisation of sub-pixel sized clouds, and particularly the boundary layer clouds that are more sensitive to instrumental resolution changes (Wielecky, 1992).
- AVHRR takes pictures of a same area every 6 hours when two satellites are operational, this delay is large enough to let think that AVHRR cloud classification has not really proved to be stable with changes in illumination conditions. The study of this stability becomes possible with GOES prototype, with its half hourly cycle introducing only slight illumination changes from one picture to its successive. Most of the thresholding techniques apply to daytime conditions alone or to nighttime conditions alone, so that

there may appear a loss of continuity at sunset and sunrise. Animation of CT pictures is a particularly interesting tool for a visual study of the stability of the results.

2.2.3. Cloud type inputs

The CT has been prototyped with AVHRR images and GOES-East imagery locally received at CMS. The input and output data for these two prototypes are slightly different, as the AVHRR prototype is based on an existing software and the GOES-East prototype is a completely new scheme.

<u>The input for the GOES-East prototype are :</u>

- satellite imagery (see annex A.1.3) :

4 window channels (0.6 µm, 3.9 µm, 11 and 12 µm) over the Extended Northern Hemisphere at full IR spatial (the visible is averaged) every slot (i.e., every 30 minutes) in the satellite projection. Sun and satellite angles associated to GOES imagery, are computed at the segment resolution (i.e., 4*4 IR pixels).

- CMa

- NWP outputs (see annex A.2.2) :

The French NWP model ARPEGE has been used during prototyping. Six-hourly short term forecast fields of the following parameters, remapped onto satellite images (at the segment resolution, i.e. 4*4 IR pixels), are used as input (the elevation of the NWP model grid is also needed) :

  - air temperature are the following pressure levels : 850 hPa,700hPa, 500hPa, tropopause level.
  - total water vapour content of the atmosphere,

- Ancillary data sets (see annex A.2.1) :

The following ancillary data, remapped onto satellite images (at the segment resolution, i.e. 4*4 IR pixels), are used as input :

  - Land/sea/coast atlas,
  - Elevation atlas,
  - Monthly minimum SST climatology,
  - Monthly mean 0.6µm atmospheric-corrected reflectance climatology (land),

<u>The input for the AVHRR prototype are:</u>

- satellite imagery (see annex A.1.1) :

5 or 6 window channels (0.6 µm, 0.9 µm, 1.6 µm, 3.9 µm, 11 and 12 µm) at full spatial resolution in the satellite projection. Only 4 passes are processed every day. Sun and satellite angles associated to AVHRR imagery, are computed every HIRS FOV (i.e., 34*39 AVHRR pixels).

- CMa

- NWP outputs (see annex A.2.2) :

The French NWP model ARPEGE has been used during prototyping. Six-hourly short term forecast fields of the following parameters, remapped onto satellite images (at the HIRS spatial resolution, i.e. 34*39 AVHRR pixels), are used as input (the elevation of the NWP model grid is also needed) :

  - air temperatures at 700 and 500 hPa.

- Ancillary data sets (see annex A.2.1) :

The following ancillary data, remapped onto satellite images (at the HIRS spatial resolution, i.e. 34*39 AVHRR pixels), are used as input :

  - Land/sea/coast atlas,
  - Elevation atlas,
  - Monthly minimum SST climatology,
  - Monthly mean 0.6µm atmospheric-corrected reflectance climatology (land),

2.2.4. Cloud type outputs

The CT output for the GOES-East prototype are available over the Northern Hemisphere at full spatial resolution for every slots (i.e., every 30 minutes). They follow most of the specification retained for SEVIRI. These outputs are :

- The CT itself is coded on a short unsigned integer and contains twenty-one categories:
  - not processed : containing no data or corrupt data,
  - land not contaminated by clouds, aerosol or snow,
  - sea not contaminated by clouds, aerosol or ice/snow,
  - land contaminated by snow,
  - sea contaminated by ice/snow,
  - very low clouds. 2 possible classes: cumuliform & stratiform,
  - low clouds. 2 possible classes: cumuliform & stratiform,
  - medium clouds. 2 possible classes: cumuliform & stratiform,
  - high opaque clouds. 2 possible classes: cumulonimbus & not cumulonimbus,
  - semitransparent ice clouds: 4 possible classes : 3 according to thickness plus a class of cirrus above lower clouds,
  - fractional clouds,
  - aerosol clouds, 2 possible classes : volcanic & sand,
  - unclassified,
- Cloud phase flag
- Quality flag:

The quality flag (coded on a short unsigned integer) encloses :

  - one bit to flag not-processed pixels,
  - six bits to identify the conditions in which the product has been processed: use of NWP outputs in the processing, illumination conditions (day, night, dawn, sunglint), high viewing angles, missing channels,
  - one flag to indicate whether the separation between stratiform and cumuliform clouds has been attempted,

In practice, separation between stratiform and cumuliform clouds has not been studied. Moreover, during prototyping, we have defined a new cloud class (very high opaque cloud). As this class was not initially planned, we have chosen to assign in the GOES prototype « high opaque not cumuliform clouds » to opaque high clouds and « high opaque cumuliform » to very high opaque clouds.

The CT output for the AVHRR prototype are available at full spatial resolution for every processed pass. These outputs are coded on a short unsigned integer as described below. They do not follow the specifications retained for SEVIRI, because the AVHRR prototype is an adaption of an existing software.

- one bit to flag not processed area (i.e., containing no data or corrupted data),
- two bits to aerosols (sand, volcanic ash),
- one bit to flag cloud with water droplets,
- four bits to describes the cloud types (cloud free, snow/ice, very low, low, medium or high thick clouds (each time, two possible classes : stratiform or cumuliform), broken clouds, cirrus clouds (4 possible classes), not processed or not classified).

2.3. Algorithm detailed description

2.3.1. Algorithm outline

The CT prototype classification is a threshold algorithm applied at the pixel scale, based on the use of CMa and spectral & textural features computed from the multispectral satellite images and

compared with a set of thresholds. The set of thresholds to be applied depends mainly on the illumination conditions. The values of the thresholds themselves may depend on the illumination, the viewing geometry, the geographical location and NWP data describing the water vapour content and a coarse vertical structure of the atmosphere. Most of the thresholds are experimental and have been deduced from the statistical study of a training data set.

First, main cloud types are separable within two sets ; the semitransparent & fractional clouds, from the low/medium/high clouds. These two systems are distinguished using spectral features : T11µm-T12µm, T39µm-T11µm, and T11µm in night-time conditions, and R0.6µm, T11µm-T12µm in day-time conditions. Then within these two sets fractional and semitransparent are separated using either both textural features (variance T11µm coupled to variance R0.6µm) and T11µm-T12µm in day-time conditions, or only spectral features T11µm-T12µm and T3.9µm-T11µm in night-time conditions. The remaining clouds are distinguished through the comparison of their T11µm to NWP forecast temperatures at several pressure levels.

2.3.2. *Main cloud type identification*

2.3.2.1. Semitransparent and fractional clouds identification at nighttime

The semitransparent clouds can be distinguished from opaque clouds using the T11µm-T12µm or T3.9µm-T11µm feature. Indeed, T11µm-T12µm is usually higher for cirrus clouds than for thick clouds. Inoue (1985), Wu (1987) and Parol (1991) have simulated and studied the behaviour of T11µm-T12µm for cirrus clouds and have shown that this brightness temperatures difference is sensitive to the clouds' microphysical properties (phase, shape, and size distribution of cloud particles), but also to the thermal contrast between the cloud top and the surface, and of course to their cloud fractional cover or thickness. The T11µm-T3.9µm feature is also very efficient to distinguish semitransparent clouds from the opaque clouds. It is based on the fact that the contribution of the relatively warm grounds to the brightness temperature of semitransparent cloud is higher at 3.9µm than at 11µm, due to a lower ice cloud transmittance (Hunt, 1973), and to the high non-linearity of the Planck function at 3.9µm. This feature will be more efficient if the thermal contrast between cloud top and surface is large.

The fractional low clouds have also T11µm-T12µm and T11µm-T3.9µm higher than opaque clouds, which therefore may lead to confusion with high very thin cirrus. But usually fractional low clouds appears warmer than thin cirrus clouds.

From Baum (1991), we note that adding a lower level under the cirrus cloud leads to reduce T11µm-T12µm and T3.9µm-T11µm when compared to those of single level cirrus. T11µm-T12µm is more reduced than T3.9µm-T11µm, making this last feature more efficient to detect cirrus overlaying low water clouds. But it seems impossible to detect overlapping clouds with only spectral features such as T11µm-T12µm or T3.9µm-T11µm at the pixel resolution, neither with local textural features ; the GOES CT algorithm therefore does not separate cirrus overlaying low clouds from fractional cover or mid-level clouds at nighttime.

2.3.2.1.1.Description of the nighttime test serie

A pixel is classified as semitransparent if :

- T11µm < maxT11vh &
  T11µm-T12µm >Max(T11T12opaque,1.5K)
- or maxT11vh < T11µm < maxT11hi &
  T11µm-T12µm > Max(T11T12opaque, 1.5K)

- or maxT11hi < T11µm < maxT11med &
  (T3.9µm < 240K & T11µm-T12µm > Max(T11T12opaque, 1.5K)
  or (T3.9µm > 240K & T3.9µm-T11µm > Max(T39T11opaque,3.5K))
- or maxT11med< T11µm < maxT11low &
  (T3.9µm < 240K & T11µm-T12µm > T11T12thr)
  or (T3.9µm > 240K & T3.9µm-T11µm > Max(T39T11opaque,3.5K))

A pixel is classified as fractional if :

- maxt11low<T11µm< maxT11low+delta&
  T11µm-T12µm > Max(T11T12opaque, 1.5°C)
  & T39T11opaque-2°C <T3.9µm-T11µm < Max(T39T11opaque,3.5K)
- or T11µm> maxT11low+delta &
  T11µm-T12µm > T11T12thr
  & T3.9µm-T11µm > T39T11opaque-2K

Delta is aimed to allow the classification of warm cloudy pixels as semitransparent clouds, but to forbid it when their T11µm is too warm, doing so avoid misclassification of fractional clouds as semitransparent. This quantity delta is hence governed by the difference between maxT11low and the cloud free surface temperature, and affected by diurnal cycle. T11T12thr, having characteristics depending on both diurnal cycle and atmospheric water vapour content was a good candidate to simulate this quantity. Considering results observed with the interactive file, it has been empirically determined as 2*T11T12thr.
The maxT11low, maxT11med, maxT11hi and maxT11vh thresholds are explained in 2.3.2.3. The thresholds applied to T11µm-T12µm (T11T12opaque and T11T12thr) and to T3.9µm-T11µm (T39T11opaque) are explained below.

2.3.2.1.2.Nighttime thresholds computation

The thresholds to be applied to T11µm-T12µm and T3.9µm-T11µm should be higher than the usual values observed for opaque clouds, which depend on the water vapour content above the cloud and on the satellite zenith angle (see figure 2.3.2.11). To estimate this dependency, we have applied RTTOV to radio-soundings from TIGR dataset, using emissivities equal to unity and air temperature equal to surface temperature and derived tables with water vapour content (above the cloud) and satellite zenith angle as input. The dependency for opaque clouds of T11µm-T12µm and T3.9µm-T11µm with the atmospheric integrated water vapour content (computed from the surface and not above the cloud) has also been regressed from the interactive file, and the comparison with the simulation shows an agreement for the shape of the curves, but with difficulties to observe same values for high water vapour contents. Finally, the thresholds are computed as follows :

- T11T12opaque and T39T12opaque are interpolated from the precomputed tables of RTTOV simulated thresholds, water vapour content and satellite zenith angle.
- T11T12thr is the threshold used to separate cloudy from cloud-free pixels (see 1.3.3.3).

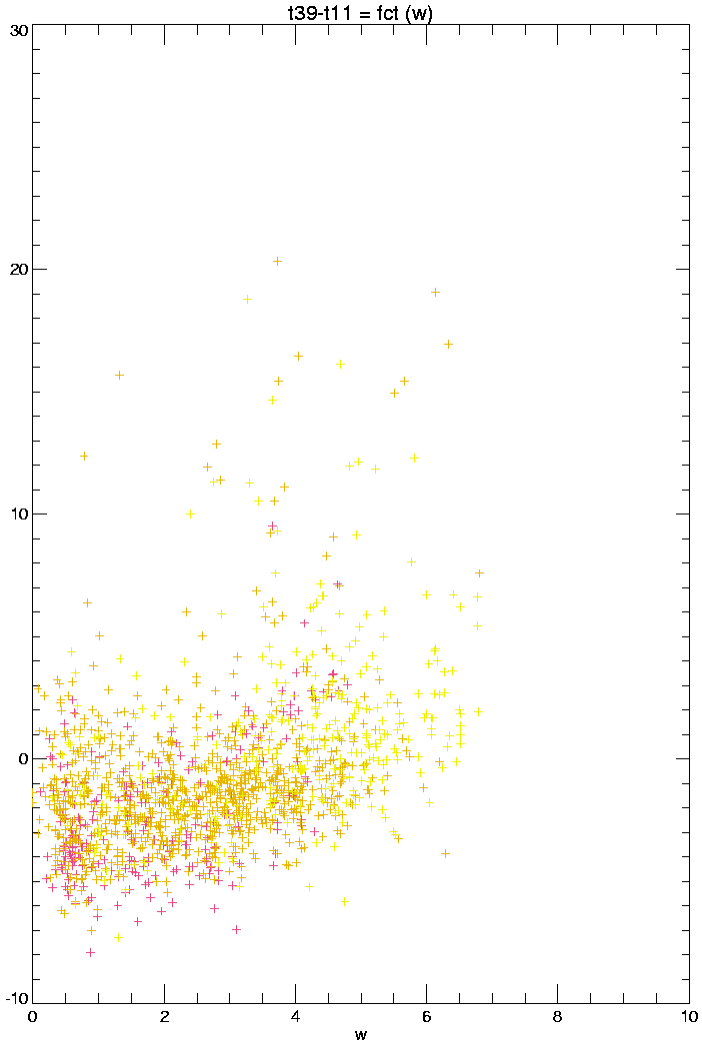

Figure 2.3.2.1.1 Observed T3.9µm-T11µm for low clouds as function of total water vapour content (computed above the surface)

2.3.2.2. Semitransparent and fractional clouds identification at daytime

At daytime, the 0.6µm channel can be used to identify semitransparent or fractional clouds, presenting lower R0.6µm reflectances than opaque clouds having the same radiative temperature. This is obvious when looking at figure 2.3.2.2.1 where R0.6µm are plotted versus T11µm for all the clouds of the interactive file at daytime. This figure shows that space R0.6µm versus T11µm can be roughly divided into two areas ; one where semitransparent clouds represent the most frequent clouds (low R0.6µm) but where also fractional low clouds can be seen, and another one where only few semitransparent clouds are observed among low water clouds or more opaque high clouds. It is also noticeable that R0.6µm of semitransparent clouds increases as their brightness temperature decreases. The set of thresholds used for the identification is based on this behaviour of R0.6µm as a function of T11µm.

The second feature used is T11µm-T12µm as for nighttime conditions, as T11µm-T12µm of semitransparent clouds is higher than for other clouds.

The separation of semitransparent and fractional is finally performed using R0.6µm and T11µm local variances : high semi-transparent clouds being highly spatially variable in temperature and fractional clouds highly inhomogeneous in reflectance, as is illustrated on figure 2.3.2.2.2.

Semitransparent over low or medium clouds could also be identified : they appear rather bright and cold, but are characterised by rather high T11µm-T12µm (if the thermal contrast between cirrus and lower cloud layer top temperature is large enough).

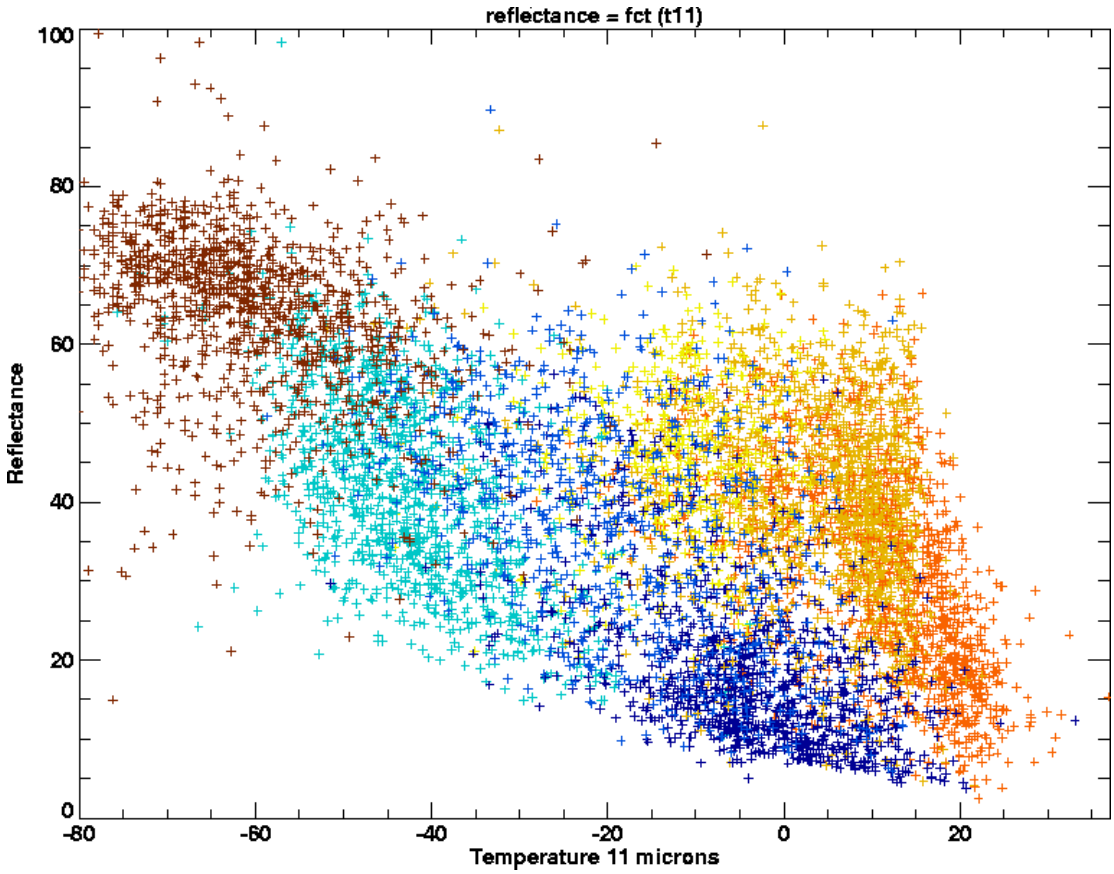

Figure 2.3.2.2.1 Illustration with the interactive file, of the separability of semitransparent and fractional clouds from opaque clouds using R0.6µm and T11µm.

[Colour convention : orange for very low clouds (stratus and cumulus, ochre for low clouds, yellow for mid-level clouds, dark blue for thin cirrus, blue for cirrus and cirrostratus, clear blue for cirrus over low or medium level clouds, brown for isolated or merged thick cumulonimbus]

2.3.2.2.1.Description of the daytime test serie

A pixel is classified as semitransparent if :

- T11µm < maxT11vh &
  T11µm-T12µm > Max(T11T12opaque,1.5K)
- or maxT11vh < T11µm < maxT11hi &
  T11µm-T12µm > Max(T11T12opaque, 1.5K)
- or maxT11hi < T11µm < maxT11med &
  R0.6µm < maxCiCh1
  & T11µm-T12µm > Max(T11T12opaque, 1.5K))
- or maxT11med < T11µm < maxT11low &
  [R0.6µm > maxCiCh1 &
  T11µm-T12µm > Max(T11T12opaque, 1.5K) &
  varilogt11/varilogvis > varilogthr]
  or [R0.6µm < maxCiCh1 &
  T11µm-T12µm > Max(T11T12opaque, 1.5K))]
- or maxT11low < T11µm < maxT11low +delta &
  R0.6µm < maxCiCh1
  & T11µm-T12µm >t11t12thr

A pixel is classified as semitransparent over low/medium clouds if :

- maxT11hi < T11µm < maxT11med &
  R0.6µm > maxCiCh1
  & T11µm-T12µm > Max(T11T12opaque, 1.5K)

A pixel is classified as fractional if :

- maxT11med< T11µm < maxT11low &
  R0.6µm < maxCiCh1
  & T11µm-T12µm< Max(T11T12opaque, 1.5K)
- or maxT11low < T11µm < maxT11low +delta &
  [R0.6µm > maxCiCh1
  & T11µm-T12µm > T11T12_edge]
  or [R0.6µm < maxCiCh1
  & T11µm-T12µm < T11T12_edge]
- or maxT11low +delta < T11µm &
  T11µm-T12µm > T11T12_edge
  or R0.6µm < minLowCh1

The maxT11low, maxT11med, maxT11hi and maxT11vh thresholds are explained in 2.3.2.3. Thresholds applied to T11µm-T12µm (T11T12_edge and T11T12opaque), R0.6µm (maxCiCh1 and minLowCh1) and to the local variance of R0.6µm and T11µm (varilogthr) are detailed below.

2.3.2.2.2.Daytime thresholds computation

The computation of T11T12opaque (threshold applied to T11µm-T12µm) has already been described in the previous paragraph.

T11T12_edge has been simply deduced from T11T12thr which is the threshold used to separate cloudy from cloud-free pixels (see 1.3.3.3) by T11T12thr, after several empirical attempts on the interactive file.

Following the observation that the two areas in the R0.6µm/T11µm space corresponding to the semitransparent/fractional clouds and the opaque clouds can be roughly separated by a straight line, the threshold applied to the R0.6µm reflectance (maxCiCh1) is obtained as a linear function of T11µm brightness determined by two reference points :

- The coldest and brighter one is determined by: (T11µm=223.15K, R0.6µm=35%).
- The warmest and darker one is depending surface effects and atmospheric effects :
  - Its reflectance depends on the surface reflectance, for which we have an indication from a sea reflectance when over sea or the monthly mean 0.6µm value from climatology when over ground. A constant safety offset of 7% is added to this reflectance to account for uncertainties on climatology, turbid waters, calibration.
  - Its temperature is estimated from the SST climatology file over sea or from NWP 2m forecast temperature over land.

Two sets (sea and land) of thresholds (slope and intercept of the straight line) are then computed by accounting for cloud bidirectional effects (using coefficients proposed by Manalo & Smith, 1996, overcast model, and with a weighting factor of 0.4 for Rayleigh part), for the visible calibration variation with time, and for the variation of earth-sun distance.

MinLowCh1 is aimed to put a minimum value to an acceptable reflectance of a low cloud, it is mainly aimed to separate fractional and low clouds. It is derived from a constant value (10%)

accounted for bidirectional effects (using coefficients proposed by Manalo & Smith, 1996, overcast model, and with a weighting factor of 0.4 for Rayleigh part).

The features used in the separation of fractional and semitransparent clouds are varilogt11=log(1+ var(T11μm)) and varilogvis=log(1+var(R0.6μm)/13.) where var stands for the standard deviation in a bin of 9 pixels centred on the pixel to classify. The threshold applied to the ratio varilogt11/varilogvis (varilogthr) is 2.2

2.3.2.2.3.Efficiency based on interactive file

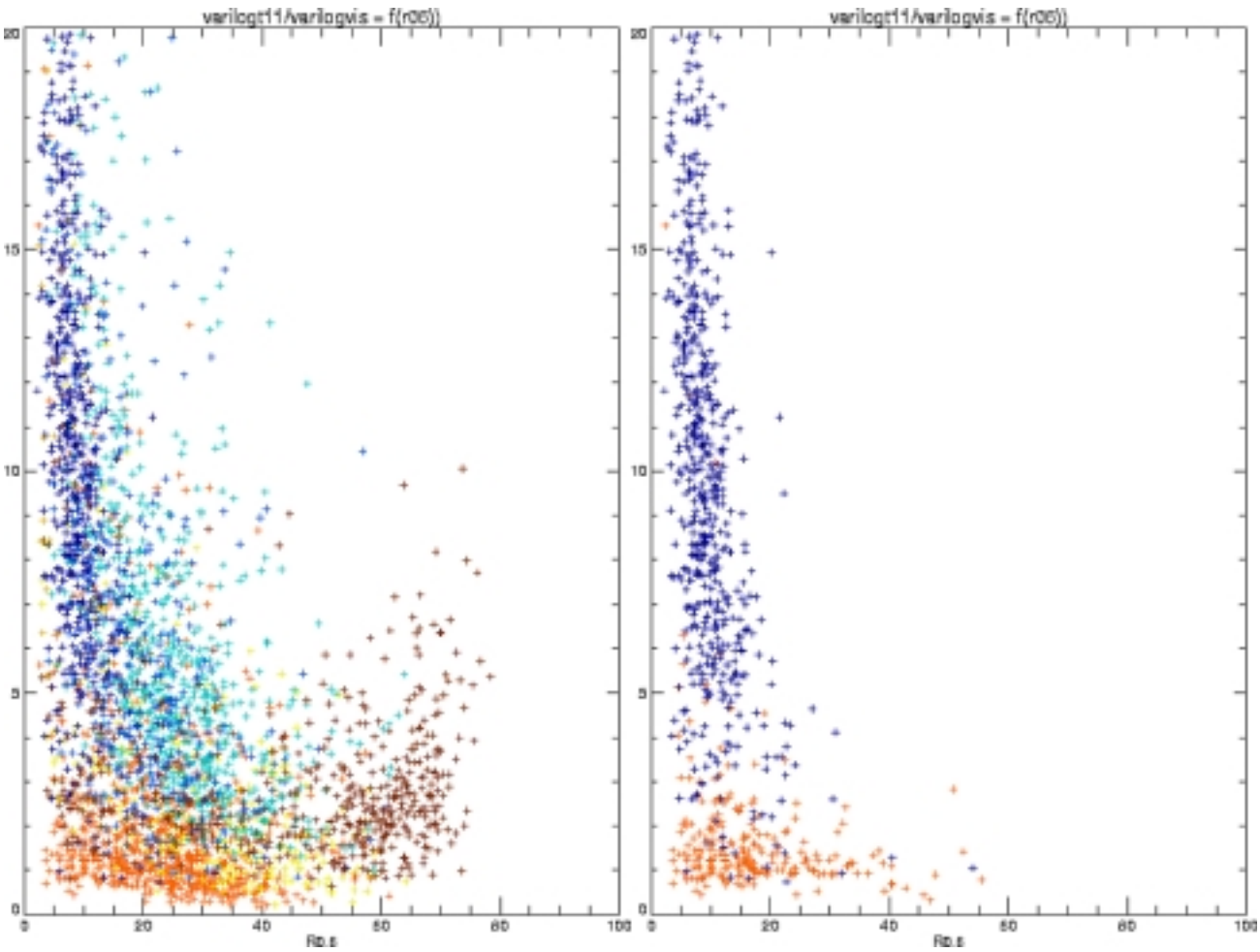

Figure 2.3.2.2.2 Illustration with the interactive file, of the separability of semitransparent from fractional clouds using ratio of T11μm and R0.6μm local variances. Left plot illustrates the features for all cloud types, right is a restriction to semitransparent and low cumuliform clouds

[Colour convention : orange for very low clouds (stratus and cumulus, ochre for low clouds, yellow for mid-level clouds, dark blue for thin cirrus, blue for cirrus and cirrostratus, clear blue for cirrus over low or medium level clouds, brown for isolated or merged thick cumulonimbus]

2.3.2.3. Low/medium/high clouds separation

When the semitransparent or fractional clouds have been identified, the classification of the remaining cloudy pixels between low, mid-level and high clouds is performed through a simple thresholding on the T11μm brightness temperature which is related to their height. In order to account for atmospheric variability on the scene to analyse, NWP forecast temperatures at several pressure levels are used to compute the thresholds that allows to separate very low from low clouds

(maxT11low), low from medium clouds (maxT11med), medium from high clouds (maxT11hi), and high from very high clouds (maxT11vh). These thresholds used in GOES CT prototype have been derived from statistical behaviour of clouds observed in the interactive file.
Note that, as the « very high cloud » class was not initially planned and as the separation between stratiform and cumuliform clouds has not been studied (see 2.3.4), we have chosen to assign, in the GOES prototype, « high opaque cumuliform » to very high opaque clouds.

2.3.2.3.1. Description of the test serie

A pixel is classified as :

- very high if not semitransparent or fractional & T11µm < maxT11vh
- high if not semitransparent or fractional & maxT11vh < T11µm < maxT11hi
- medium if not semitransparent or fractional & maxT11hi < T11µm < maxT11med
- low if not semitransparent or fractional & maxT11med < T11µm < maxT11low
- very low if not semitransparent or fractional & maxT11low < T11µm

2.3.2.3.2.2 Thresholds computation

The four thresholds have been determined according to statistical results obtained when studying the very low, low, medium, and high clouds from the interactive file. We have fitted the targets' T11µm brightness temperatures of each group of clouds with their air temperature at selected pressure levels forecast by NWP. In a second step we subtracted to these values a quantity allowing a separation between the clouds from a given level to the clouds from the upper level. The thresholds are the following :

- $maxT11vh = 0.4 * T_{500hPa} + 0.6 * T_{tropo} - 5$ K
- $maxT11h = 0.5 * T_{500hPa} - 0.2 * T_{700hPa} + 178$ K
- $maxT11me = 0.8 * T_{850hPa} + 0.2 * T_{700hPa} - 8$ K
- $maxT11low = 1.2 * T_{850hPa} - 0.2 * T_{700hPa} - 5$ K

In order to give concrete expression to them, table 2.3.2.4.1 expresses their mean and standard deviation computed from all the targets of the interactive file.

	Mean	Standard deviation
maxT11vh	226.13 K	3.9 K
maxT11h	250.93 K	2.6 K
maxT11me	275.2 K	9.2 K
maxT11low	281.3 K	9.7 K

Table 2.3.2.4.1 Mean and standard deviation of thresholds applied to T11µm before other considerations, from the whole set of targets.

2.3.2.3.3.Efficiency based on interactive file

The efficiency of each threshold for the separation of clouds' levels is illustrated on the following plots of Figure 2.3.2.3.1.

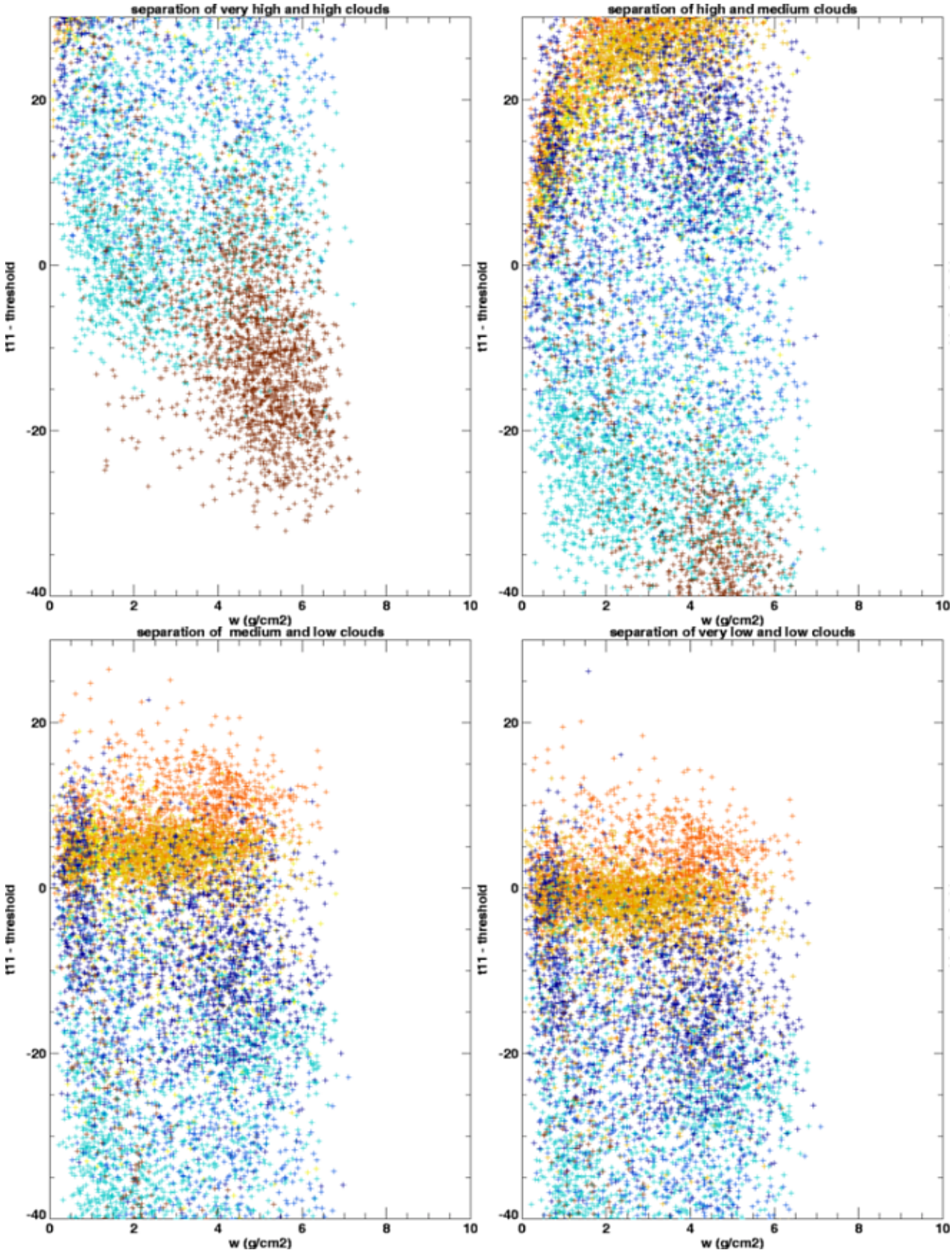

Figure 2.3.2.3.1 Illustration with the interactive file, of the separability of very low, low, medium, high and very high clouds using T11µm.
[Colour convention : orange for very low clouds (stratus and cumulus, ochre for low clouds, yellow for mid-level clouds, dark blue for thin cirrus, blue for cirrus and cirrostratus, clear blue for cirrus over low or medium level clouds, brown for isolated or merged thick cumulonimbus]

2.3.3. *Cloud phase determination*

The analysis of cloud phase determination (optional study) was planned to be performed during a visiting scientist stay in 2000, but the stay has been recently cancelled.

2.3.4. *Cumuliform clouds identification*

This optional study has not been performed, due to time constraints.

2.4. Practical application

2.4.1. *Implementation of the cloud type scheme*

2.4.1.1. AVHRR prototype

We have just modified an existing operational software described in Derrien et al ., 1993, and summed up below :

- The AVHRR imagery is processed in satellite projection
- In a first step, most of the thresholds used are computed in segments (boxes of 34*39 AVHRR pixel centred on HIRS F.O.V), using monthly climatological maps, atlas and NWP model forecast fields available at $1/6^{th}$ degree horizontal resolution on the Lannion HRPT acquisition area.
- In a second step, the cloud type is computed at the AVHRR pixel resolution using thresholds available at the segment resolution.
- The modified scheme is daily applied on a development workstation : the four AVHRR passes the most centred over France are processed every day.
- The result is available over the whole processed area in satellite projection.

2.4.1.2. GOES prototype

As already mentioned in the CMa description, the GOES prototype is a completely new scheme that fulfils most of the specifications defined for the SEVIRI software. It is detailed in this chapter.

- The software is implemented on a pre-operational workstation financed by Eumetsat for the SAFNWC project. This UNIX workstation receives half-hourly GOES images, and all the needed NWP fields (from 00h and 12h with 12h and 18h time forecast terms) to allow the cloud type computation every half an hour.
- The software may be applied to several regions (rectangular in the satellite projection) located in the GOES Extended Northern Hemisphere (illustrated in annex A.5)., and defined by their name, the location of their north-west corner and their number of rows/lines. The user may chose the whole Extended Northern Hemisphere itself.
- The user must define the size of segments for each processed regions. Segments are square boxes (in the satellite projection). All the solar and satellite angles, the NWP forecast parameters, the atlas values and the thresholds will be derived over all the

processed regions at the horizontal resolution of the segment. During the prototyping, we have usually used segment size of 4x4 GOES IR pixels, but have also tested segments of one individual GOES IR pixel (see 1.4.3). The land/sea atlas is available at the full GOES IR resolution, allowing the identification of the surface type (land or sea) of every IR pixels, whatever the segment size.

- Once the regions are defined, a script prepares (only once) the regional monthly climatological and atlas maps, as well as latitude/longitude and satellite angles information for his regions at the full IR horizontal resolution. These regional atlas and maps are extracted from maps available on the whole extended northern hemisphere, and stored on a dedicated directory., to be used during the routine processing.
- The routine processing is performed in three steps. All the regions are processed sequentially.
    - the preliminary step is the reprojection of NWP model forecast fields on the regional regions at the segment resolution. This is monitored by a crontab, twice a day, this step provides regional remapped NWP data valid for a given time. The number of regions depends on the list of regions declared by the user.
    - the preparation step includes the computation on the regional areas at the segment horizontal resolution of solar & satellite angles, monthly climatological & atlas maps, and required thresholds for the CT determination. This is also monitored by a crontab. The action is launched 48 times per day per region before the normal availability of the 48 GOES images. The ArchiPEL scheduling mechanisms guarantee that one real time action is not performed during an off-line action, so that resource sharing conflicts have not to be thought about when coding.
    - the execution step is the real-time processing of the GOES images themselves over the regions. This process is activated within the same script as the CMa i.e when all the input images (on the whole GOES Extended Northern Hemisphere) but when the associated CMa is available. The cloud type is computed at the IR GOES pixel resolution [the visible reflectances are available at 1km resolution but are averaged on the corresponding IR pixel (4km)].

2.4.2. Impact of missing NWP information

The prototypes that have been developed are not robust : they require the availability of all satellite channels and auxiliary data (climatological and atlas maps, and NWP output). Climatological and atlas maps are stored on the disk of the satellite image processing system, and therefore always available. We have never faced a situation where a single satellite channel was missing : this would happen in case a failure of the radiometer itself.. On the contrary, NWP fields are produced by a NWP model (external to the satellite processing system), transferred to the satellite processing system : there are therefore reasons why some fields may be missing.

The impact of missing NWP parameters on the results' accuracy has been estimated using the GOES interactive file. Tables 2.4.2.1 and 2.4.2.2 (see 2.5.1 for the meaning of their content) present statistics on the cloud types if needed NWP parameters are unavailable and replaced by climatological values (integrated water vapour content, air temperature at 850, 700, 500hPa see annex A.2.1) or constant values (-60°C for the tropopause temperature, as no climatology was available for this parameter). The main conclusions from this comparison are :

- an increase of the misclassification of cirrus clouds as fractional clouds

- less low clouds are classified as fractional clouds
- high thick non cumuliform clouds are more often confused with thick semi-transparent clouds
- eitherwise, as expected, the repartition between very low, low, mid-level and high clouds has been slightly changed.

	Producer accuracy (NWP used)	**Producer accuracy (Climatology used)**	**User accuracy (NWP used)**	**User accuracy (climatology used)**
Sea	96.0%	93.1%	95.5%	95.8%
Land	95.9%	89.9%	80.0%	80.8%
Ice	60.2%	60.2%	88.6%	89.2 %
Snow	52.4%	52.4%	75.6%	75.6%
Very Low	43.2%	62.6%	41.9%	43.5%
Low	53.5%	46.0%	65.2%	72.2%
Mid	62.8%	61.0%	59.1%	54.6%
Semi Above	22.0%	20.2%	40.3%	38.2%
Semi Thin	15.2%	14.0%	73.2%	69.9%
Semi Thick	51.5%	53.1%	25.6%	26.3%
High Nocu	54.3%	53.4%	41.7%	41.0%
High Cu	77.8%	74.8%	77.8%	84.5%

Table 2.4.2.1 Comparison of producer and user accuracy (for all climatic and viewing conditions) if NWP or climatological values are used.

	Sea	Land	Ice	Snow	Very Low	Low	Mid	Semi Above	Semi Thin	Semi Thick	High Nocu	High Cum	Sand	Ash	Fract	Total
Sea	**1756**	8	6	1	39	2	0	2	5	2	0	0	0	0	8	1829
Land	13	**1346**	0	1	13	7	2	1	1	1	0	0	0	0	19	1404
Ice	0	2	**124**	23	31	18	1	1	1	2	3	0	0	0	0	206
Snow	0	53	0	**133**	32	24	7	0	1	3	1	0	0	0	0	254
Very Low	24	114	1	7	**629**	351	50	9	37	6	0	0	0	0	228	1456
Low	27	64	2	1	490	**1054**	205	6	12	15	4	0	0	0	90	1970
Mid	1	13	0	0	116	120	**851**	28	14	72	117	1	0	0	23	1356
Semi Above	0	3	0	0	6	15	151	**182**	15	376	74	1	0	0	4	827
Semi Thin	7	54	7	10	30	15	81	202	**242**	839	28	0	0	0	74	1589
Semi Thick	0	0	0	0	0	0	10	11	1	**537**	416	67	0	0	0	1042
High Nocu	0	0	0	0	0	1	54	10	0	196	**703**	331	0	0	0	1295
High Cu	0	0	0	0	3	0	22	0	0	45	331	**1405**	0	0	0	1806
Sand	0	0	0	0	1	7	2	0	0	0	0	0	**0**	0	0	10
Ash	9	21	0	0	111	1	0	0	0	0	0	0	0	**0**	52	194
Total	1837	1678	140	176	1501	1615	1436	452	329	2094	1677	1805	0	0	498	**15238**

	Sea	Land	Ice	Snow	Very Low	Low	Mid	Semi Above	Semi Thin	Semi Thick	High Nocu	High Cum	Sand	Ash	Fract	Total
Sea	**1720**	8	6	1	50	1	0	2	8	2	0	0	0	0	50	1848
Land	11	**1265**	0	1	58	5	5	1	1	0	0	0	0	0	60	1407
Ice	0	2	**124**	22	37	7	3	2	0	2	5	0	0	0	2	206
Snow	0	56	0	**133**	24	11	19	1	4	2	4	0	0	0	0	254
Very Low	22	91	1	7	**914**	153	62	6	37	3	0	0	0	0	164	1460
Low	21	49	2	1	561	**907**	317	6	9	15	3	0	0	0	82	1973
Mid	0	9	0	0	159	113	**830**	29	15	74	89	2	0	0	40	1360
Semi Above	0	4	0	0	35	22	132	**167**	20	361	68	1	0	0	18	827
Semi Thin	7	46	6	11	95	28	54	191	**223**	739	24	0	0	0	167	1591
Semi Thick	0	0	0	0	1	1	12	12	0	**554**	421	40	0	0	2	1043
High Nocu	0	0	0	0	9	6	61	20	2	298	**692**	206	0	0	1	1295
High Cu	0	0	0	0	0	0	20	0	0	59	377	**1356**	0	0	0	1812
Sand	0	0	0	0	0	9	1	0	0	0	0	0	**0**	0	0	10
Ash	14	31	0	0	150	1	0	0	0	0	0	0	0	**0**	20	215
Total	1795	1561	139	176	2103	1254	1515	437	318	2109	1683	1604	0	0	606	**15301**

Table 2.4.2.2 Error matrix for all climatic and viewing conditions.(Top if NWP parameters are used ; bottom if climatological values are used)

2.4.3. Estimation of needed informatic resources

CPU and virtual memory size required by both the preparation step (offline computation of thresholds) and the execution step (real time computation of the Cloud Type) have been estimated in the GOES prototype for a 512 by 512 IR pixels region and a segment size of 4 by 4 :

- CT preparation : CPU time : 31 seconds Virtual memory Size : 6312 Kbytes
- CT execution : CPU time : 14 seconds Virtual Memory Size : 14096 Kbytes

CPU time and Virtual Memory Size have been measured on a development workstation Sun ULTRA Creator 140E running under SunOS 5.7 for tasks compiled without any optimisation. The exact meanings of « CPU time » and « Virtual Memory Size » are those of the **ps** UNIX command.

2.5. Validation

2.5.1. Comparison with interactive file

The comparison with the interactive file of the cloud types, as determined by the GOES CT algorithm and as manually labelled, is an indicator of the CT algorithm's quality but also of the separability of the cloud classes, and a way to understand how the CT algorithm manages classes. The results presented in this paragraph are a first attempt to assess the GOES CT accuracy, but figures must be handled carefully, because ;

- the interpretation of the observer is not 100% correct, due to the closeness of several types
- the choice for the class grouping is questionable and may act upon the numerical results
- the whole set of mid-latitude subset used for testing the CT have been used for the training of the thresholds, leading to an overestimation of the CT accuracy that the user must notice
- the fractional clouds is not a class of the observers' types, therefore it can never be well classified, but is taken into account for the statistics.

Thirty eight classes can be identified by the observer labelling its selected target from the satellite picture, and twenty one classes are potentially identified by CT prototype, so that there is no bijection between the two sets. In order to make feasible a comparison, we have grouped together types from the interactive data set as indicated in the first column of table 2.5.1.1 Their equivalent in the CT types is given in the second column of table 2.5.1.1 The most questionable "group classes" are those related to semitransparent above lower clouds and the separation between thin and thick semitransparent clouds because this separation is really subjective.

Group Class name	Target type	CT type
Sea	Open sea, Sea with haze, Sea with shadow, Sea with sunglint	Sea not contaminated by clouds, aerosol or ice/snow
Land	Land, land with haze, land with shadow,	Land not contaminated by clouds, aerosol or snow
Ice	Ice, ice with shadow	Sea contaminated by ice/snow
Snow	Snow, snow with shadow	Land contaminated by snow
Very Low	Fog, stratus, small cumulus over land, small cumulus over sea	Very low clouds
Low	Stratocumulus, stratocumulus with shadow,	Low clouds
Mid-level cloud	Altocumulus, Altostratus, cumulus congestus over land and sea	Medium clouds
Semitransparent Above lower clouds	Thin cirrus above stratus or stratocumulus or cumulus	Cirrus above lower clouds
Semitransparent Thin	Thin cirrus over sea, thin cirrus over land, thin cirrus over snow, thin cirrus over ice.	Thin cirrus
Semitransparent Thick	Cirrostratus	Mean and thick cirrus
High opaque no cum.	Cirrostratus over Altocumulus or Altostratus. Thin cirrus over Ac As	High opaque clouds not cumulonimbus
High opaque cum	Isolated or merged Cb	High opaque clouds
Sand	Sand above sea, sand above land	Aerosol sand
Ash	Volcanic ash over sea Volcanic ash over land	Aerosol volcanic ash
		Fractional clouds

Table 2.5.1.1 Equivalence between targets and CT types

The result of CT over a 5x5 target is compared with the class of the target given by the observer. There is an agreement if the most probable CT "group class" (i.e. the most frequent "group class" among the 9 central pixels of the target) is the same as the Observer "group class".

In order to measure the accuracy of GOES CT prototype to separate low, mid-level , semitransparent and high clouds we have also created "metaclasses" by gathering very low and low into low, all semitransparent clouds into a single semitransparent and high opaque clouds into a single high class, and by removing sand and ash cases from the interactive data set.

A first indication of the accuracy of the GOES CT prototype is given by the overall accuracy (total correctly classified targets divided by total number of targets, given in tables 2.5.1.2 and 2.5.1.3), computed for the "metaclasses" and for the "group classes" according to the equivalence between given by table 2.5.1.1. The better results for the global set are certainly due to the fact that the whole interactive file has been used to train the thresholds, which are then used in the algorithm. Table 2.5.1.3 shows that introducing details into the "metaclasses" decreases the overall accuracy by 20% from about 80% to about 60%.

	Whole Set	Mid-latitude subset
all targets	80.1%	77.3%
daytime	78.7%	78.0%
nighttime	82.8%	78.7%
twilight	80.7%	77.5%

Table 2.5.1.2 Overall accuracy of GOES CT prototype for classification of "metaclasses" (sea, land, snow /ice, low clouds, mid level clouds, semitransparent, and high clouds).

	Whole Set	Mid-latitude subset
all targets	57.6%	56.9%
daytime	60.9%	58.5%
nighttime	59.0%	53.7%
twilight	50.2%	54.1%

Table 2.5.1.3 Overall accuracy of GOES CT prototype for classification of "group classes" as defined in table 2.5.1.1

Another indicator of the CT classifier is given by error matrixes (also called contingency tables). They are computed for the "metaclasses" and for the "group classes" of the CT GOES prototype, for different illuminations conditions (daytime, nighttime and twilight). The full tables are available in the annex 6 (tables A.6.1 for the metaclasses and tables A.6.2 for the group classes). In those error matrixes the rows represent the observers' classes (considered as reference) while the columns figures represents the CT classifier results. Therefore, the total figure at the end of each row is the number of targets in the group class of the reference set, and the total figure at the end of each column is the number of targets classified in the "group class" by the CT classification algorithm. The producer's accuracy, which represents the probability of a target being correctly classified, and the user's accuracy , which represents the probability of a pixel classified into a category on a picture to really belong to that category are also given, and their variation with illumination conditions and geographic areas are synthesised and displayed on figures 2.5.1.1 - 2.5.1.4 (full tables available in annex 6 (table A.6.3 and A.6.4)). They are more interesting measures than the overall accuracy and show details in the behaviour of the classifier.

Main comments about the results are :

- Concerning "metaclasses" :
  - The overall accuracy figures is above 75%, the best being observed at nighttime. The comparison of these results with the overall accuracy of CMa (table 1.5.1.2) shows that introducing snow and ice classes and detailing the cloudy targets into four main classes leads to decrease the overall accuracy from about 96% to about 80%.
  - From the user point of view, the less reliable class among the "metaclasses" is the mid level clouds class, with a user accuracy of 60%. It can be understood by the weak spectral separability of the medium clouds. For all the other cloud "metaclasses", the user accuracy is above 75%, and it is noticeable that except for mid level cloud the user accuracy is good and quite the same as the one measured for the land class.

- Only 9% of low clouds and 2% of mid level clouds are classified as fractional, but 2% of the semitransparent clouds are really misclassified as fractional. For the user, 75.6% of the pixels identified as fractional cloud are low or mid level clouds while 17.7% of them should probably be semitransparent. The relatively weak number of fractional clouds at nighttime conditions, when compared to the one obtained at daytime conditions is still to be explained (algorithm ? diurnal effects ?...)
- When analysing the CT classes users' accuracy behaviour with changes in daytime and nighttime conditions one can note their stability (except for snow (non detected at nighttime) and fractional clouds (much less frequent at nighttime)), indicating a certain independency of the CT classifier behaviour to the illumination conditions.

- Concerning all CT "group classes" :
  - When detailing the cloud "metaclasses" into CT "group classes" the overall accuracy decreases down to 60%.
  - An overall accuracy of 56% for the mid-latitude subset is not so good, but it carries the difficulty to separate several classes of low cloud and semitransparent clouds, belonging to same "metaclass". A misclassification inside a given "metaclass" having the same weight as an error between two classes really different. This difficulty which is also present in the observer's classification contributes to make the reference dependent on the observer's skill.
  - Very low and low clouds are a little bit more difficult to "produce" than the medium clouds (the last being in fact in fact less reliable for the user), with a user's accuracy for very low clouds artificially reduced by the fact that about 15% (small cumulus) of them are well classified as fractional clouds, but counted as erroneous.
  - Thin semitransparent clouds are the most difficult clouds to "produce" by CT classifier and particularly at nighttime. But when classified their probability to be really thin semitransparent is good (>90%) at night.
  - The distinction between several semitransparent classes decreases also the accuracy of the classifier, mainly due to a really poor separability of thick cirrus, cirrus above clouds (not identifiable at nighttime and then increasing the misclassifications for the other classes), and high not cumuliform clouds.
  - High opaque cumuliform clouds are well typed with a users' accuracy of 78%, being generally misclassified as high opaque not cumuliform.

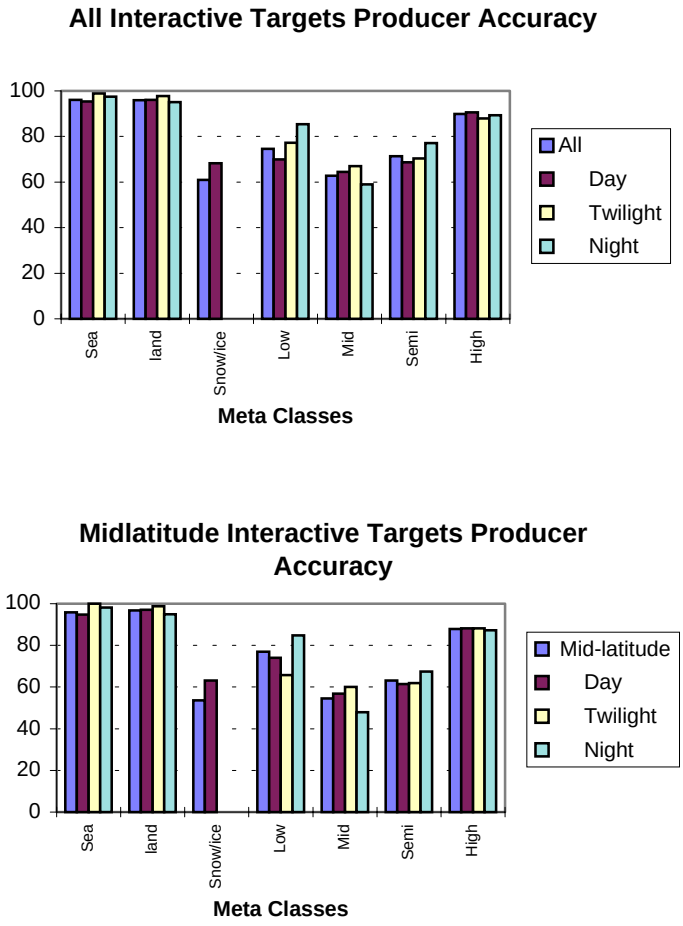

Figure 2.5.1.1 Variation of producer accuracy of meta classes from interactive file for whole set and midlatitude area with illumination conditions

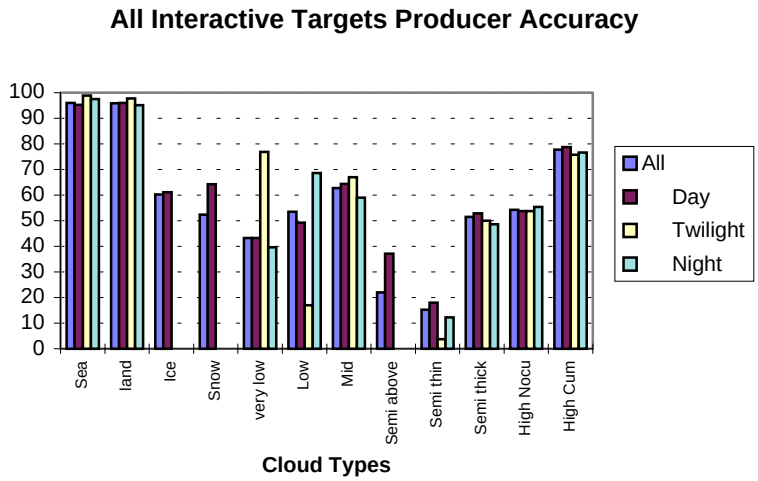

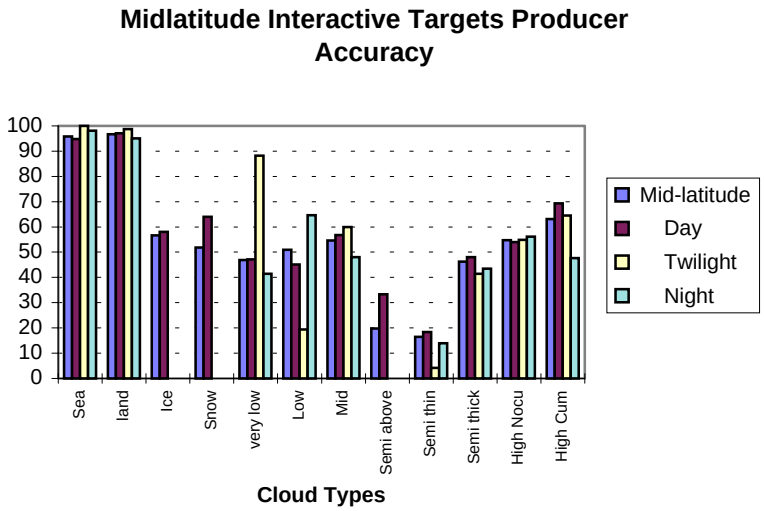

Figure 2.5.1.2 Variation of producer accuracy of group classes from interactive file for whole set and midlatitude area with illumination conditions

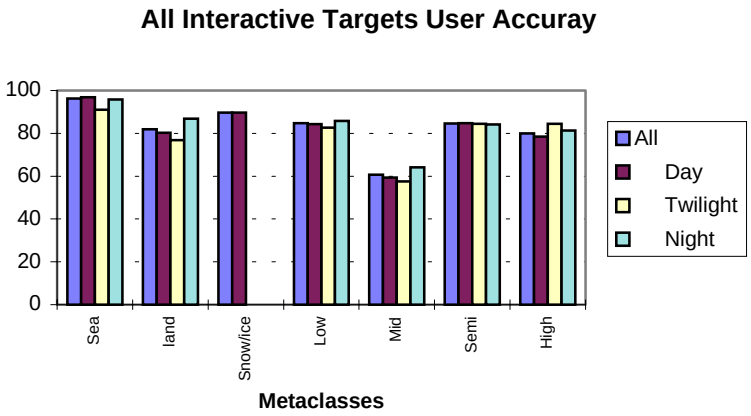

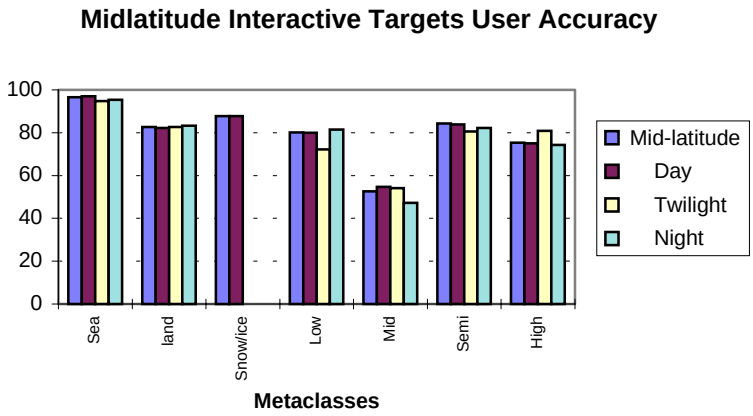

Figure 2.5.1.3 Variation of user accuracy of meta classes from interactive file for whole set and midlatitude area with illumination conditions

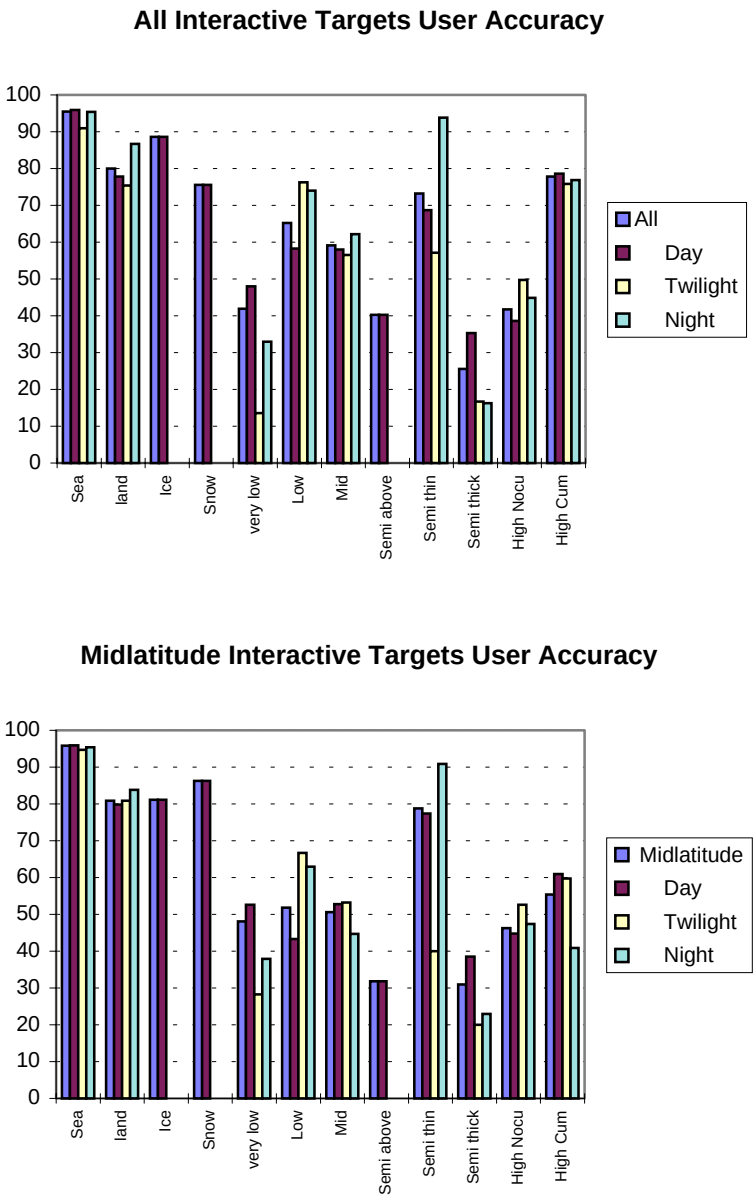

Figure 2.5.1.4 Variation of user accuracy of group classes from interactive file for whole set and midlatitude area with illumination conditions

2.5.2. Comparison with surface observation

The quantitative comparison of the GOES CT prototype with surface synoptic observations has been made possible thanks to the use of the coincident satellite targets and SYNOP data gathered from the two years from July 1st 1997 to July 1st 1999. From the SYNOP data set (see A.3.2), total cloud cover and partial cloud covers for low, medium and high levels are available. We have applied the CT classifier to the coincident GOES-08 data set, satellite cloud type is then the result of the CT classification for the central pixel of the satellite target and its surroundings. The satellite pixels, supposed to be within the field of view of the surface observer, are used to simulate the surface observation. No attempt has been made to take into account the complexity of the observation, and all the nine pixels inside the central part of the satellite data target are used for the evaluation. The slots retained for the satellite target selections starts at about 15 minutes before the UTC reference time of the SYNOP observation and ends at about 3 minutes after the reference time, so that they can be considered as really coincident. During the two years of data gathering, a pre-processing random error of scan line numbering occurred, adding some noise to the geographical collocation of the ground and satellite observations.

The equivalence of the CT prototype types [the most frequent CT type among the 9 central pixels of the target is retained except for cloud free type (corresponds to more than 6 cloud free pixels)], and the cloud layers reported in SYNOP is indicated in table 2.5.2.1. During the comparison:

- Snow cover has not been analysed: the cloud free cases include situations with ground covered by snow.
- A distinction was done among the cloud layers reported in SYNOP between those corresponding to a total cloud cover lower than 5 octas or higher than 6 octas.

Main class name	SYNOP cloud layers	CT types
cloud free	-Total cloudiness lower or equal 2 octas	-land not contaminated by cloud, -land contaminated by snow
low	-Sky not observed, due to fog -Stratus (except bad weather stratus) without overlying cloud layer reported -Stratocumulus without overlying cloud layer reported -Cumulus humilis	-very low clouds, -low clouds
mid-level cloud	-Dominant cloud layer: Cumulus mediocris -Dominant cloud layer: opaque altostratus or altocumulus (without cirrus clouds)	-medium clouds
high cloud	-Sky not observed due to rain or showers -Dominant cloud layer: cumulonimbus -Bad weather stratus -Altocumulus or altostratus overlaid by dense cirrus or cirrostratus	-high opaque clouds
semitransparent	-Dominant cloud layer: cirrus, cirrostratus or cirrocumulus -Dominant cloud layer: semitransparent altostratus or altocumulus	-thin, mean and thick cirrus
multi-layer	-Remaining cloud observations	
fractional		-fractional
cirrus above lower clouds		-cirrus above lower clouds

Table 2.5.2.1 Equivalence between CT types and SYNOP cloud layers

Contingency tables, user and producer's accuracies (defined in paragraph 2.5.1) have been computed for various illumination conditions, and different geographic areas. They are provided in annex 6 (tables A.6.5, A.6.6 and A.6.7). User and producer's accuracies, plotted below in figure 2.5.2.1, 2.5.2.2 and 2.5.2.3, give a synthetic view of the impact of the illumination conditions (day, night, twilight) and the geographic area (tropical, mid-latitude or polar regions) on the classification of each cloud class, whereas each contingency table allows a finer analysis of the confusion between cloud classes for a given illumination condition and geographic area.

The comparison between the GOES CT classes and the ground-based cloud cover gives much less good results than those obtained when using the interactive file (see 2.5.1). The reasons may be the following:

- The cloud layers reported in the SYNOP may be questionable:
    - high level clouds overlying a lower cloud layer may not be reported in SYNOP
    - at nighttime clouds may be not reported in SYNOP if their base is too high to be reached by the telemeter and if they cannot be seen by the observer, this leads to underestimate particularly middle and high cloud covers.
- Often more than one cloud layer is reported in SYNOP, indicating high frequencies of mixed layers, and the uncertainty to get the lower layers by the top-down satellite observation
- The area analysed by the observer is not perfectly coincident with the 9 by 9 IR pixels targets extracted from the satellite imagery.

In mid-latitude regions,

- The low clouds are the best typed clouds, with user and producer's accuracies above 40% (which is much less than what was observed with the interactive file):
    - As already noticed with the interactive file, the difficulty to detect small cumulus, and their possible classification by CT algorithm as fractional clouds are the main reasons, linked to the CT algorithm, to decrease the producer's accuracy of low clouds having total cloudiness reported in SYNOP lower than 5 octas. This drawback is also emphasized by the fact that surface observers are known to overestimate the coverage of scattered cumulus.
    - The incapacity of the surface observer to see thin high level clouds when a lower cloud layer fills his field of view is highlighted by the contingency tables especially at daytime: this artificially lowers the producer's accuracy of low clouds having total cloudiness reported in SYNOP higher than 6 octas.
- The other clouds are not well typed, especially if the total cloudiness reported in SYNOP is lower than 5 octas (much lower producer's accuracies). The mid-level clouds are the less well typed cloud class, as already noticed with the interactive file.
- Cloud cover classified by CT algorithm as fractional clouds mainly correspond to low and semi-transparent cloud layers (as already noticed with interactive file), or cloud free areas. Very few fractional cloud class are output by CT algorithm in nighttime condition (already observed with interactive file).
- The impact of illumination conditions depends on the cloud type:
    - For cirrus clouds, the user's accuracy is higher at daytime than at nightime, which is not observed with the interactive file. In fact, numerous nighttime situations reported in SYNOP as cloud free are classified as covered by cirrus (as shown by the contingency table). This must be an artefact due to cirrus cloud cover not seen by the surface observer in dark situations. On the contrary, the producer's accuracy is much higher at nightime than at daytime, which was also observed with the interactive file. This is due to a much better detection of cirrus clouds at nightime. Three explanations can be proposed: -the use of T11μm-T3.9μm (used during nightime) is very efficient to detect cirrus clouds at nighttime; -the surface observer is able to see very thin cirrus clouds at daytime, which are difficult to detect from satellite imagery; -cirrus are more frequently confused as fractional clouds at daytime than at nighttime.
    - For low clouds, the producer's accuracy is much lower at twilight. As shown by the contingency tables, this is due to a difficulty to detect them.
    - For cloud free areas, the user's accuracy is lower in twilight conditions, indicating more undetected clouds.

The impact of geographical area depends on the cloud type:

- The low cloud user and producer's accuracies are much higher in mid-latitude regions: misclassification of cloud free areas with low clouds is rather frequent for nordic region (leading to lower user accuracy), whereas difficulties to detect low clouds (with partial cover, i.e. cumulus) in tropical regions lead to lower producer accuracy.
- The cloud free user and producer's accuracies are generally higher in mid-latitude regions, which indicates that the cloud detection algorithm is better tuned for mid-latitude.

Figure 2.5.2.3 describing the distribution of ground-based observations correspond to CT clear sky misclassifications per illumination and geographical area is an interpretation of clear failures. For the global set two cases rise up from the graphs ; the cloud covers corresponding to dominant semitransparent clouds (failures a little more frequent in daytime conditions), and the cloud covers corresponding to low clouds with a total coverage greater than 6 octas (failures more frequent in nighttime conditions). Their analysis for midlatitude area shows that failures of semitransparent clouds occurs mostly when N<5,at daytime, while low clouds are missed mainly at nighttime and twilight with large covers.

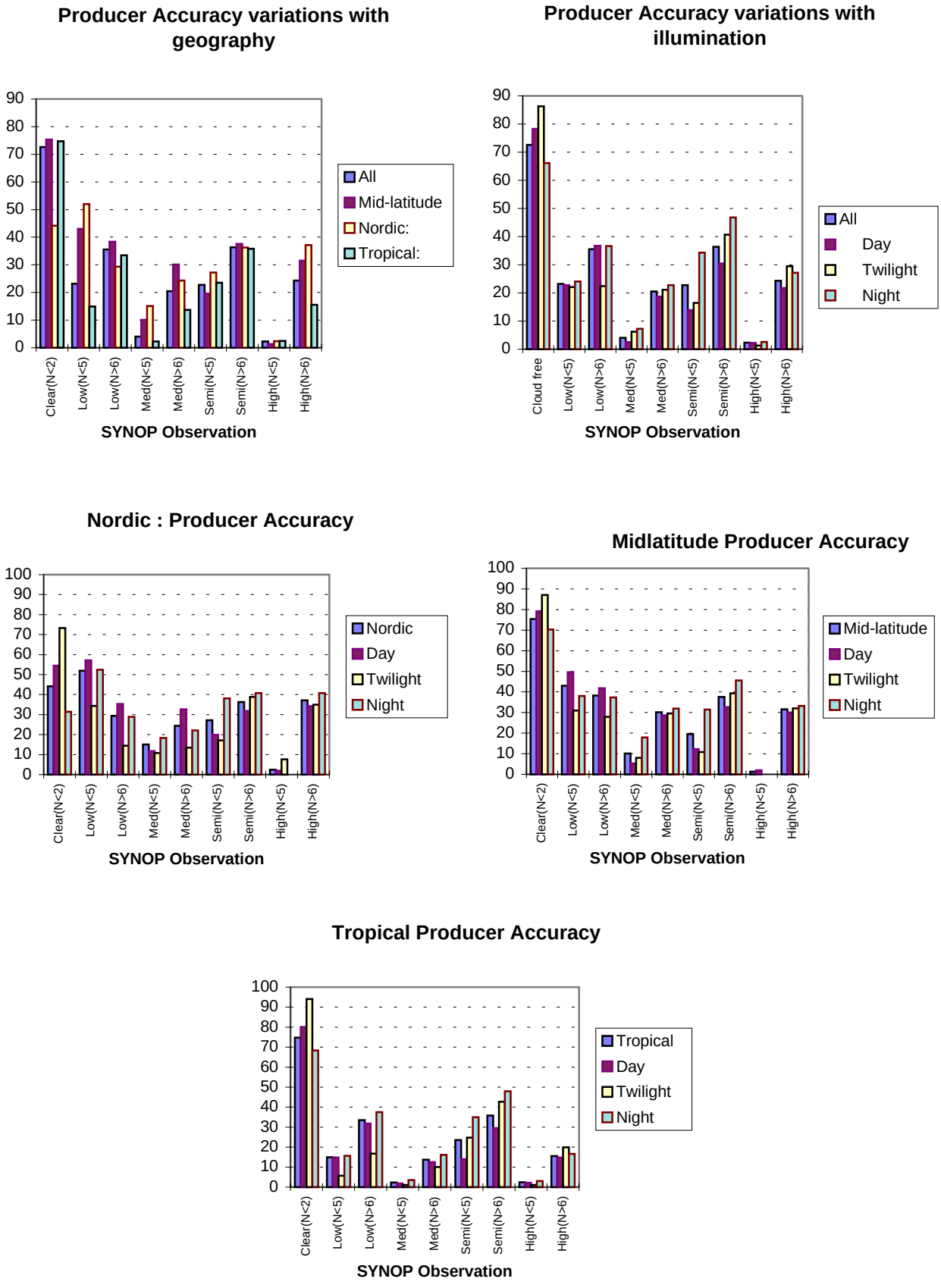

Figure 2.5.2.1 Producer Accuracy variations with geography and illumination, related to classes from SYNOP observations

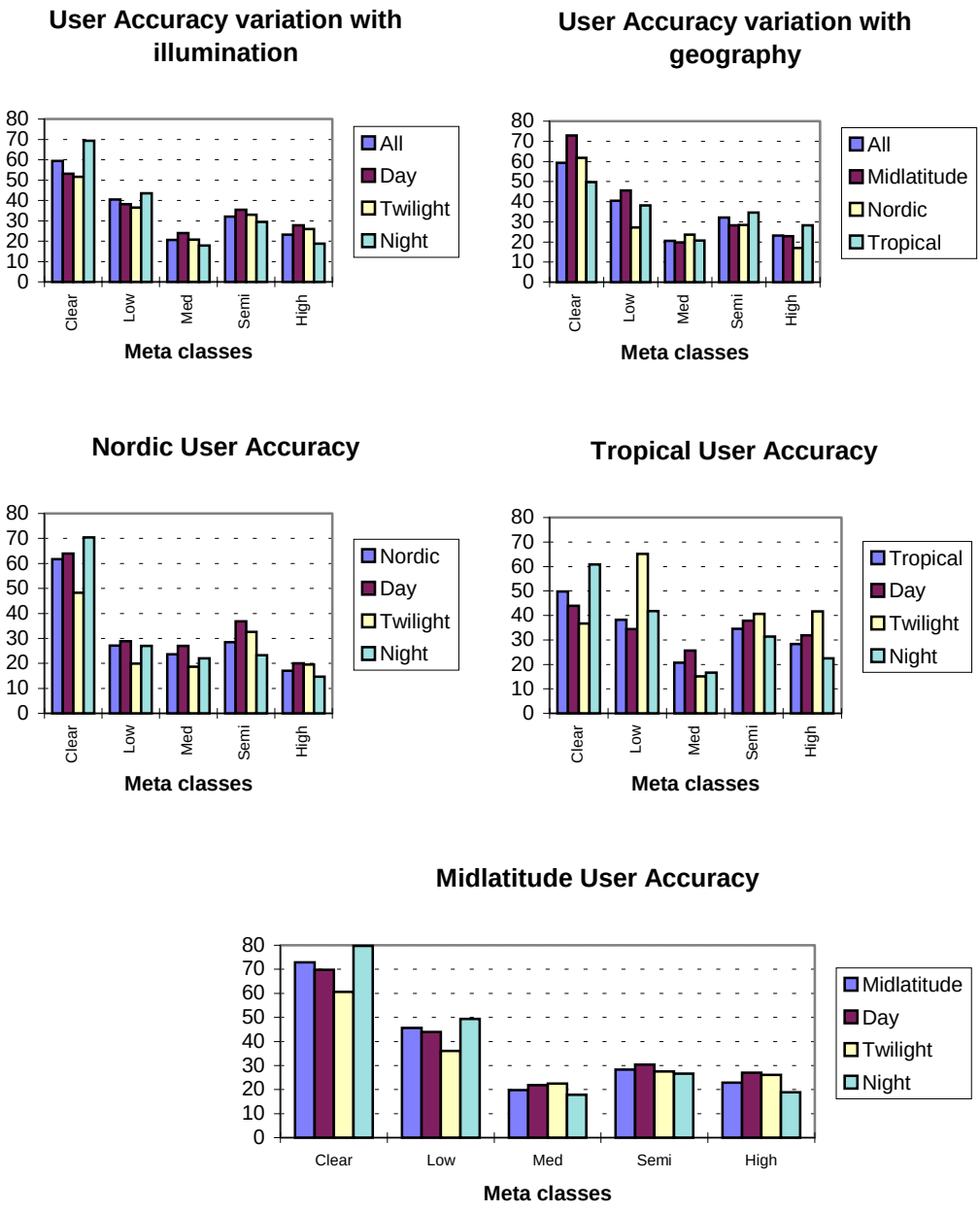

Figure 2.5.2.2Variation of user accuracy with geography and illumination, related to classes from SYNOP observations

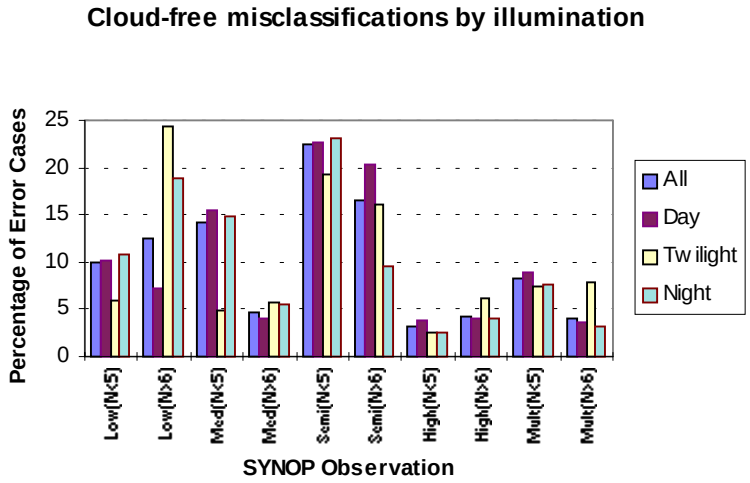

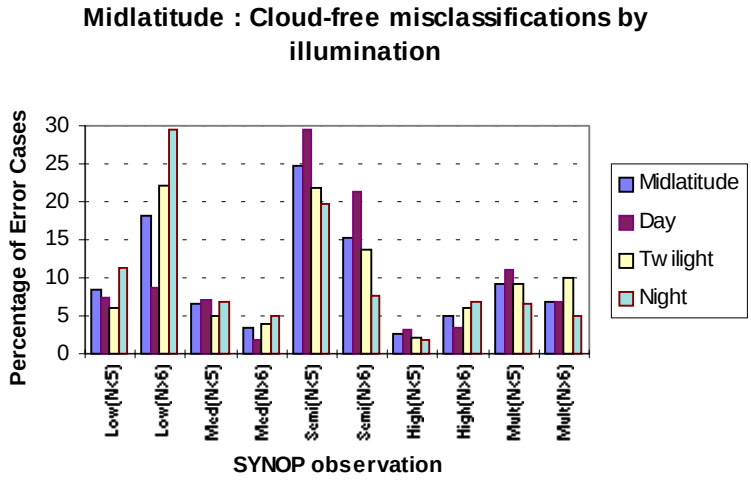

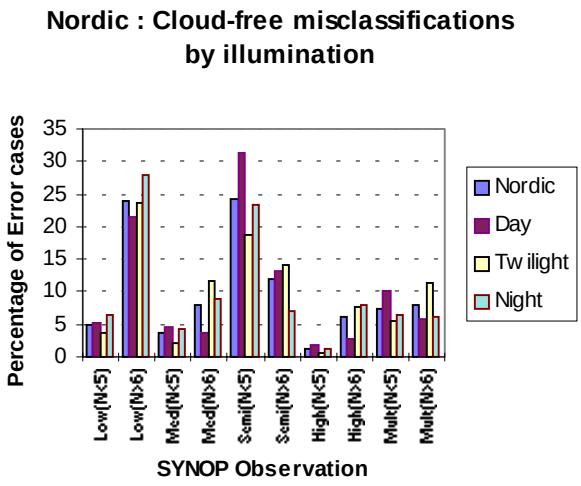

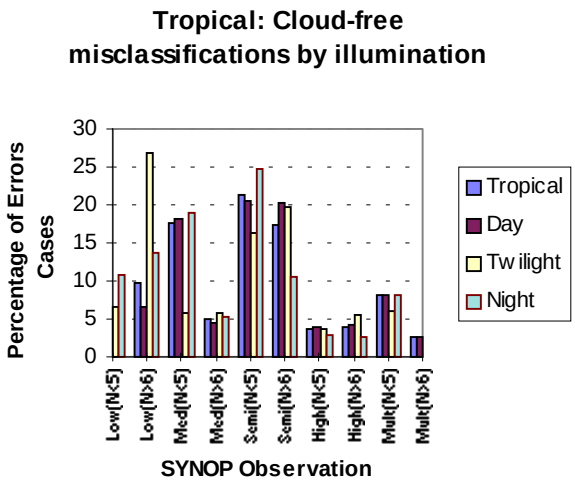

Figure 2.5.2.3 CT Cloud-free misclassifications : variations related to SYNOP observations with geography and illumination.

2.6. The Demonstration experiment

A description of the demonstration experiment is given in annex 5. During this experiment (8th November 1999 - 8th December 1999), half-hourly cloud type maps over the Extended Northern Hemisphere were made available in GIF format for visualisation.

A special validation of the cloud type with SYNOP measurement during the demonstrator experiment has not been performed, as the results of an extensive validation with SYNOP covering two years are available (see 2.5.2).

2.6.1. Cloud type examples

The first example given in Figure 2.6.1 is one of the CT products that were available every half hour for free evaluation by the users' community during the demonstrator experiment. It has been chosen because it contains a day/twilight/night transition, which is the major problem for an homogeneous cloud type restitution. Some traces of this transition can be distinguished between the South of the Galapagos islands and Ecuador, with an artificial linear border between semitransparent clouds and semitransparent overlapping lower clouds, a cloud type that can be retrieved only on a sunlit area.

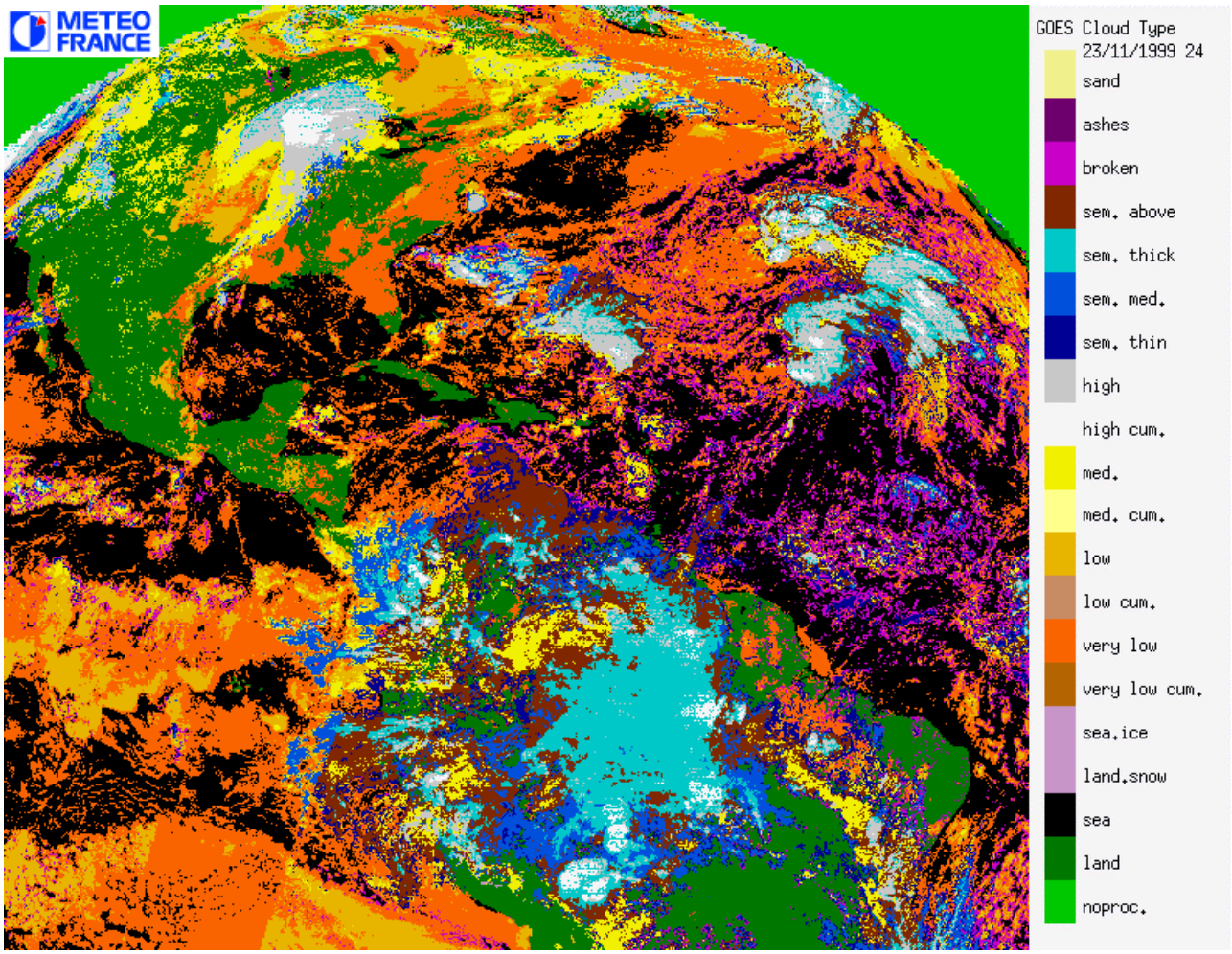

Figure 2.6.1 Example of cloud type prototyped with GOES08 data, on 23 November 1999 12:15 UTC, and available during demonstrator experiment

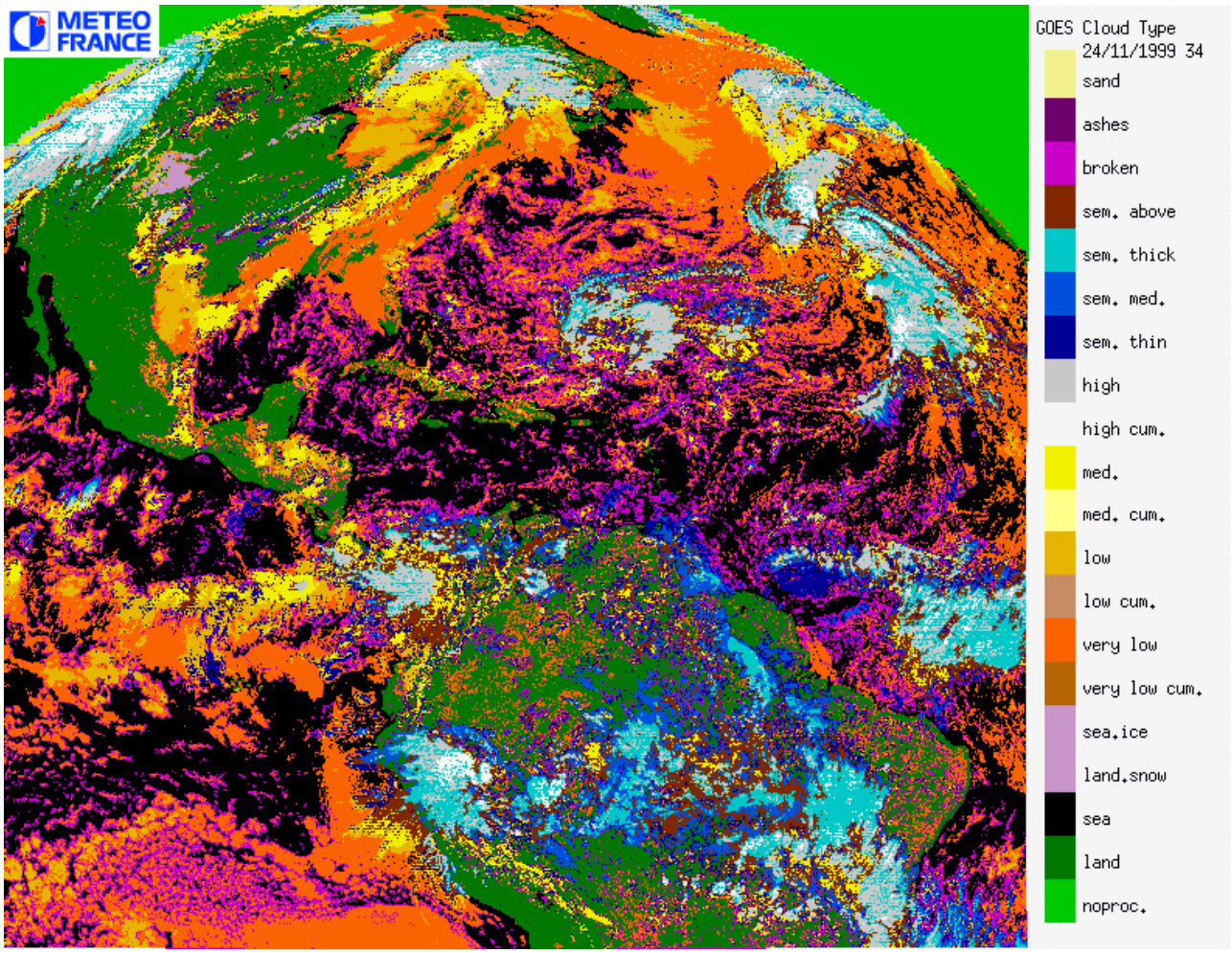

Figure 2.6.2 Example of cloud type fromGOES08 data, on 24 November 1999 16:45 UTC,

The second example given in Figure 2.6.2 illustrates three significant events over the United Sates :

- arrival of an intense and strong storm over western United States
- snow cover identification for the first major snow event of the season in the central United States
- extended area of dense fog and low clouds over the eastern United States, source of many travel problems reported that day

2.6.2. Interpretation of the cloud type

When analysing the cloud type maps one must be aware of the results of the validation. In practical, the CT images should be used with their associated quality flags where the viewing conditions, that are important in the result understanding, can be found.

In any case a CT picture should not be used without knowing the previous results, hence an animation of the last pictures should be kept accessible to the user. As an example, the replacement of a snowy area by a low cloud between two successive pictures may be due only to the transition from day to night, as the snow detection is not possible at nighttime.

2.7. Future application to SEVIRI

2.7.1. Conclusion from prototyping :

The prototyping with AVHRR and GOES has allowed to gain experience for the development of the algorithm and software to process SEVIRI :

- we have checked the technical feasibility of real time cloud classification using GOES imagery
- we have quantified the accuracy that can be expected if a limited set of SEVIRI channels is used (i.e., those available on GOES).
- we have visually estimated CT quality in Europe using AVHRR

Taking into account the result of prototyping, we propose to implement the algorithm described below :

Input data (M indicates mandatory input) :

- Satellite imagery from current slot (see annex A.1.3 ; availability of data checked for every pixel) :
  - 0.6µm (M), 1.6µm, 3.9µm (M), 8.7µm, 11µm (M), 12 µm (M) at full IR spatial resolution
  - Sun and satellite angles associated to SEVIRI imagery (M).
- CMa (M)
- NWP parameters (see annex A.2.2) :

Forecast fields of the following parameters (minimum frequency : 4 per days), remapped onto satellite images (at the segment resolution), are used as input :

  - air temperature are the following pressure levels : 850 hPa,700hPa, 500hPa, tropopause level.
  - total water vapour content of the atmosphere,
  - elevation of the NWP model grid (required if NWP are used as input)

- Ancillary data sets (see annex A.2.1) :

The following ancillary data, remapped onto satellite images, are used as input :

  - Land/sea atlas (M)
  - Elevation atlas (M)
  - Monthly minimum SST climatology (M)
  - Monthly mean 0.6µm atmospheric-corrected reflectance climatology (land) (M)
  - Monthly integrated atmospheric water vapor content climatology (M)
  - Monthly climatology of air temperature at 850hPa, 700 and 500 hPa (M)

Output data :

The content of the CT is the following :

- 5 bits to describe cloud types

21 classes are available :

0	non-processed	containing no data or corrupted data
1	cloud free land	no contamination by snow/ice covered surface, no contamination by clouds ; contamination by thin aerosol (dust clouds or volcanic plume) possible
2	cloud free sea	no contamination by snow/ice covered surface, no contamination by clouds ; contamination by thin aerosol (dust clouds or volcanic plume) possible
3	land contaminated by snow	
4	sea contaminated by snow/ice	
5	very low and cumuliform clouds	
6	very low and stratiform clouds	
7	low and cumuliform clouds	
8	low and stratiform clouds	

9 medium and cumuliform clouds
10 medium and stratiform clouds
11 high opaque and cumuliform clouds
12 high opaque and stratiform clouds
13 very high opaque and cumuliform clouds
14 very high opaque and stratiform clouds
15 high semitransparent thin clouds
16 high semitransparent meanly thick clouds
17 high semitransparent thick clouds
18 high semitransparent above low or medium clouds
19 fractional clouds
20 undefined (undefined by CM)

- 10 bits for quality

3 bits to define illumination and viewing conditions:
0 Undefined (space)
1 Night
2 Twilight
3 Day
4 Sunglint

2 bits to describe NWP input data
0 Undefined (space)
1 All NWP parameters available (no low level inversion)
2 All NWP parameters available (low level inversion)
3 At least one NWP parameter missing

2 bits to describe SEVIRI input data
0 Undefined (space)
1 All useful SEVIRI channels available ;
2 At least one useful SEVIRI channel missing

2 bits to describe the quality of the processing itself:
0 Non processed (containing no data or corrupted data)
1 Good quality (high confidence)
2 Poor quality (low confidence)
3 Reclassified after spatial smoothing (very low confidence)

1 bit set to 1 to indicate that the separation between cumuliform and stratiform clouds has been performed.

- 2 bits for cloud phase

0 Non processed (containing no data or corrupted data)
1 water cloud
2 ice cloud
3 undefined (due to known separability problems)

Algorithm outline :

The CT algorithm is a threshold algorithm applied at the pixel scale, based on the use of CMa and spectral & textural features computed from the multispectral satellite images and compared with a set of thresholds. It will be very similar to the GOES prototype : the improvement using the new channels (1.6µm and 8.7µm) will be considered only when SEVIRI images are available.

We recall the outline of the chosen algorithm. The set of thresholds to be applied depends mainly on the illumination conditions, whereas the values of the thresholds themselves may depend on the illumination, the viewing geometry, the geographical location and NWP data describing the water vapour content and a coarse vertical structure of the

atmosphere. First, main cloud types are separable within two sets ; the semitransparent & fractional clouds, from the low/medium/high clouds. These two systems are distinguished using spectral features : T11µm-T12µm, T39µm-T11µm, and T11µm in night-time conditions, and R0.6µm, T11µm-T12µm in day-time conditions. Then within these two sets fractional and semitransparent are separated using either both textural features (variance T11µm coupled to variance R0.6µm) and T11µm-T12µm in day-time conditions, or only spectral features T11µm-T12µm and T3.9µm-T11µm in night-time conditions. The remaining clouds are distinguished through the comparison of their T11µm to NWP forecast temperatures at several pressure levels.

Depending on the result of the study performed within the visiting scientist activity, a special dedicated algorithm will be applied to extract the cloud phase.

2.7.2. Pre-launch activity :

The CT phase 1 prototype will be used to develop PGE02 (Product Generation Element 02 : the software to extract the Cloud Type (CT) from SEVIRI images).

- PGE02 will :
  use as much as possible SAFNWC common functions
  be spectrally tuned to process both GOES and SEVIRI channels
- PGE02 will be tested with GOES images by comparison with CT phase-1 prototype : this validates PGE02 if the mandatory set of SEVIRI channels is used.
- PGE-02 will be implemented in a CMS pre-operational SEVIRI environment to prepare their full validation as soon as SEVIRI images are available at CMS.

2.7.3. Post-launch activity :

- The PGE02 will be run in a CMS pre-operational SEVIRI environment. It will include a visual inspection.
- As during the prototyping phase-1, test and validation files will be gathered interactively (with a procedure based on the WAVE commercial software see annex A.3.1) and automatically (collocated satellite imagery and surface observations extracted from SYNOP, see annex A.3.2).
- The products will be validated, and the algorithm tuned if needed (especially, the use of the new channel 8.7µm).
- A scientific report, including validation results, will be written.

2.7.4. Integration activity :

- The PGE02 will be prepared for their delivery to INM (systematic use of common functions),
- The informatic documentation will be written,
- A test case will be defined : the PGE02 to be delivered to INM will be validated at CMS (must give same result as PGE02 implemented at CMS),
- The PGE02, the test case and the informatic documentation will be made available to INM.

3. Cloud top temperature and height prototyping

3.1. Introduction

This chapter is a scientific description of the cloud top temperature and height (CTTH) prototyping performed by Météo-France during the SAF NWC first development phase.

The development of techniques to retrieve cloud top temperature of broken or semitransparent clouds using window channels only are studied by SMHI and presented in a separate document.

3.2. Overview

3.2.1. Objective

The cloud top temperature and height (CTTH), developed within the SAF NWC context, aims to support nowcasting applications. The main use of this product is the analysis and early warning of thunderstorm development. Other applications include the cloud top height assignment for aviation forecast activities. The product may also serve as input to mesoscale models or to other SAF NWC product generation elements.

The CTTH product contains information on the cloud top temperature and height for all pixels identified as cloudy in the satellite scene.

The main application is nowcasting over the MSG N area. The consequences are twofold :

- the cloud top temperature and height prototypes have been developed, keeping in mind that the final software must be efficient in term of computing time and that all the ancillary data needed by the software must be available in real time.
- the prototypes have been validated only in mid-latitude regions.

3.2.2. Background

The temperature at the top of an opaque cloud is retrieved using IR measurements in an atmospheric window channel provided that an additional correction for contributions from water vapour above the cloud is applied. The cloud top height may then be derived from the top temperature using atmospheric temperature profiles from NWP output.

For semitransparent and broken cloud layers this straightforward approach does not work. The IR brightness temperature is contaminated by radiation contributions from the surface, from lower cloud layers and from the atmosphere beneath the cloud layer. Thus, the brightness temperature depends on at least two parameters; the effective cloudiness (fractional cloudiness times cloud emissivity) and the cloud temperature, and both need to be retrieved.

Two different approaches have be tested for semitransparent or broken clouds :

- Approach 1, Window channels histogram analysis :

  By making histogram analysis on a large area of pixels, using information from more than one window channel (or spectral feature) it may be possible to separate the signal from the cloud

tops and the surface at the same time. One candidate method is the spatial coherence method (Coakley and Bretherton, 1982). In ideal situations (for a true sub-pixel opaque cloud regime over a homogenous surface), a two-dimensional histogram of the local spatial variance of the T11µm brightness temperature versus the brightness temperature itself defines an arched curve with the two feet defining the surface and the cloud top temperature. Another candidate method is using two thermal window channels and the different behaviour of cloud transmissivity with thickness (Inoue, 1985). The brightness temperature difference between 11µm and 12µm channels is low and only affected by the atmosphere (mainly water vapour) over cloud free pixels, and close to zero for opaque clouds. For semitransparent and sub-pixel clouds, the difference is higher. Thus a curve (much like the arch discussed above) may be fitted to such a histogram, and the cloud top temperature could then be derived from the point of the curve where the brightness temperatures are equal in both channels.

- Approach 2, Radiance ratioing and Intercept methods:

The radiance ratioing method makes use of the fact that the variation of the radiance with height and cloudiness is not the same for a window channel as for a CO_2 sounding channel. Knowing the clear sky radiances and transmittances at various levels of the atmosphere for both channels, and assuming a simple relationship between the cloud emissivities in the two channels (a constant ratio between the two effective cloud emissivities, equal or different from one) the cloud top pressure may be estimated for every pixel (Menzel et al., 1983). An alternative approach called the H_2O/IRW intercept method (based on a infrared window and a water vapour channel histogram analysis) is currently applied to Meteosat imagery for cloud height assignment in the operational Cloud Motion Wind retrieval at EUMETSAT (Schmetz et al., 1993). RTM calculations are needed to get the radiance that would be measured for the opaque cloud layer set at different atmospheric levels.

The first approach will be tested by SMHI and detailed in a separate document. The prototyping of algorithms using the second approach for semitransparent or broken clouds is described in this document.

3.2.3. Cloud top temperature and height inputs

The CTTH has been prototyped with NOAA HIRS and AVHRR data, and with GOES-East imagery both locally received at CMS. The input and output data for these two prototypes are very different, as the NOAA prototype is based on an existing software and the GOES-East prototype is a completely new scheme.

<u>The input for the GOES-East prototype are :</u>

- satellite imagery (see annex A.1.3) :

2 IR window channels (11 and 12 µm) and 1 WV channel (6.7 µm) over the Extended Northern Hemisphere at full spatial resolution every slot (i.e., every 30 minutes) in the satellite projection. Sun and satellite angles associated to GOES imagery, are computed at the segment resolution (i.e., 32*32 IR pixels).

- CMa and CT.

- NWP outputs (see annex A.2.2) :

The French NWP model ARPEGE has been used during prototyping. Six-hourly short term forecast fields of the following parameters, remapped onto satellite images (at the segment resolution, i.e. 32*32 IR pixels), are used as input (the elevation of the NWP model grid is also needed) :

  - air temperature and relative humidity on the ARPEGE 20 standard pressure levels,
  - surface pressure,
  - air temperature and relative humidity at 2m,

- surface temperature,

- Ancillary data sets (see annex A.2.1) :

The following ancillary data, remapped onto satellite images (at the segment resolution, i.e. 32*32 IR pixels), are used as input :

- Monthly mean 0.6 µm atmospheric-corrected reflectance climatology (land),
- Land/sea/coast atlas,
- Elevation atlas,
- Monthly minimum SST climatology,

The input for the NOAA prototype are:

- HIRS satellite data (see annex A.1.2) :

12 window channels are used (10 channels in the 15 µm CO2 absorption band and 2 WV channels)) at the HIRS spatial resolution in the satellite projection. Only 4 passes are processed every day.

- AVHRR satellite imagery (see annex A1.1) :

2 IR window channels (11 and 12 µm) at full spatial resolution in the satellite projection. Only 4 passes are processed every day. Sun and satellite angles associated to AVHRR imagery, are computed every HIRS FOV (i.e., 34*39 pixels). The AVHRR and HIRS data are collocated and used simultaneously during the prototyping.

- CMa and CT.

- NWP outputs (see annex A.2.2) :

The French NWP model ARPEGE has been used during prototyping. Six-hourly short term forecast fields of the following parameters, remapped onto satellite images (at the HIRS spatial resolution, i.e. 34*39 AVHRR pixels), are used as input (the elevation of the NWP model grid is also needed) :

- air temperature and relative humidity on the ARPEGE 20 standard pressure levels,
- surface pressure,
- air temperature and relative humidity at 2m,
- surface temperature,

- Ancillary data sets (see annex A.2.1) :

The following ancillary data, remapped onto satellite images (at the HIRS spatial resolution, i.e. 34*39 AVHRR pixels), are used as input :

- Land/sea/coast atlas,
- Elevation atlas,
- Monthly minimum SST climatology,
- Monthly mean 0.6µm atmospheric-corrected reflectance climatology (land),

3.2.4. Cloud top temperature and height outputs

The CTTH output for the GOES-East prototype are available over the Northern Hemisphere at full spatial resolution for every slots (i.e., every 30 minutes). They follow most of the specifications retained for SEVIRI. These outputs are :

- The cloud top temperature coded on a short unsigned integer in 1/100 K
- The cloud top pressure coded on a short unsigned integer in 1/10 hPa.
- The cloud top altitude coded on a short integer in meters
- The cloud effective cloudiness (amount times emissivity) coded on a short unsigned integer in 1/10 %
- A quality flag, coded on a short unsigned integer, encloses :
  - one bit to flag not-processed pixels,
  - one bit to flag the lack of NWP fields,
  - one bit to flag temperature inversion in the lower troposphere (obtained from NWP forecast fields),

- one bit to flag the lack of RTM simulations,
- three bits are used to describe the quality of each methods that has been tested : one bit to indicate if the final result has been obtained with this method, two bits to indicate whether the method has been successful and inform on the confidence in the result (good or bad),

The CTTH output for the NOAA prototype does not at all meet the specifications retained for SEVIRI, because it is an adaption of an existing software. Only Cloud top temperature and pressure, and the cloud effective cloudiness are computed. No quality indicators are stored. All the outputs are available at the HIRS spatial resolution. Only the cloud top temperature derived from AVHRR IR window channel can also be displayed at the AVHRR spatial resolution.

3.3. Algorithm detailed description

Prototyping has been performed using NOAA-AVHRR, NOAA-HIRS and GOES imagery :

- The aim of the NOAA prototype is to compare techniques to retrieve cloud top for semitransparent clouds, using window channels (AVHRR prototype) or sounding channels (HIRS prototype). Some lidar measurements collocated with satellite measurements are available for validation.
- The GOES prototype is very similar to the scheme that will be developed for SEVIRI : different techniques are implemented to retrieve cloud top temperature and height for all cloud types.

3.3.1. Algorithm outline

The schemes used to retrieve the cloud top from AVHRR, HIRS and GOES imagery are outlined in this paragraph. Individual retrieval techniques used in these three schemes are then detailed in 3.3.2, whereas general modules are only shortly presented in 3.3.3.

3.3.1.1. NOAA-AVHRR algorithm outline

We have used an already existing scheme (described in Derrien et al., 1988) which is applied to already cloud-classified AVHRR image :

- The cloud top temperature of opaque clouds are computed at the individual AVHRR pixel scale by applying an empirical atmospheric correction to T11μm. This correction is calculated from a precomputed table [with the satellite zenith angle and the T11μm brightness temperature of the pixel as input] which has been set up by applying RTTOV to radio-soundings from TIGR dataset. These cloud top temperatures are also averaged in 34*39 pixels box centred on a HIRS measurement. This step is detailed in 3.3.2.1.
- The cloud top temperature of semitransparent ice clouds is computed at the individual HIRS pixel scale, by analysing the (T11μm-T12μm) versus T11μm histogram built using AVHRR pixels contained in a 34*39 pixels box centred on a HIRS measurement. This step is detailed in 3.3.2.3.
- The cloud top pressure is then retrieved (at the HIRS spatial resolution) from its temperature by using the vertical temperature profile forecast by ARPEGE NWP model (see general module in 3.3.3).

3.3.1.2. NOAA-HIRS algorithm outline

During a visiting scientist stay, the radiance ratioing method, as described in Menzel et al, 1983, has been implemented and applied to HIRS data for semitransparent or broken clouds. The following process is applied to each HIRS F.O.V :

- The identification of semitransparent or broken clouds is performed using the cloud types of all the AVHRR pixels inside the HIRS FOV.
- RTTOV infrared radiative transfer model is applied on the vertical temperature and humidity profile forecast by ARPEGE NWP model to simulate infrared HIRS radiances for cloud free atmosphere and for opaque clouds at various vertical levels.
- The top pressure of these clouds is then retrieved by applying the radiance ratioing method to six pairs of HIRS H_2O or CO_2 sounding channel (13.3µm/11.1µm, 13.7µm/11.1µm, 14.0µm/11.1µm, 7.34µm/11.1µm, 6.75µm/11.1µm, 6.75µm/7.34µm). The simulated radiances are used in this process. This step is detailed in 3.3.2.4.
- Finally, the cloud top temperature is retrieved from its pressure by using the vertical temperature profile forecast by ARPEGE NWP model (see general module in 3.3.3).

3.3.1.3. GOES algorithm outline

The GOES algorithm has been developed in the frame of SAF NWC and meets most of the specifications retained for SEVIRI. The different steps of the processing, applied to cloud-classified image, are listed below :

- RTTOV infrared radiative transfer model is applied using the vertical temperature and humidity profile forecast by ARPEGE NWP model to simulate 11µm and 6.7µm radiances & brightness temperatures for cloud free atmosphere and for opaque clouds at various vertical levels. The vertical profiles used are temporally interpolated to the exact slot time from the two nearest in time NWP output fields. This process is performed in each segment of the image (i.e., box of 32*32 GOES IR pixels).
- The technique used to retrieve the cloud top pressure depends on the cloud's type :
    - For low, medium of high thick clouds : The cloud top pressure is retrieved on a pixel basis and corresponds to the best fit between the simulated and the measured 11µm radiances. The simulated radiances, initially computed at the segment resolution, are spatially interpolated to individual pixels during this process. This step is detailed in 3.3.2.2. For high clouds, if the estimated quality is poor, the techniques developed for cirrus are used instead.
    - For cirrus clouds, two methods are implemented (detailed in 3.3.2.4 and 3.3.2.5) :
        - the radiance ratioing method, as described in Menzel et al. 1982, is applied to the 11µm and 6.7µm pair of channels to retrieve the cloud top pressure at a pixel basis.
        - the H_2O/IRW intercept method, based on a 11µm and 6.7µm histogram analysis [very similar to the Eumetsat method (Schmetz et al., 1993)] is also implemented and allows the retrieval of cloud top pressure at the segment spatial resolution (i.e., 32*32 GOES IR pixels).

Only the cloud top retrieved with H2O/IRW intercept is retained in the final results, except for thick cirrus : the radiance ratioing technique is used instead if its quality is good.

- For low broken clouds, the water vapour channel is not sensitive to low broken clouds, and is therefore useless in presence of such clouds. The 11µm and 12µm channels are surface contaminated and cannot therefore be used as for thick clouds. Techniques relying on window channels should have been developed by SMHI to be implemented in the GOES prototype : this has not been possible due to delay during the development phase. No technique is therefore implemented for low broken clouds.

- Cloud top temperature and height are then computed from their pressure using general modules described in 3.3.3. During these processes, the atmospheric vertical profiles used are temporally interpolated to the exact slot time using the two nearest in time NWP outputs fields, and spatially interpolated to individual pixels.

3.3.2. Cloud top retrieval techniques

3.3.2.1. Opaque Cloud Top Temperature retrieved from one window channel

This empirical technique allows to retrieve the cloud top temperature of opaque clouds on a pixel basis, even if the atmospheric vertical profile is not available, which is the case in our AVHRR prototype.

The cloud top temperature is calculated from the 11µm brightness temperature by adding an offset that accounts for the atmospheric absorption. This offset, which should be higher for low clouds and high viewing angles, is estimated from a pre-computed table with the 11µm brightness temperature of the pixel (indicating the cloud height) and the viewing angle as input.

This pre-computed table has been elaborated off-line using RTTOV simulations : T11µm brightness temperatures have been simulated from mid-latitude radio-soundings (available in TIGR dataset) by assuming opaque clouds at various pressure levels in the troposphere. The values of the pre-computed table (see table 3.3.2.1) have been regressed from these simulations.

	Secante=1.0	**secante=1.25**	**secante=1.5**	**secante=1.75**	**secante=2.0**
T11µm=220 K	-0.01	-0.01	-0.01	-0.01	-0.01
T11µm=230 K	0.01	0.01	0.01	0.01	0.01
T11µm=240 K	0.03	0.03	0.04	0.04	0.05
T11µm=250 K	0.06	0.07	0.08	0.09	0.10
T11µm=260 K	0.11	0.13	0.15	0.17	0.19
T11µm=270 K	0.22	0.26	0.29	0.33	0.36
T11µm=280 K	0.43	0.51	0.58	0.64	0.71
T11µm=290 K	0.89	1.04	1.18	1.34	1.52
T11µm=300 K	1.64	1.91	2.17	2.30	2.36
T11µm=310 K	2.40	2.79	3.16	3.25	3.21

Table 3.3.2.1 The offset (expressed in Kelvin) used to retrieve the cloud temperature from its T11µm brightness temperature (in Kelvin) for various secantes of the satellite zenith angle.

3.3.2.2. Opaque Cloud top pressure retrieved from one window channel

This technique is applied in the GOES prototype and allows to retrieve the cloud top pressure of opaque clouds on a pixel basis. It relies on the support of on-line RTTOV simulations and therefore requires the availability of the atmospheric vertical profile. These atmospheric profiles are forecast by a NWP model (ARPEGE and ECMWF model have been used) and temporally interpolated to the exact slot. The RTTOV simulations, initially computed on segments of 32*32 IR pixels, are then spatially interpolated to the processed pixel.

Top of Atmosphere T11μm brightness temperatures are simulated assuming opaque clouds at the different pressure levels of the atmospheric vertical profile. The appropriate cloud top pressure corresponds to the best fit between the measured and the simulated T11μm brightness temperature. In case of low level thermal inversion, the cloud is assumed to be above it ; this assumption avoids too sharp transitions in the result for low or medium clouds.

The quality of the technique is estimated on-line by retrieving the cloud top pressure from both the T11μm and T12μm brightness temperatures, the result being ideally equal. A bad quality flag is set if the difference between the results obtained from these two wavelengths is larger than 0.5°C. Moreover, the presence of thermal inversion in the forecast vertical temperature profile is also flagged.

Cloud top pressures retrieved with this technique are higher than those being directly retrieved from the 11μm brightness temperatures (see 3.3.3.2) without atmospheric correction. This cloud pressure difference, estimated on average over the Extended Northern Hemisphere for the period February-June 1999, is 35hPa (30hPa rms error) for low clouds and only 5hPa (5hPa rms error) for medium clouds. This corresponds to a temperatures difference of 2°C (1°C rms) for low clouds and 0.4°C (0.3°C rms error) for medium clouds.

3.3.2.3. Cloud Top Temperature retrieved from two window channels' histogram

This technique (detailed in Derrien et al, 1988) allows to retrieve the cloud top temperature of semitransparent ice clouds at a rough spatial resolution. It has been implemented in the NOAA-AVHRR prototype only. It consists in an automatic adjustment of a curve on the bi-dimensionnal histogram T11µm-T12µm versus T11µm, made up with the AVHRR pixels located in a 34*39 pixel box centred around each HIRS measurements. A single top temperature is retrieved in each HIRS box.

3.3.2.3.1.The scientific basis

The method relies on the different values of semitransparent ice clouds emissivities at 11µm and 12µm. Neglecting the non-linearity of the Planck function at these wavelengths, the brightness temperatures are (same for $T12_{\mu m}$) :

$T11_{\mu m}=(1-N*\varepsilon_{11})*T_{s11}+N*\varepsilon_{11}*T_{cld}$, where

$\varepsilon 11$ is the cloud emissivity at 11µm,
T_{s11} is the cloud-free brightness temperature at 11µm,
T_{cld} is the cloud top temperature
N is the fractional cloudiness

The emissivity is related to the absorption coefficient by : $\varepsilon_{11}=1-\exp(-\beta_{11}*z/\cos(\theta))$ where β_{11} is the absorption coefficient at 11µm, z is the cloud thickness and θ the viewing angle.

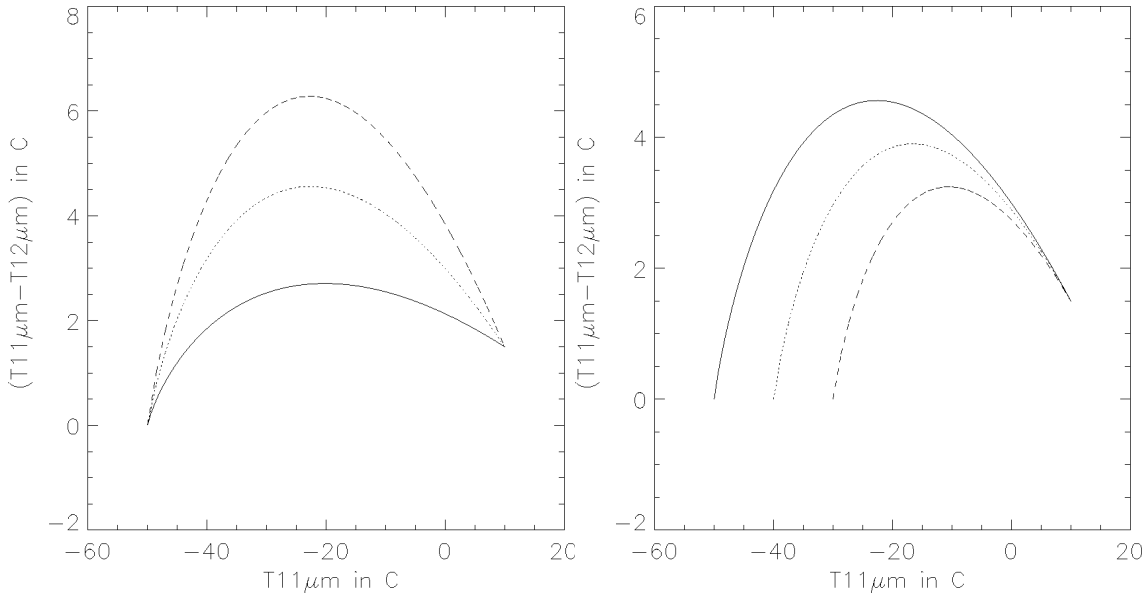

Figure 3.3.2.3.1 Examples of brightness temperatures curves. Ts_{11}=10°C, Ts_{11}-Ts_{12}=1.5°C :Left : for a range of absorption coefficient ratios (β=1.1 (solid), 1.2 (dot), 1.3 (dash)), T_{cld}=-50°C.Right : For a range of cloud top temperatures (T_{cld}=-50°C, -40°C, -50°C), β=1.2.

If the fractional cloudiness is assumed to be unity (reasonable assumption for semitransparent cloud layers) and if the brightness temperature difference is assumed be zero for cloud emissivity equal to unity, the difference between the 11µm and 12µm brightness temperatures is a function of $T11_{\mu m}$, whose shape depends on the cloud absorption coefficients and top temperature, and the surface cloud-free brightness températures (see figure 3.3.2.3.1) :

$T11_{\mu m}-T12_{\mu m} = (\tau-\tau^{\beta})*(T_{s11}- T_{cld}) +\tau^{\beta}*(T_{s11}- T_{s12})$ where

$\tau = (T11\mu m - T_{cld})/(T_{s11} - T_{cld})$ and
$\beta = \beta_{11}/\beta_{12}$ is the ratio of the absorption coefficients at 11µm and 12µm.

3.3.2.3.2.Implementation in the AVHRR prototype

Histogram preparation : For each HIRS F.O.V, a histogram T11µm-T12µm versus T11µm is built up using all semitransparent or high thick clouds AVHRR pixels within a 34*39 pixel box centred on the HIRS measurement. This histogram is then averaged (steps of 3°C for T11µm) to save computation time, and gathered with the histograms of the 8 surrounding HIRS F.O.V to increase the total number of semitransparent cloud pixels used, thus improving the curve adjustment. Usually, as illustrated on figure 3.3.2.3.2, the histograms have an arch-like structure (as expected from theory), but the colder part of the arch (i.e., the crossing of this arch with the X-axis) is not available. It means that no part of the semitransparent cloud layer is thick enough to directly retrieve the cloud top temperature; finding the intersection of the adjusted curve on this histogram with X-axis retrieves the cloud top temperature.

Curve adjustment : The curve, described in 3.3.2.3.1, is non-linearly adjusted on the averaged T11µm-T12µm versus T11µm histogram. The two unknown parameters are the absorption coefficient ratio, and the cloud top temperature. The cloud free brightness temperatures are either computed with cloud-free AVHRR pixels available in the HIRS F.O.V, either estimated from the 2m air temperature (forecast by ARPEGE) and pre-computed tables (elaborated using RTTOV radiative transfer model applied to mid-latitude TIGR radio-soundings ; input of these tables : 2m air temperature and viewing angles).

Quality flag computation : Theoretically, the technique cannot give reliable result if no part of the cloud layer has emissivity higher that 0.5 : in that case the decreasing part of T11µm-T12µm with decreasing T11µm cannot be observed in the histogram, and the method is bound to fail.

The quality of the retrieved cloud top temperature (T_{cld}) is described in a quality flag:

- results obtained with too few cloudy pixels are flagged as bad quality
- cases where a decrease of T11µm-T12µm with decreasing T11µm is not observed in the histogram are flagged as bad quality
- the cloud emissivity of the coldest pixels [i.e., the thicker part of the semitransparent cloud layer] is used to quantify the result's quality (four quality classes are defined : emissivity lower than 0.6, between 0.6 and 0.75, between 0.75 and 0.90, higher than 0.90).

Examples of such adjustments are given on figure 3.3.2.3.2.

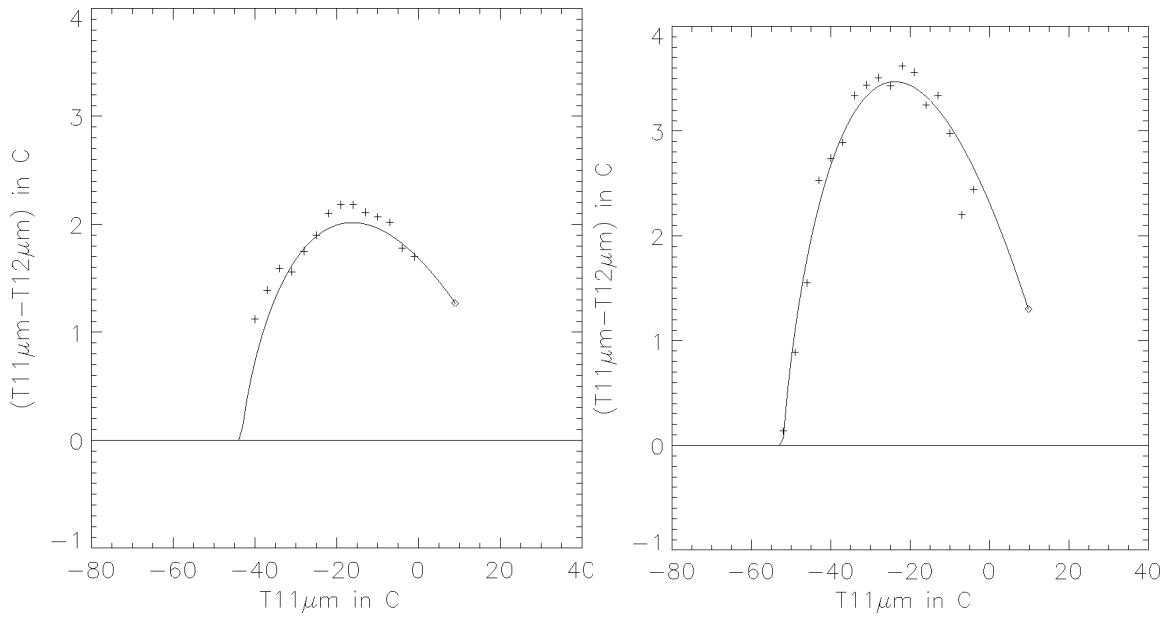

Figure 3.3.2.3.2 Examples of automatic curve adjustment (solid line) on averaged T11µm-T12µm versus T11µm histogram (crosses).

3.3.2.4. Cloud Top Pressure retrieved using radiance ratioing technique

The radiance ratioing technique allows to retrieve broken or semitransparent cloud top pressure at a pixel scale from two infrared channels, one of these channels being a sounding channel. It relies on on-line RTTOV simulations and therefore requires the availability of the atmospheric vertical profile. It has been implemented in the NOAA-HIRS prototype using different pairs of CO_2 channels and in the GOES prototype to the 11µm window channel and the 6.7µm water vapour channel.

3.3.2.4.1.The scientific basis :

This technique is detailed in Menzel et al., 1983. The basic equation of the method is the following:

$$\frac{R_{m1} - R_{clear1}}{R_{m2} - R_{clear2}} = \frac{N\varepsilon_1 (R_{op1} - R_{clear1})}{N\varepsilon_2 (R_{op2} - R_{clear2})}$$

where R_m is the measured radiance, R_{clear} is the clear radiance, R_{op} is the opaque cloud radiance, N is the cloud amount and ε is the cloud emissivity. The terms of denominators on both side come from the same channel (index 2) and the nominators from the other one of the pair (index 1).

Assuming that the ratio of the emissivities is close to one the equation becomes simpler:

$$\frac{R_{m1} - R_{clear1}}{R_{m2} - R_{clear2}} = \frac{R_{op1} - R_{clear1}}{R_{op2} - R_{clear2}} \qquad \text{Eq. 3.3.2.4.1.}$$

Both side of this equation depends on the chosen channels, surface temperature, vertical temperature and absorbing material profiles. The right side of the equation also depends on the cloud pressure due to R_{op}. Consequently if we use a fixed surface temperature and vertical profiles, the right side becomes a function depending on the pressure, the left side being a constant. The retrieved cloud top pressure corresponds to the pressure that satisfies the equation 3.3.2.4.1. In practice the clear sky radiances R_{clear} are simulated values in the HIRS prototype and either measured or simulated for GOES, the opaque cloud radiances R_{op} are simulated values, while the R_m is the measured data.

3.3.2.4.2.Implementation in the NOAA-HIRS prototype

This implementation has been performed during a visiting scientist stay by M.Putsay from Hungarian Meteorological Institute, and has been fully documented in a separate report.

The radiance ratioing technique performs cloud top pressure retrievals for semitransparent clouds and broken clouds for each HIRS F.O.V. The process is split up into several steps detailed below.

Simulation of the HIRS radiances

TOA infrared HIRS radiances for clear atmosphere and for opaque clouds at various pressure levels, simulated with RTTOV, are available.

Calculation of the cloud top pressure

Using the simulated and the measured radiances, we calculate the simulated ratio as a function of the cloud top pressure (left side of the equation 3.3.2.4.1), and the measured ratios (right side of the equation 3.3.2.4.1). The difference between the simulated and the measured ratios is a function of RTTOV pressure levels and is illustrated on figure 3.3.2.4.1. The retrieved pressure level corresponds to this difference equal to zero.

This process has been implemented using six pairs of HIRS channels : 11.1µm/13.3µm, 11.1µm/13.7µm, 11.1µm/14.0µm, 11.1µm/7.34µm, 11.1µm/6.75µm, 7.34µm/6.75µm. Therefore six retrieved cloud top pressures are available.

Calculation of the effective emissivity

The effective emissivity is calculated from the 11µm window channel, using the retrieved cloud pressure.

Rejection

The retrieved cloud pressure is assumed to be unreliable in the following cases :

- the difference of the measured radiance and the simulated clear sky radiance (R_m - R_{clear}) is within five times the instrument noise level.
- the measured radiance is bigger than the simulated clear sky radiance ($R_m > R_{clear}$). This can be happen if the forecast surface temperature is too cold or in the case of a temperature inversion with a low cloud warmer then the surface. This case produces a negative measured ratio (left side of equation 3.3.2.4.1.), while the right side is normally positive. If $R_m > R_{clear}$ in both channels then the ratio will not be negative but according to our experiences the retrieval will not be good even in that case.
- the equation 3.3.2.4.1 has no solution : i.e., the measured ratio is bigger or smaller than all simulated ratios between 1000hPa and 150hPa.
- the equation 3.3.2.4.1. has more than one solution. The simulated ratio is normally monotone function of the pressure [denominator and nominator channels are chosen so that ratios increase while pressure decreases]. However in temperature inversion situation or even if only the surface is colder than the air above it, the simulated ratio may be a non monotonic function in the lower part of the atmosphere. In that case we can have more than one solutions. To filter out a part of the problem with inversions we take into account only those solutions of equation 3.3.2.4.1. which are in the rising parts of the curve.
- the retrieved pressure is lower than 150hPa or higher the surface pressure.
- the retrieved emissivity is outside the [0, 1.01] interval.

Selecting the best retrieval

Calculating the retrieved parameters from every channel pairs separately, we can have six different retrieved cloud top pressures and effective emissivities. The best retrieved cloud top pressure minimises the discrepancy between the measured and the simulated radiances for the four following wavelength : 13.3µm, 13.7µm, 14.0µm and 14.2µm.

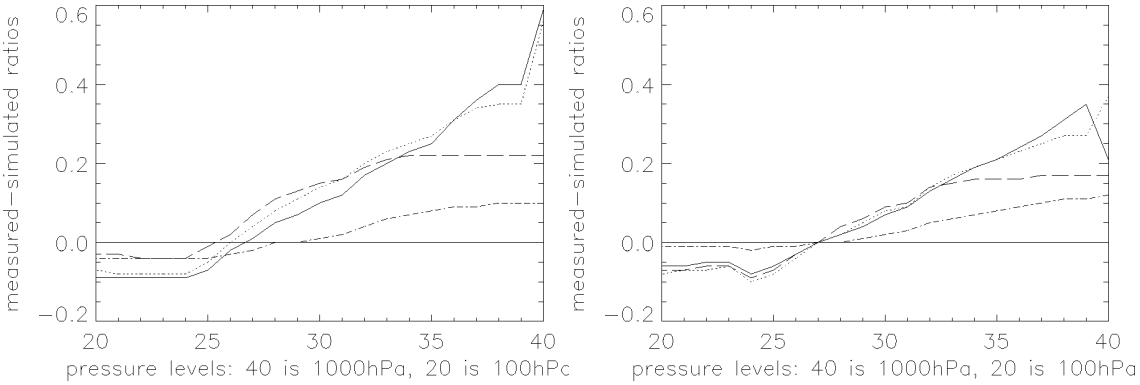

Figure 3.3.2.4.1.Examples of measured minus simulated ratios as a function of the pressure level. The cloud top pressure level corresponds to the crossing of the curves with the X-axis. The four curves corresponds to different channel pairs : 11.1µm/13.3µm (solid), 11.1µm/13.7µm (dot), 11.1µm/7.34µm (dash-dot), 7.34µm/6.75µm (long dash).

3.3.2.4.3.Implementation in the GOES prototype

The radiance ratioing technique is applied to the 11µm window channel and the 6.7µm water vapour channel and allows to retrieve cloud top pressure for semitransparent ice clouds and some high thick clouds (for which the method used for opaque clouds leads to poor quality) on a pixel basis. The process is performed in several steps described below.

Simulation of the GOES radiances

TOA infrared 11µm and 6.7µm GOES radiances for clear atmosphere and for opaque clouds at various pressure levels have been previously simulated with RTTOV.

Modification of simulated radiances

The method very much depends on the cloud free and opaque clouds values. As the simulated values for the water vapour channels are not reliable enough, the following process is applied to modify them:

- modification of cloud free 11µm simulated radiances : cloud free 11µm radiances are computed over the whole image at the segment spatial resolution (i.e., 32*32 pixels) from cloud free individual pixels. When available, these observed cloud free values replace the simulated ones.
- modification of cloud free 6.7µm simulated radiances : cloud free 6.7µm radiances are computed over the whole image at the segment spatial resolution (i.e., 32*32 pixels) from cloud free individual pixels and pixels containing opaque clouds too low to affect the 6.7µm measurements. These observed 6.7µm radiances values are then spread in areas where they could not be computed. They are used instead the simulated ones.
- modification of opaque 6.7µm simulated radiances : the cloudy 6.7µm radiances are modified to account for the discrepancy between the simulated and observed cloud free 6.7µm radiance : the radiance for clouds at the tropopause remain unchanged, the radiance for the lowest clouds are replaced by the cloud free observed radiance, whereas the modification for the other clouds is linearly linked to its 11µm radiance.

Calculation of the cloud top pressure

Using the simulated and the measured radiances, we calculate the simulated ratio as a function of the cloud top pressure (left side of the equation 3.3.2.4.1), and the measured ratios (right side of the equation 3.3.2.4.1). The retrieved pressure level corresponds to this difference equal to zero.

Calculation of the effective emissivity

The effective emissivity is calculated from the 11μm window channel, using the retrieved cloud pressure.

Rejection

The retrieved cloud pressure is assumed to be unreliable in the following cases :

- the difference of measured radiance and the simulated clear sky radiance (R_m - R_{clear}) is within three times the instrument noise level.
- the retrieved pressure is lower than the tropopause's pressure or higher than 500hPa.
- the retrieved 11μm emissivity is lower than 0.5 or larger than 1.

Quality flag

The pressure retrieval is flagged as of bad quality if :

- the cloud free cluster is derived from simulation.
- either the 11μm or 6.7μm simulated radiances is higher than the measured one.

This technique is very much sensitive to the noise (especially for very thin clouds), and to the inaccuracy of the water vapour channel simulated radiances, due to bad water vapour forecast.

3.3.2.5. Cloud Top Pressure retrieved using H2O/IRW Intercept method

The H_2O/IRW intercept method, based on a 11µm and 6.7µm histogram analysis [very similar to the Eumetsat method (Schmetz et al., 1993)] has been implemented in the GOES prototype, and allows the top pressure retrieval at the segment spatial resolution (i.e., 32*32 GOES IR pixels) for semitransparent ice cloud and some high thick clouds (for which the method used for opaque clouds leads to poor quality). It makes use of on-line RTTOV simulations and therefore requires the availability of the atmospheric vertical profile. Part of this work has been performed during a visiting scientist stay (M.Ringer from UK meteorological Office).

3.3.2.5.1.The scientific basis :

The fundamental assumption of the method is that there is a linear relationship between measurements in the two spectral bands observing a single cloud layer. In particular, all pairs of measurements in the 6.7µm and 11µm channels viewing a cloud layer at pressure p_c will lay along a straight line, the spreading along the line corresponding to changes in cloud amounts. On the other hand, the pairs of 11µm and 6.7µm of opaque clouds at different pressure levels will lay along a curve that can be calculated from the atmospheric vertical structure using RTTOV radiative transfer model. Therefore, the cloud top pressure for semitransparent ice clouds is retrieved as the intersection between the linear fit to the observations and the simulated opaque cloud curve. This is illustrated on figure 3.3.2.5.1.

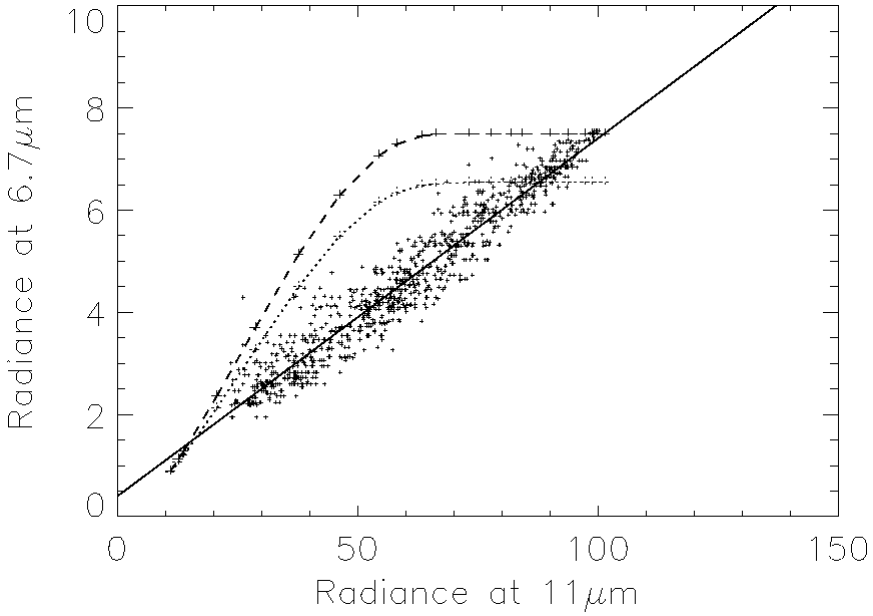

Figure 3.3.2.5.1 Illustration of the H_2O/IRW intercept method with GOES radiances (expressed in $Wm^{-2}sr^{-1}cm$).

The dotted curve simulates the 11µm and 6.7µm radiances of opaque clouds at various pressure levels.
The dashed curve is the dotted curve modified to fit cloud free observations.
The crosses represents radiances of clouds at the same height, but with varying thickness, and the radiance of cloud free pixels.
The top pressure of the semitransparent cloud layer is retrieved from the intersection between the simulated curve (dashed curve) and the regression line.

3.3.2.5.2.Implementation in the GOES prototype

The process is performed in several steps detailed below :

<u>Simulation of the GOES radiances</u>

TOA infrared 11µm and 6.7µm GOES radiances for clear atmosphere and for opaque clouds at various pressure levels have been previously simulated with RTTOV.

Modification of simulated radiances

As the method very much depends on the opaque clouds values, and as these simulations for the water vapour channels are not very reliable, the following process is applied to modify the simulated values :

- modification of cloud free 6.7µm simulated radiances : cloud free 6.7µm radiances are computed over the whole image at the segment spatial resolution (i.e., 32*32 pixels) from cloud free individual pixels and pixels containing opaque clouds too low to affect the 6.7µm measurements. These observed 6.7µm radiances values are then spread in areas where they could not be computed. They are used instead the simulated ones.
- modification of opaque 6.7µm simulated radiances : the cloudy 6.7µm radiances are modified to account for the discrepancy between the simulated and observed cloud free 6.7µm radiance : the radiance for clouds at the tropopause remain unchanged, the radiance for the lowest clouds are replaced by the cloud free observed radiance, whereas the modification for the other clouds is linearly linked to its 11µm radiance.

Calculation of the cloud top pressure

A straight line is adjusted, using the 6.7µm and 11µm radiances of all pixels previously classified as semitransparent, high thick clouds or cloud-free. The intersection of this straight line with the opaque cloud curve will give the cloud top pressure. This process is illustrated on figure 3.3.2.5.1.

Calculation of the effective emissivity

The effective emissivity of each pixel is calculated from the 11µm window channel, using the retrieved cloud pressure.

Rejection

The retrieved cloud pressure is assumed to be unreliable in the following cases :

- unreliable regression :
  - less than 50 pixels
  - less than 15 mWm^{-2} sr^{-1} cm. between the 11µm radiance of the coldest and the warmest pixels
  - correlation coefficient lower than 0.7
- not adequate regression line :
  - slope of the regression line too small : $\delta(R6.7)/\delta(R11) < 0.005$
  - regression line too close to opaque cloud curve : maximum difference in the 6.7µm radiance less than one tenth of the cloud free 6.7µm radiance.
- if the retrieved pressure is lower than the tropopause's pressure or higher than 500 hPa.

If no intersection has been found, but if the regression seems reliable (more than 75 pixels, large spread of the pixels in the 11µm channel (more than 23 mWm^{-2} sr^{-1} cm between the 11µm radiance of the coldest and the warmest pixels), correlation coefficient larger than 0.9, high regression's slope : $\delta(R6.7)/\delta(R11) > 0.015$), then the cloud top pressure is assumed to be the tropopause's pressure, but the retrieval is flagged as bad quality.

Quality flag

The pressure retrieval is flagged as good quality if :

- more than 100 pixels are used,
- a large spread of the pixes in the 11μm channel is observed (more than 23 mWm^{-2} sr^{-1} cm between the 11μm radiance of the coldest and the warmest pixels),
- a correlation coefficient larger than 0.8
- a high regression's slope : $\delta(R6.7)/\delta(R11) > 0.015$.

3.3.3. General modules

3.3.3.1. Cloud Top Height retrieved from its pressure

In the NOAA (AVHRR and HIRS) prototype, the standard OACI atmosphere has been assumed to retrieve the cloud top height from its pressure. The following analytical formulae is therefore used :

$p=1013.25*[(288.15-0.0065*z)/288.15]^{5.26}$ where z is the height in meters and p the pressure in hPa.

In the GOES prototype, a module is used to compute the height vertical profile from the corresponding vertical profile of pressure, temperature & water vapour mixing ratio, the surface height and the latitude. The cloud height is then interpolated using the height of the two nearest pressure levels in the vertical profile. The interpolation used is linear in logarithm of the pressure.

3.3.3.2. Cloud Top Pressure retrieved from its temperature

A vertical temperature profile in pressure levels and the pressure level of the tropopause are needed in this process. We first check for the presence of a low level thermal inversion. The vertical profile is then inspected from surface level (or from the top of the thermal inversion, if it exists) up to the tropopause level : we look for two consecutive pressure levels having temperatures respectively higher and lower than the cloud top temperature ; the final cloud top pressure is obtained by a linear interpolation (logarithm of pressure used) between these two temperatures. The most important point to notice is the uncertainty of the result in case of the thermal inversion in the lowest troposphere. We have assumed a cloud above the top of the inversion to avoid sharp spatial variation in the result.

3.3.3.3. Cloud Top Temperature retrieved from its pressure

A vertical temperature profile in pressure levels is needed in this process. The cloud temperature is interpolated using the temperature of the two nearest pressure levels in the vertical profile. The interpolation used is linear in logarithm of the pressure.

3.3.3.4. Tropopause height estimation

The module used has been developed by the aeronautic forecast service in Toulouse. The pressure and height of the tropopause is extracted from a vertical profile (temperature, height and pressure), the ground height and the latitude. The tropopause estimation is mainly based on the WMO definition of the tropopause : the lowest level (above 5000m) corresponding to a temperature decrease of less than 2°C/km during 2km. A maximum height of the tropopause level is assumed (20km at the equator, 12-13km at the poles) to check the result's coherency.

3.3.3.5. Application of RTTOV to vertical profiles

RTTOV radiative transfer model (version 3) simulates radiances through a cloud-free atmosphere described in 40 standard pressure levels. The vertical profiles forecast by ARPEGE are first pre-processed before being interfaced with RTTOV :

- The temperature and humidity vertical profile forecast by ARPEG NWP model are interpolated (linearly in logarithm of the pressure) to the RTTOV pressure levels that are below the upper ARPEGE pressure level.

- The temperature vertical profile for RTTOV pressure levels above the upper ARPEGE pressure level (i.e., in the high stratosphere) is extrapolated depending on the location, the day and time of the day of the vertical profile.
- The ozone profile is extracted from the US standard atmosphere (76).
- The surface emissivity is assumed to be 0.96 for continental surface, and is computed from Masuda tables (Masuda et al., 1988) over the sea.

The outputs of RTTOV that have been used in the NOAA and GOES prototypes are the brightness temperatures and the radiances of the simulated channels for cloud-free atmosphere and assuming opaque clouds at the 40 standard pressure level of RTTOV.

3.4. Practical application

3.4.1. Implementation of the Cloud Top Temperature and Height scheme

3.4.1.1. NOAA-AVHRR prototype

The software to extract the cloud top temperature and height from AVHRR has been developed in 1988 (see Derrien et al., 1988). It is applied to AVHRR imagery that has been previously processed to extract the cloud type. The result is available on the whole processed pass at the HIRS spatial resolution, and can also be remapped onto a limited area in a stereographic grid. Since end 1998, this scheme has been daily applied on a development workstation to the four NOAA passes the most centred over France, allowing the computation of statistics on the comparison of different methods applied to AVHRR and HIRS measurements.

3.4.1.2. NOAA-HIRS prototype

The software to extract the cloud top pressure from HIRS measurements has been developed during a visiting scientist stay in 1998. This process, applied to HIRS measurements, requires two preprocessing steps : a remapping of temperature and humidity profiles (forecast par ARPEGE) onto the HIRS grid ; the analysis of the AVHRR imagery to extract the cloud type present in the HIRS's F.O.V. The result is available on the whole processed pass at the HIRS spatial resolution. Since end 1998, this scheme has been daily applied on a development workstation to the four NOAA passes the most centred over France, allowing the computation of statistics on the comparison of different methods applied to AVHRR and HIRS measurements.

3.4.1.3. GOES prototype

As already mentioned, the GOES prototype is a completely new scheme that meets most of the specifications defined for the SEVIRI software. It is detailed in this paragraph.

- The software is implemented on a pre-operational workstation financed by Eumetsat. This workstation receives half-hourly GOES images, and all the needed NWP fields to allow the cloud top computation every half an hour. The cloud top computation is performed after the cloud types extraction.
- The software may be applied to several regions (rectangular in the satellite projection) located in the GOES Extended Northern Hemisphere (illustrated in the annex 5), and defined by their name, the location of their north-west corner and their number of rows/lines. The user may chose the whole Extended Northern Hemisphere itself.

- Segments are defined as square boxes (in the satellite projection) of 32 by 32 GOES IR pixels. Histogram analysis, needed to retrieve cloud top pressure, are performed in these segments. All the solar and satellite angles, the NWP model forecast values, the atlas values and the thresholds will be derived over all the processed regions at the horizontal resolution of the segment.
- When the regions are defined, a script prepares for the user (only once) the regional monthly climatological and atlas maps, as well as latitude/longitude and satellite angles information for his regions at the full IR horizontal resolution. These regional atlas and maps are extracted from maps available on the whole extended northern hemisphere, and stored on a dedicated directory, to be used during the routine processing.
- The routine processing is performed in three steps. All the regions are processed sequentially.
    - the preliminary step is the reprojection of NWP model forecast fields on the regional regions at the segment horizontal resolution. This is monitored by a crontab.
    - the preparation step (monitored by crontab) includes the computation on the regional areas at the segment horizontal resolution of :
        - the satellite & solar angles,
        - the monthly climatological and atlas maps, and
        - the simulated cloud free & opaque cloud radiances with RTTOV.
    - the execution step is the real-time processing of the GOES images itself over the regions. This process is activated by a home-made scheduler (called ARCHIPEL2) when all the input images (including the cloud type) are available on the whole GOES northern hemisphere.

3.4.2. Impact of missing NWP information

The prototypes that have been developed are not robust : they require the availability of all satellite channels and auxiliary data (climatological and atlas maps, and NWP output). Climatological and atlas maps are stored on the disk of the satellite image processing system, and therefore always available. We have never faced a situation where a single satellite channel was missing : this would happen in case a failure of the radiometer itself. On the contrary, NWP fields are produced by a NWP model (external to the satellite processing system), transferred to the satellite processing system : there are therefore reasons why some fields may be missing.

The needed NWP inputs are air temperature and relative humidity on 20 pressure levels and 2m level, plus surface pressure. The surface parameters (surface temperature and pressure, air temperature and relative humidity at 2m) are mandatory, but the prototypes are able to use a temperature and relative humidity vertical profile where some pressure levels are lacking, the missing information being interpolated using the two nearest pressure levels. The impact of the missing levels on the quality of the retrieved parameters has not been estimated.

3.4.3. Estimation of needed informatic resources

CPU and virtual memory size required by both the preparation step (off-line simulation of radiances) and the execution step (real time computation of the Cloud Top Temperature and Height) have been estimated in the GOES prototype for a 512 by 512 IR pixels region :

- CTTH preparation : CPU time : 3 seconds Virtual memory Size : 9512 Kbytes
- CTTH execution : CPU time : 41 seconds Virtual Memory Size : 35016 Kbytes

CPU time and Virtual Memory Size have been measured on a development workstation Sun ULTRA Creator 140E running under SunOS 5.7 for tasks compiled without any optimisation. The exact meanings of « CPU time » and « Virtual Memory Size » are those of the **ps** UNIX command.

3.5. Validation

As the method used to extract the cloud top height product is dependent on the cloud type, the quality may be poor if the cloud type is wrong (for example : the retrieved pressure of a low cloud mis-classified as cirrus cloud will be much too low, if the intercept method is applied to this pixel). The validation presented in this paragraph does not examine the impact of cloud misclassification on its top temperature or pressure.

Validation is more difficult than for cloud mask or type : it has only been performed for semitransparent ice clouds, low opaque clouds, and at a lower extent for medium opaque clouds.

3.5.1. Semitransparent ice clouds

3.5.1.1. Semitransparent ice clouds : comparison with ground-based lidar

Cloud top height of semitransparent ice clouds retrieved with NOAA-AVHRR and HIRS data have been compared with ground-based lidar measurements performed at Lannion (see A.3.3). Seventeen situations could be gathered in 1998 and 1999, corresponding to rather thin cirrus whose top could be observed by the lidar. Satellite and lidar were coincident in time for 13 situations ; less than 90 minutes separates the satellite and lidar measurements for the remaining situations.

The semitransparent cloud top pressures are retrieved for each HIRS F.O.V, using the radiance ratioing techniques applied to six HIRS channels pairs (see 3.3.2.4) and from AVHRR imagery using T11μm and T12μm histogram technique (see 3.2.3.2). For each tested technique, two values were used in the comparison :

- the retrieved cloud pressure of the HIRS F.O.V collocated over Lannion ; if this value is not available, the retrieved cloud top pressure corresponding to the higher retrieved emissivity within the 3*3 HIRS F.O.V around Lannion is retained;
- the retrieved cloud pressure averaged over 5*5 HIRS F.O.V around Lannion.

The lidar measurements retrieves the top height (in km) of thin cloud layers. The cloud top pressure is then obtained assuming a standard atmosphere (see 3.3.3.1). For some situations, two (and even three) cirrus layers could be observed : an averaged top pressure together with the minimum and maximum top pressure were used in the comparison.

The comparison between satellite retrieved and lidar derived cloud top pressures is illustrated on the next five figures (3.5.1.1-3.5.1.5) for five satellite retrieval techniques (radiance ratioing applied to the following HIRS channels pairs : 11.1μm/13.3μm, 11.1μm/13.7μm, 11.1μm/14.0μm, 11.1μm/7.34μm, and AVHRR T11μm and T12μm histogram technique).

The comparison was hindered by some encountered difficulties :

- only the top height of rather thin clouds can be retrieved from lidar measurements, whereas the satellite cloud top retrieval techniques cannot be applied to too thin cloud layers. This partly explains why so few comparison cases could be gathered.

- lidar measurements are ponctual, whereas HIRS F.O.V covers an extensive area. Moreover, the lidar and satellite data are not completely collocated and coincident in time. An attempt to overcome this problem is to analyse the lidar signal during 30 minutes, which allows to have an insight of the cirrus layer spatial homogeneity and information on multiple cloud layers.

The main conclusions from this comparison are the following :

- The best fit between lidar and satellite cloud pressure is obtained with the radiance ratioing technique applied to the 11.1µm window IR & 13.7µm (peaking at 800hPa).
- All techniques overestimate the cloud top pressure : the averaged difference between satellite and lidar pressure takes values from 20hPa (for the ratioing technique applied to 11.1µm & 13.7µm) up to 100hPa for the AVHRR histogram technique, with rms eror from around 50-60hPa (100hPa for the radiance ratioing technique using the 7.34µm water vapour channel).
- The AVHRR T11µm/T12µm histogram technique gives the worst results. In fact, the comparison cases correspond to rather thin cirrus clouds, for which the histogram retrieval technique is not adequate (as stated in 3.3.2.3, this technique assumes that part of the cirrus layer is thick enough (emissivity larger than 0.5)).
- The radiance ratioing technique using the 11.1µm window IR & 7.34µm water vapour channel (peaking at approximately 700hPa) can be applied on only 8 cases, and gives the larger scatter. This must be due to the fact that the 7.34µm simulation is not accurate, due to the water vapour vertical profile uncertainty.
- Usually, the larger cloud top pressure overestimation is observed for the thinner cirrus. This is the case for the ratioing technique applied to 11.1µm and 13.3µm : the differences between the satellite and the lidar cloud top pressure were within +/-100hPa, except for low cloud emissivities (overestimation up to 200hPa).

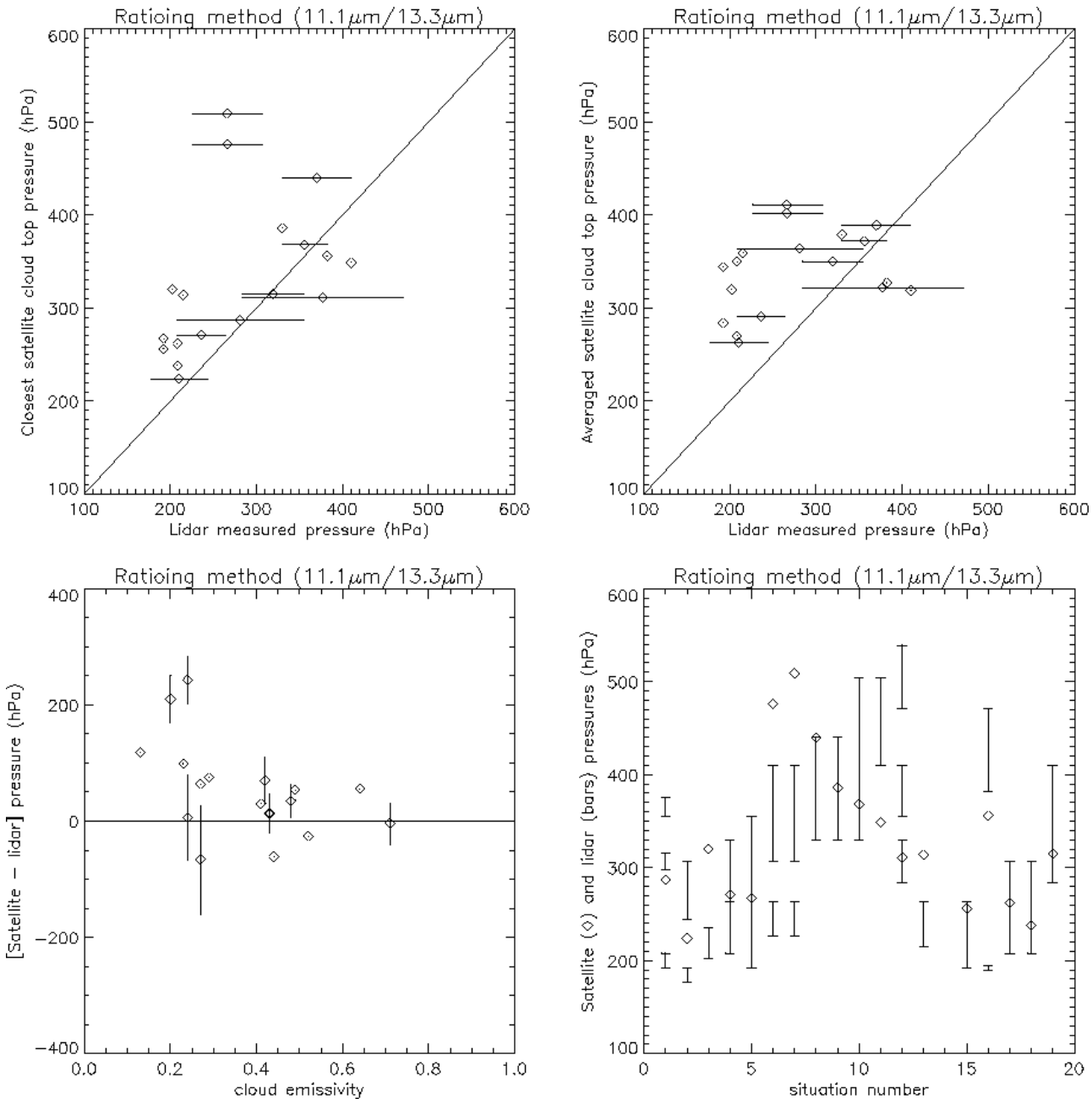

Figure 3.5.1.1 Comparison between satellite and lidar cloud top pressure. For the radiance ratioing technique applied to the 11.1µm/13.3µm HIRS channel pairs.

Note : The horizontal and vertical bars (top figures and bottom left figure) indicate the minimum and maximum top pressure observed with the lidar (the diamond symbol corresponds to the averaged lidar cloud top pressure). Each vertical bars on the bottom right figure corresponds to a cirrus layer observed with the lidar.

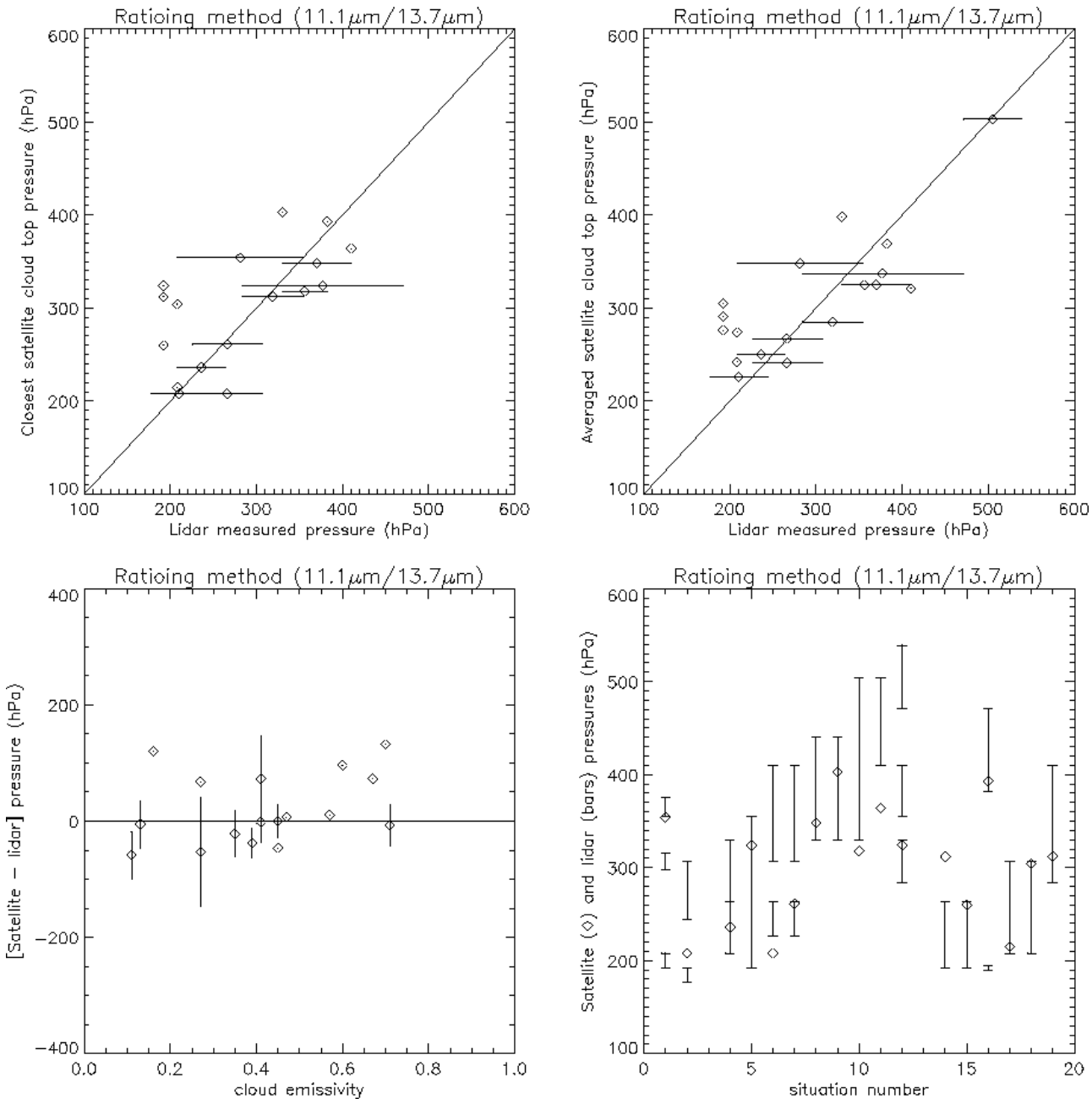

Figure 3.5.1.2 Same as 3.5.1.1 for the radiance ratioing technique applied to the 11.1μm/13.7μm HIRS channel pairs.

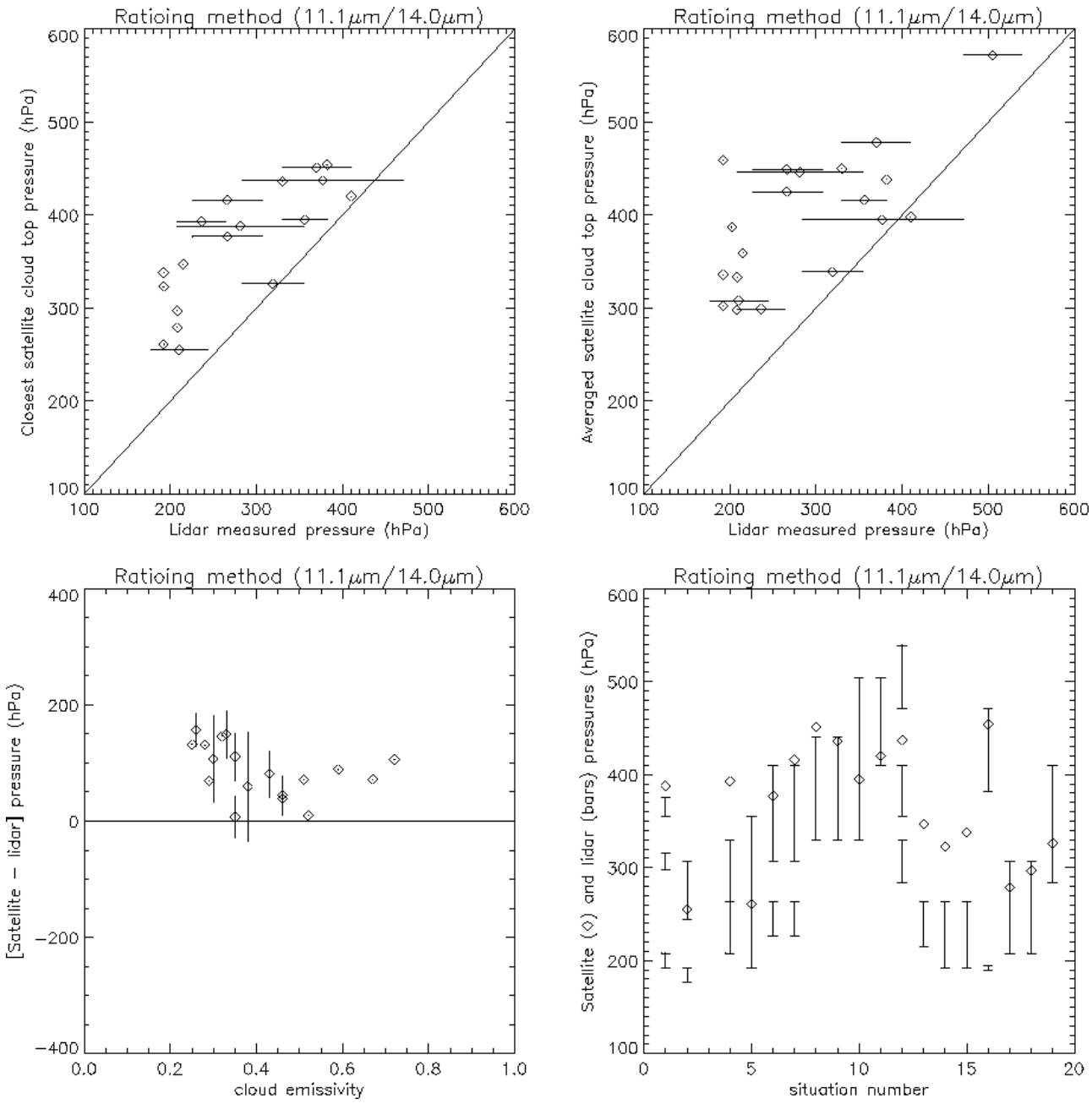

Figure 3.5.1.3 Same as 3.5.1.1 for the radiance ratioing technique applied to the 11.1μm/14.0μm HIRS channel pairs.

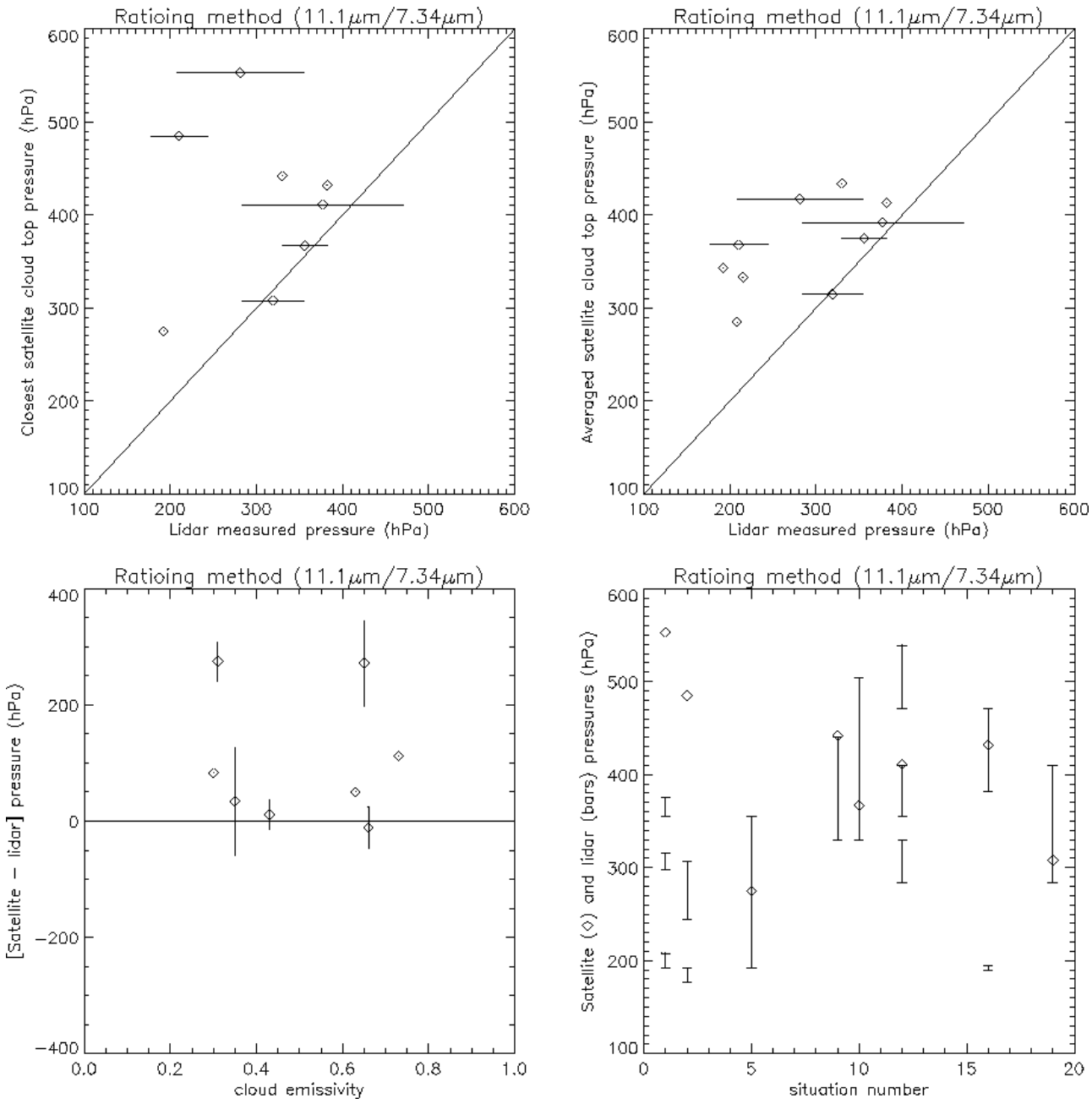

Figure 3.5.1.4 Same as 3.5.1.1 for the radiance ratioing technique applied to the 11.1μm/7.34μm HIRS channel pairs.

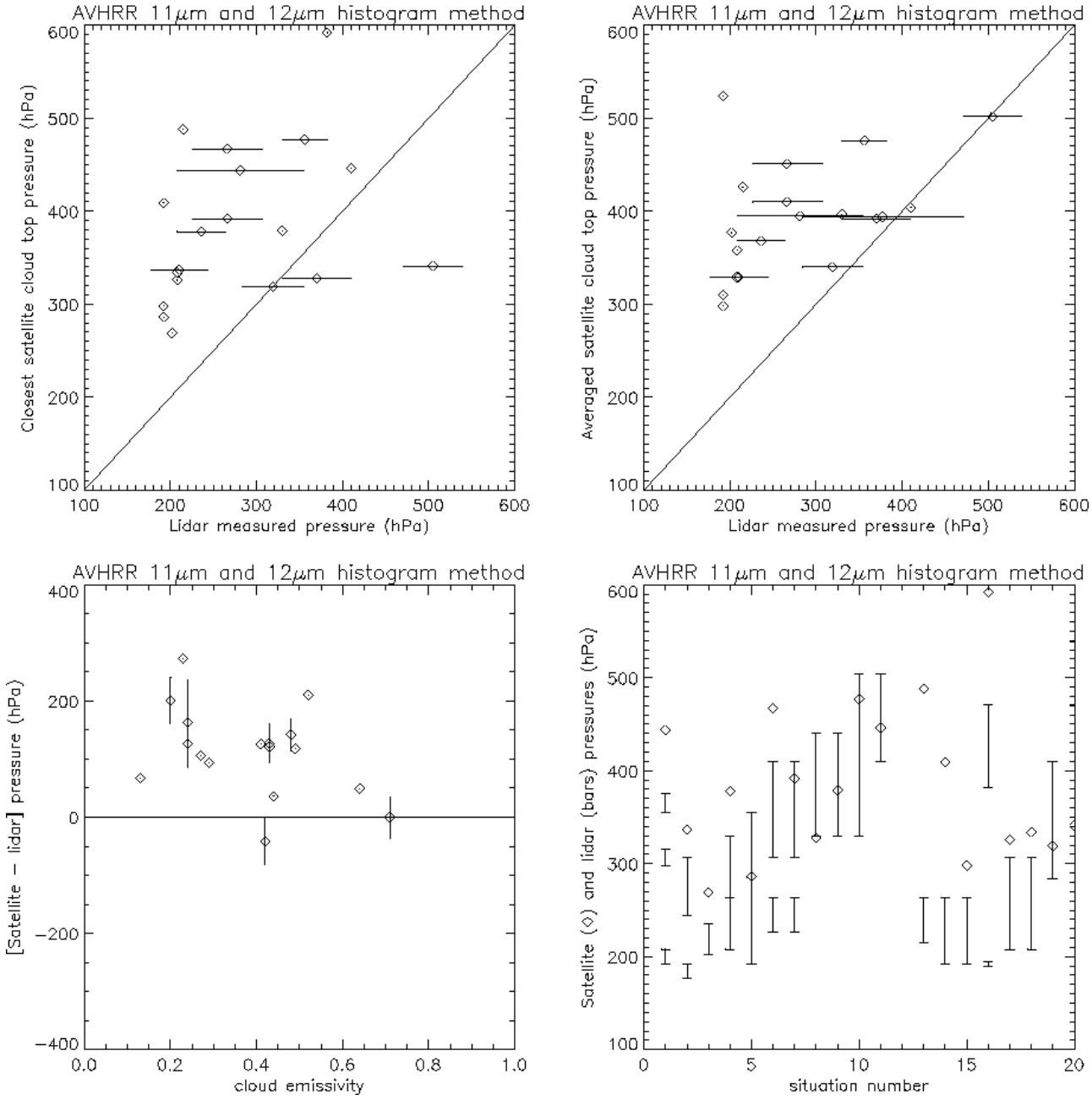

Figure 3.5.1.5 Same as 3.5.1.1 for the AVHRR T11μm and T12μm histogram technique.

3.5.1.2. Semitransparent ice cloud :inter-comparison of different methods

The NOAA and GOES prototypes have been used to gather statistics on retrieved semitransparent cloud top pressure by different methods:

- The NOAA prototype has allowed to analyse and compare the radiance ratioing technique applied to various HIRS channels pairs (11.1µm/13.3µm, 11.1µm/13.7µm, 11.1µm/14.0µm, 11.1µm/7.34µm, 11.1µm/6.75µm, 7.34µm/6.75µm) and the T11µm & T12µm histogram method applied to AVHRR. statistics are illustrated on figures 3.5.1.6 and 3.5.1.7.
- The GOES prototype has allowed to compare the radiance ratioing technique (applied to individual pixels) to the H2O/IRW intercept method (applied to histograms) and check their temporal consistency. Statistics are illustrated on figures 3.5.1.8 and 3.5.1.9.

NOAA statistics have allowed to compare HIRS radiance ratioing technique and AVHRR histogram method (figure 3.5.1.6) :

- The cloud top pressures, retrieved with the AVHRR histogram method, are on average between 10 and 50hPa lower than with the radiance ratioing techniques. This result is apparently in contradiction with the comparison with lidar measurements, which indicates larger retrieved cloud top pressure with the AVHRR histogram technique. The reason may be that only very thin cirrus were used during the comparison with lidar, whereas the statistics include thicker cirrus also.
- The radiance ratioing technique, applied to various HIRS channels pairs, gives similar results (average values within 20hPa), except for the 11.1µm/7.34µm pair for which larger retrieved pressures are obtained.
- The averaged differences between results obtained from the radiance ratioing techniques and the AVHRR histogram methods are satellite-dependent : 20hPa difference is observed for the 11.1µm/7.34µm pair between NOAA-12 and NOAA-15. It may be due to the radiative transfer's accuracy which plays a major role in the radiance ratioing technique.
- The differences between the cloud top pressure retrieved with the radiance ratioing technique and the AVHRR histogram show large rms error (50hPa, 60hPa for NOAA-12).

An attempt has been made to assess the accuracy of each tested method by using the retrieved cloud parameters to simulate HIRS brightness temperatures (figures 3.5.1.7). An error in the cloud height estimation should induce an error in HIRS sounding channels' simulation : systematic errors should lead to a bias in the statistics, whereas random errors should increase the associated rms error. The difficulty is that an error in the height estimation leads to an error in the emissivity (computed using T11µm brightness temperature) and both errors may compensate for themselves in the HIRS simulation [this should be less true for infrared short-wave channels at 4µm, due to the Planck effect] :

- As expected, statistics for channel 14.5µm (peaking at 100hPa and therefore nearly insensitive to clouds) are nearly the same for cloud-free and cloudy (opaque or semitransparent) situations.
- Statistics of simulated minus measured brightness temperatures for semitransparent clouds present higher rms error when the AVHRR histogram method is used, which indicates that this technique induces higher random errors than the radiance ratioing techniques.
- Concerning statistics of simulated minus measured brightness temperatures at 14.2µm, 14.0µm and 13.7µm, the bias and rms error for semitransparent clouds [when radiance

ratioing technique applied to HIRS channels in the CO_2 absorption band at 15µm is used to estimate cloud parameters] are similar to that obtained for opaque clouds. Note that results for channels at 14.0µm and 13.7µm must be handled cautiously as these channels are used in the retrieval by the radiance ratioing technique itself.

- Concerning statistics of simulated minus measured brightness temperatures at 4.40µm and 4.47µm, the rms errors for semitransparent clouds [when radiance ratioing technique are used to estimate cloud parameters] are similar to that obtained for opaque clouds, which indicates that the radiance ratioing performs rather well.

GOES statistics have showed that :

- the cloud top pressures retrieved with the radiance ratioing technique are on average between 10 and 20hPa larger than if obtained with the H2O/IRW intercept method ; the scatter between both methods is rather large (a rms error of 50hPa is observed) [see figure 3.5.1.8].
- as shown on figure 3.5.1.9, the transparency correction performed by the H2O/IRW intercept method presents a diurnal effect of about 50hPa (5°C) : it is larger for slot 36. This can be due to the fact that this method is supposed to correct the 11µm infrared measurement from the surface contribution which is larger when the ground is overheated (i.e., for the slot 36).

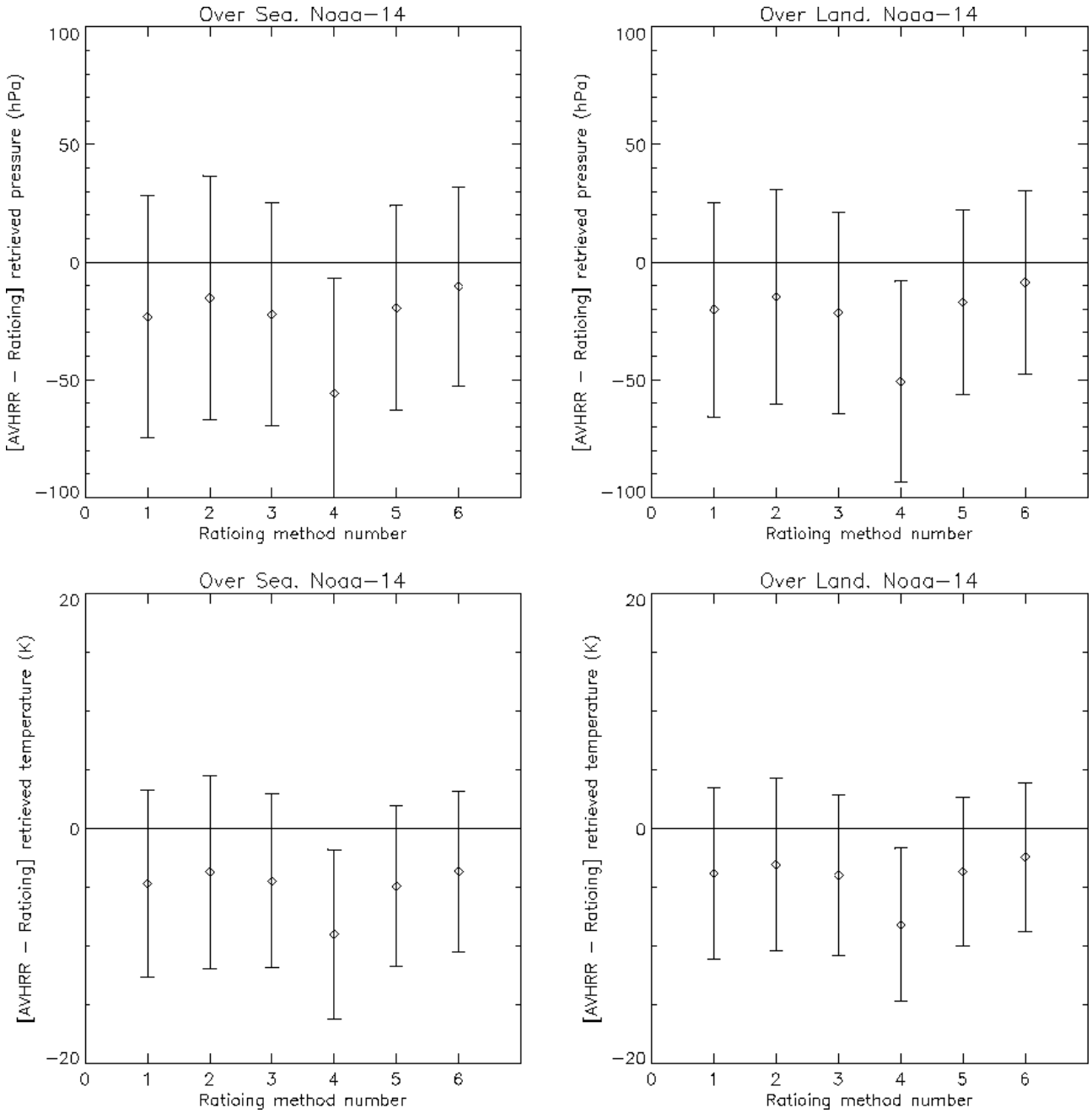

Figure 3.5.1.6 Comparison of semitransparent ice cloud top pressure and temperature retrieved with the radiance ratioing technique (applied to 6 HIRS channel pairs (11.1µm/13.3µm, 11.1µm/13.7µm, 11.1µm/14.0µm, 11.1µm/7.34µm, 11.1µm/6.75µm, 7.34µm/6.75µm)) and the AVHRR $T11_{\mu m}/T12_{\mu m}$ histogram method.

The diamond symbols and the vertical bars correspond respectively to the mean and rms error values. Statistics are computed on a six-month period [End 1998-mid1999].

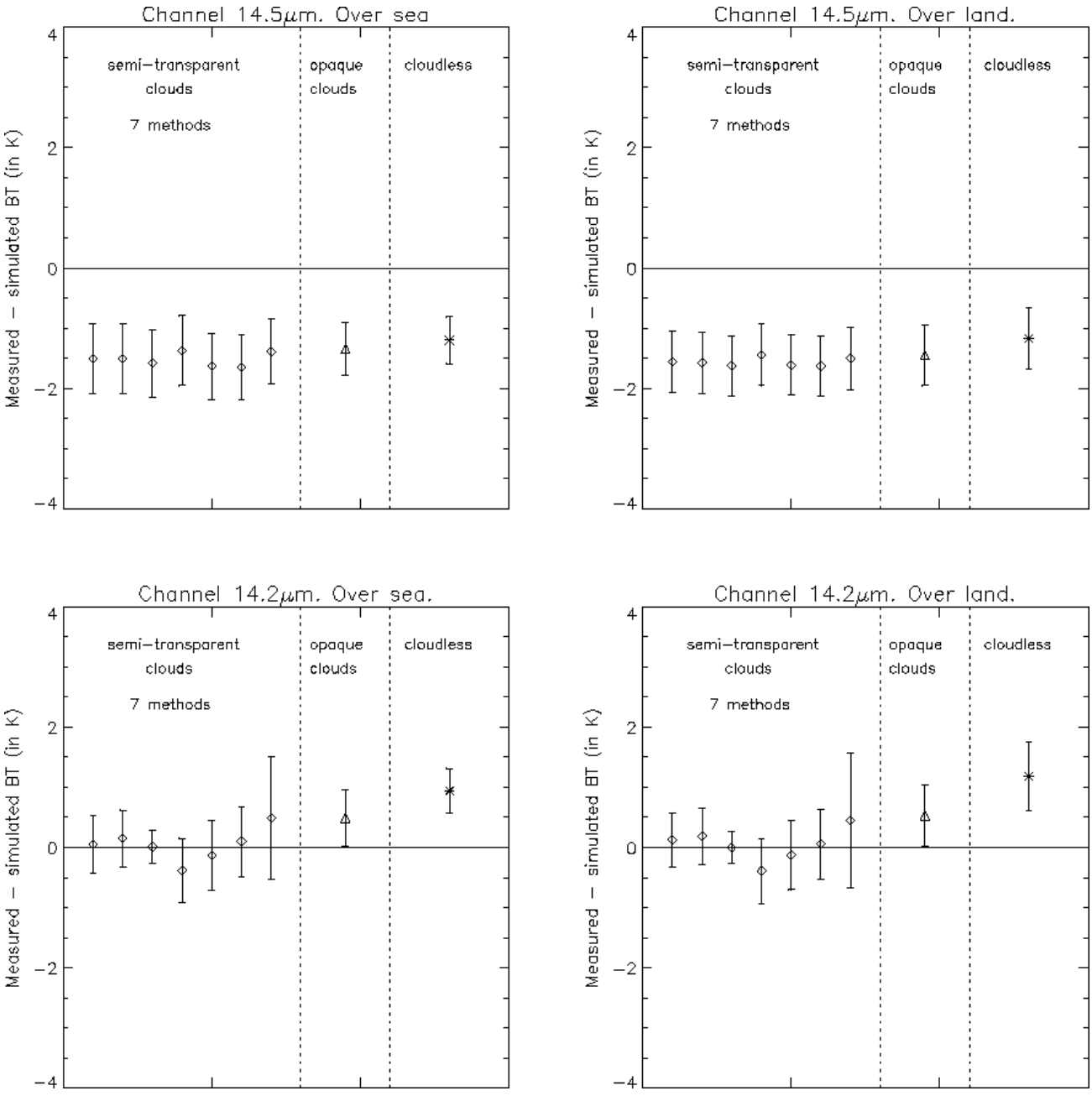

Figure 3.5.1.7(a) Comparison of measured and simulated brightness temperatures for NOAA-14/HIRS channels at 14.5µm (peaking at 100hPa) and at 14.2µm (peaking at 400hPa).
The brightness temperatures' simulations use : -forecast ARPEGE vertical temperature and humidity profiles ; -semitransparent cloud top pressure and emissivity retrieved with the radiance ratioing technique applied to six HIRS channel pairs (11.1µm/13.3µm, 11.1µm/13.7µm, 11.1µm/14.0µm, 11.1µm/7.34µm, 11.1µm/6.75µm, 7.34µm/6.75µm) and the AVHRR T11µm/T12µm histogram method. The symbols and the vertical bars corresponds respectively to the mean and rms error values. Statistics are computed on a six-month period [End 1998-mid1999].

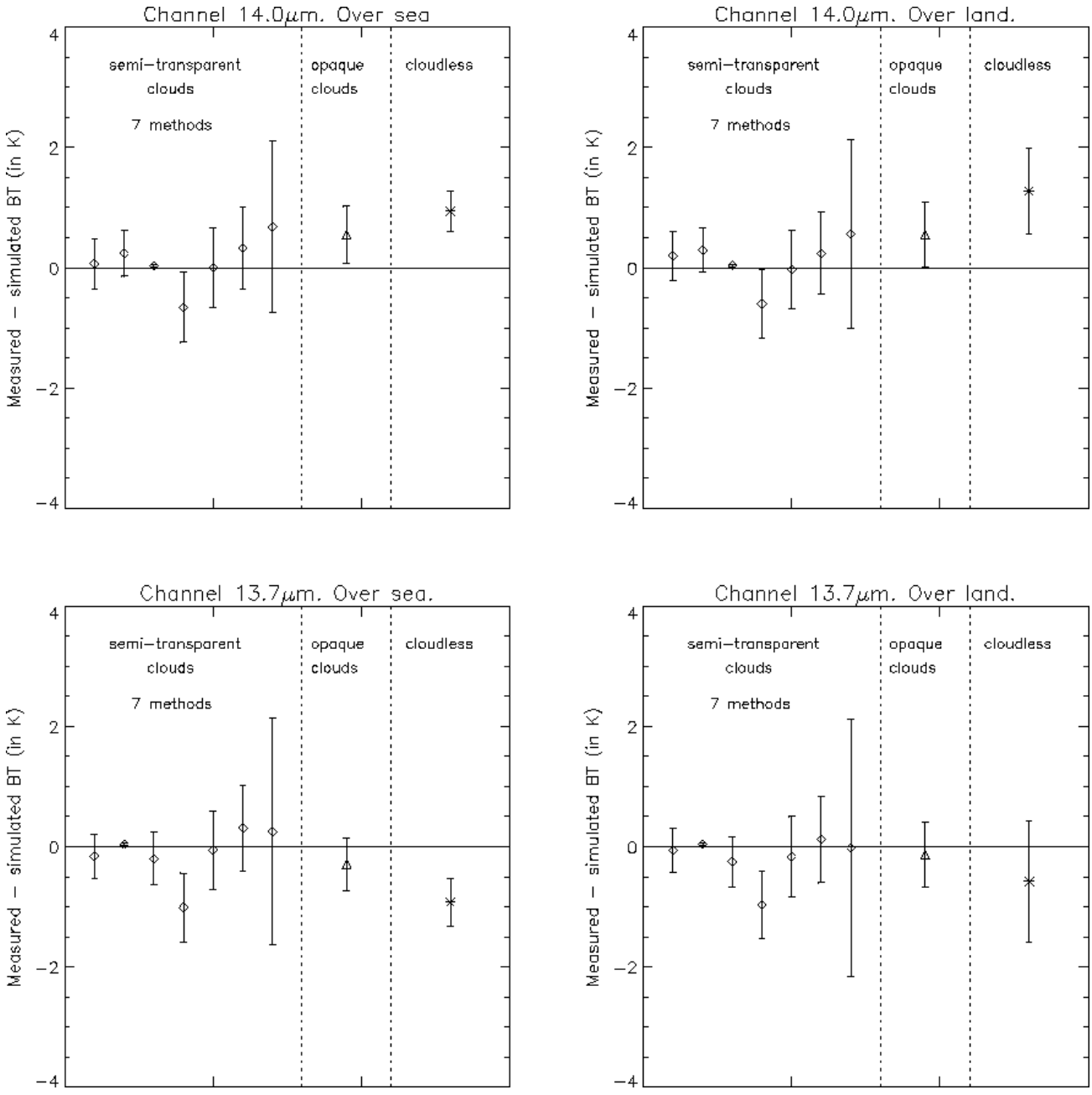

Figure 3.5.1.7(b) Same as figure 3.5.1.7(a) for NOAA-14/HIRS channels at 14.0μm (peaking at 600hPa) and at 13.7μm (peaking at 900hPa).

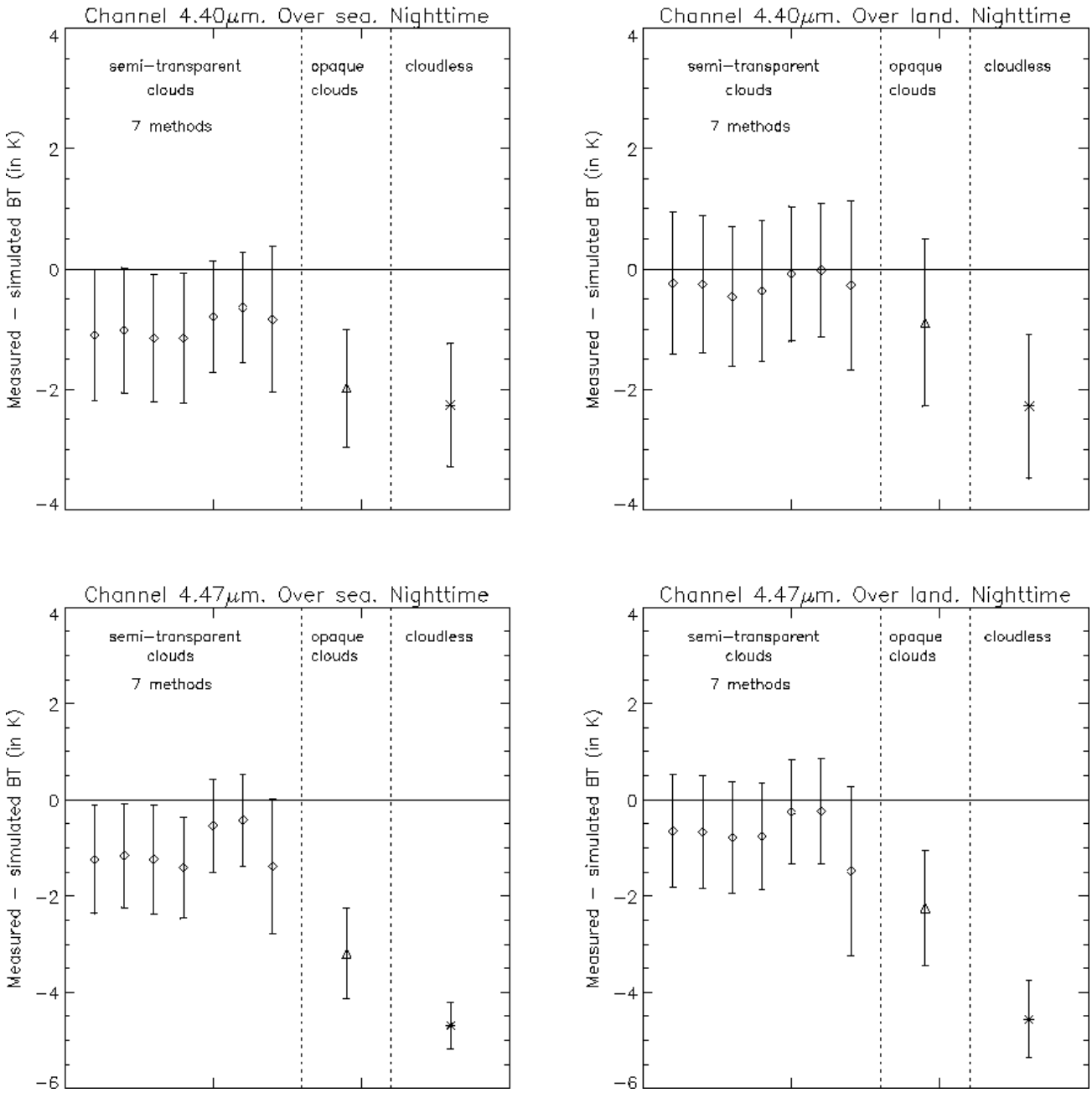

Figure 3.5.1.7(c) Same as figure 3.5.1.7(a) for NOAA-14/HIRS channels at 4.40µm (peaking at 400hPa) and at 4.47µm (peaking at 800hPa). Only night-time measurements are used, as these channels may be contaminated by solar irradiation.

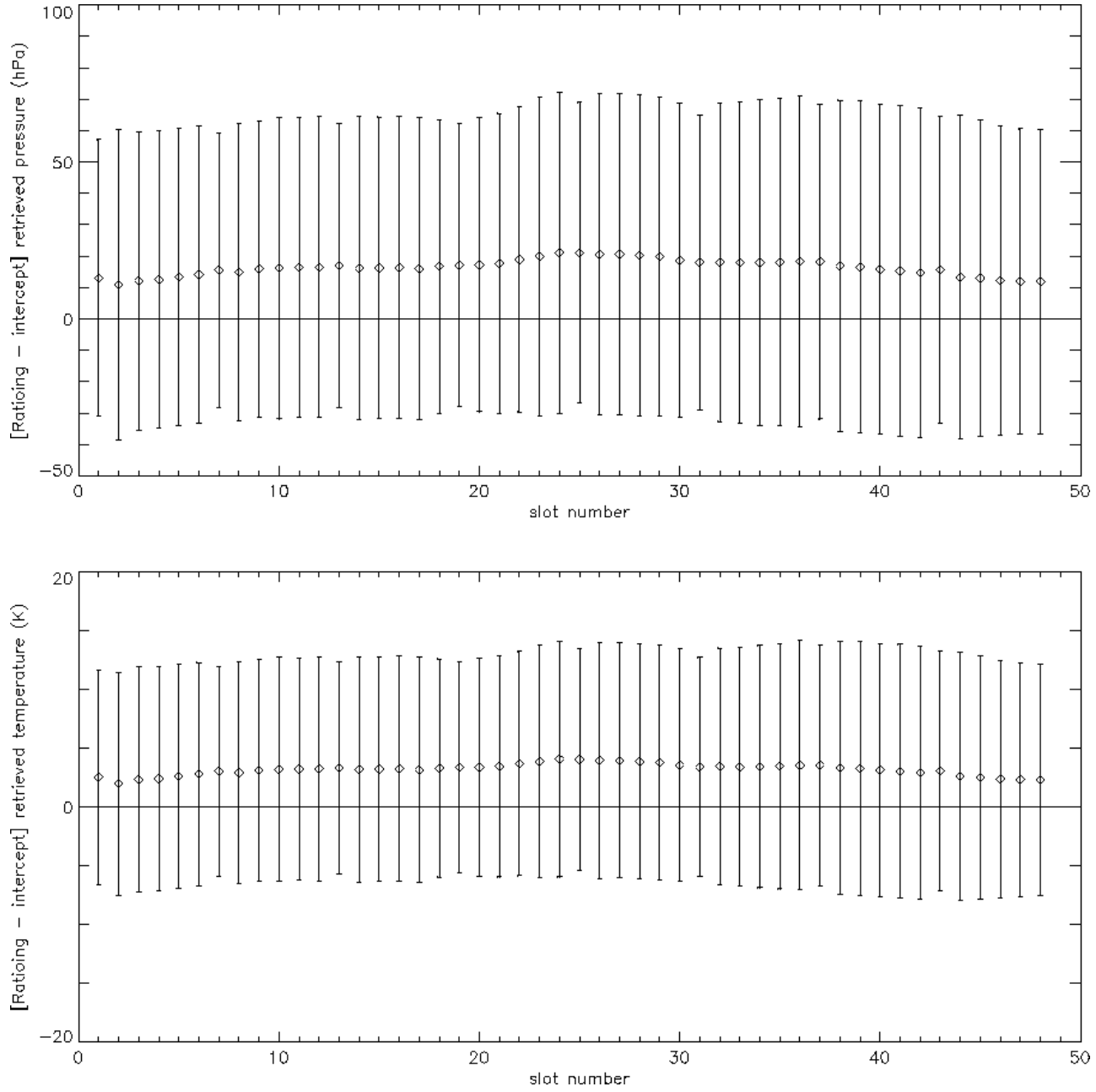

Figure 3.5.1.8 Comparison of semitransparent ice cloud top pressure and temperature retrieved with the radiance ratioing technique and the H2O/IRW intercept method for each GOES slot. The diamond symbols and the vertical bars corresponds respectively to the mean and rms error values. Statistics are computed on a five-month period [February-June 1999].

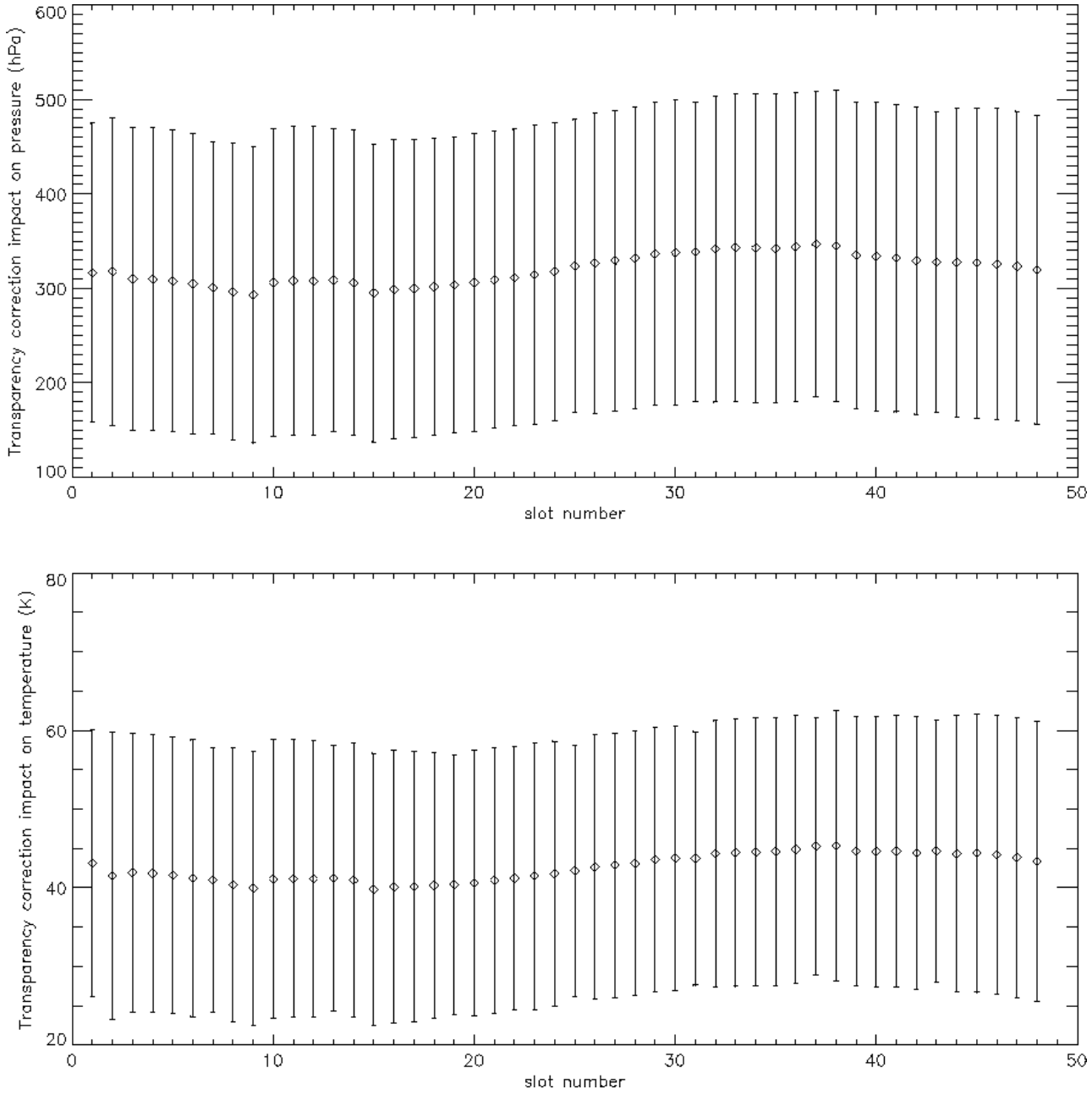

Figure 3.5.1.9 Mean and rms error of the transparency correction applied to semitransparent ice clouds for each GOES slot. [The transparency correction is defined by the difference between cloud top directly retrieved from 11µm brightness temperature and retrieved with the H2O/IRW intercept method]. The statistics are computed on a five-month period [February-June 1999].

3.5.1.3. Semitransparent ice clouds : impact of NWP forecast vertical profile on H2O/IRW intercept method applied to GOES imagery

To analyse the impact of the NWP forecast vertical profile, the H2O/IRW intercept method has been applied to retrieve the cloud top pressure of semitransparent clouds, using ARPEGE forecast fields and ECMWF analysed fields. The comparison of the retrieved cloud top pressure using both NWP models gives an insight of the impact of the model in the result.

This procedure has been applied to GOES imagery (slot 24, i.e. 12 UTC) for three days (11-07-1999,12-07-1999 and 15-08-1999). The difference between both retrieved pressures is small : the bias is smaller than 6 hPa with a rms error lower than 16 hPa.

3.5.2. Low opaque clouds :

3.5.2.1. Low opaque clouds : impact of NWP forecast vertical profile (GOES prototype)

To analyse the impact of the NWP forecast vertical profile, the cloud top pressure has been retrieved using ARPEGE forecast fields and ECMWF analysed fields. The comparison of these retrieved cloud top pressure using both NWP models gives an insight of the impact of the model in the result.

This procedure has been applied GOES imagery (slot 24, i.e. 12 UTC) for three days (11-07-1999,12-07-1999 and 15-08-1999). The difference between both retrieved pressure is relatively high : the bias is around -8 hPa for very low clouds and 5 hPa for low clouds, with high rms error varying between 15 and 30hPa depending on the situation. This seems to indicate, that when retrieving low cloud top pressure from its radiative temperature, the vertical structure of the lower atmosphere (not well described in the NWP forecast fields used during our prototyping) has a rather high impact in the result.

3.5.2.2. Low opaque clouds : comparison with cloud top estimated from radio-soundings

A comparison of low cloud top pressure & temperature retrieved from GOES imagery and estimated from radio-sounding has been performed. During a one month-period (12/07/99-18/08/99), we have selected radio-soundings available in East of North America (only 00 UTC and 12UTC) using the following procedure : -a single layer of stratus or stratocumulus is observed at the radio-sounding station; -low clouds are detected in the GOES imagery around the radio-sounding station. For the 37 selected cases, cloud top pressure and temperature retrieved from satellite imagery (in a 9*9 IR pixel area) are compared to cloud top pressure estimated from radio-sounding.

The comparison is illustrated on figures 3.5.2.1 and 3.5.2.2. The difference between the cloud top retrieved from satellite and that estimated from the radio-sounding is on average -24 hPa (50hPa rms error) in pressure and 0.5°C (1.9°C rms error) in temperature.

A finer analysis indicates that the error in pressure can be partly explained in case of a strong thermal inversion in the atmospheric vertical profile : in the prototype, the cloud is not allowed to be below a thermal inversion, whereas the estimation of cloud top pressure from the radio-sounding usually leads to a cloud below strong inversions. This is illustrated on figure 3.5.2.1 (bottom left). The satellite-retrieved cloud top temperature does not seems to be affected by thermal inversion (figure 3.5.2.2 bottom left). In the GOES prototype, the quality flag appended to the cloud top

product indicates if a the thermal inversion has been detected in the forecast atmospheric vertical profile.

Another potential source of error seems to be the influence of ground temperature on the result (figure 3.5.2.2 bottom right) : the strongest cloud top temperature overestimations seem to be associated to strong surface overheating, as if the cloud was not fully opaque and therefore contaminated by the surface. In the GOES prototype, the quality flag indicates a bad quality for opaque clouds if different results is obtained using 11µm and 12µm infrared window channels, which means that the cloud was not completely opaque.

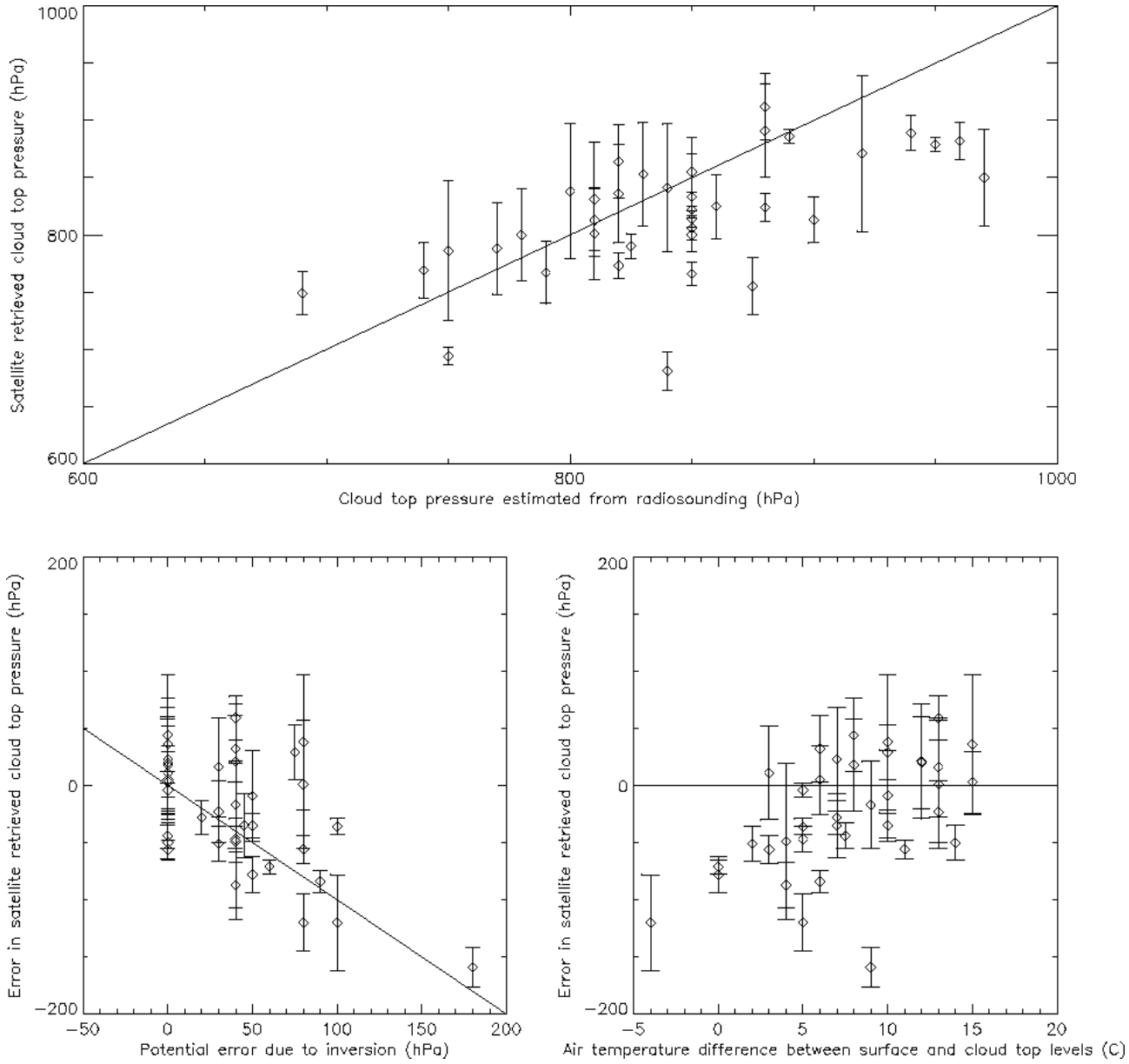

Figure 3.5.2.1 Comparison between cloud top pressure retrieved from satellite and estimated from radio-soundings (over North-East America, 12/07/99-18/08/99). The error in satellite retrieved cloud top pressure stands for : pressure retrieved from satellite minus pressure estimated from radio-soundings . The potential error due to inversion is estimated from the radio-soundings : it corresponds to the pressure difference between the two levels having the cloud temperature (possible only if the estimated cloud is below a thermal inversion).

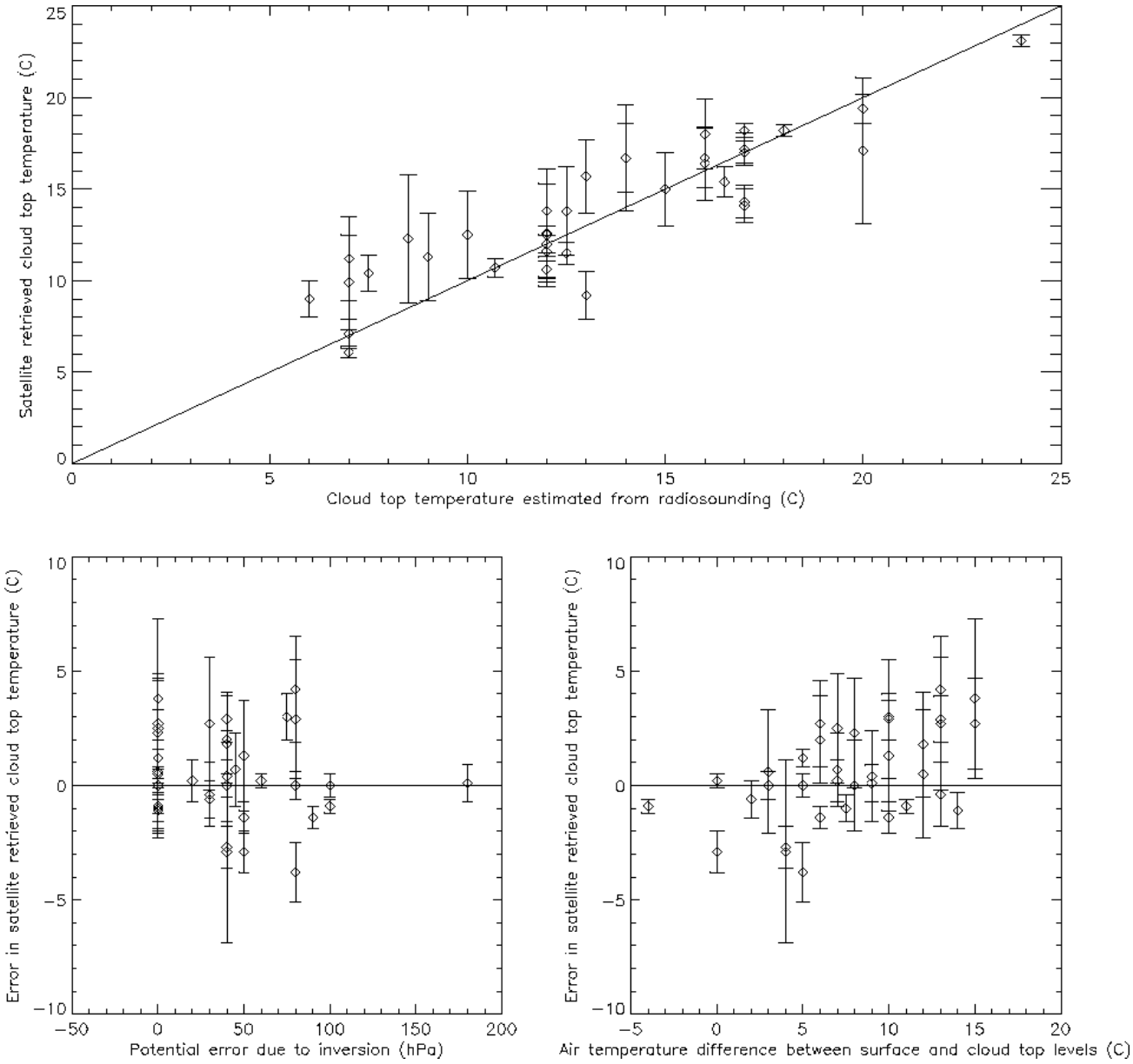

Figure 3.5.2.2 Comparison between cloud top temperature retrieved from satellite and estimated from radio-soundings (over North-East America, 12/07/99-18/08/99). The error in satellite retrieved cloud top pressure stands for : pressure retrieved from satellite minus pressure estimated from radio-soundings . The potential error due to inversion is estimated from the radio-soundings : it corresponds to the pressure difference between the two levels having the cloud temperature (possible only if the estimated cloud is below a thermal inversion).

3.5.3. Medium opaque clouds

3.5.3.1. Medium opaque clouds : impact of NWP forecast vertical profile (GOES prototype)

The procedure described in 3.5.2.1 has been applied GOES imagery (slot 24, i.e. 12 UTC) for three days (11-07-1999,12-07-1999 and 15-08-1999). The difference between both retrieved pressures is low : the bias is smaller than 2 hPa with a rms error less than 8 hPa.

3.6. The Demonstration experiment

A description of the demonstration experiment is given in annex A.5. During this experiment (8th November 1999 - 8th December 1999), half-hourly GOES cloud top pressure over the Extended Northern Hemisphere were made available for visualisation in GIF format (see figure 3.6.1).

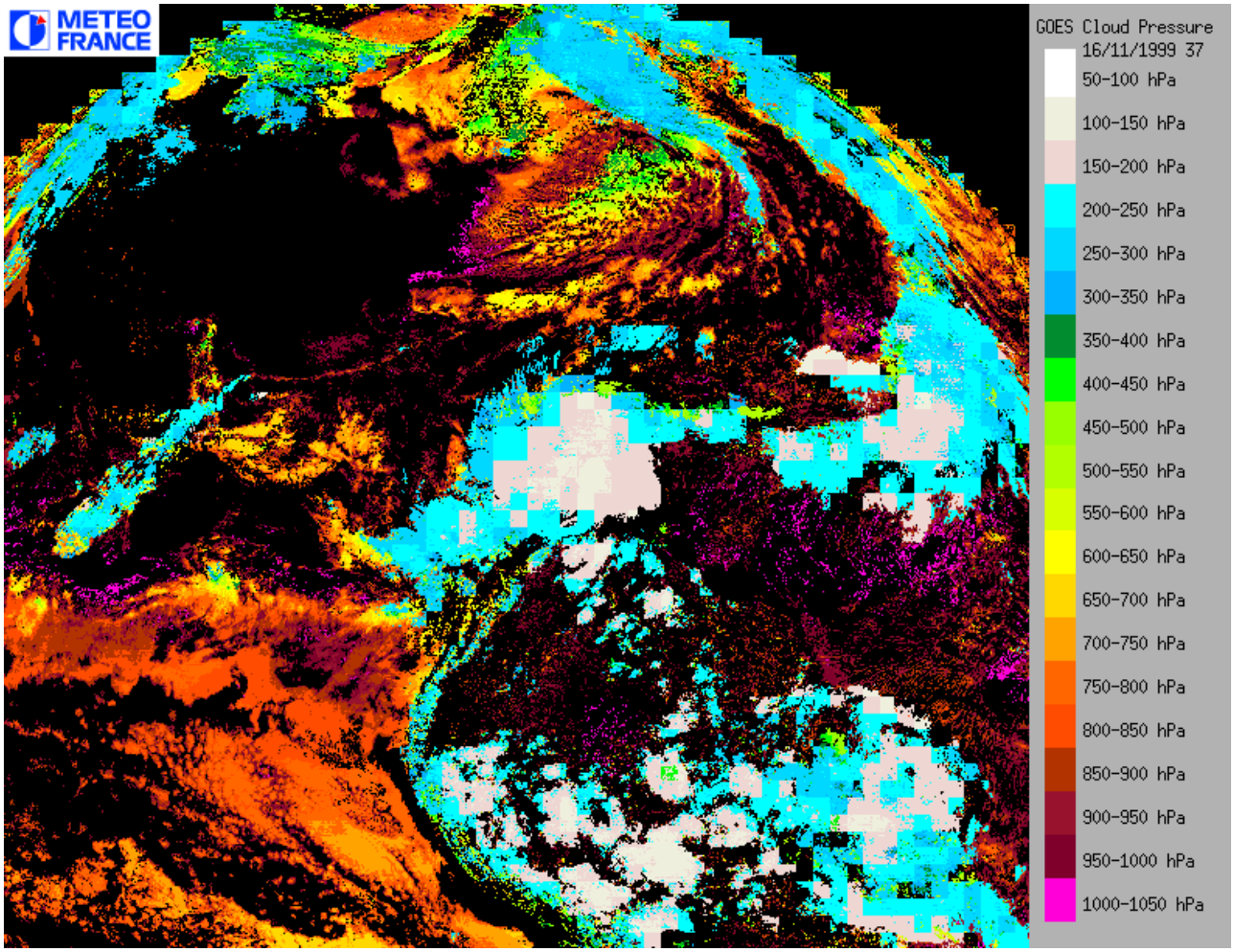

Figure 3.6.1 Example of cloud top pressure prototyped with GOES and available during demonstrator experiment.

A comparison of low clouds top pressure retrieved from GOES imagery and estimated from radiosondes, has been performed during the demonstrator experiment using a procedure slightly different from the one described in 3.5.2.2. Experienced forecasters at CMS have daily used SYNERGYE (the workstation available to french forecasters for visualisation of satellite imagery,

NWP model outputs...) to display the cloud type and top pressure prototyped with GOES. Using tools available on SYNERGYE workstation, they have analysed the radiosondes (0 and 12 UTC) in areas where low clouds were detected with satellite images, to determine the cloud top pressure. The cloud top is placed at the bottom of the temperature inversion plus approximately 5 to 10 hPa, considering a sufficient humidity at this level. These cloud top pressures extracted from radiosondes are finally compared with cloud top pressures retrieved from GOES imagery close to the radiosondes (see figure 3.6.2). This comparison, performed during November which more favours the presence of low clouds and low level inversion in North America than August studied in 3.5.2.2, confirms the results presented in 3.5.2.2 : a systematic bias (the cloud top pressure is underestimated by 52 hPa) and a higher rms error (69hPa) are also observed. These bias and rms error are nearly the same in the evening at 0UTC (48hPa and 71hPa) as in the morning at 12UTC (48hPa and 67hPa).

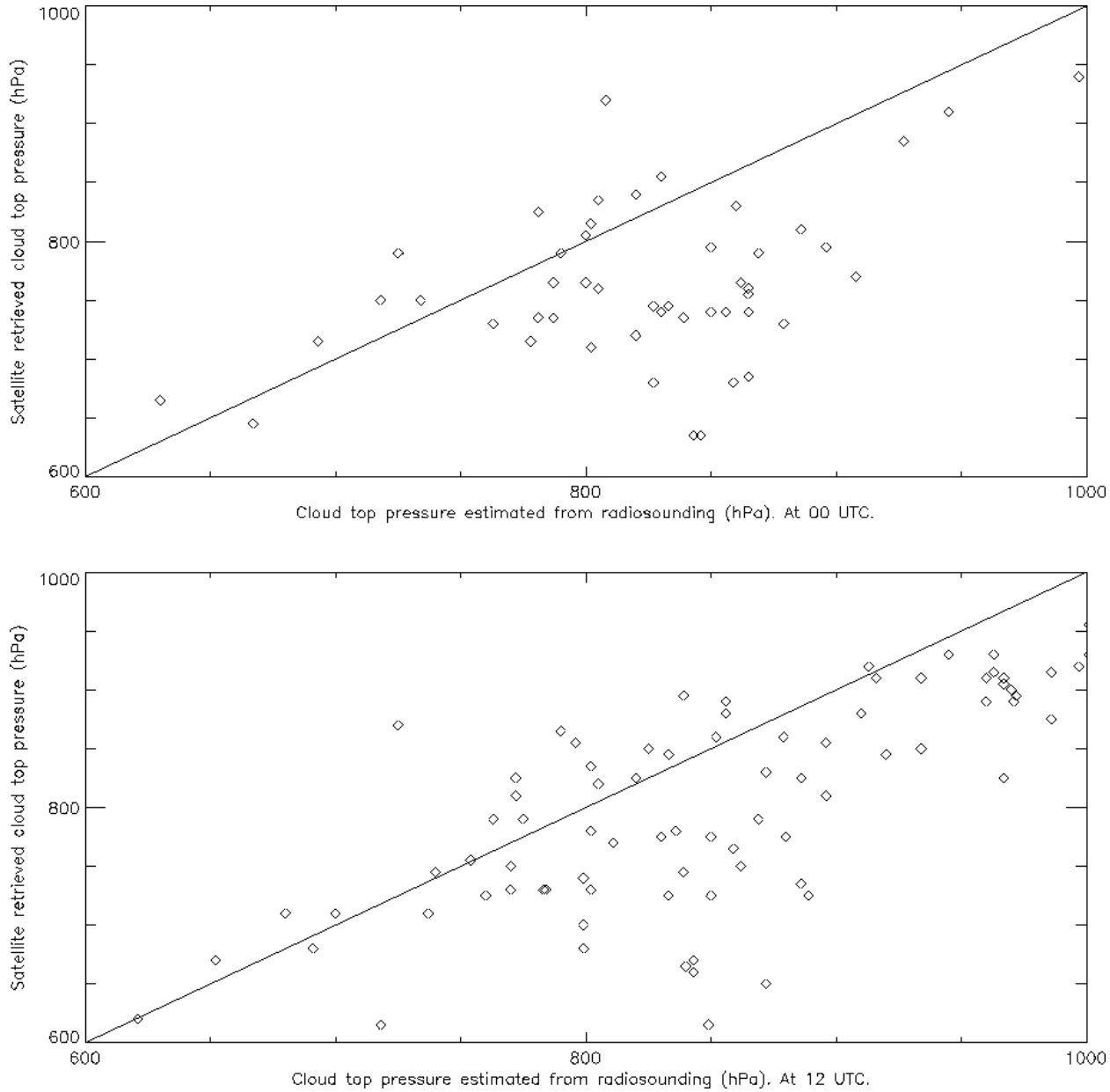

Figure 3.6.2 Comparison between cloud top pressure retrieved from satellite and estimated from radio-soundings (over North-East America, during Demonstrator experiment)

3.7. Future application to SEVIRI

3.7.1. Conclusion from prototyping :

The prototyping with NOAA and GOES has allowed to gain experience for the development of the algorithm and software to process SEVIRI :

- we have checked the technical feasibility of real time cloud top estimation using GOES imagery
- we have quantified accuracy that can be expected for low clouds (with GOES imagery) and high semitransparent clouds (with NOAA data)
- we have compared different methods for high semitransparent cloud top retrieval with NOAA and GOES

Taking into account the result of prototyping, we propose to implement the algorithm described below :

Input data (M indicates mandatory input) :

- Satellite imagery from current slot (see annex A.1.3; availability of data checked for every pixel):
  - 6.2µm, 7.3µm, 13.4µm (at least one of these three channels is Mandatory to process high semitransparent clouds), 11µm (M), 12 µm (M) at full IR spatial resolution
  - Satellite angles associated to SEVIRI imagery (M).
- CMa (M) and CT (M)
- NWP parameters (see annex A.2.2) :

Forecast fields of the following parameters (minimum frequency : 4 per days), remapped onto satellite images (at the segment resolution), are used as input :

- elevation of the NWP model grid (M)
- air temperature and relative humidity on pressure levels (Mandatory : at least one pressure level every 100hPa layer from 1000hPa up to 50hPa)
- surface pressure (M)
- surface temperature (M)
- air temperature and relative humidity at 2m (M)

If those NWP are not input to the software, only the cloud top temperature of opaque clouds will be computed.

- Ancillary data sets (see annex A.2.1) :

The following ancillary data, remapped onto satellite images, are used as input :

- Land/sea atlas (M)
- Elevation atlas (M)
- Monthly minimum SST climatology (M)
- Monthly mean 0.6µm atmospheric-corrected reflectance climatology (land) (M)
- rttov coefficients (M)

Output data :

The content of the CTTH is the following :

- 6 bits for cloud top pressure

Cloud pressure : from 0hPa up to 1050hPa ; step : 25hpa

Linear conversion from count to pressure :

$$\text{Cloud Pressure} = \text{gain} * \text{Count}_{6\text{bits}} + \text{intercept}$$

where intercept = -250 hPa
gain = 25 hPa/count

Special count = 0 used when no cloud pressure is available

- 7 bits for cloud top height

Cloud height : from -400m up to 20000m ; step : 200m

Linear conversion from count to height :

Cloud Height = gain * $Count_{7bits}$ + intercept

where intercept = -2000m
gain = 200m/count

Special count = 0 used when no cloud height is available

- 8 bits for cloud top temperature

Cloud temperature : from 180K up to 320K ; step : 1K

Linear conversion from count to temperature :

Cloud Temperature = gain * $Count_{8bits}$ + intercept

where intercept = 150K
gain = 1K/count

Special count = 0 used when no cloud temperature is available

- 5 bits for effective cloudiness

Effective cloudiness : from 0% up to 100% ; step : 5%

Linear conversion from count to cloudiness :

Cloudiness= gain * $Count_{5bits}$ + intercept

where intercept = -50%
gain = 5%/count

Special count = 0 used when no cloudiness is available

- 14 bits for quality

2 bits to define processing status:

0 non-processed. encompasses :
-CM and/or CT Non-processed or undefined,
-Image areas that may not be processed [when the images'size is not a multiple of the PGE03 segment size]

1 non-processed because FOV is cloud free

2 processed because cloudy, but without result

3 processed because cloudy, with result

1 bit set to 1 when RTTOV IR simulations are available

3 bits to describe NWP input data

0 undefined (space)

1 All NWP parameters available, no thermal inversion

2 All NWP parameters available, thermal inversion present

3 Some NWP pressure levels missing, no thermal inversion

4 Some NWP pressure levels missing, thermal inversion present

2 bits to describe SEVIRI input data

0 undefined (space)

1 all SEVIRI useful channels available

2 at least one SEVIRI useful channel missing

4 bits to describe which method has been used

0 Non-processed

1 Opaque cloud, using rttov

2 Opaque clouds, not using rttov

3 Intercept method 11µm/13.4µm :
4 Intercept method 11µm/6.2µm :
5 Intercept method 11µm/7.3µm :
6 Radiance Ratioing method 11µm/13.4µm
7 Radiance Ratioing method 11µm/6.2µm
8 Radiance Ratioing method 11µm/7.3µm
9-15 Spare for not yet defined methods

2 bits to describe quality of the processing itself
0 No result (Non-processed, cloud free, no reliable method)
1 Good quality (high confidence)
2 Poor quality (low confidence)

Algorithm outline :

The different steps of the processing, applied to cloud-classified image, are listed below :

- RTTOV infrared radiative transfer model is applied on the temperature and humidity vertical profile forecast by NWP model to simulate 6.2µm, 7.3µm, 13.4µm, 11µm, and 12µm radiances and brightness temperatures for cloud free atmosphere and for opaque clouds for the vertical pressure levels defined in RTTOV code. The input vertical profiles used are temporally interpolated to the exact slot time using the two nearest in time NWP outputs fields. This process is performed in each segment of the image (i.e., box of 32*32 SEVIRI IR pixels).
- The technique used to retrieve the cloud top pressure depends on the cloud's type :
    - For low, medium of high thick clouds : The cloud top pressure is retrieved on a pixel basis and corresponds to the best fit between the simulated and the measured 11µm radiances. The simulated radiances, initially computed at the segment resolution, are spatially interpolated to individual pixels during this process. For high clouds, if the estimated quality is poor, the techniques developed for cirrus are used instead. If simulated radiances are not available, a climatological atmospheric correction will be applied using look-up tables to compute the cloud top temperature.
    - For cirrus clouds, two methods are implemented:
        - the radiance ratioing method, as described in Menzel et al. 1982, is applied to the 11µm and 13.4µm pair of channels to retrieve the cloud top pressure at a pixel basis. If 13.4µm channel is not available, the 6.2µm or 7.3µm channels is used instead.
        - the H_2O/IRW intercept method, based on a 11µm and 13.4µm histogram analysis [very similar to the Eumetsat method (Schmetz et al., 1993)] is also implemented and allows the retrieval of cloud top pressure at the segment spatial resolution (i.e., 32*32 SEVIRI IR pixels). If 13.4µm channel is not available, the 6.2µm or 7.3µm channels is used instead.
        - the radiance ratioing technique result is retained unless its quality is not good (the result obtained with the intercept method is then used)
    - For low broken clouds : No technique is yet proposed for low broken clouds.
- Cloud top temperature and height are then computed from their pressure using general modules. During these processes, the atmospheric vertical profiles used are temporally interpolated to the exact slot time using the two nearest in time NWP outputs fields, and spatially interpolated to individual pixels.

3.7.2. Pre-launch activity :

The CTTH phase 1 prototype will be used to develop PGE03 (Product Generation Element 03 : the software to extract the Cloud Top Temperature and Height (CTTH) from SEVIRI images).

- PGE03 will :
  follow previous description
  use as much as possible SAFNWC common functions

be spectrally tuned to process both GOES and SEVIRI channels

- PGE03 will be tested with GOES images by comparison with CTTH phase-1 prototype : this validates PGE03 if the minimum set of SEVIRI channels is used.
- PGE-03 will be implemented in a CMS pre-operational SEVIRI environment to prepare their full validation as soon as SEVIRI images are available at CMS.

3.7.3. Post-launch activity :

- The PGE03 will be run in a CMS pre-operational SEVIRI environment. It will include a visual inspection.
- As during the prototyping phase-1, validation files will be automatically gathered : collocated satellite imagery and radiosondes, and possibly lidar measurements.
- The products will be validated and the algorithm tuned if needed.
- A scientific report, including validation results, will be written.

3.7.4. Integration activity :

- The PGE03 will be prepared for their delivery to INM (systematic use of common functions),
- The informatic documentation will be written,
- A test case will be defined : the PGE03 to be delivered to INM will be validated at CMS (must give same result as PGE03 implemented at CMS),
- The PGE03, the test case and the informatic documentation will be made available to INM.

Annex

Annex 1. Satellite dataset

A 1.1 AVHRR imagery

We describe here only the last AVHRR instrument on NOAA-15 satellite. For details on previous AVHRR refer to the NOAA Polar Orbiter Data User's Guide, a document that describes the orbital and spacecraft characteristics, instruments, data formats, etc. of the TIROS-N, NOAA-6 through NOAA-14 polar orbiter series of satellites.

The AVHRR/3 is a six channel scanning radiometer providing three solar channels in the visible-near infrared region and three thermal infrared channels. The AVHRR/3 has two one-micrometer wide channels between 10.3 and 12.5 micrometers. The instrument utilizes a 20.32 cm (8 inch) diameter collecting telescope of the reflective Cassegrain type. Cross-track scanning is accomplished by a continuously rotating mirror directly driven by a motor. The three thermal infrared detectors are cooled to 105 Kelvin (K) by a two-stage passive radiant cooler. Although AVHRR/3 is a six channel radiometer, only five channels are transmitted to the ground at any given time. Channels 3A and 3B cannot operate simultaneously. The data from the six channels are simultaneously sampled at a 40 kHz rate and converted to 10-bit binary form within the instrument. The data samples from each channel are output in a non-continuous burst of 10 space samples, 2048 Earth samples, and 10 internal calibration target samples per scan.

A summary of the AVHRR/3 spectral characteristics are given in Table A.1.1 (from NOAA-K,L,M user's guide)

Parameter	Ch. 1	Ch. 2	Ch. 3A	Ch. 3B	Ch. 4	Ch. 5
Spectral Range (micrometers)	0.58-0.68	.725-1.0	1.58-1.64	3.55-3.93	10.3-11.3	11.5-12.5
Detector type	Silicon	Silicon	InGaAs	InSb	HgCdTe	HgCdTe
Resolution (km)	1.09	1.09	1.09	1.09	1.09	1.09
IFOV* (milliradian)	1.3 sq.	1.3 sq.	1.3 sq.	1.3 sq.	1.3 sq.	1.3 sq.
S/N @ 0.5% albedo	9:1	9:1	20:1	-	-	-
NEdT @ 300K	-	-	-	.12K	.12K	.12K
MTF @ 1.09 km	>.30	>.30	>.30	>.30	>.30	>.30
Temperature Range (K)	-	-	-	180 - 335	180 - 335	180 - 335

Table A.1.1. Summary of AVHRR/3 Spectral Channel Characteristics

A 1.2 HIRS sounder

The High Resolution Infrared Radiation Sounder (HIRS/3) is a discrete stepping, line-scan instrument designed to measure scene radiance in 20 spectral bands to permit the calculation of the vertical temperature profile from Earth's surface to about 40 km.

Multispectral data from one visible channel (0.69 micrometers), seven shortwave channels (3.7 to 4.6 micrometers) and twelve longwave channels (6.5 to 15 micrometers) are obtained from a single telescope and a rotating filter wheel containing twenty individual filters. An elliptical scan mirror provides cross-track scanning of 56 increments of 1.8 degrees. The mirror steps rapidly (<35 msec), then holds at each position while the 20 filter segments are sampled. This action takes place each 100 msec. The instantaneous FOV for each channel is approximately 1.4 degrees in the visible and shortwave IR and 1.3 degrees in the longwave IR band which, from an altitude of 833 kilometers, encompasses an area of 20.3 kilometers and 18.9 kilometers in diameter, respectively, at nadir on the Earth.

Channel Number	**Central Wavenumber (cm^{-1})**	**Wavelength (micrometers)**	**Half Power Bandwidth (cm^{-1})**	**Noise Equivalent Delta Radiance $mW/(m^2\text{-}sr\text{-}cm^{-1})$**
1	669	14.95	3	3.00
2	680	14.71	10	0.67
3	690	14.49	12	0.50
4	703	14.22	16	0.31
5	716	13.97	16	0.21
6	733	13.64	16	0.24
7	749	13.35	16	0.20
8	900	11.11	35	0.10
9	1,030	9.71	25	0.15
10	802	12.47	16	0.15
11	1.365	7.33	40	0.20
12	1,533	6.52	55	0.20
13	2,188	4.57	23	0.006
14	2,210	4.52	23	0.003
15	2,235	4.47	23	0.004
16	2,245	4.45	23	0.004
17	2,420	4.13	28	0.002
18	2,515	4.00	35	0.002
19	2,660	3.76	100	0.001
20*	14,500	0.690	1,000	0.10% albedo
*Visible Channel				

Table A.1.2 HIRS/3 Spectral Characteristics

A 1.3 GOES imagery

The GOES I-M Imager is a five-channel (one visible, four infrared) imaging radiometer designed to sense radiant and solar reflected energy from sampled areas of the earth. By means of a servo-driven, two-axis gimballed mirror scan system in conjunction with a Cassegrain telescope, the Imager's multispectral channels can simultaneously sweep an 8-kilometer (5-statute mile) north-to-south swath along an east-to-west/west-to-east path, at a rate of 20° (optical) east-west per second. (source GOES Data Book)

Channels Number	**Wavelength Range (μm)**	**Range of Measurement Resolution**	**Resolution**	**Meteorological Objective and Maximum Temperature Range**
1	0.55 to 0.75	1.6 to 100% albedo	1 km	Cloud cover
2 (GOES-I/J/K) 2 (GOES-L/M)	3.80 to 4.00 3.80 to 4.00	4 to 320 K 4 to 335 K 4 km	4 km	Nighttime clouds (space – 340 K)
3 (GOES-I/J/K/L) 3 (GOES-M)	6.50 to 7.00 13.0 to 13.7	4 to 320 K 4 to 320 K	8 km 8 km	Water vapor (space – 290 K) Cloud cover and height
4	10.2 to 11.20	4 to 320 K	4 km	Sea surface temperature and water vapor (space – 335 K)
5 (GOES-I/J/K/L) 5 (GOES-M)	11.5 to 12.5 5.8 to 7.3	4 to 320 K 4 to 320 K	4 km 8 km	Sea surface temperature and water vapor (space – 335 K) Water vapor

Table A.1.3.1 GOES Imager Spectral Characteristics

Several events related to the CMS preprocessing quality have to be noted ;

- July 1st 1996 correction of visible channel calibration
- December 9th 1996 modification to parameters of IR calibration.
- July 1st 1997 shift IR channels one scan line towards south (mis-registration between VIS and IR channels in CMS ingest)

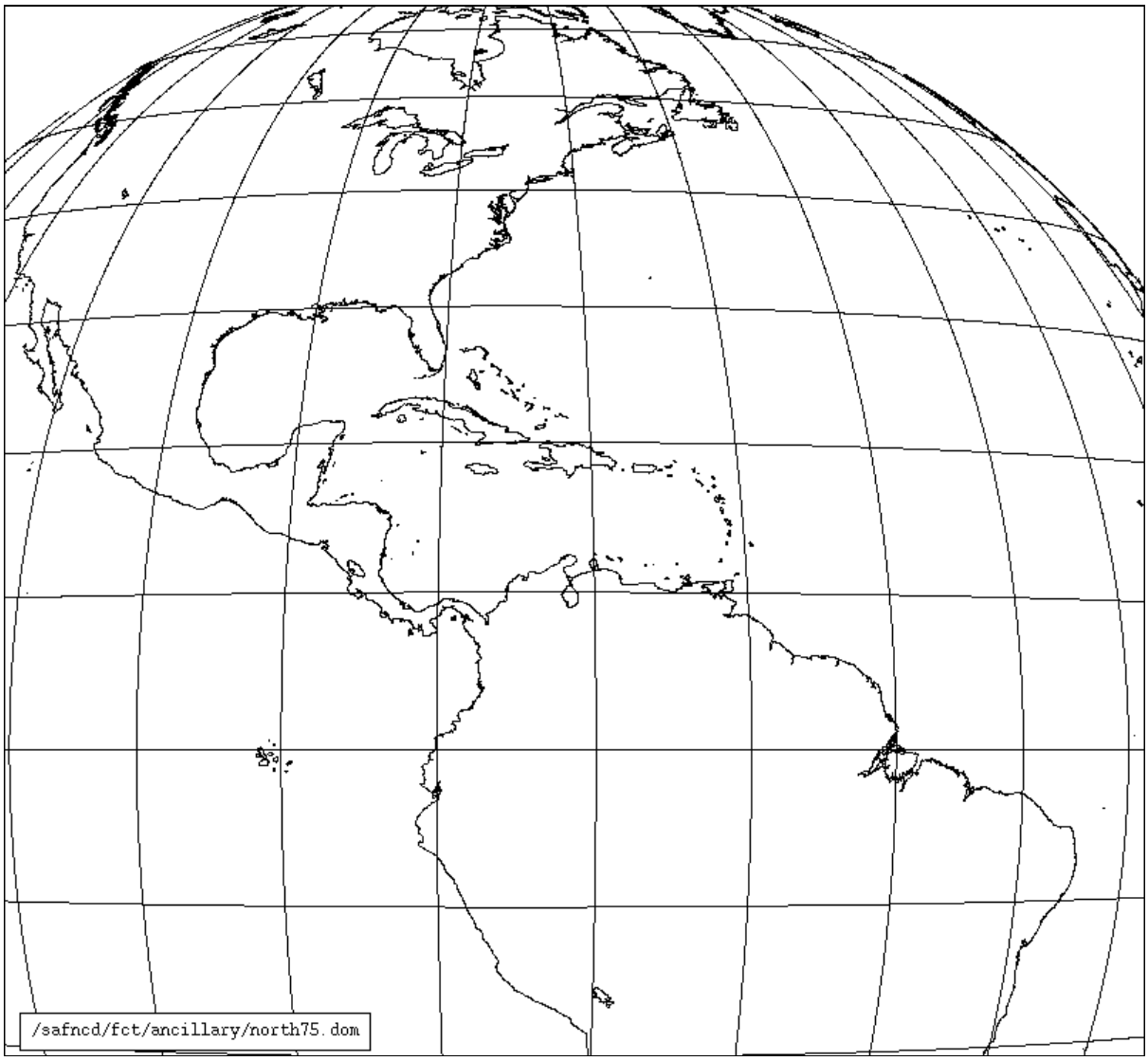

Figure A.1.3 GOES-EAST Extended Northern Hemisphere Area for a nominal position at 75W

Channel	Rows	Columns	Total size
1	7296	7920	115.6 M Bytes
2	1824	1980	7.2 M Bytes
3	912	990	1.8 M Bytes
4	1824	1980	7.2 M Bytes
5	1824	1980	7.2 M Bytes

Table A.1.3.2 GOES-EAST Extended Northern Hemisphere Image sizes

A 1.4 SEVIRI imagery

The 12 SEVIRI images correspond to the following spectral bands. Table A.1.4 presents the spectral characteristics, the dynamic range, the operating temperature of the detectors, the number of detectors simultaneously acquiring image information during each satellite revolution and the sampling distance of the level 1.0 image data:

Channel	Bands	Centre Frequ.	Spectral Band (99% energy limits)	Dynamic Range	Operating Temp.	Detectors per channel	Sample distance at SSP
		µm	µm		°K		km
HRV	Visible &	(0.75)	broadband (peak within 0.6 - 0.9)	0 - 459 W/m^2 sr µm (scaled at centre frequency)	300	9	1
VIS0.6		0.635	0.56 - 0.71	0 - 533 W/m^2 sr µm		3	3
VIS0.8	Near	0.81	0.74 - 0.88	0 - 357 W/m^2 sr µm			
IR1.6	IR	1.64	1.50 - 1.78	0 - 75 W/m^2 sr µm			
IR3.8 (IR3.9)		3.80 (3.92)	3.40 - 4.20 (3.48 - 4.36) (98% energy limits)	0 - 335 K	85-95		
IR8.7	Window	8.70	8.30 - 9.10 (98% energy limits)	0 - 300 K			
IR10.8		10.80	9.80 - 11.80 (98% energy limits)	0 - 335 K			
IR12.0		12.00	11.00 - 13.00 (98% energy limits)	0 - 335 K			
IR6.2	Water Vapor	6.25	5.35 - 7.15	0 - 300 K			
IR7.3		7.35	6.85 - 7.85 (98% energy limits)	0 - 300 K			
IR9.7	Ozone	9.66	9.38 - 9.94	0 - 310 K			
IR13.4	Carbon-dioxide	13.40	12.40 - 14.40 (96% energy limits)	0 - 300 K			

Table A.1.4 SEVIRI Spectral Channels definition

Several areas candidate as pre-defined SAFNWC region, containing 262144 points or less, and covering entirely France have been proposed to the forecasters. The selected region that is shown in figure A.1.4, its characteristics are ;

- centre position (45.0 N,0.8 E)
- size (576 points, 448 lines)

It will be the proposed as the pre-defined France region at the SAFNWC software installation.

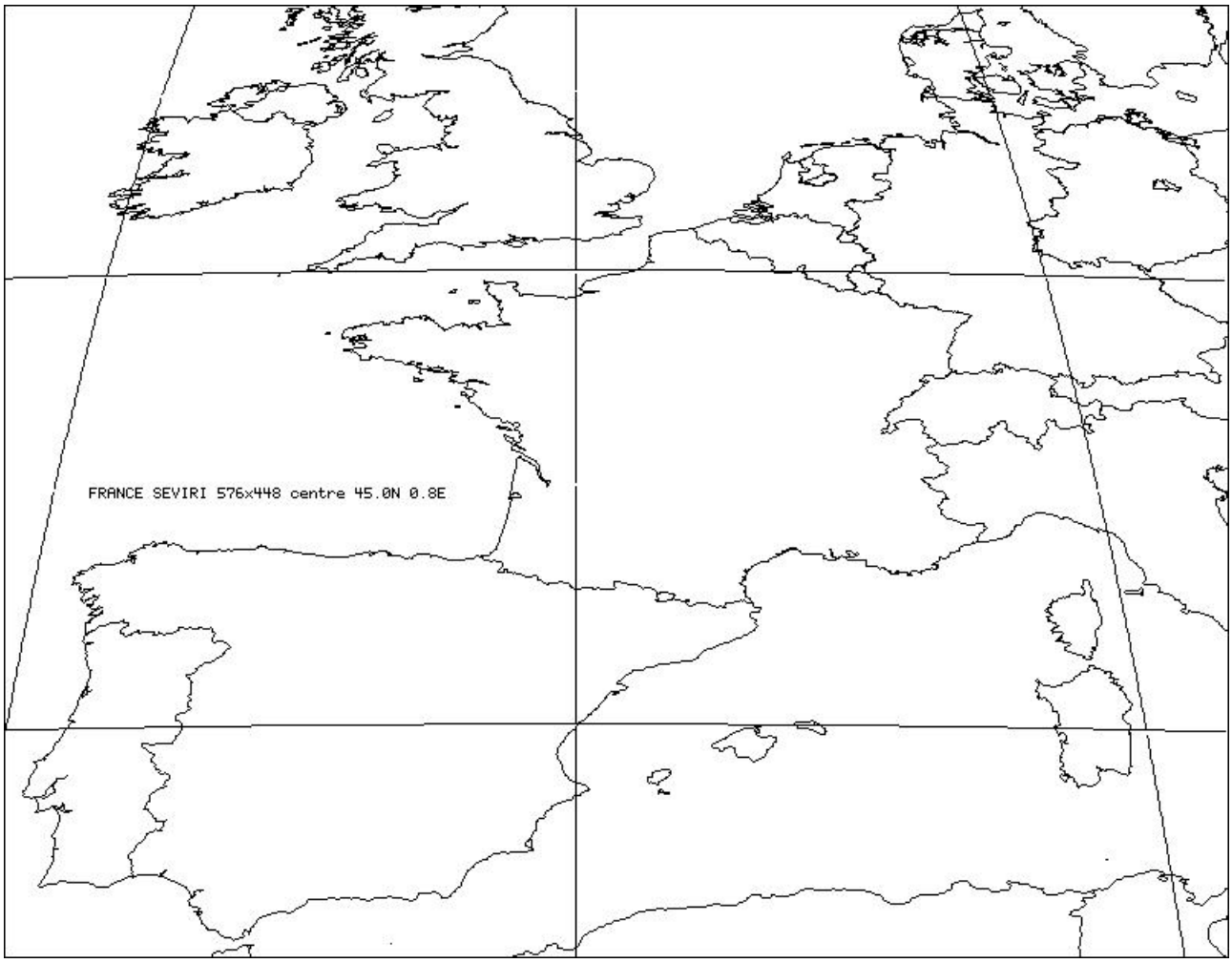

Figure A.1.4 Region proposed as pre-defined region for France at SAFNWC installation

Annex 2. Ancillary data set

A 2.1 Atlas

A 2.1.1 Land/sea/coast atlas

For the AVHRR prototype, we have used an already available land/sea/coast atlas covering the processed region at 10 minutes spatial resolution. This atlas is coded in FIS format (the image standard used at CMS) on one BYTE (1 for coast, 2 for sea and 3 for land).

For GOES prototypes (Extended Northern Hemisphere only), we have used the GMT tool version 3.0 (see Wessel et al., 1995, code available on internet (http ://www.soest.hawaii.edu /gmt)) to extract a land/sea atlas at 0.6 minutes spatial resolution (the lakes with a size lower than the spatial resolution have not been considered). This land/sea atlas was then remapped in the GOES visible grid (1km spatial resolution) using the nearest information. A land/sea atlas in the GOES IR grid (4km spatial resolution) was finally derived from the 1km file by keeping the dominant surface type (sea or land). This final atlas is coded in FIS format on one BYTE (0 for space, 2 for sea and 3 for land).

A 2.1.2 Elevation atlas

The initial source is the terrainbase 5 minute global digital elevation model (version 1.0) obtained in 1996 from the National Geophysical Data Center (contact : info@ngcd.noaa.gov). The accuracy of this DTM is better than the famous ETOPO05 (initially developed in 1985). Both topography and bathymetry are available in this file.

For the AVHRR prototype, the global terrainbase was first remapped on the processed region at 1.25 minutes spatial resolution. Then an elevation atlas at 10 minutes spatial resolution was obtained by averaging the height values of each 1.25 minutes land pixels located inside the 10 minutes-pixels. The final atlas is coded in FIS format on two BYTES (in meters, 0 for sea).

For GOES prototypes (Extended Northern Hemisphere only), the global terrainbase was remapped on the GOES visible grid (1km spatial resolution) using the nearest information. An elevation atlas in the GOES IR grid (4km spatial resolution) was finally derived by averaging the height values of each 1km land pixel located inside the 4km pixels. This final atlas is coded in FIS format on two BYTES (in meters, -10000 for space and sea).

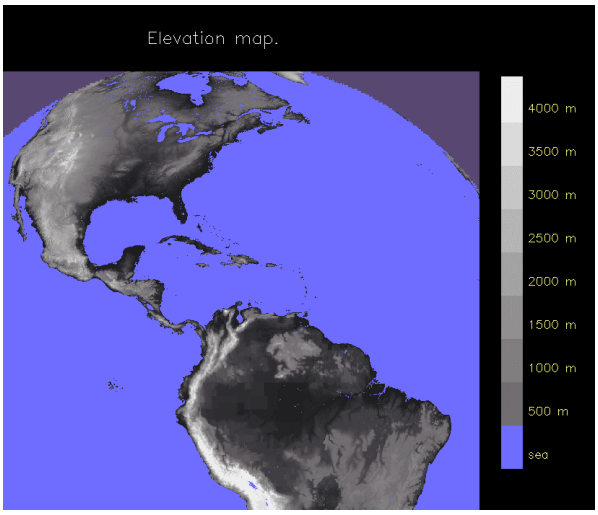

Figure A.2.1.2 Elevation map on the GOES Extended Northern Hemisphere.

A 2.1.3 Monthly Minimum Sea Surface Temperature climatology

The initial sources are :

- the global Reynolds climatology at 1 degree spatial resolution contains 12 monthly mean SST maps,
- the global Pathfinder climatology at 1/9th degree spatial resolution contains monthly mean SST maps over 5 years, from which a global minimum monthly climatology can be derived,

Twelve global monthly minimum SST maps were elaborated at 1/9th degree spatial resolution by remapping both fields on the same grid and using the Reynolds mean SST climatology to fill gaps in the Pathfinder minimum SST climatology.

For the AVHRR prototype, each monthly global SST map was remapped on the processed region at 1.25 minutes spatial resolution. Then a minimum SST atlas at 10 minutes spatial resolution is obtained by retaining the minimum value of the 1.25 minutes sea pixels located inside the 10 minutes-pixels. The final atlas (in FIS format) contains twelve channels (one for each month) coded on two BYTES (in 1/10th degree Kelvin, 0 for land).

For GOES prototypes (Extended Northern Hemisphere only), each monthly global SST map was remapped on the GOES visible grid (spatial resolution 1km) using the nearest information. Monthly minimum SST atlas in the GOES IR grid (4km spatial resolution) were finally derived by retaining the minimum value of the 1km sea pixel located inside the 4km pixels. The final twelve monthly minimum SST maps are coded in FIS format on two BYTES (in 1/100 Celsius, -10000 for space and land).

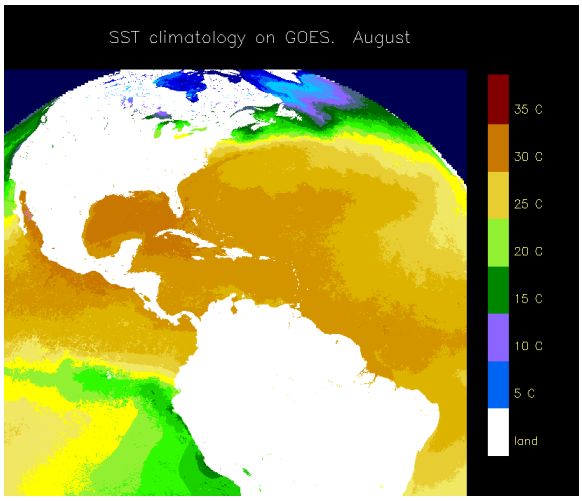

Figure A.2.1.3 Monthly SST climatology on the GOES Extended Northern Hemisphere : August.

A 2.1.4 Monthly visible atmospheric-corrected reflectances climatology

The initial source is a 10 minutes spatial resolution global climatology of Top Of Atmosphere monthly visible reflectances derived by NOAA from AVHRR GAC measurements (see Gutman et al., 1995).

These TOA reflectances have been roughly corrected from atmospheric effects. The values corresponding to snowy targets have been replaced, either with the nearest in time value, either by a constant value (20%). The data have been finally spread spatially in the coastal areas.

For the AVHRR prototype, each monthly global reflectance map was remapped on the processed region at 1.25 minutes spatial resolution. Then a reflectance atlas at 10 minutes spatial resolution is obtained by averaging the values of the 1.25 minutes land pixels located inside the 10 minutes-pixels. The final atlas (in FIS format) contains twelve channels (one for each month) coded on two BYTES (in $1/100^{th}$ % reflectance, 0 for sea).

For GOES prototypes (Extended Northern Hemisphere only), each monthly global reflectance map was remapped on the GOES visible grid (1km spatial resolution) using the nearest information. Monthly reflectance atlas in the GOES IR grid (4km spatial resolution) were finally obtained by averaging the values of the 1km land pixel located inside the 4km pixels (a constant value of 20% was used to fill gaps, mainly small islands). The twelve final monthly reflectance maps are coded in FIS format on two BYTES (in $1/100^{th}$ % reflectance, -10000 for space and sea).

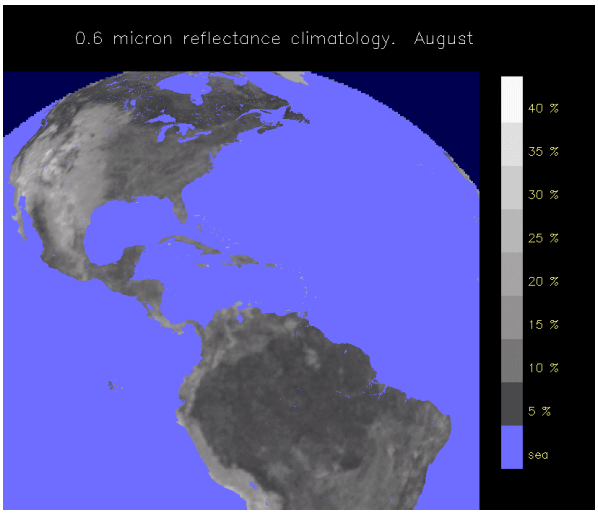

Figure A.2.1.4 Visible reflectance climatology on the GOES Extended Northern Hemisphere : August.

A 2.1.5 Monthly atmospheric integrated water vapour content climatology

The initial source is a 2.5 degrees spatial resolution global monthly climatology of specific humidity on 11 pressure levels (1000, 950, 900, 850, 700, 500, 400, 300, 200, 100, and 50 hPa), elaborated by Oort from a collection of 15 years of global rawinsonde data (Oort, 1983).

This file has first been remapped on the GOES grid (Extended Northern Hemisphere only) at 4km spatial resolution (spatial smoothing using bi-linear interpolation in latitude/longitude). The integrated water vapor content is then computed from the specific humidity of pressure levels above the surface level (whose pressure is derived from the height map (described in A 2.1.2) using a standard OACI standard atmosphere for the height/pressure conversion). The final twelve monthly integrated water vapor content maps are coded in FIS format on two BYTES (in 1/100 g/cm^2, -9999 for space).

A 2.1.6 Monthly air temperature (at 1000, 850, 700, 500 hPa) climatology

The initial source is a 1.5 degrees spatial resolution global monthly climatology of air temperatures at 1000hPa, 850hPa, 700hPa and 500hpa derived from the ECMWF model.

These fields have been remapped on the GOES grid (Extended Northern Hemisphere only) at 4km spatial resolution (spatial smoothing using bi-linear interpolation in latitude/longitude). The final monthly temperature maps are coded in FIS format on two BYTES (in 1/100 K, -9999 for space).

A 2.2 NWP data fields

The NWP data fields used both in the training and validation files come from the BDAP database from the French DIAPASON system. The parameters are those handled by the Arpege and ECMWF models. They are stored in the BDAP data base in the WMO FM-92 GRIB format and pre-processed on several areas with several spatial resolution. For the SAFNWC development phase we have gathered the Arpege forecast parameters at the global coverage using equidistant cylindrical (or plate carrée) grid with a regular spatial resolution of 1.5 degrees (GLOB15 grid). Their characteristics are summarized in the table A2.2.1 and table A2.2.2

Domain Name	Number of Rows	Number of Columns	Minimum Latitude	Minimum Longitude	Maximum Latitude	Maximum Longitude	Latitude Step	Longitude Step
GLOB15	121	240	90S	0	90N	358.5	1.5	1.5

Table A.2.2.1 Geographical characteristics of the NWP meteorological fields

The forecast fields are those computed by Arpege twice a day for analysis time 00h and 12h. The forecast ranges used are 12h and 18h. Each parameter for a given level at an analysis time for a given forecast range is coded in a GRIB file. The GRIB files of a given analysis time are gathered in a single file.

The archive of the GRIB files has started on July 1997, the archive of the wind speed at 10 m has started on October 1st 1997.

Parameter	**Code**	**Level type**	**Level**
Ground Pressure	1	1	0
Surface Temperature	11	1	0
Wind speed	32	105	10m
Tropopause Pressure	1	7	0
Tropopause Temperature	11	7	0
Temperature 2m	11	105	2m
Relative humidity 2m	52	105	2m
Temperature	11	100	20 pressure levels : 10,20,30,50,70,100,150, 200,250,300,400,500,600, 700,800,850,900,925,950,1000 hPa
Relative humidity	52	100	same 20 pressure levels from10 to 1000 hPa

Table A.2.2.2 Meteorological fields content

The model land/sea file and the model altitude file are also required for the preprocessing of the meteorological data.

The forecast fields every six hours over GLOB15 grid are used to determine the atmospheric parameters necessary for the thresholds computation. A simple bilinear interpolation in the original GLOB15 regular grid is used to estimate the atmospheric parameters at the segment centre. For surface temperature, before spatial interpolation the forecast surface temperature from the land grid points is spread on the neighbour sea grid points. This avoids influence of oceanic surface temperature into land surface segments.

Linear interpolation between the two nearest forecast times is used to estimate the parameters at each picture time when computing the thresholds depending on NWP data.

The tropopause temperature and pressure are ARPEGE outputs that are available in BDAP data base. If missing, they can be estimated from the NWP temperature, geopotential and pressure

profiles, according to an interpolation of mixed criteria between WMO (strict and relaxed), and maximum gradient levels.

A 2.3 TIGR dataset

We have used the radio-sounding database which is available in the TIGR (Tovs Initial Guess Retrieval) dataset that has been built by Laboratoire de Météorologie Dynamique. Each of these radio-soundings contains the temperature and humidity profile on 40 vertical levels from 1013 hPa up to 0.05 hPa [1013, 955., 900., 850., 800., 725., 651., 585., 525., 472., 424., 380., 342., 307., 276., 250., 222., 200., 162., 131., 106., 86., 70., 57., 46., 37., 25., 17., 11., 7.5, 5., 3.3, 2.2, 1.5, 1., 0.55, 0.3, 0.17, 0.09, 0.05]. The surface temperature available in the dataset has not been used.

The objective of TIGR is to be representative of all atmospheric conditions on earth. TIGR-2 dataset contains 1751 radio-soundings, including 436 polar situations (latitude lower that 63 degrees South or higher that 75 degrees North), 507 continental, 477 maritime and 341 coastal situations. Statistics on the total water vapour content and the air temperature at 1013 hPa are shown on the following figures A.2.3.1-A.2.3.4.

The TIGR dataset has been used at CMS for the preparation of IR thresholds to be used in the cloud masking. By applying RTTOV on selected TIGR radio-soundings with different viewing angles, surface temperatures and emissivities, we prepare pre-computed tables of IR cloud free brightness temperatures as a function of viewing angles and water vapour content. These tables, which are computed for various IR channels combinations over sea, vegetated or arid areas, in daytime or night-time conditions, are then used in the cloud masking process to compute IR thresholds to be applied to each pixels.

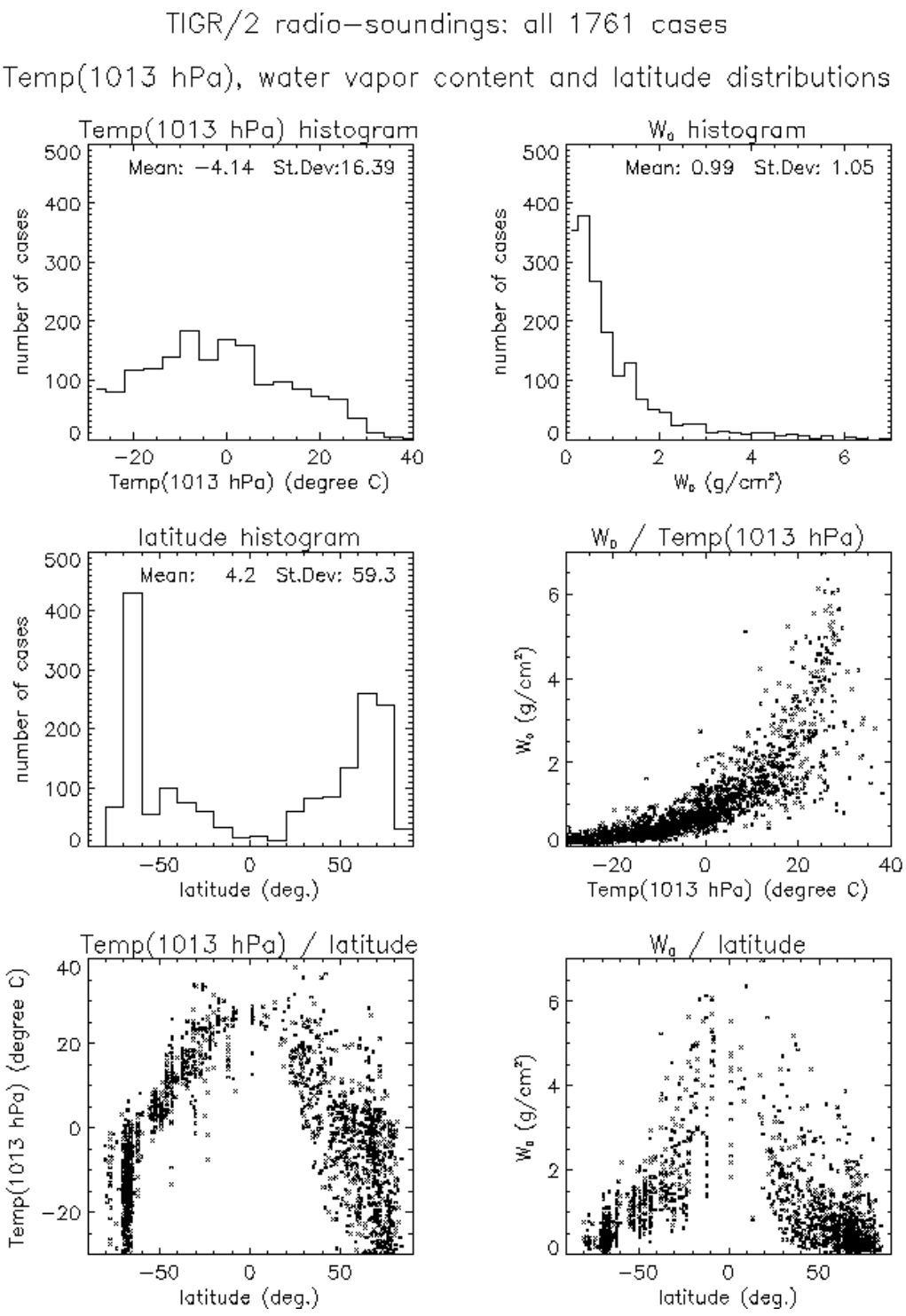

A.2.3.1 Statistics on all TIGR radio-soundings

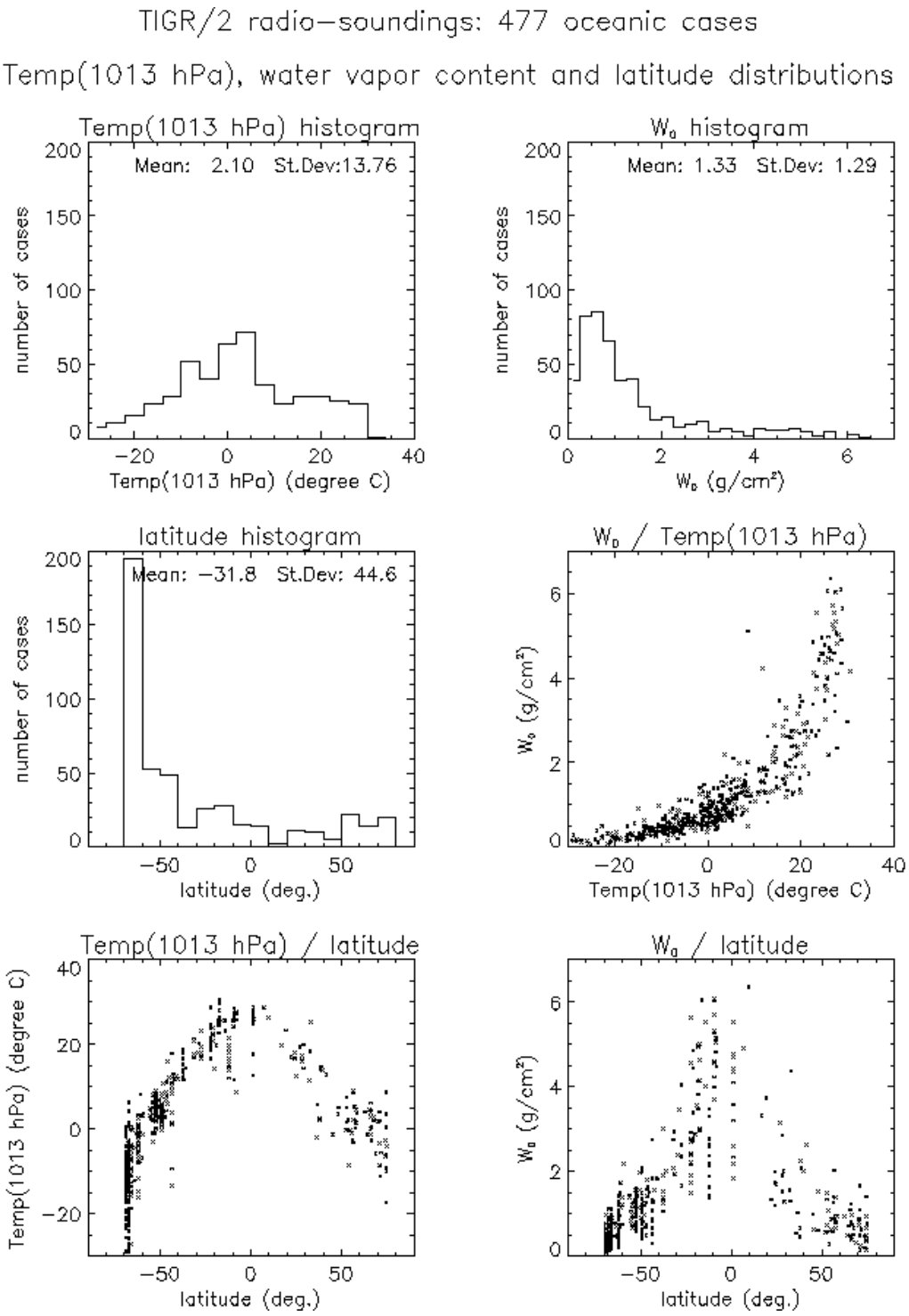

Figure A.2.3.2 Statistics on TIGR Oceanic radio-soundings

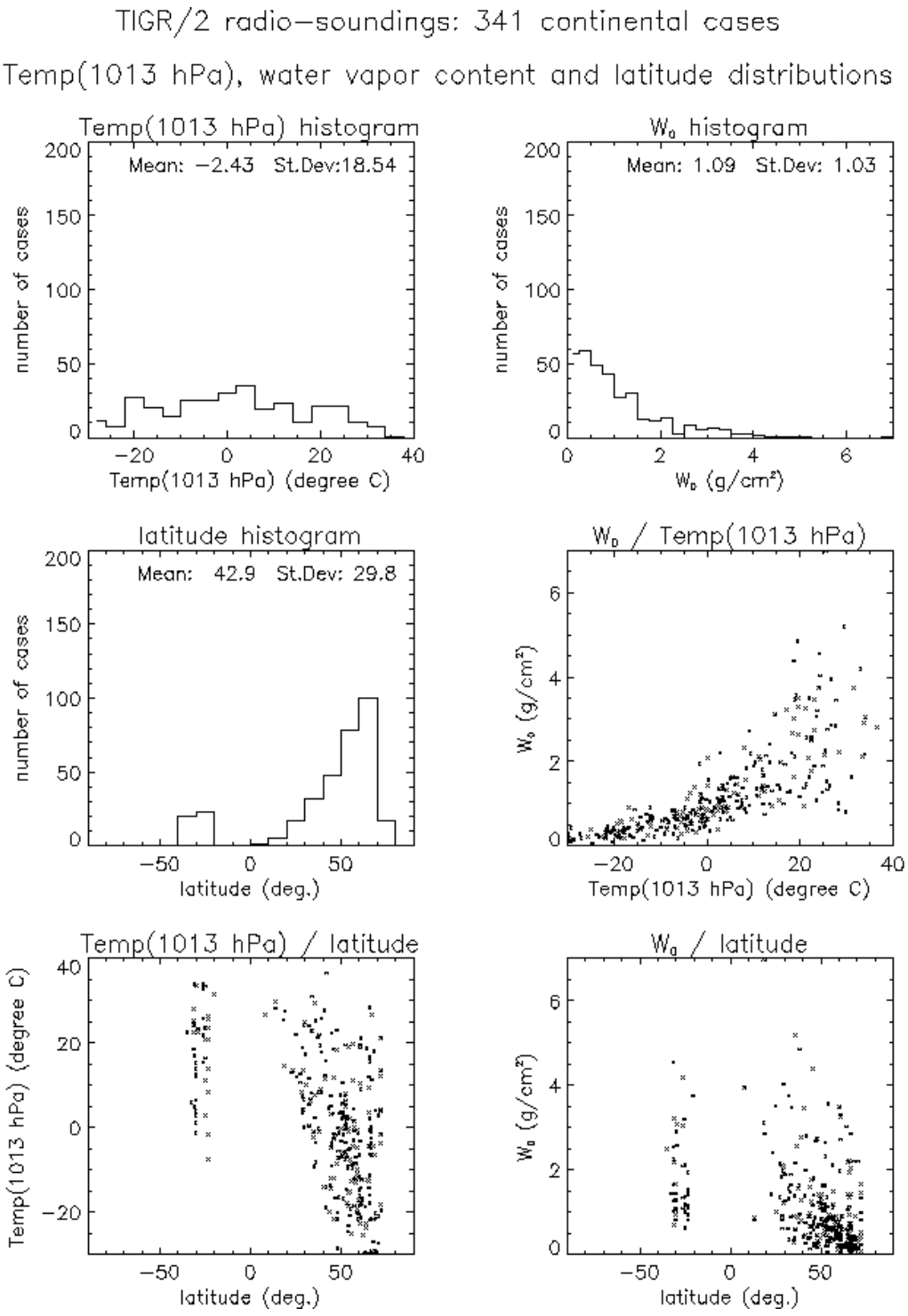

Figure A.2.3.3 Statistics on TIGR continental radio-soundings

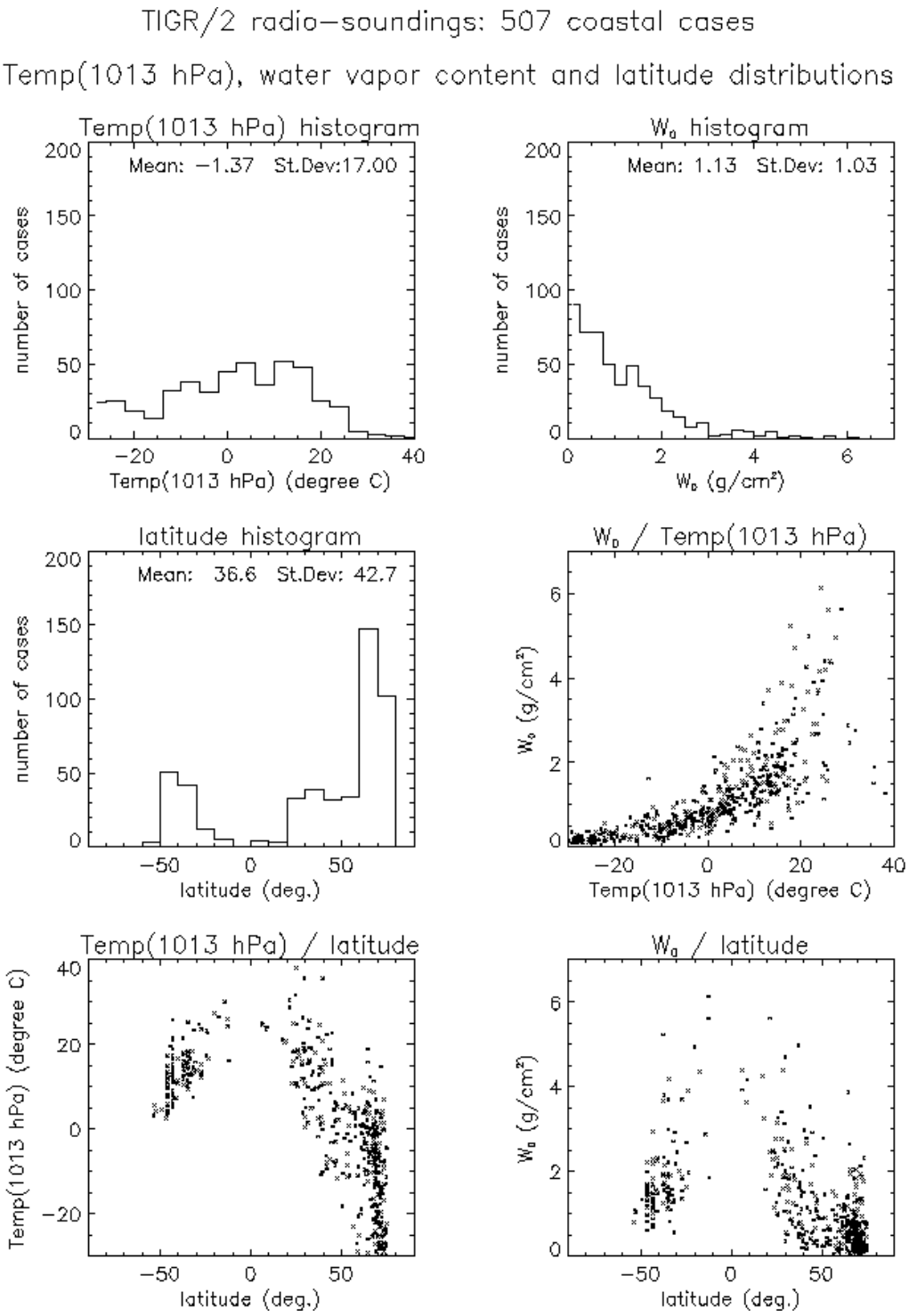

Figure A.2.3.4 Statistics on TIGR coastal radio-soundings

Annex 3. Test and Validation dataset

A 3.1 Interactive test file

An interactive tool (see figure A.3.1.1), based on the use of the commercial image processing software WAVE, has been used by three experienced operators for the extraction of visually identified targets in GOES images (area : Extended Northern hemisphere, i.e. corresponding to latitudes between 20 degrees south and 60 degrees north) and NOAA-12, NOAA-14 and NOAA-15 AVHRR images (Over Europe and adjacent seas). The result of this work is a dedicated database for spectral signature studies that we call the interactive test file. Such a database has been already been gathered in 1992 from NOAA-11 and NOAA-12 AVHRR images. For GOES targets (generally chosen in slots 12, 24, 36, 48 only, except for volcanic ash targets), we have chosen every types of clouds and conditions. For AVHRR (chosen in any passes), we have focused on aerosol (sand dust, volcanic plumes), snow and ice and on the new AVHRR 1.6μm channel. The GOES targets have been mainly gathered by three experienced operators (58.5%, 24% and 16% of the targets respectively) and by the two developers (M.Derrien and H.LeGleau : only 1.5% of the targets).

The interactive procedure allows :

- the display of various channels combination (GOES full resolution in satellite projection, AVHRR in stereographic projection (sampled at 2km spatial resolution))
- the zoom of an area
- the choice of small square targets (5*5 GOES IR pixels, 10*10 2km AVHRR)
- the labelling of the targets through a menu

For each target, the interactive test file gather :

- the label given by the operator to the target (list displayed in table A.3.1.3),
- the full satellite information in the square targets together with satellite & solar angles and time information,
- the collocated and nearest in time meteorological information extracted from ARPEGE forecast fields (see A.2.2),
- collocated atlas values (see A.2.1).

This database has been fed since June 1997. Statistics are sum up in Tables A.3.1.1 and A.3.1.2.

This database has been used at CMS in various way :

- the cloud free measurements has allowed to check the validity of RTM cloud free simulation to compute the thresholds used in the cloud masking,
- the bi-directional effects in cloud reflectances have been analysed,
- knowledge about the new 1.6 μm channel has been gained,
- the cloud free and cloudy targets have allowed to check the efficiency of the cloud mask and cloud type algorithm in various conditions,
- the aerosol targets have allowed to check the efficiency of published algorithms

	total number	polar	mid-latitude	tropical	Daytime	Nighttime	Twilight
GOES	20359	4.2 %	55.4 %	40.4 %	64.4 %	29.2 %	6.4 %
AVHRR	4307	17.8 %	82.2 %	0 %	82.7 %	8.4 %	8.9 %
1992-AVHRR	6882	3.5 %	96.5 %	0 %	69 %	7.5 %	23.5 %

Table A.3.1.1 Statistics on locations and solar illuminations of the Interactive test files' targets

	sea	land	snow & ice	St/Sc	Ac/As	Cu	Cb	Ci over clouds	Ci	Cs over Ac,As	aerosol
GOES	11.2 %	9.5 %	5.9 %	17.1 %	5.5 %	8.2 %	12.8 %	8.1 %	15.8 %	4.8 %	1.1 %
AVHRR	17.6 %	15.7 %	9.3 %	22 %	3.6 %	3.8 %	2.3 %	4.5 %	6.1 %	4.0 %	10.5 %
1992-AVHRR	20.0 %	23.7 %	2.4 %	25.3 %	6.1 %	2.3 %	3.5 %	4.7 %	8.5 %	3.5 %	0 %

Table A.3.1.2 Statistics on cloud and earth's types available in the Interactive test files.

Open sea (101)	Sea with shadow (102)	Sea with sand aerosols (103)	Sea with ash (volcanic or fire) (104)
Sea with haze (105)	Sea with sunglint (106)		
Land (151)	Land with shadow (152)	Land with sand aerosol (153)	Land with ash (volcanic or ash) (154)
Land with Haze (155)	Ice (181)	Ice with shadow (182)	Snow (191)
Snow with shadow (192)	Unclassified (cloudy or cloudfree) (200)	Cloudy (unknown) (900)	
fog (501)	stratus (502)	stratocumulus (503)	shadow over low clouds (504)
small cumulus over sea (601)	Cumulus congestus over sea (606)	small cumulus over land (602)	Cumulus congestus over land (607)
Cumulonimbus (608)	Extensive cumulonimbus (609)	Thin cirrus over sea (701)	Thin Cirrus over ice (703)
Thin cirrus over land (702)	Thin cirrus over snow (704)	Thin cirrus over St/Sc (705)	Thin cirrus over Cu (706)
Thin cirrus over Ac/As (707)	Altocumulus/Altrostratus (801)	Altocumulus (802)	Cirrostratus (811)
Cirrostratus over Ac/As (812)			

Table A.3.1.3 List of cloud & earth types available in the Interactive Test files.

(The coding number stored in the interactive file is also indicated for each type.)

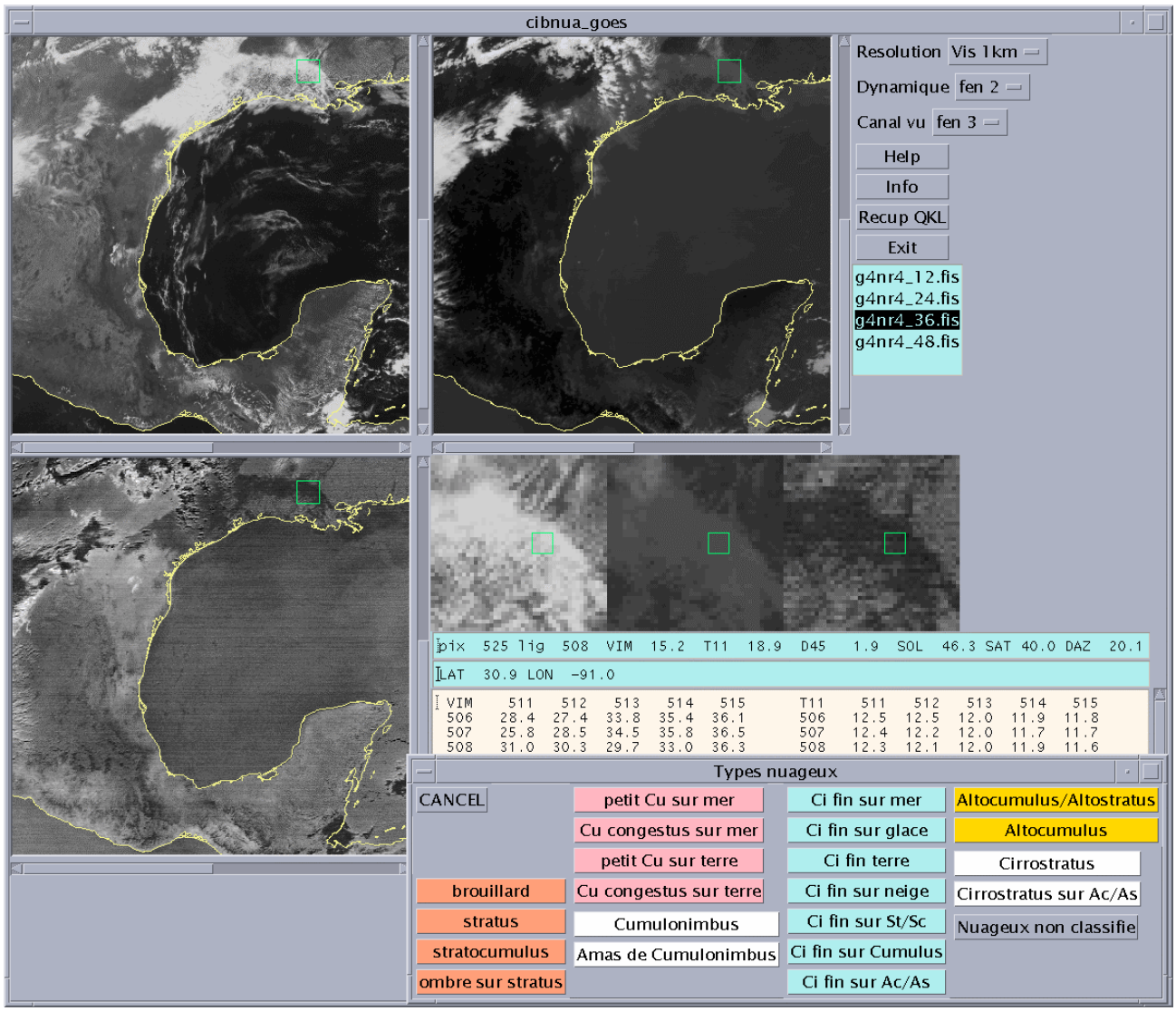

Figure A.3.1.1 Interactive tool graphic interface (based on WAVE software)

Internal format for GOES interactive training target files :

The size of each satellite target window is :
for 4km IR channel : 5 columns by 5 rows
for 8km WV channel : 3 columns by 3 rows
for 1km Vis channel : 20 columns by 20 rows

Full satellite information in the square targets, together with satellite & solar angles and time information :

type	a*2 target type (in for interactive)
observer	a*10 user name of the person who has analysed the target
lat	i*4 latitude of the centre of the target (1000th of degrees)
lon	i*4 longitude of the centre of the target (1000th of degrees)
date	i*4 julian day (count from 00h, 1 Jan 1950)
hour	i*4 UTC time of day in milliseconds
nbp	i*2 number of columns expressed in 4km IR coordinates
nbl	i*2 number of rows expressed in 4km IR coordinates
nbc	i*2 number of channels (5 or 4, according to day/night consideration)
valcan_IR1	i*2 indicator of IR 3.7 mm availability [-1 =not in the file
valcan_IR2	i*2 indicator of IR 11 mm availability [0 =is missingt
valcan_IR3	i*2 indicator of IR 12 mm availability [>0 =mean value in the
valcan_WV	i*2 indicator of IR 6.7 mm availability [target)]
valcan_VIS	i*2 indicator of VIS channel availability
canal IR1	x i*2 window from the IR 3.7 mm channel (x = nbp*nbl)
canal IR2	x i*2 window from the IR 11 mm (x = nbp*nbl)
canal IR3	x i*2 window from the IR 12 mm (x = nbp*nbl)
canal WV	y i*2 window from the IR 6.7 mm (y = (nbp/2+0.5)*(nbl/2+0.5))
canal VIS	z i*2 window from the VIS channel (z = (nbp*4)*(nbl*4))) [NOT corrected from solar elevation]
solzen	i*2 solar zenith angle (100th of degrees)
satzen	i*2 satellite zenith angle (100th of degrees)
daz	i*2 local azimuth angle (100th of degrees)s
typ_cloud	i*2 target code (given by the observer) [coding value : see table A.3.1.3]

The record size is 220 bytes for a nighttime target (slot 12) and 1020 bytes for a daytime (slots 24,36,48). Note that the procedure was initially written to cope only with slots 12, 24, 36, 48. For the other slots (only available for volcanic ash targets), the record size is 1020 even in nighttime conditions (then visible value is off course meaningless !).

Collocated and nearest in time meteorological information extracted from ARPEGE forecast fields (temperature & humidity vertical profile) [missing values : -9999] :

lat_met	i*4 latitude of the NWP measurement (1000th of degrees)
lon_met	i*4 longitude of the NWP measurement(1000th of degrees)
atm	a*4
date	i*4 julian day of forecast day (count from 00h, 1 Jan 1950)
res	i*4 hour of forecast
ech	i*4 forecast term (in hour)
psol	i*4 ground pressure (1/100 hPa)
tsol	i*4 ground temperature (1/100 K)
t2m	i*4 2m air temperature (1/100 K)
hu2m	i*4 2m air relative humidity (1/100 %)
pniv	20 i*4 pressure level (20) (in hPa)
tniv	20 i*4 temperature at 20 pressure levels (1/100 K)
huniv	20 i*4 relative humidity at 20 pressure levels (1/100 %)
ptropo	i*4 pressure at tropopause level (1/100 hPa)
ttropo	i*4 temperature at tropopause level (1/100 K)

ff10m	i*4 10m wind speed (1/10 m/s)

Collocated atlas values and spare values :

land/sea	x i*1 land/sea atlas (space=0, sea=2, land=3), (x = nbp*nbl)
height	x i*2 height atlas value (in meters), (x = nbp*nbl)
stt	x i*2 sst climatological value (in 1/100 C), (x = nbp*nbl)
albedo	x i*2 visible reflectance climatological value (in 1/100 %), (x = nbp*nbl)
W	i*4 integrated water vapor content (in 1/100 kg/m2)
spare	30 i*4 spare data (not used)

CMS Internal format for interactive training target files from NOAA data

The size of each satellite target window is 5 lines by 5 pixels.

Full satellite information in the square targets, together with satellite & solar angles and time information :

type	a*2 target type (in for interactive)
observer	a*10 user name of the person who has analysed the target
lat	i*4 latitude of the centre of the target (1000th of degrees)
lon	i*4 longitude of the centre of the target (1000th of degrees)
date	i*4 julian day (count from 00h, 1 Jan 1950)
hour	i*4 UTC time of day in milliseconds
nbp	i*2 number of columns expressed in 4km IR coordinates
nbl	i*2 number of rows expressed in 4km IR coordinates
nbc	i*2 number of channels (6 or 4, according to day/night consideration)
valcan_VIS1	i*2 indicator of VIS channel 1 availability
valcan_VIS	i*2 indicator of VIS channel 2 availability
valcan_IR3	i*2 indicator of IR 3.7 mm or 1.6 mm availability [-1 =not in the file
valcan_IR4	i*2 indicator of IR 11 mm availability [0 =is missingt
valcan_IR5	i*2 indicator of IR 12 mm availability [0 =is missingt
valcan_classif	i*2 indicator of classification availability [>0 =mean value in the

daytime cases:

canal 1	x i*2 window from the VIS channel 1 (x = nbp*nbl) [corrected from solar elevation]
canal 2	x i*2 window from the VIS channel 2 (x = nbp*nbl)) [corrected from solar elevation]
canal3	x i*2 window from the VIS channel 3 or IR 3 (x = nbp*nbl)) [1.6µm corrected from solar elevation]
canal 4	x i*2 window from the IR channel 4 (x = nbp*nbl)
canal 5	x i*2 window from the IR channel 5 (x = nbp*nbl)
canal 6	x i*2 window containing the classification (x = nbp*nbl)

nighttime cases

canal 3	x i*2 window from the IR channel 3 (x = nbp*nbl)
canal 4	x i*2 window from the IR channel 4 (x = nbp*nbl)
canal 5	x i*2 window from the IR channel 5 (x = nbp*nbl)
canal 6	x i*2 window containing the classification (x = nbp*nbl)

solzen	i*2 solar zenith angle (100th of degrees)
satzen	i*2 satellite zenith angle (100th of degrees)
daz	i*2 local azimuth angle (100th of degrees)s
typ_cloud	i*2 target code (given by the observer) [coding value : see table A.3.1.3]

The record length is 254 bytes for a nighttime target and 354 bytes for a daytime.

Collocated and nearest in time meteorological information extracted from ARPEGE forecast fields (temperature & humidity vertical profile) [missing values : -9999] :

lat_met	i*4 latitude of the NWP measurement (1000th of degrees)
lon_met	i*4 longitude of the NWP measurement(1000th of degrees)

atm	a*4
date	i*4 julian day of forecast day (count from 00h, 1 Jan 1950)
res	i*4 forecast hour
ech	i*4 forecast term (in hours)
psol	i*4 ground pressure (1/100 hPa)
tsol	i*4 ground temperature (1/100 K)
t2m	i*4 2m air temperature (1/100 K)
hu2m	i*4 2m air relative humidity (in 1/100 %)
pniv	20 i*4 pressure level (20) (in hPa)
tniv	20 i*4 temperature at 20 pressure levels (1/100 K)
huniv	20 i*4 relative humidity at 20 pressure levels (in 1/100 %)
ptropo	i*4 pressure at tropopause level (in 1/100 hPa)
ttropo	i*4 temperature at tropopause level (1/100 K)
ff10m	i*4 10m wind speed (1/10 m/s)

Collocated atlas values and spare values :

land/sea	x i*1 land/sea atlas (space=0, sea=2, land=3), (x = nbp*nbl)
height	x i*2 height atlas value (in meters), (x = nbp*nbl)
stt	x i*2 sst climatological value (in 1/100 C), (x = nbp*nbl)
albedo	x i*2 visible reflectance climatological value (in 1/100 %), (x = nbp*nbl)
W	i*4 integrated water vapor content (in 1/100 kg/m2)
spare	30 i*4 spare data (not used)

A 3.2 Surface observations (SYNOP)

The data used is the routine weather observations, coded by the observers into the WMO synoptic code, gathered at Toulouse and made available to users through a METEO-FRANCE data base. From this data base we extract all the synoptic reports from a list of 650 selected land stations, 307 over the European area and 343 over the American area, and code ASCII files containing a part of the SYNOP reports. The SYNOP reports are normally made every three hours (79 over Europe and 143 over America), but some of them are made every one hour (228 over Europe) and a few (200 over America) every 6 hours. The figures A3.2.1 illustrate the spatial coverage of the selected land stations.

The archive of the ASCII files containing a part of the SYNOP reports collocated with the GOES-08 satellite data has started **on November 14th1996**. For AVHRR collocated data, this archive has started also on **September 1st 1996**.

As automated GOES-08 data coincident and collocated with SYNOP observations have been stored with one shifted IR scan line until July 1997, only newer than **July 1st 1997** have been used for validation purposes.

The ASCII files have been coded according to the format and content described in table A.3.2.1 .

The SYNOP reports covering GOES area have been limited to stations making only human observations of cloud cover, i.e. the stations producing SYNOP containing Cl,Cm,Ch descriptions when cloud cover is not 0 or 9.This filter on the stations is justified by the fact some stations produce automatic cloud covers (ASOS, Automated Surface Observing System) leading to cloud cover reported equal to 0 when clouds layers are above 12000 feet. This leads to a reduced set of 114 stations whose spatial coverage is illustrated on figure A3.2.2., 6 belong to the nordic area, 48 to the midlatitude area, and 60 to the tropical.

ASCII	content
1x	blank
i2.2	WMO region code
i3.3	WMO station code
i2.2	station type
i4.4	station altitude (m)
i6	latitude of the station (1/100 degree)
i6	longitude of the station (1/100 degree)
i4.4	year of the report
i2.2	month of the report
i2.2	day of the report
i2.2	hour of the report
i2.2	minute of the report
1x	blank
a2	ground status code
a3	ground snow thickness (cm)
1x	blank
a5	Pressure at the station level (decapascal)
a2	wind direction (1/10 degree)
a2	wind speed (m/s)
1x	blank
a4	air temperature (1/10 Celsius)
a4	dew point temperature (1/10 Celsius
a3	relative humidity (%)
a4	horizontal visibility (decameters)
a3	present weather (WMO code)
a2	past weather1 (WMO code)
a2	past weather2 (WMO code)
1x	blank
a1	total cloud cover (eigth od cloud cover)
a1	lower cloud amount (eigth od cloud cover
a4	base height of the lowest cloud (WMO code)
a1	low cloud type (cl WMO code)
a1	middle cloud type (cm WMO code)
a1	high cloud type (ch WMO code)
a1	cloud cover 1 (eigth)
a1	cloud type 1 (WMO code)
a4	base height 1 (decameters)
a1	cloud cover 2 (eigth)
a1	cloud type 2 (WMO code)
a4	base height 2 (decameters)
a1	cloud cover 3 (eigth)
a1	cloud type 3 (WMO code)
a4	base height 3 (decameters)
a1	cloud cover 4 (eigth)
a1	cloud type 4 (WMO code)
a4	base height 4 (decameters)

Table 3.2.1 Content of the extracted SYNOP reports ASCII files

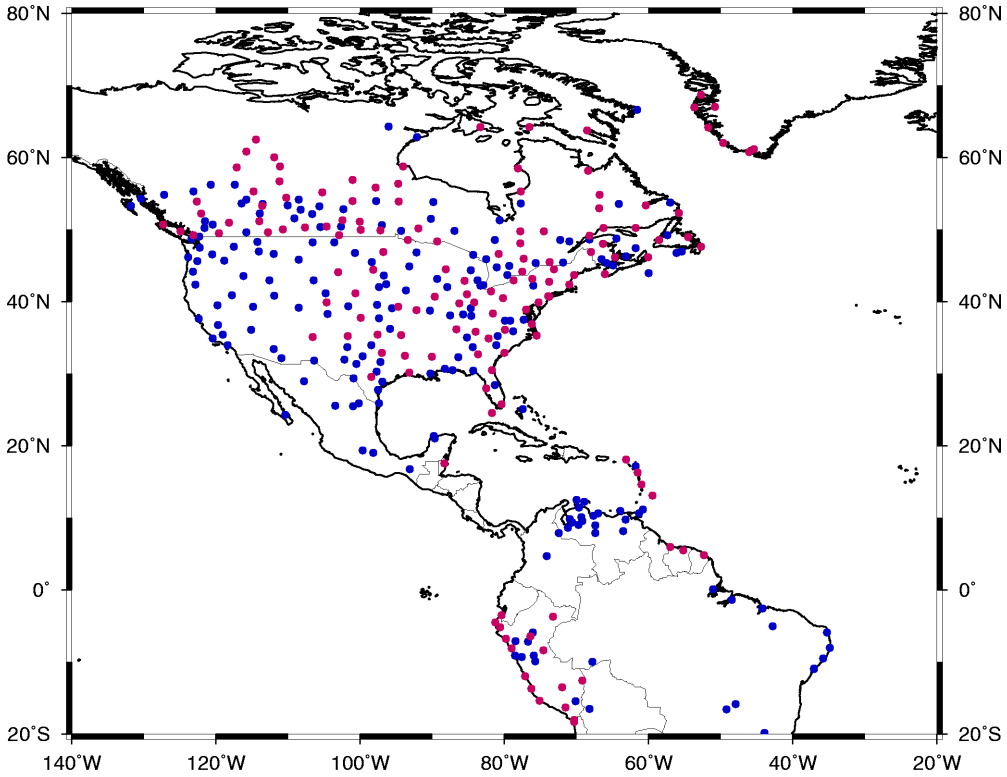

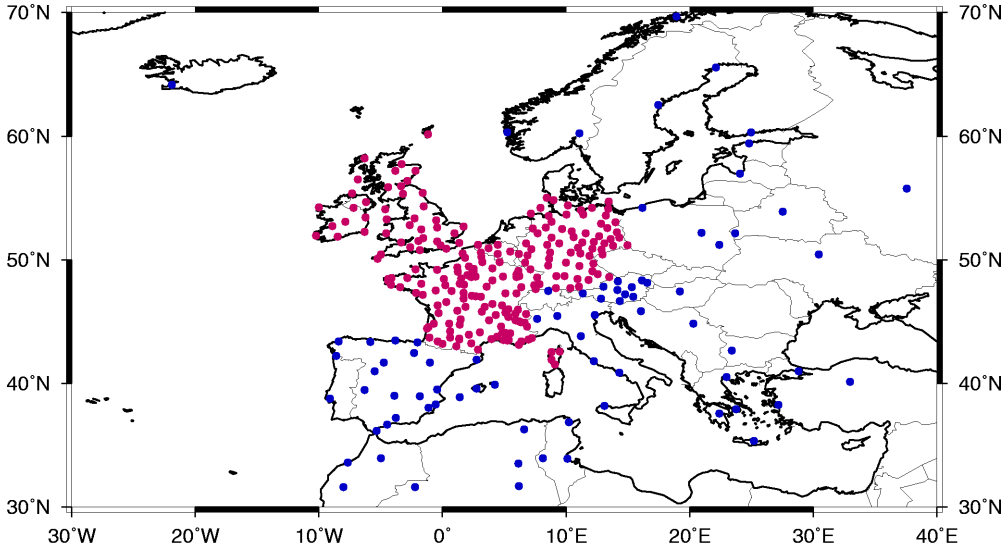

Figure A.3.2.1 Geographical location of the weather observation stations selected for the Cloud products evaluation

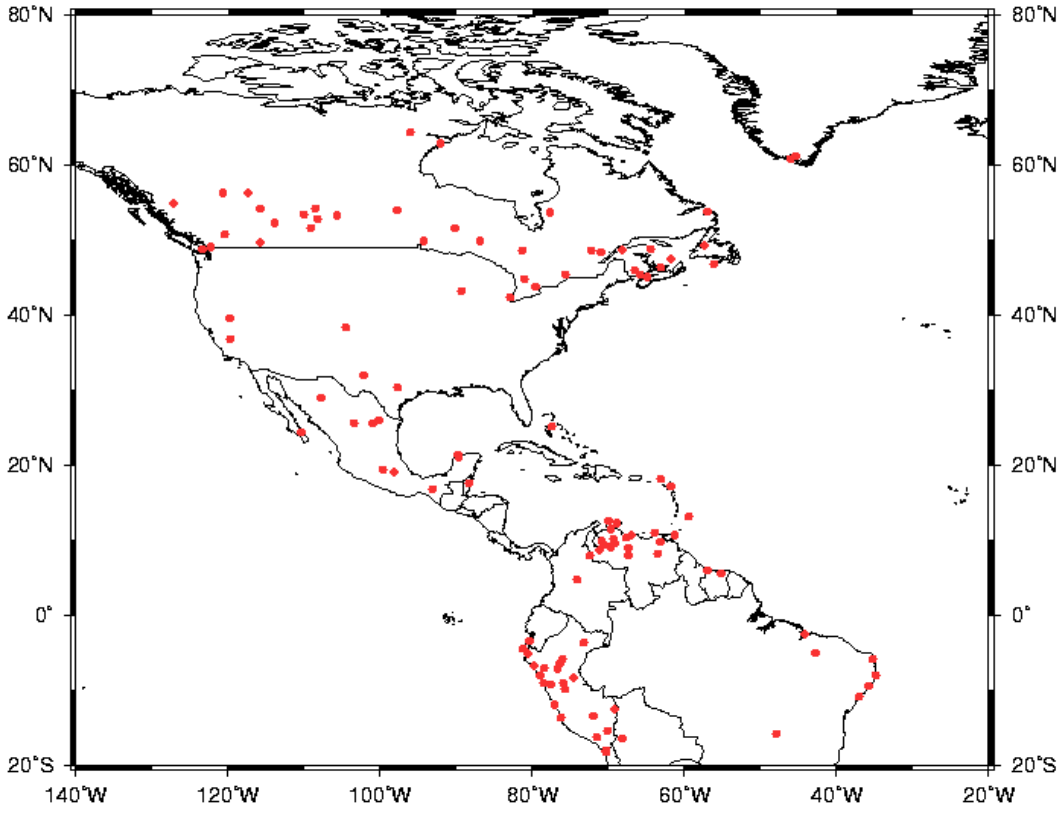

Figure A.3.2.2 Geographical location of the final set of 114 weather observation stations selected for the GOES Cloud products evaluation

A 3.3 Lidar measurements

Lidar measurements are performed at the « Laboratoire d'Optronique » of ENSSAT, Lannion France (contact : ladobord@enssat.fr). The lidar operates at 0.532 µm, and its range is 0-40km in cloud free atmosphere. This powerful lidar has been designed with the aim of producing measurements on clouds optical properties. It easily allows to retrieve the cloud basis and cloud top height for clouds that are not too thick, as well as the phase of the cloud basis. Presently, two studies on the retrieval of cirrus characteristics, and on the retrieval of water clouds droplet distribution are on-going at ENSSAT.

Lidar measurements are occasionally performed, coincident with the NOAA satellite HIRS and AVHRR measurements. Coincident lidar and satellite observations of semi-transparent clouds are available for the following situations : 09-02-98, 11-02-98, 12-02-98, 19-06-98, 23-06-98, 21-09-98, 28-11-98, 12-02/99 (9h & 14h), 09-03-99, 10-03-99, 15-03-99 (14h & 17h), 19-03-99, 31-03-99, 06-04-99, 16-04-99. They have been used by CMS for the validation of semi-transparent cloud top height retrieved from satellite data. We plan to gather a similar coincident data set for low clouds to be used during the cloud phase study to be performed during a visiting scientist stay.

The lidar signal, averaged every one minute, is available during at least 30 minutes and gives an indication of the temporal stability of the semi-transparent cloud cover. A vertical profile of the lidar signal, averaged over the whole period, helps to determine the cloud top height.

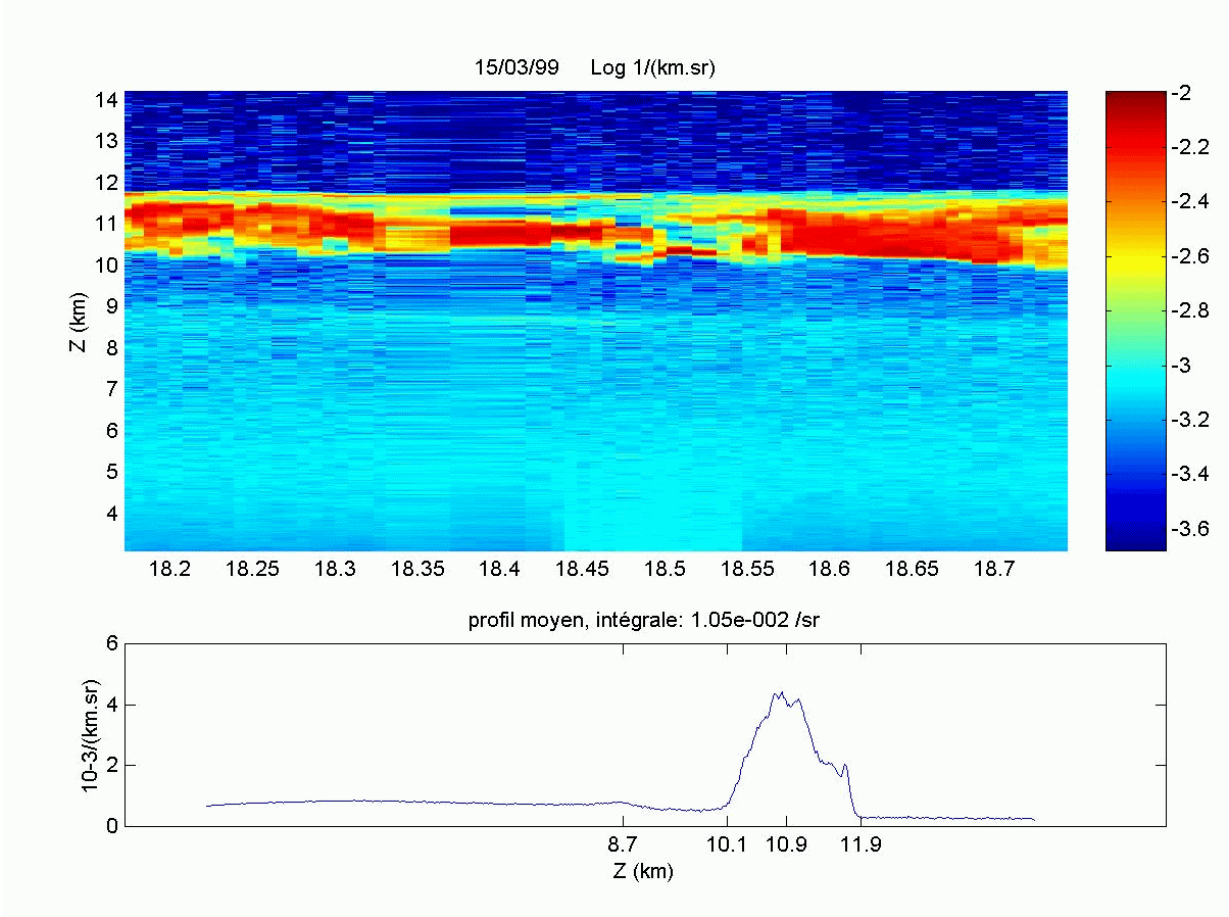

Figure A.3.3 Example of lidar information used for semi-transparent cloud top height retrieval . 15/03/99. Starting at 18h09 (local time)

Annex 4. Radiative Transfer Model

A 4.1 RTTOV

RTTOV is a radiative transfer model developed by J.Eyre. This parametrized model allows the very fast simulation of IR/MW radiances through a cloud-free atmosphere (described on 40 standard vertical levels), averaged over the spectral response of the considered channel. It was initially designed for HIRS sounding channels, but is flexible enough to allow the processing of other instrument, provided transmittance coefficients files and a set up parameters file are available for the new instrument. RTTOV is a software library containing subroutines.

The initial source code (version 3) has been obtained from ECMWF and is described by a ECMWF Technical Memorandum (Eyre et al., 1991). RTTOV code (version 3) has been slightly modified to allow the surface emissivities to differ from unity, and to improve the ozone processing. The files containing the gas transmittance for each new channel are easily elaborated at CMS using a large data base containing gas transmittance at 0.10 cm-1 spectral resolution (Brunel et al., 1992).

RTTOV has been applied off-line to the radio-soundings of the TIGR dataset for the tuning of thresholds for cloud masking. RTTOV is also routinely used on-line for cloud top pressure retrieval from NOAA/HIRS and GOES IR/WV channels.

A 4.2 6S

6S is a radiative transfer model developed by D.Tanre (University of Lille, France). This band model allows the relatively slow simulation of visible/near-infrared radiances or reflectances for pre-defined or user-defined channels (ranging from 0.25 to 4.0 μm, the spectral resolution is 0.0025 μm) through cloudless atmosphere. The main atmospheric effects (gaseous absorption by water vapour, carbon dioxide, oxygen and ozone ; scattering by molecules and aerosols) are taken into account. Non uniform surfaces may be considered, as well as bi-directional reflectances as boundary conditions. It is an interactive program easy to use. It is scientifically documented in a user's guide (see also Tanre et al., 1990).

The source code and the associated documentation have been obtained through ftp on the site : kratmos.gsfc.nasa.gov. The contact person is Eric vermote (eric@kratmos.gsfc.nasa.gov). We have used the version 4.1.

6S has been used at CMS mainly to tune a very fast model (developed at CMS) to simulate visible and near-infrared cloud-free reflectances for various satellites (NOAA, GOES-East and finally SEVIRI). In fact, this very fast model needs look-up tables for the computation of the gaz absorption, the Rayleigh & aerosol scattering transmittance and reflectances. We have modified the 6S main program to process new channels (add new filters), and to loop on satellite and sun angles, on ozone and water vapour content to pre-compute these look-up tables (see Brunel et al., 1991). The very fast simulation model is used on line for the cloud masking.

A 4.3 STREAMER

Streamer is a radiative transfer model developed by J.R.Key (Department of geography, Boston University). This band model allows the computation of either radiances (intensities) or irradiances (fluxes) for a wide variety of atmospheric (including clouds) and surface conditions. Its interface is

performed through a ASCII file. It is scientifically documented in a user's guide (see also Key et al., 1998).

The source code and the associated documentation have been obtained through ftp on the site : stratus.bu.edu (/pub/streamer/docs/userman.ps & refman.ps for the documentation, /pub/streamer/streamer.tar for the code). We have used the version 2.4.1 (September 17, 1998).

We will used Streamer for cloud radiance simulations during a cloud phase retrieval study (performed by a Visiting Scientist at CMS). The main advantage of this code, as compared to MODTRAN, is that Streamer computes the optical properties of clouds defined by the user (only their thickness, height, effective radius, ice/water concentration are needed), which is not the case for MODTRAN. But this code has some drawbacks, as indicated in the user's guide : the spectral definition is rough as compared to MODTRAN (predefined spectral bands are used : 24 between 0 and 4 μm, 75 between 4 and 16 μm), the long-wave cloud optical properties are computed using Mie theory, which is not adequate for ice clouds, and finally the cloud phase function is approximated using the asymmetry factor, and the Henvey-Greenstein function, which may lead to significant errors in radiances computations.

A 4.4 MODTRAN

MODTRAN is a radiative transfer model developed by Phillips Laboratory/Geophysics Directorate. This band model allows the relatively slow computation of radiances for a few surface conditions, but a wide variety atmospheric conditions (including clouds, aerosol...). Its interface is performed through cards in a ASCII file. It is scientifically documented in a user's guide (see also Anderson et al., 1995).

The source code and the associated documentation have been obtained through ftp on the site : 146.153.100.3. The contact person is G.P. Anderson (Phillips Laboratory/Geophysics Directorate Hanscom AFB, MA 01731). We have used the MODTRAN 3.5 version 1.2 (April 1997).

We have used MODTRAN mainly for cloud and aerosol simulations. The main difficulty to use this code for cloud simulations is that the standard clouds do not seem realistic, and that a cloud must be defined by the user through its cloud optical properties, which must therefore be computed outside MODTRAN. But the advantage of MODTRAN is its relatively fine spectral resolution (1 cm^{-1} resolution). An additional difficulty is that it is not possible to define a channel filter in MODTRAN: we have processed individual wavelengths and then apply the channel filter outside MODTRAN.

Annex 5. Demonstration Experiment

During the SAFNWC demonstration experiment (8th November 1999-8th December 1999), Météo-France provided half-hourly cloud types and cloud top pressure extracted from GOES-East imagery over the Extended Northern Hemisphere. The GOES prototype, with its high temporal frequency (thus allowing animation of products), its ability to analyse cloud cover both at daytime and night-time (thanks to the 3.9µm channel) illustrates the cloud parameters' minimum quality that can be expected with MSG SEVIRI. The Météo-France's contribution to SAF NWC demonstration experiment is summarised below :

- products' description :
  - cloud type, cloud top pressure and corresponding IR images (scale documented)
  - sampled every 3*3 IR pixels (i.e., 12*12km at satellite nadir)
  - over the Extended Northern Hemisphere (see figure A.5.1)
  - every 30 minutes
  - in GIF format
- products' availability :
  - the products corresponding to the 48 slots from the day before
  - updated only once every day (at 4 UTC)
  - on the Météo-France ftp public server (ftp ://www.meteo.fr) on the directories /pub/SAFNWC/DEMO/CT (for the cloud types) [respectively CTTH (for the cloud top pressure) and IR (for the IR images)]
- The demonstration experiment has no operational status :
  - no spare workstation is used
  - prototype's software is not robust in case of missing channels or ancillary data.

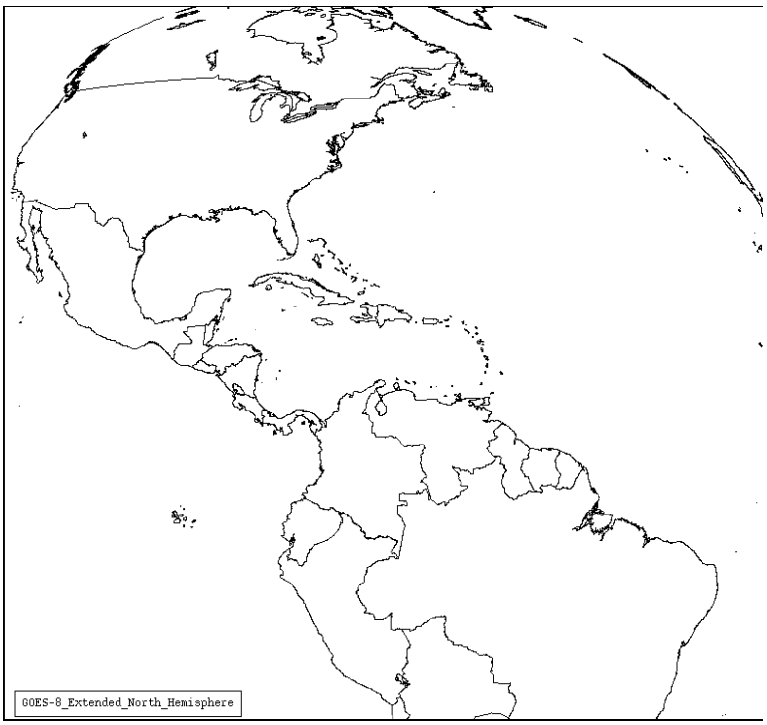

Figure A.5.1 Illustration of the GOES processed area (Extended Northern Hemisphere)

Annex 6. Contingency, producer and user accuracy's tables for CT

The following definitions are used in this annex :

- In the error matrixes the rows represent the observers' classes (considered as reference) while the columns figures represents the CT classifier results.
- The producer's accuracy represents the probability of a target being correctly classified.
- The user's accuracy represents the probability of a pixel classified into a category on a picture to really belong to that category.

	Sea	**Land**	**Snow/Ice**	**Low**	**Mid**	**Semi**	**High**	**Fract**	**Total**	**Producer**
Sea	**1756**	8	7	41	0	9	0	8	1829	96.0%
Land	13	**1346**	1	20	2	3	0	19	1404	95.9%
Snow/Ice	0	55	**280**	105	8	8	4	0	460	60.9%
Low	48	169	11	**2555**	252	82	4	305	3426	74.6%
Mid	1	13	0	236	**851**	114	118	23	1356	62.8%
Semi	7	53	13	57	215	**2466**	572	75	3458	71.3%
High	0	0	0	4	75	234	**2788**	0	3101	89.9%
Total	1825	1644	312	3018	1403	2916	3486	430	**15034**	
User	96.2%	81.9%	89.7%	84.7%	60.7%	84.6%	80.0%			

Table A.6.1a Validation of Cloud Type (CT) with interactive file. Error matrix and producer and user accuracy for meta-classes for all climatic and illumination conditions

	Sea	**Land**	**Snow/Ice**	**Low**	**Mid**	**Semi**	**High**	**Fract**	**Total**	**Producer**
Sea	**1230**	5	7	35	0	8	0	6	1291	95.3%
Land	8	**869**	1	5	2	3	0	17	905	96.0%
Snow/Ice	0	17	**280**	96	6	8	3	0	410	68.3%
Low	29	133	11	**1592**	147	65	2	300	2279	69.9%
Mid	0	10	0	128	**515**	63	62	22	800	64.4%
Semi	4	48	13	30	157	**1485**	362	64	2163	68.7%
High	0	0	0	3	40	120	**1570**	0	1733	90.6%
Total	1271	1082	312	1889	867	1752	1999	409	**9581**	
User	96.8%	80.3%	89.7%	84.3%	59.4%	84.8%	78.5%			

Table A.6.1b Same as A.6.1a, for daytime conditions and all climatic areas.

	Sea	Land	Snow/Ice	Low	Mid	Semi	High	Fract	Total	Producer
Sea	**434**	3	0	5	0	1	0	2	445	97.5%
Land	3	**391**	0	15	0	0	0	2	411	95.1%
Snow/Ice	0	32	**0**	9	2	0	1	0	44	0%
Low	15	18	0	**811**	87	13	2	4	950	85.4%
Mid	1	3	0	90	**271**	48	45	1	459	59.0%
Semi	0	3	0	14	36	**795**	174	9	1031	77.1%
High	0	0	0	1	27	87	**963**	0	1078	89.3%
Total	453	450	0	945	423	944	1185	18	**4418**	
User	95.8%	86.9%	0%	85.8%	64.1%	84.2%	81.3%			

Table A.6.1c Same as A.6.1a, for nighttime conditions and all climatic areas.

	Sea	Land	Snow/Ice	Low	Mid	Semi	High	Fract	Total	Producer
Sea	**91**	0	0	1	0	0	0	0	92	98.9%
Land	2	**86**	0	0	0	0	0	0	88	97.7%
Snow/Ice	0	6	**0**	0	0	0	0	0	6	0%
Low	4	18	0	**152**	18	4	0	1	197	77.2%
Mid	0	0	0	18	**65**	3	11	0	97	67.0%
Semi	3	2	0	13	22	**185**	36	2	263	70.3%
High	0	0	0	0	8	27	**255**	0	290	87.9%
Total	100	112	0	184	113	219	302	3	**1033**	
User	91.0%	76.8%	0%	82.6%	57.5%	84.5%	84.4%			

Table A.6.1d Same as A.6.1a, for twilight conditions and all climatic areas.

	Sea	Land	Snow/Ice	Low	Mid	Semi	High	Fract	Total	Producer
Sea	**858**	1	6	24	0	3	0	4	896	95.8%
Land	7	**913**	0	16	2	3	0	3	944	96.7%
Snow/Ice	0	53	**171**	82	8	4	1	0	319	53.6%
Low	23	88	7	**1441**	137	36	3	140	1875	76.9%
Mid	0	5	0	192	**394**	48	68	15	722	54.6%
Semi	1	45	11	41	146	**1212**	396	65	1917	63.2%
High	0	0	0	4	62	131	**1426**	0	1623	87.9%
Total	889	1105	195	1800	749	1437	1894	227	**9296**	
User	96.5%	82.6%	87.7%	80.1%	52.6%	84.3%	75.3%			

Table A.6.1e Same as A.6.1a, for midlatitude areas and all illumination conditions.

	Sea	Land	Snow/Ice	Low	Mid	Semi	High	Fract	Total	Producer
Sea	**615**	1	6	21	0	2	0	4	649	94.8%
Land	6	**609**	0	4	2	3	0	3	627	97.1%
Snow/Ice	0	16	**171**	74	6	4	0	0	271	63.1%
Low	12	68	7	**930**	70	29	2	137	1255	74.1%
Mid	0	5	0	108	**264**	34	39	15	465	56.8%
Semi	1	42	11	24	108	**774**	240	59	1259	61.5%
High	0	0	0	3	33	77	**843**	0	956	88.2%
Total	634	741	195	1164	483	923	1124	218	**5482**	
User	97.0%	82.2%	87.7%	79.9%	54.7%	83.9%	75.0%			

Table A.6.1f Same as A.6.1a, for midlatitude areas and daytime condition.

	Sea	Land	Snow/Ice	Low	Mid	Semi	High	Fract	Total	Producer
Sea	**207**	0	0	3	0	1	0	0	211	98.1%
Land	0	**228**	0	12	0	0	0	0	240	95.0%
Snow/Ice	0	31	**0**	8	2	0	1	0	42	0%
Low	10	10	0	**459**	55	4	1	2	541	84.8%
Mid	0	0	0	71	**97**	12	22	0	202	48.0%
Semi	0	3	0	10	28	**368**	131	5	545	67.5%
High	0	0	0	1	23	42	**448**	0	514	87.2%
Total	217	272	0	564	205	427	603	7	**2295**	
User	95.4%	83.8%	0%	81.4%	47.3%	86.2%	74.3%			

Table A.6.1g Same as A.6.1a, for midlatitude areas and nighttime conditions.

	Sea	Land	Snow/Ice	Low	Mid	Semi	High	Fract	Total	Producer
Sea	**36**	0	0	0	0	0	0	0	36	100.0%
Land	1	**76**	0	0	0	0	0	0	77	98.7%
Snow/Ice	0	6	**0**	0	0	0	0	0	6	0%
Low	1	10	0	**52**	12	3	0	1	79	65.8%
Mid	0	0	0	13	**33**	2	7	0	55	60.0%
Semi	0	0	0	7	10	**70**	25	1	113	61.9%
High	0	0	0	0	6	12	**135**	0	153	88.2%
Total	38	92	0	72	61	87	167	2	**519**	
User	94.7%	82.6%	0%	72.2%	54.1%	80.5%	80.8%			

Table A.6.1h same as A.6.1a, for midlatitude areas and twilight conditions.

	Sea	Land	Ice	Snow	Very Low	Low	Mid	Semi Above	Semi Thin	Semi Thick	High Nocu	High Cum	Sand	Ash	Fract	Total
Sea	**1756**	8	6	1	39	2	0	2	5	2	0	0	0	0	8	1829
Land	13	**1346**	0	1	13	7	2	1	1	1	0	0	0	0	19	1404
Ice	0	2	**124**	23	31	18	1	1	1	2	3	0	0	0	0	206
Snow	0	53	0	**133**	32	24	7	0	1	3	1	0	0	0	0	254
Very Low	24	114	1	7	**629**	351	50	9	37	6	0	0	0	0	228	1456
Low	27	64	2	1	490	**1054**	205	6	12	15	4	0	0	0	90	1970
Mid	1	13	0	0	116	120	**851**	28	14	72	117	1	0	0	23	1356
Semi Above	0	3	0	0	6	15	151	**182**	15	376	74	1	0	0	4	827
Semi Thin	7	54	7	10	30	15	81	202	**242**	839	28	0	0	0	74	1589
Semi Thick	0	0	0	0	0	0	10	11	1	**537**	416	67	0	0	0	1042
High Nocu	0	0	0	0	0	1	54	10	0	196	**703**	331	0	0	0	1295
High Cu	0	0	0	0	3	0	22	0	0	45	331	**1405**	0	0	0	1806
Sand	0	0	0	0	1	7	2	0	0	0	0	0	**0**	0	0	10
Ash	9	21	0	0	111	1	0	0	0	0	0	0	0	**0**	52	194
Total	1837	1678	140	176	1501	1615	1436	452	329	2094	1677	1805	0	0	498	**15238**

Table A.6.2a: Validation of Cloud Type (CT) with interactive file. Error matrix for all climatic and illumination conditions.

	Sea	Land	Ice	Snow	Very Low	Low	Mid	Semi Above	Semi Thin	Semi Thick	High Nocu	High Cum	Sand	Ash	Fract	Total
Sea	**1230**	5	6	1	33	2	0	2	5	1	0	0	0	0	6	1291
Land	8	**869**	0	1	4	1	2	1	1	1	0	0	0	0	17	905
Ice	0	0	**124**	23	31	17	1	1	1	2	3	0	0	0	0	203
Snow	0	17	0	**133**	30	18	5	0	1	3	0	0	0	0	0	207
Very Low	13	105	1	7	**518**	248	34	9	37	4	0	0	0	0	224	1200
Low	17	34	2	1	270	**531**	115	6	7	5	2	0	0	0	89	1079
Mid	0	10	0	0	58	70	**515**	28	14	21	61	1	0	0	22	800
Semi Above	0	1	0	0	0	5	104	**182**	14	134	49	1	0	0	1	491
Semi Thin	4	51	7	10	20	8	62	202	**178**	369	15	0	0	0	65	991
Semi Thick	0	0	0	0	0	0	6	11	0	**360**	269	35	0	0	0	681
High Nocu	0	0	0	0	0	1	30	10	0	91	**369**	186	0	0	0	687
High Cu	0	0	0	0	2	0	11	0	0	28	181	**824**	0	0	0	1046
Sand	0	0	0	0	1	7	2	0	0	0	0	0	**0**	0	0	10
Ash	9	21	0	0	111	1	0	0	0	0	0	0	0	**0**	52	194
Total	1281	1113	140	176	1078	909	887	452	258	1019	949	1047	0	0	476	**9785**

Table A.6.2b Same as A.6.2a, for daytime only and all climatic conditions

	Sea	Land	Ice	Snow	Very Low	Low	Mid	Semi Above	Semi Thin	Semi Thick	High Nocu	High Cum	Sand	Ash	Fract	Total
Sea	**434**	3	0	0	5	0	0	0	0	1	0	0	0	0	2	445
Land	3	**391**	0	0	9	6	0	0	0	0	0	0	0	0	2	411
Ice	0	2	**0**	0	0	1	0	0	0	0	0	0	0	0	0	3
Snow	0	30	0	**0**	2	6	2	0	0	0	1	0	0	0	0	41
Very Low	9	6	0	0	**91**	102	16	0	0	2	0	0	0	0	4	230
Low	8	13	0	0	120	**494**	72	0	3	8	2	0	0	0	0	720
Mid	1	3	0	0	43	47	**271**	0	0	48	45	0	0	0	1	459
Semi Above	0	1	0	0	3	8	29	**0**	0	186	22	0	0	0	3	252
Semi Thin	0	2	0	0	2	4	14	0	**60**	389	11	0	0	0	7	489
Semi Thick	0	0	0	0	0	0	3	0	1	**141**	120	25	0	0	0	290
High Nocu	0	0	0	0	0	0	17	0	0	78	**261**	115	0	0	0	471
High Cu	0	0	0	0	1	0	10	0	0	12	119	**465**	0	0	0	607
Sand	0	0	0	0	0	0	0	0	0	0	0	0	**0**	0	0	0
Ash	0	0	0	0	0	0	0	0	0	0	0	0	0	**0**	0	0
Total	455	451	0	0	276	668	434	0	64	865	581	605	0	0	19	**4418**

Table A.6.2c Same as A.6.2a, for nighttime only and all climatic conditions

	Sea	Land	Ice	Snow	Very Low	Low	Mid	Semi Above	Semi Thin	Semi Thick	High Nocu	High Cum	Sand	Ash	Fract	Total
Sea	**91**	0	0	0	1	0	0	0	0	0	0	0	0	0	0	92
Land	2	**86**	0	0	0	0	0	0	0	0	0	0	0	0	0	88
Ice	0	0	**0**	0	0	0	0	0	0	0	0	0	0	0	0	0
Snow	0	6	0	**0**	0	0	0	0	0	0	0	0	0	0	0	6
Very Low	2	3	0	0	**20**	1	0	0	0	0	0	0	0	0	0	26
Low	2	17	0	0	100	**29**	18	0	2	2	0	0	0	0	1	171
Mid	0	0	0	0	15	3	**65**	0	0	3	11	0	0	0	0	97
Semi Above	0	1	0	0	3	2	18	**0**	1	56	3	0	0	0	0	84
Semi Thin	3	1	0	0	8	3	5	0	**4**	81	2	0	0	0	2	109
Semi Thick	0	0	0	0	0	0	1	0	0	**35**	27	7	0	0	0	70
High Nocu	0	0	0	0	0	0	7	0	0	27	**73**	30	0	0	0	137
High Cu	0	0	0	0	0	0	1	0	0	5	31	**116**	0	0	0	153
Sand	0	0	0	0	0	0	0	0	0	0	0	0	**0**	0	0	0
Ash	0	0	0	0	0	0	0	0	0	0	0	0	0	**0**	0	0
Total	100	114	0	0	147	38	115	0	7	209	147	153	0	0	3	**1033**

Table A.6.2d Same as A.6.2a, for twilight and all climatic conditions

	Sea	Land	Ice	Snow	Very Low	Low	Mid	Semi Above	Semi Thin	Semi Thick	High Nocu	High Cum	Sand	Ash	Fract	Total
Sea	**858**	1	5	1	22	2	0	1	1	1	0	0	0	0	4	896
Land	7	**913**	0	0	11	5	2	1	1	1	0	0	0	0	3	944
Ice	0	1	**43**	2	18	10	1	1	0	0	0	0	0	0	0	76
Snow	0	52	0	**126**	30	24	7	0	1	2	1	0	0	0	0	243
Very Low	19	55	0	6	**438**	276	31	4	15	3	0	0	0	0	87	934
Low	4	41	0	1	231	**480**	108	3	7	6	3	0	0	0	57	941
Mid	0	5	0	0	91	101	**394**	15	6	27	67	1	0	0	15	722
Semi Above	0	1	0	0	4	12	96	**75**	6	132	47	1	0	0	4	378
Semi Thin	1	47	5	10	23	8	63	117	**145**	376	18	0	0	0	64	877
Semi Thick	0	0	0	0	0	0	9	10	1	**306**	275	61	0	0	0	662
High Nocu	0	0	0	0	0	1	41	9	0	119	**532**	268	0	0	0	970
High Cu	0	0	0	0	3	0	22	0	0	14	202	**412**	0	0	0	653
Sand	0	0	0	0	1	5	2	0	0	0	0	0	**0**	0	0	8
Ash	6	10	0	0	38	1	0	0	0	0	0	0	0	**0**	7	62
Total	895	1126	53	146	910	925	776	236	183	987	1145	743	0	0	241	**8366**

Table A.6.2e Same as A.6.2a, for mid-latitude areas only and all illumination conditions

	Sea	Land	Ice	Snow	Very Low	Low	Mid	Semi Above	Semi Thin	Semi Thick	High Nocu	High Cum	Sand	Ash	Fract	Total
Sea	**615**	1	5	1	19	2	0	1	1	0	0	0	0	0	4	649
Land	6	**609**	0	0	3	1	2	1	1	1	0	0	0	0	3	627
Ice	0	0	**43**	2	18	9	1	1	0	0	0	0	0	0	0	74
Snow	0	16	0	**126**	29	18	5	0	1	2	0	0	0	0	0	197
Very Low	11	53	0	6	**351**	195	20	4	15	3	0	0	0	0	85	743
Low	1	21	0	1	140	**231**	51	3	3	3	2	0	0	0	56	512
Mid	0	5	0	0	49	59	**264**	15	6	13	38	1	0	0	15	465
Semi Above	0	0	0	0	0	4	68	**75**	5	43	28	1	0	0	1	225
Semi Thin	1	45	5	10	17	5	46	117	**113**	184	10	0	0	0	60	613
Semi Thick	0	0	0	0	0	0	6	10	0	**202**	172	31	0	0	0	421
High Nocu	0	0	0	0	0	1	23	9	0	64	**291**	151	0	0	0	539
High Cu	0	0	0	0	2	0	11	0	0	9	106	**289**	0	0	0	417
Sand	0	0	0	0	1	5	2	0	0	0	0	0	**0**	0	0	8
Ash	6	10	0	0	38	1	0	0	0	0	0	0	0	**0**	7	62
Total	640	760	53	146	667	531	499	236	145	524	647	473	0	0	231	**5552**

Table A.6.2f Same as A.6.2a, for mid-latitude areas only and daytime conditions

	Sea	Land	Ice	Snow	Very Low	Low	Mid	Semi Above	Semi Thin	Semi Thick	High Nocu	High Cum	Sand	Ash	Fract	Total
Sea	**207**	0	0	0	3	0	0	0	0	1	0	0	0	0	0	211
Land	0	**228**	0	0	8	4	0	0	0	0	0	0	0	0	0	240
Ice	0	1	**0**	0	0	1	0	0	0	0	0	0	0	0	0	2
Snow	0	30	0	**0**	1	6	2	0	0	0	1	0	0	0	0	40
Very Low	7	2	0	0	**72**	80	11	0	0	0	0	0	0	0	2	174
Low	3	8	0	0	69	**237**	45	0	2	2	1	0	0	0	0	367
Mid	0	0	0	0	32	39	**97**	0	0	12	22	0	0	0	0	202
Semi Above	0	1	0	0	2	6	22	**0**	0	77	18	0	0	0	3	129
Semi Thin	0	2	0	0	2	3	13	0	**30**	156	7	0	0	0	3	216
Semi Thick	0	0	0	0	0	0	2	0	1	**87**	86	24	0	0	0	200
High Nocu	0	0	0	0	0	0	13	0	0	40	**191**	96	0	0	0	340
High Cu	0	0	0	0	1	0	10	0	0	3	77	**83**	0	0	0	174
Sand	0	0	0	0	0	0	0	0	0	0	0	0	**0**	0	0	0
Ash	0	0	0	0	0	0	0	0	0	0	0	0	0	**0**	0	0
Total	217	272	0	0	190	376	215	0	33	378	403	203	0	0	8	**2295**

Table A.6.2g Same as A.6.2a, for mid-latitude areas only and nighttime conditions

	Sea	Land	Ice	Snow	Very Low	Low	Mid	Semi Above	Semi Thin	Semi Thick	High Nocu	High Cum	Sand	Ash	Fract	Total
Sea	**36**	0	0	0	0	0	0	0	0	0	0	0	0	0	0	36
Land	1	**76**	0	0	0	0	0	0	0	0	0	0	0	0	0	77
Ice	0	0	**0**	0	0	0	0	0	0	0	0	0	0	0	0	0
Snow	0	6	0	**0**	0	0	0	0	0	0	0	0	0	0	0	6
Very Low	1	0	0	0	**15**	1	0	0	0	0	0	0	0	0	0	17
Low	0	12	0	0	22	**12**	12	0	2	1	0	0	0	0	1	62
Mid	0	0	0	0	10	3	**33**	0	0	2	7	0	0	0	0	55
Semi Above	0	0	0	0	2	2	6	**0**	1	12	1	0	0	0	0	24
Semi Thin	0	0	0	0	4	0	4	0	**2**	36	1	0	0	0	1	48
Semi Thick	0	0	0	0	0	0	1	0	0	**17**	17	6	0	0	0	41
High Nocu	0	0	0	0	0	0	5	0	0	15	**50**	21	0	0	0	91
High Cu	0	0	0	0	0	0	1	0	0	2	19	**40**	0	0	0	62
Sand	0	0	0	0	0	0	0	0	0	0	0	0	**0**	0	0	0
Ash	0	0	0	0	0	0	0	0	0	0	0	0	0	**0**	0	0
Total	38	94	0	0	53	18	62	0	5	85	95	67	0	0	2	**519**

Table A.6.2h Same as A.6.2a, for mid-latitude areas only and twilight conditions

	Sea	land	Snow/ice	Low	Mid	Semi	High
All	96.2	81.9	89.7	84.7	60.7	84.6	80.0
Day	96.8	80.3	89.7	84.3	59.4	84.8	78.5
Twilight	91.0	76.8	0	82.6	57.5	84.5	84.4
Night	95.8	86.9	0	85.8	64.1	84.2	81.3
Mid-latitude	96.5	82.6	87.7	80.1	52.6	84.3	75.3
Day	97.0	82.2	87.7	79.9	54.7	83.9	75.0
Twilight	94.7	82.6	0	72.2	54.1	80.5	80.8
Night	95.4	83.3	0	81.4	47.3	82.2	74.3

Table A.6.3a Validation of Cloud Type (CT) with interactive file. Variation of user accuracy percentage with climatic areas and illumination conditions for "metaclass".

	Sea	land	Ice	Snow	very low	Low	Mid	Semi above	Semi thin	Semi thick	High Nocu	High Cum
All	95.5	80.0	88.6	75.6	41.9	65.2	59.1	40.3	73.2	25.6	41.7	77.8
Day	95.9	77.8	88.6	75.6	48.0	58.3	58.0	40.3	68.7	35.3	38.6	78.6
Twilight	91.0	75.4	0	0	13.6	76.3	56.5	0	57.1	16.7	49.7	75.8
Night	95.4	86.7	0	0	33.0	74.0	62.2	0	93.8	16.3	44.9	76.9
Mid-latitude	95.8	80.9	81.1	86.3	48.1	51.8	50.6	31.8	78.8	31.0	46.3	55.4
Day	95.9	79.8	81.1	86.3	52.6	43.3	52.8	31.8	77.4	38.5	44.8	61.0
Twilight	94.7	80.9	0	0	28.3	66.7	53.2	0	40.0	20.0	52.6	59.7
Night	95.4	83.8	0	0	37.9	63.0	44.7	0	90.9	23.0	47.4	40.9

Table A.6.3b Validation of Cloud Type (CT) with interactive file. Variation of user accuracy percentage with climatic areas and illumination conditions for "group-class".

	Sea	land	Snow/ice	Low	Mid	Semi	High
All	96.0	95.9	60.9	74.6	62.8	71.3	89.9
Day	95.3	96.0	68.2	69.9	64.4	68.7	90.6
Twilight	98.9	97.7	0	77.2	67.0	70.3	87.9
Night	97.5	95.1	0	85.4	59.0	77.1	89.3
Mid-latitude	95.8	96.7	53.6	76.9	54.6	63.2	87.9
Day	94.8	97.1	63.1	74.1	56.8	61.5	88.2
Twilight	100.0	98.7	0	65.8	60.0	61.9	88.2
Night	98.1	95.0	0	84.8	48.0	67.5	87.2

Table A.6.4a Validation of Cloud Type (CT) with interactive file. Variation of producer accuracy percentage with climatic areas and illumination conditions for "metaclass".

	Sea	land	Ice	Snow	very low	Low	Mid	Semi above	Semi thin	Semi thick	High Nocu	High Cum
All	96.0	95.9	60.2	52.4	43.2	53.5	62.8	22.0	15.2	51.5	54.3	77.8
Day	95.3	96.0	61.1	64.3	43.2	49.2	64.4	37.1	18.0	52.9	53.7	78.8
Twilight	98.9	97.7	0	0	76.9	17.0	67.0	0	3.7	50.0	53.8	75.8
Night	97.5	95.1	0	0	39.6	68.6	59.0	0	12.3	48.6	55.4	76.6
Mid-latitude	95.8	96.7	56.6	51.9	46.9	51.0	54.6	19.8	16.5	46.2	54.8	63.1
Day	94.8	97.1	58.1	64.0	47.2	45.1	56.8	33.3	18.4	48.0	54.0	69.3
Twilight	100.0	98.7	0	0	88.2	19.4	60.0	0	4.2	41.5	54.9	64.5
Night	98.1	95.0	0	0	41.4	64.6	48.0	0	13.9	43.5	56.2	47.7

Table A.6.4b Validation of Cloud Type (CT) with interactive file. Variation of producer accuracy percentage with climatic areas and illumination conditions for "group-class"

	Cloud free	Low	Med	Semi	High	Semi above	Fract	Total
Cloud free	**45999**	5887	1905	4383	1173	193	3799	63339
Low (N≤5)	3107	**1640**	274	772	80	81	1109	7063
Low (N≥6)	3961	**11266**	6106	4215	3564	1239	1369	31720
Med (N≤5)	4438	1823	**404**	1127	138	159	1897	9986
Med (N≥6)	1450	2191	**4014**	5564	3835	1462	1078	19594
Semi (N≤5)	7065	1730	887	**3464**	290	359	1445	15240
Semi (N≥6)	5229	2057	2287	**8599**	1741	1902	1850	23665
High (N≤5)	1028	361	113	700	**66**	73	546	2887
High (N≥6)	1344	1686	2705	4385	**3824**	1123	659	15726
Mult (N≤5)	2620	1200	327	1023	78	**152**	861	6261
Mult (N≥6)	1245	2099	2447	3309	1946	**1079**	687	12812
Total	77486	31940	21469	37541	16735	7822	15300	**208293**

Table A.6.5a. Validation of Cloud Type (CT) with SYNOP. Error matrix for all climatic and illumination conditions (N stands for total cloud cover reported in the SYNOP)

	Cloud free	Low	Med	Semi	High	Semi above	Fract	Total
Cloud free	**21053**	2039	277	747	126	193	2472	26907
Low (N≤5)	1890	**961**	87	227	24	81	948	4218
Low (N≥6)	1356	**5098**	2186	1483	1272	1239	1235	13869
Med (N≤5)	2870	1298	**163**	491	54	159	1564	6599
Med (N≥6)	741	1279	**1963**	2421	1696	1462	919	10481
Semi (N≤5)	4225	884	218	1070	61	359	899	7716
Semi (N≥6)	3774	1119	1016	**4384**	799	1902	1432	14426
High (N≤5)	710	254	65	**231**	**38**	73	360	1731
High (N≥6)	749	892	1432	2176	**1910**	1123	513	8795
Mult (N≤5)	1644	746	132	420	26	152	680	3800
Mult (N≥6)	669	1330	1319	1738	1015	1079	588	7738
Total	39681	15900	8858	15388	7021	7822	11610	**106280**

Table A.6.5b. Same as A.6.5a, for daytime conditions and all climatic areas

	Cloud free	Low	Med	Semi	High	Semi above	Fract	Total
Cloud free	**3725**	349	60	130	24	0	28	4316
Low (N≤5)	207	**64**	3	12	2	0	2	290
Low (N≥6)	846	**597**	371	423	368	0	57	2662
Med (N≤5)	172	67	**19**	34	6	0	7	305
Med (N≥6)	202	109	**285**	375	359	0	19	1349
Semi (N≤5)	671	112	52	**171**	12	0	21	1039
Semi (N≥6)	562	148	175	**738**	146	0	46	1815
High (N≤5)	87	16	7	18	**2**	0	24	154
High (N≥6)	212	102	215	417	**408**	0	28	1382
Mult (N≤5)	258	65	20	40	0	0	4	387
Mult (N≥6)	270	186	255	399	254	0	14	1378
Total	7212	1815	1462	2757	1581	0	250	**15077**

Table A.6.5c. Same as A.6.5a, for twilight conditions and all climatic areas

	Cloud free	Low	Med	Semi	High	Semi above	Fract	Total
Cloud free	**21221**	3499	1568	3506	1023	0	1299	32116
Low (N≤5)	1010	**615**	184	533	54	0	159	2555
Low (N≥6)	1759	**5571**	3549	2309	1924	0	77	15189
Med (N≤5)	1396	458	**222**	602	78	0	326	3082
Med (N≥6)	507	803	**1766**	2768	1780	0	140	7764
Semi (N≤5)	2169	734	617	**2223**	217	0	525	6485
Semi (N≥6)	893	790	1096	**3477**	796	0	372	7424
High (N≤5)	231	91	41	451	**26**	0	162	1002
High (N≥6)	383	692	1058	1792	**1506**	0	118	5549
Mult (N≤5)	718	389	175	563	52	0	177	2074
Mult (N≥6)	306	583	873	1172	677	0	85	3696
Total	30593	14225	11149	19396	8133	0	3440	**86936**

Table A.6.5d. Same as A.6.5a, for night conditions and all climatic areas

	Cloud free	Low	Med	Semi	High	Semi above	Fract	Total
Cloud free	**22051**	2729	1020	1709	780	83	886	29258
Low (N≤5)	687	**755**	70	88	21	5	129	1755
Low (N≥6)	1478	**6051**	3349	1704	2345	385	476	15788
Med (N≤5)	542	490	**166**	217	47	35	144	1641
Med (N≥6)	270	842	**1986**	1339	1694	323	145	6599
Semi (N≤5)	2031	592	335	**826**	138	71	224	4217
Semi (N≥6)	1258	687	681	**2479**	815	377	293	6590
High (N≤5)	207	65	26	70	**6**	13	76	463
High (N≥6)	410	925	1553	1318	**2132**	277	146	6761
Mult (N≤5)	749	441	92	225	19	26	147	1699
Mult (N≥6)	556	1346	1586	1728	1358	524	272	7370
Total	30239	14923	10864	11703	9355	2119	2938	**82141**

Table A.6.5e. Same as A.6.5a, for midlatitude areas and all illuminations conditions

	Cloud free	Low	Med	Semi	High	Semi above	Fract	Total
Cloud free	**9061**	955	125	387	93	83	745	11449
Low (N≤5)	287	**419**	10	18	1	5	104	844
Low (N≥6)	337	**2717**	1200	595	834	385	439	6507
Med (N≤5)	280	299	**47**	91	8	35	120	880
Med (N≥6)	70	491	**880**	488	703	323	124	3079
Semi (N≤5)	1156	291	77	**251**	24	71	180	2050
Semi (N≥6)	836	375	283	**1195**	328	377	266	3660
High (N≤5)	126	48	14	37	**6**	13	49	293
High (N≥6)	131	422	733	634	**991**	277	114	3302
Mult (N≤5)	430	283	31	104	4	26	125	1003
Mult (N≥6)	267	845	837	968	698	524	245	4384
Total	12981	7145	4237	4768	3690	2119	2511	**37451**

Table A.6.5f. Same as A.6.5a, for midlatitude areas and daytime conditions

	Cloud free	Low	Med	Semi	High	Semi above	Fract	Total
Cloud free	**2440**	212	36	86	17	0	12	2803
Low (N≤5)	98	**47**	3	2	1	0	1	152
Low (N≥6)	352	**402**	229	193	244	0	20	1440
Med (N≤5)	79	48	**14**	25	4	0	5	175
Med (N≥6)	63	79	**208**	164	185	0	5	704
Semi (N≤5)	349	71	34	**56**	3	0	6	519
Semi (N≥6)	217	101	89	**321**	78	0	9	815
High (N≤5)	33	8	3	3	**0**	0	6	53
High (N≥6)	97	69	157	207	**255**	0	11	796
Mult (N≤5)	145	47	9	19	0	0	2	222
Mult (N≥6)	157	162	203	291	191	0	7	1011
Total	4030	1246	985	1367	978	0	84	**8690**

Table A.6.5g. Same as A.6.5a, for midlatitude areas and twilight conditions

	Cloud free	Low	Med	Semi	High	Semi/lower	Fract	Total
Cloud free	**10550**	1562	859	1236	670	0	129	15006
Low (N≤5)	302	**289**	57	68	19	0	24	759
Low (N≥6)	789	**2932**	1920	916	1267	0	17	7841
Med (N≤5)	183	143	**105**	101	35	0	19	586
Med (N≥6)	137	272	**898**	687	806	0	16	2816
Semi (N≤5)	526	230	224	**519**	111	0	38	1648
Semi (N≥6)	205	211	309	**963**	409	0	18	2115
High (N≤5)	48	9	9	30	**0**	0	21	117
High (N≥6)	182	434	663	477	**886**	0	21	2663
Mult (N≤5)	174	111	52	102	15	0	20	474
Mult (N≥6)	132	339	546	469	469	0	20	1975
Total	13228	6532	5642	5568	4687	0	343	**36000**

Table A.6.5h. Same as A.6.5a, for midlatitude areas and night conditions

	Cloud free	Low	Med	Semi	High	Semi above	Fract	Total
Cloud free	**2186**	1306	302	550	328	14	262	4948
Low (N≤5)	68	**131**	15	15	9	1	13	252
Low (N≥6)	326	**839**	730	275	610	37	42	2859
Med (N≤5)	49	128	**57**	88	26	6	24	378
Med (N≥6)	110	254	**563**	477	848	48	11	2311
Semi (N≤5)	330	225	102	**297**	61	38	38	1091
Semi (N≥6)	162	144	169	**481**	303	56	10	1325
High (N≤5)	18	38	10	11	**2**	0	5	84
High (N≥6)	82	182	336	220	**508**	32	7	1367
Mult (N≤5)	100	131	47	53	10	4	31	376
Mult (N≥6)	109	196	298	269	287	53	20	1232
Total	3540	3574	2629	2736	2992	289	463	**16223**

Table A.6.5i. Same as A.6.5a, for nordic areas and all illumination conditions

	Cloud free	Low	Med	Semi	High	Semi above	Fract	Total
Cloud free	**832**	432	28	80	17	14	125	1528
Low (N≤5)	24	**56**	3	3	0	1	11	98
Low (N≥6)	100	**391**	279	56	205	37	39	1107
Med (N≤5)	21	55	**17**	27	5	6	14	145
Med (N≥6)	17	108	**260**	93	265	48	6	797
Semi (N≤5)	147	113	25	**88**	5	38	27	443
Semi (N≥6)	62	85	86	**192**	114	56	9	604
High (N≤5)	9	26	6	6	**1**	0	5	53
High (N≥6)	13	82	151	73	**186**	32	7	544
Mult (N≤5)	48	80	18	25	1	4	28	204
Mult (N≥6)	27	120	154	118	132	53	19	623
Total	1300	1548	1027	761	931	289	290	**6146**

Table A.6.5j. Same as A.6.5a, for nordic areas and day conditions

	Cloud free	Low	Med	Semi	High	Semi above	Fract	Total
Cloud free	**488**	128	22	20	7	0	1	666
Low (N≤5)	20	**11**	0	1	0	0	0	32
Low (N≥6)	124	**59**	77	46	101	0	0	407
Med (N≤5)	12	18	**4**	1	2	0	0	37
Med (N≥6)	61	23	**48**	93	132	0	0	357
Semi (N≤5)	98	33	11	**31**	7	0	1	181
Semi (N≥6)	74	15	21	**101**	49	0	0	260
High (N≤5)	4	4	2	2	**1**	0	0	13
High (N≥6)	40	27	40	49	**84**	0	0	240
Mult (N≤5)	29	13	10	12	0	0	0	64
Mult (N≥6)	60	20	43	49	52	0	0	224
Total	1010	351	278	405	435	0	2	**2481**

Table A.6.5k. Same as A.6.5a, for nordic areas and twilight conditions

	Cloud free	Low	Med	Semi	High	Semi above	Fract	Total
Cloud free	**866**	746	252	450	304	0	136	2754
Low (N≤5)	24	**64**	12	11	9	0	2	122
Low (N≥6)	102	**389**	374	173	304	0	3	1345
Med (N≤5)	16	55	**36**	60	19	0	10	196
Med (N≥6)	32	123	**255**	291	451	0	5	1157
Semi (N≤5)	85	79	66	**178**	49	0	10	467
Semi (N≥6)	26	44	62	**188**	140	0	1	461
High (N≤5)	5	8	2	3	**0**	0	0	18
High (N≥6)	29	73	145	98	**238**	0	0	583
Mult (N≤5)	23	38	19	16	9	0	3	108
Mult (N≥6)	22	56	101	102	103	0	1	385
Total	1230	1675	1324	1570	1626	0	171	**7596**

Table A.6.5l. Same as A.6.5a, for nordic areas and night conditions

	Cloud free	Low	Med	Semi	High	Semi above	Fract	Total
Cloud free	**21762**	1852	583	2124	65	96	2651	29133
Low (N≤5)	2352	**754**	189	669	50	75	967	5056
Low (N≥6)	2157	**4376**	2027	2236	609	817	851	13073
Med (N≤5)	3847	1205	**181**	822	65	118	1729	7967
Med (N≥6)	1070	1095	**1465**	3748	1293	1091	922	10684
Semi (N≤5)	4704	913	450	**2341**	91	250	1183	9932
Semi (N≥6)	3809	1226	1437	**5639**	623	1469	1547	15750
High (N≤5)	803	258	77	619	**58**	60	465	2340
High (N≥6)	852	579	816	2847	**1184**	814	506	7598
Mult (N≤5)	1771	628	188	745	49	122	683	4186
Mult (N≥6)	580	557	563	1312	301	502	395	4210
Total	43707	13443	7976	23102	4388	5414	11899	**109929**

Table A.6.5m. Same as A.6.5a, for tropical areas and all illumination conditions

	Cloud free	Low	Med	Semi	High	Semi above	Fract	Total
Cloud free	**11160**	652	124	280	16	96	1602	13930
Low (N≤5)	1579	**486**	74	206	23	75	833	3276
Low (N≥6)	919	**1990**	707	832	233	817	757	6255
Med (N≤5)	2569	944	**99**	373	41	118	1430	5574
Med (N≥6)	654	680	**823**	1840	728	1091	789	6605
Semi (N≤5)	2922	480	116	**731**	32	250	692	5223
Semi (N≥6)	2876	659	647	**2997**	357	1469	1157	10162
High (N≤5)	575	180	45	188	**31**	60	306	1385
High (N≥6)	605	388	548	1469	**733**	814	392	4949
Mult (N≤5)	1166	383	83	291	21	122	527	2593
Mult (N≥6)	375	365	328	652	185	502	324	2731
Total	25400	7207	3594	9859	2400	5414	8809	**62683**

Table A.6.5n. Same as A.6.5a, for tropical areas and day conditions

	Cloud free	Low	Med	Semi	High	Semi above	Fract	Total
Cloud free	**797**	9	2	24	0	0	15	847
Low (N≤5)	89	**6**	0	9	1	0	1	106
Low (N≥6)	370	**136**	65	184	23	0	37	815
Med (N≤5)	81	1	**1**	8	0	0	2	93
Med (N≥6)	78	7	**29**	118	42	0	14	288
Semi (N≤5)	224	8	7	**84**	2	0	14	339
Semi (N≥6)	271	32	65	**316**	19	0	37	740
High (N≤5)	50	4	2	13	**1**	0	18	88
High (N≥6)	75	6	18	161	**69**	0	17	346
Mult (N≤5)	84	5	1	9	0	0	2	101
Mult (N≥6)	53	4	9	59	11	0	7	143
Total	2172	218	199	985	168	0	164	**3906**

Table A.6.5o. Same as A.6.5a, for tropical areas and twilight conditions

	Cloud free	Low	Med	Semi	High	Semi above	Fract	Total
Cloud free	**9805**	1191	457	1820	49	0	1034	14356
Low (N≤5)	684	**262**	115	454	26	0	133	1674
Low (N≥6)	868	**2250**	1255	1220	353	0	57	6003
Med (N≤5)	1197	260	**81**	441	24	0	297	2300
Med (N≥6)	338	408	**613**	1790	523	0	119	3791
Semi (N≤5)	1558	425	327	**1526**	57	0	477	4370
Semi (N≥6)	662	535	725	**2326**	247	0	353	4848
High (N≤5)	178	74	30	418	**26**	0	141	867
High (N≥6)	172	185	250	1217	**382**	0	97	2303
Mult (N≤5)	521	240	104	445	28	0	154	1492
Mult (N≥6)	152	188	226	601	105	0	64	1336
Total	16135	6018	4183	12258	1820	0	2926	**43340**

Table A.6.5p. Same as A.6.5a, for tropical areas and night conditions

	Cloud free	Low (N≤5)	Low (N≥6)	Med (N≤5)	Med (N≥6)	Semi (N≤5)	Semi (N≥6)	High (N≤5)	High (N≥6)
All :	72.62	23.22	35.52	4.05	20.49	22.73	36.34	2.29	24.32
Day	78.24	22.78	36.76	2.47	18.73	13.87	30.39	2.20	21.72
Twilight	86.31	22.07	22.43	6.23	21.13	16.46	40.66	1.30	29.52
Night	66.08	24.07	36.68	7.20	22.75	34.28	46.83	2.59	27.14
Mid-latitude:	75.37	43.02	38.33	10.12	30.10	19.59	37.62	1.30	31.53
Day	79.14	49.64	41.76	5.34	28.58	12.24	32.65	2.05	30.01
Twilight	87.05	30.92	27.92	8.00	29.55	10.79	39.39	0.00	32.04
Night	70.31	38.08	37.39	17.92	31.89	31.49	45.53	0.00	33.27
Nordic:	44.18	51.98	29.35	15.08	24.36	27.22	36.30	2.38	37.16
Day	54.45	57.14	35.32	11.72	32.62	19.86	31.79	1.89	34.19
Twilight	73.27	34.38	14.50	10.81	13.45	17.13	38.85	7.69	35.00
Night	31.45	52.46	28.92	18.37	22.04	38.12	40.78	0.00	40.82
Tropical:	74.70	14.91	33.47	2.27	13.71	23.57	35.80	2.48	15.58
Day	80.11	14.84	31.81	1.78	12.46	14.00	29.49	2.24	14.81
Twilight	94.10	5.66	16.69	1.08	10.07	24.78	42.70	1.14	19.94
Night	68.30	15.65	37.48	3.52	16.17	34.92	47.98	3.00	16.59

Table A.6.6 Validation of Cloud Type (CT) with SYNOP. Variation of producer accuracy percentage with climatic areas and illuminations conditions

	Cloud free	**Low**	**Med**	**Semi**	**High**
All :	59.36	40.41	20.58	32.13	23.24
Day	53.06	38.11	24.00	35.44	27.75
Twilight	51.65	36.42	20.79	32.97	25.93
Night	69.37	43.49	17.83	29.39	18.84
Mid-latitude:	72.92	45.61	19.81	28.24	22.85
Day	69.80	43.89	21.88	30.33	27.02
Twilight	60.55	36.04	22.54	27.58	26.07
Night	79.76	49.31	17.78	26.62	18.90
Nordic:	61.75	27.14	23.58	28.44	17.05
Day	64.00	28.88	26.97	36.79	20.09
Twilight	48.32	19.94	18.71	32.59	19.54
Night	70.41	27.04	21.98	23.31	14.64
Tropical:	49.79	38.16	20.64	34.54	28.30
Day	43.94	34.36	25.65	37.81	31.83
Twilight	36.69	65.14	15.08	40.61	41.67
Night	60.77	41.74	16.59	31.42	22.42

Table A.6.7 Validation of Cloud Type (CT) with SYNOP. Variation of user accuracy percentage with climatic areas and illuminations conditions

Annex 7. References

Ackerman S.A., 1989, Using the Radiative Temperature Difference at 3.7 and 11μm to track Dust Outbreaks, *Remote Sensing of Environment, **27**, 129-133*.

Ackerman S.A and Strabala K.I., 1994, Satellite remote sensing of H_2SO_4 aerosol using the 8-12mm window region : Application to Mount Pinatubo, *Journal of geophysical Research, **99(D9)** 18639-18649*.

Anderson G. et al., 1995, Fascode/Modtran/Lowtran : past/present/future. *Proc. 18th Annual Review Conference on Atmospheric Transmission Models, 6-8th June 1995.*

Baum, B. A., Arduini, R. F., Wielicki B. A., Minnis, P., Tsay, S., 1994 : Multilevel cloud retrieval using multispectral HIRS and AVHRR data : Nighttime oceanic analysis. *J. Geophys. Res*., **99, D3**, 5499-5514.

Brunel P., Derrien M., LeGleau H., Marsouin A., 1991, Routine mapping of vegetation index with the AVHRR of NOAA11, *Proceeding of the 5th International colloquium Physical Measurements and signatures in Remote Sensing, Courchevel, France 14-18 January 1991, ESA SP-319*, pp61-64.

Brunel P., Lavanant L., and Rochard G., 1992, Transmittance coefficients generation for fast radiative transfer model, *Proc. Central Symposium of the ISY Conference, Munich, ESA SP-341*, pp229-233.

Coakley J.A., and Bretherton F.P., 1982, Cloud cover from high resolution scanner data : detection and allowing for partially filled fields of view, *J.Geophys.Res*., **87**, 4917-4932.

Congalton R., 1991 : A review of assessing the accuracy of classifications of remotely sensed data.. *Remote Sensing of Environment*,**37**, 35-46.

Cox C., and Munck W., 1954, Measurements of the roughness of the sea surface from the sun's glitter. *J.Opt.Soc.Am*., **44**, 838-850.

Derrien M., Lavanant L., Le Gléau H., 1988, Retrieval of the top temperature of semi-transparent clouds with AVHRR. *Proc. IRS'88 Conf, Lille, France*, pp 199-202.

Derrien M, Farki B., Harang L., Le Gléau H., Noyalet A., Pochic D., Sairouni A., 1993, Automatic cloud detection applied to NOAA-11 / AVHRR imagery, *Remote Sensing of Environment*, **46**, pp246-267.

Derrien M and LeGleau H., 1999, Cloud classification extracted from AVHRR and GOES imagery, *Proceeding of the 1999 Eumetsat Meteorological Satellite Data user' conference, Copenhague 6-10 September 1999.*

Eyre J., 1991, A Fast radiative transfer model for satellite sounding systems. *ECMWF Res.Dep.Tech.Mem 176. ECMWF, Reading, United Kinkdom*.

Gesell G., 1989, An algorithm for snow and ice detection using AVHRR data. An extension to the APOLLO software package. *Int.J.Remote Sensing*, **10**, 897-905.

Gutman G., Tarpley D., Ignatov A., and Olson S., 1995, The enhanced NOAA global land dataset from the Advanced Very High Resolution Radiometer, *Bulletin of the American Society*, 76 (7) 1141-1156.

Hall D.K., Riggs G.A., and Salomonson V., 1995, Development of methods for mapping global snow cover using moderate resolution imaging spectroradiometer data. *Remote Sensing of Environment*, **54**, 127-140.

Hunt, G.E., 1973, Radiative properties of terrestrial clouds at visible and infra-red thermal window wavelengths, *Quart.J.Roy.Meteorol.Soc*, 99 : 346-369.

Inoue, T., 1985 , On the temperature and effective emissivity détermination of semi-transparent Cirrus clouds by bi-spectral measurements in the 10μm window region, *J.Meteorol.Soc.Jpn*, **63**, 88-99.

Jankowiak I. and Tanre D., 1992, Satellite Climatology of Saharian Dust outbreaks : Method and Preliminary results, *Journal of Climate, 5, 646-656*.

Karrlsson K.G.,1993, Comparison of Operational AVHRR-Based Cloud Analyses with Surface Observations. *Proc. of the 6th AVHRR Data Users' Meeting, Belgirate , Italy, 29th June- 2nd July 1993*, EUM P 12, 223-229

Key J., Schweiger, 1998, Tools for atmospheric radiative transfer : Streamer and FluxNet, *Computers & Geosciences*, **24**(5), 443-451.

Kriebel K.T., Gesell G.,Gratzki A., Kästner M., Mannstein H., Schickel K.P., Seyerlin R., 1997,Comparison of AVHRR Derived Cloud Cover with Surface Observations. *Proc. of the 1997 Meteorological Satellite Data Users' Conference, Brussels, EUM P 21 ,107-114*

LeRoux C., LeNoble J., Deuzé J.L., Goloub P., Sergent C., Fily M., 1996, Modelling and Measurements of snow reflectance from visible to nrear-infrared. *Proceeding of IRS'96 : Current Problem in Atmospheric Radiation*. pp 37-40.

Luo, G., Davis, P. A., Stowe, L. , McLain, E. P., 1995 : A pixel-scal algorithm of cloud type, layer and amount for AVHRR data. Part 1 : Nighttime. *J. Atmos. Oceanic Technol*., **12**, 1013-1037.

Manalo-Smith N., Smith G.L., Tiwari S.N., and Staylor W.F., 1998, Analytical forms of bidirectional reflectance functions for application to Earth radiation budget studies, *Journal of Geophysical Research*, **103 (D16**) 19733-19751.

Masuda K., Takashima T., Takayama Y., 1988, Emissivity of pure and sea waters for the model sea surface in the infrared window regions, *Remote Sensing of Environment* 24 :313-329.

Menzel W.P., Smith W.L., and Stewart T.R., 1983, Improved Cloud Motion Wind Vector and Altitude Assignment using VAS, *Journal of Climate and Applied meteorology*, **22**, 377-384.

Oort A.H., 1983, Global atmospheric circulation statistics, 1958-1973. NOAA professional Paper No. 14.

Parol, F., Buriez, J.C., Brogniez, G., Fouquart, Y ., 1991, Information content of AVHRR channels 4 and 5 with respect to the effective radius of cirrus cloud particles. *J. Appl. Meteor* ., **30**, 973-984.

Prata A.J., 1989, Observations of volcanic ash clouds in the 10-12μm window using AVHRR/2 data, *Int.J.Remote Sensing, **10**, 751-761*.

Putsay M, Derrien M., LeGleau H. and Monnier G., 1999Comparison of two methods to estimate the cloud top temperature and pressure for NOAA-AVHRR and HIRS data, *Proceeding of the 1999 Eumetsat Meteorological Satellite Data user' conference, Copenhague 6-10 September 1999.*

Roujean J.L., LeRoy M., and Deschamps P.Y, 1992, A bidirectional reflectance model of the earth's surface for the correction of Remote sensing data, *Journal of geophysical research*, **97**, 20445-20468.

Ruff I. and Gruber A., 1983, Multispectral Identification of clouds and earth surfaces using AVHRR data. *Proceeding of the 5th Conference on Atmospheric Radiation. Baltimore. 31 October-4 November 1983*, pp 475-478.

Salisbury J.W., D'Aria D.M., 1992, Emissivity of terrestrial materials in the 8-14 μm atmospheric window, *Remote Sensing of Environment* 42 :83-106

Salisbury J.W., D'Aria D.M., 1994, Emissivity of terrestrial materials in the 3-5μm atmospheric window, *Remote Sensing of Environment* 47 :345-361

Sassen K., Mace G.G., Wang Z., Poellot M., Sekelsky S., McIntosh R.E., 1999, Continental Stratus Clouds : A Case Study Using Coordinated Remote Sensing and Aircraft Measurements. *J. Atmos. Sci*., **56**, 2345-2358.

Schmetz J., Hollmund K., Hoffman J. and B.Strauss, 1993, Operational cloud motion winds from Meteosat infrared images. *J.Appl.Meteor*, 32, 1207-1225.

Serdan J-M., Le Gléau H., Zwatz-Meise V., and Dybbroe A., 1998, The Satellite Application Facility - SAF - of EUMETSAT to support Nowcasting : An introduction, *Proc. 9th Conf.on Sat. Meteorology and Oceanography, Paris, France, 25-29 May 1998*, pp 319-322.

Tanre D., Deroo C., Duhaut P., Herman M., Morcrette J.J., Perbos J. and Deschamps P.Y., 1990, Description of a computer code to simulate the satellite signal in the solar spectrum : the 5S code, *Int.J.Remote Sensing*, **11**, 659-668.

Visa A., Iivarinen J., 1997, Evolution and Evaluation of a Trainable Cloud Classifier. *IEEE Trans. Geosci. Remote Sensing*, Vol. **35** n°**5**, 1307-1315

Wen A., and Rose W.I., 1994, Retrieval of sizes and total masses of particles in volcanic clouds using AVHRR band 4 and 5, *Journal of Geophysical Research*, **99 (D3)**, 5421-5431.

Wessel P., Smith W.H.F., 1995, New version of the Generic Mapping Tools released, *EOS Trans. Amer. Geophys. U. Electronic.* Vol 76 (33), 329

Wielecky B., Parker L., 1992, On the determination of cloud cover from satellite sensors : The effect of sensor resolution. *J.Geophys.Res*., **97**, 12,799-12,823.

Wu, M. C., 1987 : A method for remote sensing the emissivity, fractional cloud cover, and cloud top temperature of high-level, thin clouds. *J. Climate Appl. Meteor*., **26**, 225-233.

Annex 8. Acronyms

5S	Simulation of Satellite Signal in the Solar Spectrum
6S	Second Simulation of Satellite Signal in the Solar Spectrum
ATOVS	Advanced TOVS
ASOS	Automated Surface Observing System
AVHRR	Advanced Very High Resolution Radiometer
BDRF	Bi-directional Reflectance Functions
CLA	Cloud Analysis
CMa	Cloud Mask (also PGE01)
CMS	Centre de Meteorologie Spatiales (Météo-France, satellite reception centre in Lannion)
CTH	Cloud Top Height
CTTH	Cloud Top Temperature and Height
CT	Cloud Type
DTM	Digital Terrain Model
ECMWF	European Centre for Medium range Weather Forecast
EUMETSAT	European Meteorological Satellite Agency
FASCOD	Fast Code (for atmospheric transmission)
FIS	Format Image Standard (the image format used at CMS)
FOV	Field Of View
GOES	Geostationary Operational Environmental Satellite
GVAR	Geostationary I-M Variable
HIRLAM	High Resolution Limited Area Model
HIRS	High Resolution Infrared Sounder
HRIT	High Rate Information Transmission
HRPT	High Resolution Picture Transmission
INM	Instituto Nacional de Meteorología
IR	Infrared
MB	Mega-Bytes
Metop	The satellites in the EPS
MODTRAN	Moderate Resolution for Atmospheric TRANsmissions
MPEF	Meteorological Product Extraction Facility
MSG	Meteosat Second Generation
MTR	Mid-Term Review
NDVI	Normalised Differential Vegetation Index
NIR	Near Infra-Red

NMS	National Meteorological Service
NOAA	National Oceanic and Atmospheric Administration
PGE	product Generation Element
RTM	Radiative Transfer Models
R0.6μm	0.6 visible reflectance
RTTOV	Rapid Transmissions for TOVs
RTATOV	Rapid Transmissions for ATOVs
SAF	Satellite Application Facility
SAF NWC	SAF to support NoWCasting and VSRF
SAF O&SI	Ocean and Sea Ice SAF
SCANDIA	SMHI Cloud Analysis model using digital AVHRR data
SEVIRI	Spinning Enhanced Visible & Infrared Imager
SMHI	Swedish Meteorological and Hydrological Institute
SST	Sea Surface Temperature
SW	Software
T11μm	11 micrometer infrared brightness temperature
TBC	To Be Confirmed
TBD	To Be Defined
TIGR	Tovs Initial Guess Retrieval
TOA	Top Of Atmosphere
TOVS	Tiros Operational Vertical Sounder
URD	User Requirements Document
UTC	Coordinated Universal Time
VIS	Visible
VNIR	Visible and near IR
VSRF	Very Short Range Forecasting